



Durham E-Theses

A study of the interactions between ylidic phosphorus species and s-blockmetals

Bolton, Philip D.

How to cite:

Bolton, Philip D. (2000) *A study of the interactions between ylidic phosphorus species and s-blockmetals*, Durham theses, Durham University. Available at Durham E-Theses Online: <http://etheses.dur.ac.uk/4340/>

Use policy

The full-text may be used and/or reproduced, and given to third parties in any format or medium, without prior permission or charge, for personal research or study, educational, or not-for-profit purposes provided that:

- a full bibliographic reference is made to the original source
- a [link](#) is made to the metadata record in Durham E-Theses
- the full-text is not changed in any way

The full-text must not be sold in any format or medium without the formal permission of the copyright holders.

Please consult the [full Durham E-Theses policy](#) for further details.

A study of the interactions between ylidic phosphorus species and s-block metals

by

Philip D. Bolton
(Trevelyan College)

The copyright of this thesis rests with the author. No quotation from it should be published in any form, including Electronic and the Internet, without the author's prior written consent. All information derived from this thesis must be acknowledged appropriately.

A thesis submitted in part fulfilment of the requirements for the degree of Doctor of
Philosophy in the University of Durham.

October 2000



13 JUL 2001

Statement of Copyright

The copyright of this thesis rests with the author. No quotation from it should be published without his prior consent and information derived from it should be acknowledged.

Declaration

The work described in this thesis was carried out in the Department of Chemistry at the University of Durham between October 1997 and September 1999, and at the Department of Chemistry at the University of Bath between October 1999 and September 2000. All the work is my own unless stated to the contrary and it has not been submitted previously for a degree at this or any other university.

Financial Support

The EPSRC and ICI are gratefully acknowledged for their financial support.

For Mum and Dad.

Table of Contents.

Molecular Formulae of I-VII and 1-50	i
Acknowledgements	iii
List of Publications	iv
Abstract	v
List of Abbreviations	vi
1. Introduction	1
1.1 Ylides	2
1.2 Phosphonium Ylides	3
1.3 Iminophosphoranes	22
1.4 Hydrogen Bonding	32
2. General Experimental Techniques	34
2.1 Inert Atmosphere Techniques	34
2.2 Starting Materials and Solvents	36
2.3 Melting Point Determination	36
2.4 Infra-Red Spectroscopy (IR)	37
2.5 Nuclear Magnetic Resonance Spectroscopy (NMR)	37
2.6 Elemental Analysis	38
2.7 X-Ray Diffraction Studies	38
3. Experimental	40
3.1 Preparation of Ligands I-VII	43
3.2 Preparation of Complexes 1-8	49
3.3 Preparation of Complexes 9-21	58
3.4 Preparation of Complexes 22-27	71
3.5 Preparation of Complexes 28-50	78

4.	Group 2 Metal Complexes of Phosphonium Ylides	109
4.1	Background	109
4.2	Structural Investigation of I, II, V & VIIa-c	110
4.3	NMR Data of Complexes 1-8	114
4.4	Structural Investigation of Complexes 1-3	115
4.5	Discussion of Complexes 4-8	135
4.6	Conclusions	139
5	Group 2 Metal Complexes of Iminophosphoranes and Phosphine Oxides	140
5.1	Background	140
5.2	Structural Investigation of III, IV and VI	144
5.3	NMR Data of Complexes 9-21	145
5.4	Structural Investigation of Complexes 9-11	146
5.5	Discussion of Complexes 12-15	160
5.6	Discussion of Complexes 16-18 and Structural Investigation of Complexes 19-21	163
5.7	Conclusions	176
6.	Structural Diversity in Lithium Iminophosphorane Complexes and Related Systems	178
6.1	Introduction	178
6.2	NMR Data of Complexes 22-26	179
6.3	Discussion of Complexes 22-23	179
6.4	Discussion of Complexes 24-26	181
6.5	Compound 27 : The Search for a Di-anion	191
6.6	Conclusions	197
7.	Group 15 Salts and Ylides	198
7.1	Background	199

7.2	Discussion of Compounds 28-33	200
7.3	Discussion of Compounds 34-39	214
7.4	Discussion of Compounds 40-43	221
7.5	Discussion of Compounds 44-46	223
7.6	Discussion of Complexes 47-50	225
7.7	Conclusions	234
Appendix A – Supplementary Crystallographic Data		236
Appendix B – Conferences and Symposia Attended		294

Molecular formulae of I-VII and 1-50.

Number Used In Text	Empirical Formula
I	Ph_3PCH_2
II	$(\text{Me}_2\text{N})_3\text{PCH}_2$
III	Ph_3PNH
IV	$(\text{Me}_2\text{N})_3\text{PNH}$
V	$(\text{Ph}_2\text{PS})_2\text{NH}$
VI	Ph_3PO
VIIa-c	$\text{M}[\text{N}(\text{SiMe}_3)_2]_2$ where M = Ca, Sr & Ba for a, b & c respectively.
1	$(\text{Ph}_3\text{PCH}_2)_2 \cdot \text{Ca}[\text{N}(\text{SiMe}_3)_2]_2$
2	$(\text{Ph}_3\text{PCH}_2)_2 \cdot \text{Sr}[\text{N}(\text{SiMe}_3)_2]_2$
3	$(\text{Ph}_3\text{PCH}_2)_2 \cdot \text{Ba}[\text{N}(\text{SiMe}_3)_2]_2$
4	$[(\text{Me}_2\text{N})_3\text{PCH}_2]_2 \cdot \text{Ca}[\text{N}(\text{SiMe}_3)_2]_2$
5	$[(\text{Me}_2\text{N})_3\text{PCH}_2]_2 \cdot \text{Sr}[\text{N}(\text{SiMe}_3)_2]_2$
6	$(\text{Ph}_3\text{PCH}_2)_2 \cdot \text{Mg}\{\text{N}[\text{PPh}_2(\text{S})]_2\}_2$
7	$(\text{Ph}_3\text{PCH}_2)_2 \cdot \text{Ca}\{\text{N}[\text{PPh}_2(\text{S})]_2\}_2$
8	$(\text{Ph}_3\text{PCH}_2)_2 \cdot \text{Sr}[\text{OC}_6\text{H}_2(\text{Me})^t\text{Bu}_2]_2$
9	$(\text{Ph}_3\text{PNH})_2 \cdot \text{Ca}[\text{OC}_6\text{H}_2(\text{Me})^t\text{Bu}_2]_2$
10	$(\text{Ph}_3\text{PNH})_2 \cdot \text{Sr}[\text{OC}_6\text{H}_2(\text{Me})^t\text{Bu}_2]_2$
11	$(\text{Ph}_3\text{PNH})_2 \cdot \text{Ba}[\text{OC}_6\text{H}_2(\text{Me})^t\text{Bu}_2]_2$
12	$[(\text{Me}_2\text{N})_3\text{PNH}]_2 \cdot \text{Sr}[\text{OC}_6\text{H}_2(\text{Me})^t\text{Bu}_2]_2$
13	$(\text{Ph}_3\text{PNH})_2 \cdot \text{Sr}\{\text{N}[\text{PPh}_2(\text{S})]_2\}_2$
14	$(\text{Ph}_3\text{PNH})_2 \cdot \text{Sr}(\text{OCPh}_3)_2$
15	$(\text{Ph}_2\text{MePNH})_2 \cdot \text{Sr}[\text{OC}_6\text{H}_2(\text{Me})^t\text{Bu}_2]_2$
16	$(\text{Ph}_3\text{PO})_2 \cdot \text{Ca}[\text{N}(\text{SiMe}_3)_2]_2$
17	$(\text{Ph}_3\text{PO})_2 \cdot \text{Sr}[\text{N}(\text{SiMe}_3)_2]_2$
18	$(\text{Ph}_3\text{PO})_2 \cdot \text{Ba}[\text{N}(\text{SiMe}_3)_2]_2$
19	$(\text{Ph}_3\text{PO})_2 \cdot \text{Ca}[\text{OC}_6\text{H}_2(\text{Me})^t\text{Bu}_2]_2$
20	$(\text{Ph}_3\text{PO})_2 \cdot \text{Sr}[\text{OC}_6\text{H}_2(\text{Me})^t\text{Bu}_2]_2$
21	$(\text{Ph}_3\text{PO})_2 \cdot \text{Ba}[\text{OC}_6\text{H}_2(\text{Me})^t\text{Bu}_2]_2$
22	$\text{Ph}_3\text{PNH} \cdot \text{LiN}[\text{PPh}_2(\text{S})]_2$

23	$(\text{Ph}_2\text{MePN}^-)_2\text{Li}_3[\text{OC}_6\text{H}_2(\text{Me})^t\text{Bu}_2]$
24	$\text{Ph}_2\text{MePNH}\cdot\text{LiOS}(\text{O})(\text{CF}_3)\text{NSO}_2\text{CF}_3$
25	$\text{Ph}_3\text{PNH}\cdot\text{LiOS}(\text{O})(\text{CF}_3)\text{NSO}_2\text{CF}_3$
26	$\text{TMEDA}\cdot\text{LiOS}(\text{O})(\text{CF}_3)\text{NSO}_2\text{CF}_3$
27	$\text{Ph}_2[\text{C}(\text{H})(\text{Ph})\text{CO}_2\text{Me}]\text{PNCO}_2\text{Me}$
28	$\text{Ph}_2(\text{o}-\text{C}_6\text{H}_4\text{OMe})\text{P}^+\text{CH}_3\text{Br}^-$
29	$\text{Ph}_2(\text{o}-\text{C}_6\text{H}_4\text{OMe})\text{P}^+\text{CH}_2\text{PhBr}^-$
30	$\text{Ph}_2(\text{o}-\text{C}_5\text{H}_5\text{N})\text{P}^+\text{CH}_2\text{PhBr}^-$
31	$\text{Ph}_2(\text{o}-\text{C}_6\text{H}_4\text{CH}_2\text{NMe}_2)\text{P}^+\text{CH}_2\text{PhBr}^-$
32	$[\text{C}_6\text{H}_4(\text{o}-\text{CH}_2\text{P}^+\text{Ph}_3\text{Br}^-)]_2$
33	$\text{Ph}_2\text{P}^+(\text{CH}_3\text{Br}^-)\text{C}_4\text{H}_8\text{P}^+(\text{CH}_3\text{Br}^-)\text{Ph}_2$
34	$\text{Ph}_2(\text{o}-\text{C}_6\text{H}_4\text{OMe})\text{PCH}_2$
35	$\text{Ph}_2(\text{o}-\text{C}_6\text{H}_4\text{OMe})\text{PCHPh}$
36	$\text{Ph}_2(\text{o}-\text{C}_5\text{H}_5\text{N})\text{PCHPh}$
37	$\text{Ph}_2(\text{o}-\text{C}_6\text{H}_4\text{CH}_2\text{NMe}_2)\text{PCHPh}$
38	$\text{Ph}_2\text{MePCHPh}$
39	Ph_3AsCHPh
40	$\{\text{C}_6\text{H}_4[\text{o}-\text{C}(\text{H})\text{PPh}_3]\}_2$
41	$\text{C}_6\text{H}_4[\text{C}(\text{H})\text{PPh}_3]_2$
42	$\text{Ph}_2\text{P}(\text{CH}_2)\text{C}_4\text{H}_8\text{P}(\text{CH}_2)\text{Ph}_2$
43	$\text{Ph}_3\text{P}(\text{H})\text{CC}_3\text{H}_6\text{C}(\text{H})\text{PPh}_3$
44	$\text{Ph}_2\text{P}^+(\text{CH}_2\text{Ph})\text{NH}_2\text{Br}^-$
45	Ph_2MePNH
46	Ph_2EtPNH
47	$\text{Ph}_3\text{PNH}_2^+\cdot\text{N}[\text{PPh}_2(\text{S})]_2$
48	$\text{Ph}_3\text{PCH}_2\cdot\text{HOCPh}_3$
49	$\text{Ph}_3\text{PNH}\cdot\text{HOCPh}_3$
50	$\text{Ph}_3\text{PO}\cdot\text{HOCPh}_3$

Acknowledgements

Firstly, I would like to thank Prof. Matthew Davidson for his help, support and ideas over the last four years, both as a final year project student and as a Ph.D. student.

On the academic side, there are a great number of people without whom this work would not be possible : Prof. Judith Howard and the Durham University Crystallographic Service, most notably Drs. Andrei Batsanov, Andrés Goeta, Christian Lehmann, Dmitri Yusfit and Royston Copley. A big thank you to Charlie Broder for solving structures and for useful discussions. Thank you to Dr Mary Mahon at Bath University for the crystal structure determinations carried out over the last year. Thanks go to the departmental analytical services: (Durham) Jarika Dostal, Lenny Lauchlan, Judith Magee and Dr. Alan Kenwright as well as Ray and Gordon the glassblowers. (Bath) Alan Carver, Ahmed Sheibani and Mike Lock.

Prof. Fernando López-Ortiz (University of Almeria) is thanked for his hospitality during my two week stay as well as his useful discussions. Thanks also to Luis and Nacho for introducing me to the social side of southern Spain, and for help with the dianion chemistry.

Many people have had the pleasure of sharing a lab with me over the past years and a thank you is due to all of them for their help and camaraderie : Sarah, Christian, Patrick, Markus, Marina, Andy, Pete, Matt, Steve, Andreas, Tom and Andy J. A special thank you to Dr Richard Price for all his help, encouragement and alcoholic drink sharing over the past four years, I owe you one.

Thanks to all my friends from Durham: Rich, Helen, Fiona D, Fiona G, Caroline, Jenny, Tony, Charlie, Andy B, Allison J and Allison W and to those from home Stu and Julie. Thanks again to Rich P for sharing a flat with me in Bath, and a big thank you to Esther for her love and friendship over the past year.

Last and by no means least a big thank you to my family, Mum, Dad and Jen, who have been there for me throughout and without whom none of this would be possible.

List of Publications

- (1). The metallation of imino(triphenyl)phosphorane by ethylmagnesium chloride :
The synthesis, isolation and X-ray structure of $[\text{Ph}_3=\text{NMgCl}\cdot\text{O}=\text{P}(\text{NMe}_2)_3]_2$
Andrei. S. Batsanov, Philip. D. Bolton, Royston C. B. Copley, Matthew. G. Davidson,
Judith. A. K. Howard, Christian Lustig and Richard D. Price. *J. Organomet. Chem.*, **550**,
445 (1998).
- (2). Phosphorus Ylide Complexes of Calcium, Strontium and Barium: Structural
Models for Heavy Alkaline Earth Metal-Alkyl Bonds.
Philip D. Bolton, Charlotte K. Broder, Matthew G. Davidson, Andres E. Goeta, Judith A.
K. Howard and Richard D. Price. *Angew. Chem., Int. Ed. Engl.*, **Manuscript in
preparation.**
- (3). The First Neutral Iminophosphorane Complexes of Alkali Metals.
Andrei. S. Batsanov, Philip. D. Bolton, Charlotte K. Broder, Royston C. B. Copley,
Matthew. G. Davidson, Andres E. Goeta, Judith. A. K. Howard and Richard D. Price.
Manuscript in preparation.

Abstract

This thesis details the synthesis and characterisation of alkaline earth metal complexes of phosphonium ylides and iminophosphoranes, together with some related phosphine oxide species. This thesis also contains the synthesis and structural characterisation of a number of novel phosphonium ylides and iminophosphoranes.

Chapter 1 provides an introduction to the field of phosphonium ylides and related compounds, describing their preparation and subsequent reactivity. Chapter 2 contains an explanation of the experimental techniques and analytical tools used, whilst Chapter 3 details the syntheses and analyses for all of the complexes discussed in the thesis.

Chapter 4 discusses novel alkaline earth metal phosphonium ylide complexes. The chapter contains the first structurally characterised neutral phosphonium ylide complexes of calcium, strontium and barium with the general formula $(\text{Ph}_3\text{PCH}_2)_2\cdot\text{M}[\text{N}(\text{SiMe}_3)_2]_2$, where M = Ca, Sr and Ba.

The analogous iminophosphorane and phosphine oxide complexes are discussed in detail in chapter 5. Complexes of the general formula $(\text{Ph}_3\text{PNH})_2\cdot\text{M}[\text{OC}_6\text{H}_2(\text{Me})^t\text{Bu}_2]_2$, $(\text{Ph}_3\text{PO})_2\cdot\text{M}[\text{OC}_6\text{H}_2(\text{Me})^t\text{Bu}_2]_2$ and $(\text{Ph}_3\text{PO})_2\cdot\text{M}[\text{N}(\text{SiMe}_3)_2]_2$, are described where M = Ca, Sr and Ba.

Chapter 6 details the synthesis of novel lithiated iminophosphoranes and related compounds as well as the synthesis of a novel dianion $[\text{Ph}_2(\text{PhCH}^-)\text{PN}^-]$ for use in synthetic organic chemistry.

The final Chapter (7) details the synthesis and structural characterisation of a number of novel phosphonium ylides $\text{Ph}_2\text{R}'\text{PCHR}''$ and iminophosphoranes $\text{Ph}_2\text{R}'''\text{PNH}$ and their corresponding salts e.g. $\text{Ph}_2\text{R}'\text{P}^+\text{CH}_2\text{R}''\text{X}^-$ and $\text{Ph}_2\text{R}'''\text{P}^+\text{NH}_2\text{X}^-$.

List of Abbreviations

Ave.	average
Ar	aryl
ⁿ BuLi	n-butyllithium
^s BuLi	sec-butyllithium
^t BuLi	tert-butyllithium
COSY	correlation spectroscopy
CSD	Cambridge Structural Database
δ	chemical shift
DSC	differential scanning calorimetry
Et	ethyl
HMDS	hexamethyldisilylamide
HMPA	hexamethylphosphoramide
IR	infra-red
L	Lewis base
M	generic metal
Me	methyl
M.Pt	melting point
M _r	relative molecular mass
NMR	nuclear magnetic resonance
Ph	phenyl
ppm	parts per million
R	general aliphatic hydrocarbon group
thf	tetrahydrofuran
tol	toluene
XRD	X-ray diffraction

1. Introduction.

This thesis is concerned with phosphorus species of the general type $R_2R'PX$, where X can be CHR'', NH or O. In particular this thesis will concentrate on the synthesis of novel compounds of the above type and the subsequent complexation of them with alkaline earth metals. This chapter will serve to give a general overview of the topic, whilst more specific information will be detailed in the relevant discussion chapters.

The following monographs and review articles provide excellent background to this specific subject area and are recommended for further reading.

Phosphonium Ylides :

- A. W. Johnson with special contributions by W. C. Kaska, K. A. O. Starzewski and D. A. Dixon, '*Ylides and Imines of Phosphorus*', John Wiley & Sons Inc., New York, (1993).
D. G. Gilheany, *Chem. Rev.*, **94**, 1339 (1994).
O. I. Kolodiaznyi, '*Phosphorus Ylides*', Wiley-VCH, Weinheim & New York, (1999).

Iminophosphoranes :

- K. Dehnicke and J. Stahle, *Polyhedron.*, **8**, 707 (1989).
K. Dehnicke and F. Weller, *Coord. Chem. Rev.*, **158**, 103 (1997).
K. Dehnicke, M. Krieger and W. Massa, *Coord. Chem. Rev.*, **182**, 19 (1999).

Phosphine Oxides :

- D. B. Chesnut, *J. Am. Chem. Soc.*, **121**, 2335 (1999).
J. A. Dobado, H. Martínez-García, J. Molina-Molina and M. R. Sundberg, *J. Am. Chem. Soc.*, **122**, 1144 (2000).



1.1 Ylides

Although the first reported ylide was synthesised over a century ago by Michaelis et al¹, it was Staudinger et al² in 1919 who first proposed the structure of an ylide. The chemistry of ylides was not studied in any great detail until George Wittig's³ Nobel prize winning investigations published in 1953. His discovery that phosphonium ylides reacted with aldehydes or ketones to produce an alkene and phosphine oxide is still unsurpassed in the field of synthetic organic chemistry and is cited as '*of unmatched importance for specific introduction of C-C double bonds in a known location*'.⁴

An ylide may be defined⁵ as '*a substance in which a carbanion is attached directly to a heteroatom carrying a substantial degree of positive charge and in which the positive charge is created by the sigma bonding of substituents to the heteroatom*', which is easily described pictorially by two resonance canonical forms (Figure 1.1).

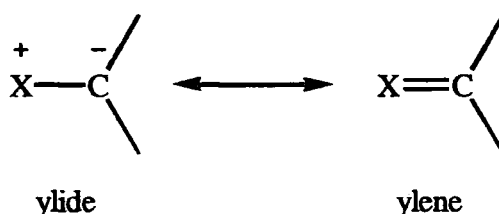


Figure 1.1 Two resonance canonical forms of an ylide

Considering the above canonical forms, it can be seen that the ylide canonical form highlights the zwitterionic nature of an onium moiety attached to the carbanionic centre, whilst the ylene form indicates a degree of electronic delocalisation of charge to give the 'double bond'.

¹ H. V. Gimborn and A. Michaelis, *Chem. Ber.*, **27**, 272 (1894).

² J. Meyer and H. Staudinger, *Helv. Chim. Acta.*, **2**, 635 (1919).

³ G. Gessler and G. Wittig, *Liebigs Ann. Chem.*, **580**, 44 (1953); G. Wittig's Nobel Prize Lecture, *Science.*, **210**, 600 (1980).

⁴ E. Vedejs, *Science.*, **210**, 42 (1980).

⁵ A. W. Johnson with special contributions by W. C. Kaska, K. A. O. Starzewski and D. A. Dixon, '*Ylides and Imines of Phosphorus*', John Wiley & Sons Inc., New York, (1993).

The word 'ylide' is the anglicised version of 'ylid' originally coined by Wittig⁶ in his native German tongue – 'yl' meaning open valence (c.f. methyl) and 'id' referring to anionicity (c.f. acetylid).

The heteroatom X can be any one of a number of Group 15 or 16 elements, (e.g. $X=R_2S$ ^{7,8} and R_3As ^{9,10}) but most commonly X is phosphorus¹¹ which has been found so far to be the most useful and as such, is the most widely studied heteroatom.

1.2 Phosphonium Ylides

1.2.1 Background

A phosphonium ylide is defined as '*an easily pyramidalised carbanion stabilised by an adjacent tetrahedral phosphonium centre*'.¹¹ They were first discovered in 1894 when Michaelis managed to isolate the ylide $Ph_3P=CHCO_2Et$. However it wasn't until 1961 that its structure was determined by Asknes,¹² by which time Staudinger² had already elucidated the structure of the simplest phosphonium ylide Ph_3PCH_2 , triphenylphosphonium methyllide, and Wittig had already reported the use of phosphonium ylides in olefin synthesis.

Phosphonium ylides are widely regarded as 'extra' stable carbanions, with the 'extra' stabilisation coming from the phosphonium group compared to say, ammonium ylides. There are three distinct but broad categories into which ylides may be placed.¹³

Stabilised ylides are usually easily isolable and have strongly electron withdrawing groups such as cyanide or a carbonyl on the ylidic carbon. They are generally unreactive and are thus stable to oxygen and moisture.

⁶ D. G. Gilheany, *Chem. Rev.*, **94**, 1339 (1994).

⁷ T. Christensen and W. G. Witmore, *Acta Cryst.*, **B25**, 73 (1969); A. F. Cook and J. G. Moffat, *J. Am. Chem. Soc.*, **90**, 740 (1968).

⁸ J. Bouma, L. Radom and B. F. Yates, *J. Am. Chem. Soc.*, **109**, 2250 (1987).

⁹ A. Strich, *New J. Chem.*, **3**, 105 (1979).

¹⁰ D. Lloyd, *Chem. Soc. Rev.*, **16**, 45 (1987).

¹¹ W. Graf, G. Muller, A. Schier, H. Schmidbaur and D. L. Wilkinson, *New J. Chem.*, **13**, 341 (1989).

¹² G. Asknes, *Scand. Chem. Acta.*, **15**, 438 (1961).

¹³ B. E. Maryanoff and A. B. Reitz, *Chem. Rev.*, **89**, 863 (1989).

Semi-stabilised ylides are more difficult to isolate and usually contain groups which are capable of moderate conjugation attached to the ylidic carbon such as a phenyl ring. Inert atmosphere techniques (see Chapter 2) are required for the handling of these compounds to ensure their preservation.

Non-stabilised ylides include those which have an alkyl group or hydrogen atom on the ylidic carbon. These ylides are of high reactivity and are usually prepared and used *in situ*. They are also intensely coloured from yellow through to dark red-purple, aiding the study of appearance and disappearance of ylides during reactions.

1.2.2 Structure and Bonding

The structure of a typical phosphonium ylide can be seen in Figure 1.2,⁶ where C_{ylidic} is the ylidic carbon atom and its substituents are represented by X and Y. R^u is known as the unique phosphorus substituent, whose P- R^u bond vector is elongated and has a wider R-P- C_{ylidic} angle in comparison to the other two substituents.

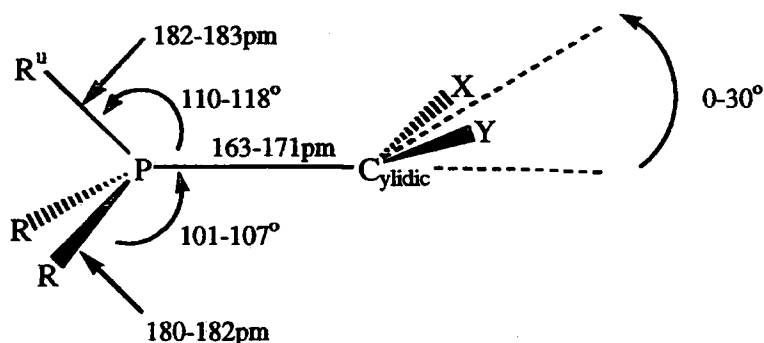


Figure 1.2 Molecular geometry of a typical phosphonium ylide

The plane defined by R^u , P and C_{ylidic} is orientated perpendicular to the plane defined by C_{ylidic} , X and Y, thereby relieving any steric strain and providing a possible site of attack beneath and perpendicular to the $C_{\text{ylidic}}XY$ plane, where the lone pair resides. The P- $C_{\text{ylidic}}XY$ moiety was originally thought to be planar, based on electron diffraction and

single crystal X-ray diffraction studies,^{14,15,16} but more recently has been shown to deviate from planarity by as much as 30°. ^{11,17} There is now evidence to suggest that stabilised ylides have trigonal planar carbanions, whereas non-stabilised ylides are slightly pyramidalised.¹⁸

The P-C_{ylidic} bond is shorter than a classical P-C single bond (1.87Å),¹⁹ typical values being in the range of 1.63 to 1.71Å.¹⁷ This shortening implies P-C double bond character but it would appear that there is only a very small barrier to rotation about the bond. Calculations have shown that for the hypothetical phosphonium ylide, H₃PCH₂ the barrier to rotation about the P-C_{ylidic} bond is 0.24kcal mol⁻¹.^{20,21} This is significantly smaller than that of the sulfonium ylide H₂SCH₃ (21.2kcal mol⁻¹),^{18,20} and also that of the ammonium ylide H₃NCH₂ (2.0kcal mol⁻¹),^{18,20} whose C-N distance of 1.457Å is typical of a carbon to nitrogen single bond.^{17,19}

The special stability of phosphonium ylides has been attributed to the positively charged phosphorus atom, and its ability, perhaps through 3d orbitals, to provide delocalisation of the negative charge on the carbanion. This makes the carbanion itself particularly stable and leads to discussion in the literature as to how this delocalisation occurs, much of which centres around the nature of the P-C bond. It is postulated that a hybrid exists between the dipolar 'ylide' species and the delocalised 'ylene' form (Figure 1.3).

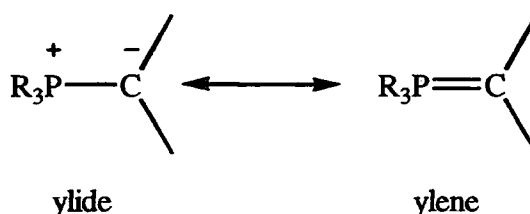


Figure 1.3 Dipolar and localised double bond forms of a phosphonium ylide

¹⁴ J. C. J. Bart, *J. Chem. Soc.*, 350 (1969).

¹⁵ E. A. V. Ebsworth, T. E. Fraser and D. W. H. Rankin, *Chem. Ber.*, **110**, 3494 (1977).

¹⁶ E. A. V. Ebsworth, T. E. Fraser, O. Gasser, D. W. H. Rankin and H. Schmidbaur, *Chem. Ber.*, **110**, 3508 (1977).

¹⁷ Ref 5 (Chp.2) and references cited therein.

¹⁸ Ref 5 (Chp.3) and references cited therein.

¹⁹ F. H. Allen, L. Brammer, O. Kennard, A. G. Orpen, R. Taylor and D. G. Watson, *J. Chem. Soc., Perkin Trans 2.*, S1-S19 (1987).

²⁰ D. A. Dixon, T. H. Dunning, R. A. Eades and P. G. Gassman, *J. Am. Chem. Soc.*, **105**, 7011 (1983).

²¹ D. A. Dixon, R. A. Eades and P. G. Gassman, *J. Am. Chem. Soc.*, **103**, 1066 (1981).

It was originally suggested^{6,22} that $d\pi$ - $p\pi$ bonding was a suitable model for the bonding in a phosphonium ylide, and was thought to occur through back-donation of electron density from the doubly occupied 2p orbital on the carbanion into a vacant 3d orbital on phosphorus (Figure 1.4). This explains why phosphonium ylides are more stable than their nitrogen (ammonium) analogues, as nitrogen has no low lying 3d orbitals²³ into which it can receive electron density and thus is incapable of this particular type of back-donation. Recently, however theoretical studies have shown that d-orbitals play little or no part in the ylidic bond,^{6,24} and thus alternative models have been sought.

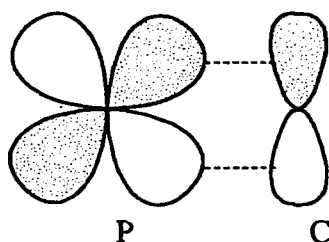


Figure 1.4 Phosphorus 3d – carbon 2p orbital overlap to give a π -type interaction

One such model^{6,25} involves donation of a lone pair of electrons from a R_3P moiety onto a carbene-like carbon atom, thus completing its octet and forming a classical σ bond. This is demonstrated in Figure 1.5 which shows the symmetry derived orbitals for the theoretical phosphonium ylide H_3PCH_2

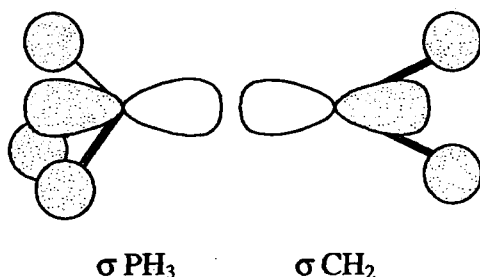


Figure 1.5 σ -bonding in H_3PCH_2

This extra charge on the carbon atom is formally a lone pair and is located in a p orbital on the ylidic carbon atom. Overlap of this p orbital with the two possible acceptor

²² A. W. Johnson, 'Ylid Chemistry,' Academic Press, New York, (1966).

²³ M. Petrovanu and I. Zugravescu, 'Nitrogen Ylid Chemistry', McGraw-Hill, New York, (1976).

²⁴ E. Magnusson, *J. Am. Chem. Soc.*, **112**, 7940 (1990).

²⁵ T. Chivers, N. Sandblom and T. Ziegler, *Can. J. Chem.*, **73**, 2363 (1996).

orbitals (anti-bonding with respect to the other ligands) on phosphorus forms a π back bond i.e. a $\pi\text{-}\sigma^*$ bond. This is called negative hyperconjugation and **Figure 1.6** shows this, with the example again being for the theoretical ylide H_3PCH_2 .

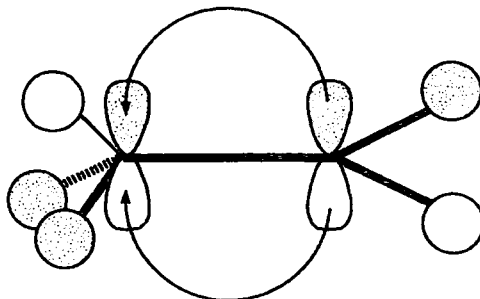


Figure 1.6 $\pi\text{-}\sigma^*$ back donation (negative hyperconjugation)

Consideration of the back-donation from $P\pi$ (HOMO) of the carbanion into the σ^* (LUMO) of the PR_3 moiety shows that an anti-bonding interaction would occur with the unique (R^u) substituent thereby weakening its P-R bond. This would in turn lead to a longer P-R bond and a wider $\text{R}^u\text{-P-C}_{\text{ylidic}}$ angle. If this is considered along with analogous phosphine oxides and transition metal phosphine complexes, in which negative hyperconjugation is believed to occur,²⁶ there is very strong evidence in favour of this theory. The ease of rotation about a phosphonium ylide bond (see earlier) is also explained by this theory as Mitchell et al²⁷ have demonstrated that back bonding is possible to antibonding orbitals in both the perpendicular and parallel conformations.

The second model describes the bonding in phosphonium ylides in terms of Ω or τ bonds^{20,28} (banana bonds²⁹ or bent multiple bonds). This unconventional approach, first introduced by Pauling in 1931,³⁰ describes neither a σ nor a π bond but instead two curved regions of electron density located between the phosphorus and carbon centres (**Figure 1.7**). Theoretical calculations have shown that the positions of the bond pairs are located close to the carbon, one of the bond pairs being noticeably closer than the other.³¹

²⁶ A. E. Reed and P. von R. Schleyer, *J. Am. Chem. Soc.*, **112**, 1434 (1990).

²⁷ D. J. Mitchell, H. B. Schlegel and S. Wolfe, *Can. J. Chem.*, **59**, 3280 (1981).

²⁸ H.-J. Freund, R. P. Messmer, P.A. Schultz and R. C. Tatar, *Chem. Phys. Lett.*, **126**, 176 (1986).

²⁹ I. N. Levine, *'Quantum Chemistry.'* 3rd Edn, Allyn and Bacon, Boston, (1983).

³⁰ L. Pauling, *J. Am. Chem. Soc.*, **53**, 1367 (1931).

³¹ M. Alajarin, F. H. Cano, J. Catalan, R. M. Claramunt, J. Elguero, M.C. Foces, C. L. Leonardo, P. Molina and J. L. G. de Paz, *J. Am. Chem. Soc.*, **111**, 355 (1989); H. Lischka, *J. Am. Chem. Soc.*, **99**, 353 (1977).

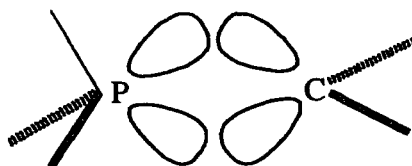
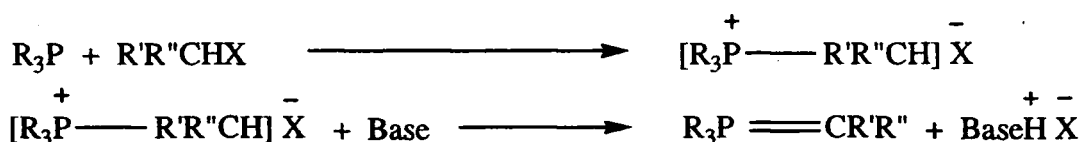


Figure 1.7 Banana bond representation for phosphonium ylides

Finally, there is a third model which attributes the length of the P-C_{ylidic} bond to electrostatic shortening.⁶ This theory considers the P-C bond to be a simple σ -bond formed by donation of the phosphorus lone pair into a vacant p orbital on the carbon atom. The phosphorus atom now carries a positive charge and the carbon a negative one, and thus there is a coulombic attraction between the two and a subsequent shortening of the bond.

1.2.3 Preparation of phosphonium ylides

Although there are various methods of preparation, dependent usually on the substituents required, the most widely used route is the 'salt' method. This process involves the removal of an α -proton from a phosphonium salt using an external base, to form the corresponding ylide. The phosphonium salt can often be made via a S_N2 quaternisation reaction (nucleophilic addition) of a trialkyl or triaryl phosphine by an alkyl halide (Scheme 1.1), or may be commercially available.



Scheme 1.1 Formation of a phosphonium salt and ylide

The reaction conditions for the formation of ylides tend to be mild – heating is seldom required. However, the choice of base is very important as it (and its conjugate acid) must: (a) be inert to reaction with the ylide, (b) produce easily separable by-products, and (c) be tolerant of any further reactions (most ylides are generated and used *in situ*). The most commonly used are carbon, nitrogen and oxygen bases (e.g. butyl lithium, sodium

amide and potassium *tert*-butoxide) and the strength of the base used depends on the nature of the phosphonium groups and the nature of the carbon substituents. The choice of solvent is also important. Generally, dry hydrocarbons and ethers are used which ensure no reaction with the bases or subsequent ylides.

Initially, ylides were made using organolithium bases, however it was soon discovered that lithium salts are able to complex with ylides and are thus capable of changing the stereochemistry of the products in a Wittig reaction. In the early 1970s Koster³² developed a 'lithium salt free' method of producing phosphonium ylides in which he used sodium amide as the base and thf as the solvent. Schmidbaur³³ later advocated the use of sodium hydride as a base but still used thf as the solvent.

Another route to making phosphonium ylides is Bestmann's 'transylidation reaction',³⁴ which avoids the need for metal bases completely. This process relies on the basicity of phosphonium ylides and involves the reaction of a phosphonium ylide with a phosphonium salt to yield the least basic phosphonium ylide as the product (Scheme 1.2). However the ylide used in the reaction must first be produced by an alternative route.



Scheme 1.2 Transylidation reaction

There are other methods of producing phosphonium ylides which tend to apply to specific cases such as ylides via vinylphosphonium salts^{35,36} and the direct addition of a carbene to a phosphine which is generally used to synthesise halo-substituted ylides.

Most common phosphonium ylide salts contain a Ph_3P group. Triphenylphosphine is cheap, safe and easy to handle as well as being both crystalline and air stable. The ipso or phosphorus bound carbon atoms in Ph_3P do not have any available protons to compete in the deprotonation step.

³² M. Grassberger, R. Koster and D. Simic, *Liebigs Ann. Chem.*, **281**, 739 (1970).

³³ H. Schmidbaur, H. Stüher and W. Vornberger, *Chem. Ber.*, **105**, 1084 (1972).

³⁴ H. J. Bestmann, *Chem. Ber.*, **95**, 58 (1962).

³⁵ H. Burger, *Dissertation at Tübingen University*, (1957).

³⁶ J. S. Fogel, J. K. Heeren and D. Seyforth, *J. Am. Chem. Soc.*, **86**, 307 (1964).

1.2.4 Phosphonium bis-ylides

Double deprotonation, where one proton is removed from each of the terminal carbons of $C-P^+-C-P^+-C$ say, results in the formation of a phosphonium 'bis' ylide. However, considering the above example, it is also possible to produce carbodiphosphoranes (both protons removed from the central carbon) and 'conjugated' bis-ylides (one proton from the central carbon and one from the terminal carbon), by double deprotonation.

$Ph_3P=CH(CH_2)_n-CH=PPh_3$ where $n = 2-5$ are known³⁷ and there is no reason why higher homologs cannot be produced. Bis-ylides are known with other chemical components between the two ylide groups e.g. $Ph_3P=CH-A-CH=PPh_3$ where $A = -C_6H_4-$ prepared from α,α' -bis(triphenylphosphonio)-p-xylene,³⁸ and the corresponding ortho isomer.^{39,40} These ylides have never previously been isolated, only prepared and used *in situ*.

Various groups have discovered that the conjugated bis-ylides are clearly energetically favoured over the isolated bis-ylides and often over the carbodiphosphoranes e.g. the carbodiphosphorane (Figure 1.8);

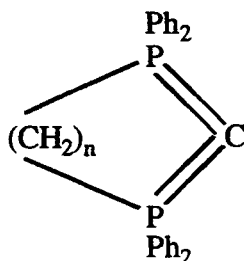


Figure 1.8

where $n = 3$ was obtained to the exclusion of the alternate isolated bis-ylide.⁴¹ Also, the conjugated ylide shown in (Figure 1.9) was obtained to the exclusion of the isolated bis-ylide of the carbodiphosphorane, even though a similar structure existed as the carbodiphosphorane.⁴²

³⁷ H. J. Bestmann, H. Haberlein and D. Kratser, *Angew. Chem., Int. Ed. Engl.*, **3**, 226 (1964).

³⁸ T. W. Campbell and R. N. McDonald, *J. Am. Chem. Soc.*, **82**, 4669 (1960).

³⁹ B. E. Douglas, C. E. Griffin and K. R. Martin, *J. Org. Chem.*, **27**, 1627 (1962).

⁴⁰ See Chapter 7 of this thesis.

⁴¹ T. Costa and H. Schmidbaur, *Chem. Ber.*, **114**, 3063 (1981).

⁴² G. A. Bowmaker, R. Herr and H. Schmidbaur, *Chem. Ber.*, **114**, 1428 (1983).

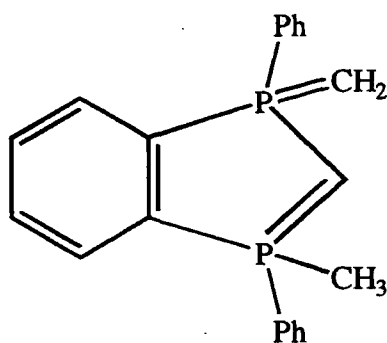


Figure 1.9

It has been concluded that conjugated bis-ylides are usually more stable than the isomeric carbodiphosphoranes and both are far more stable than the isomeric bis-ylides of which only a few examples are known e.g. Appel et al⁴³ produced the only known example of a bis-ylide of the type C=P-C-P=C (Figure 1.10),

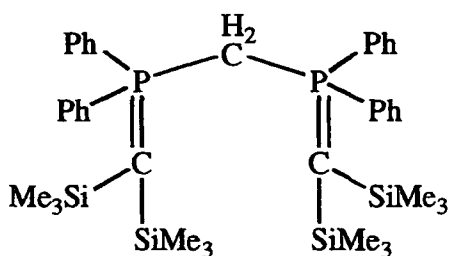


Figure 1.10

which only existed below -10°C and above which temperature it existed as the conjugated ylide shown by NMR and single crystal X-ray diffraction to be of the form (Figure 1.11);

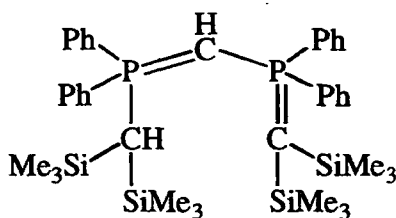


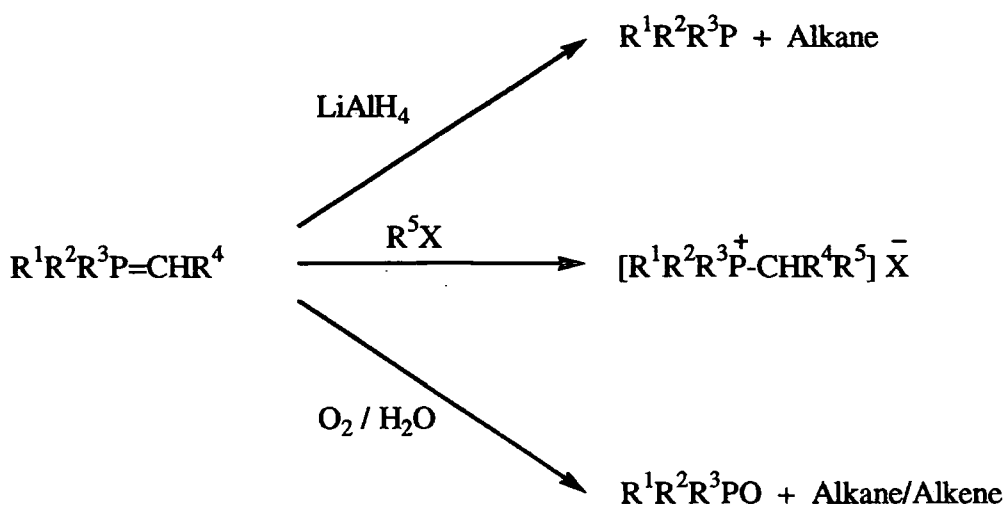
Figure 1.11

⁴³ R. Appel, G. Haubrich and F. Knoch, *Chem. Ber.*, **114**, 1428 (1983).

1.2.5 Selected reactions of phosphonium ylides

The unique electronic and molecular structure of phosphonium ylides means that they can undergo many different types of reaction. The reactions can be broadly split into two types, the ones involving only the carbanionic portion of the ylide and the reactions involving the carbanionic and phosphonium parts of the ylide, though not necessarily simultaneously.

It is beyond the scope of this introduction to detail every reaction that a phosphonium ylide can undergo, instead the reader is directed towards relevant chapters of reference 5. Some of the more useful reactions are shown in **Scheme 1.3**.



Scheme 1.3 Selected reactions of phosphonium ylides.

As can be seen from the above scheme, phosphonium ylides are particularly susceptible to hydrolytic cleavage, a general rule of thumb being that susceptibility to cleavage follows basicity i.e. the more basic the ylide, the more likely it is to undergo cleavage. The products of this reaction are a hydrocarbon and a phosphine oxide. The overall driving force for this reaction is the highly energetically stable phosphorus-oxygen bond.

The mechanism of the hydrolysis of phosphonium salts in basic conditions was established by Vanderwerf et al in 1959.⁴⁴ The reaction follows third order kinetics, first order in the phosphonium salt and second order in the hydroxide. In addition the reaction

⁴⁴ W. E. McEwen, C. A. Vanderwerf and M. Zanger, *J. Am. Chem. Soc.*, **81**, 3806 (1959).

normally occurs stereospecifically with inversion of configuration at the phosphorus resulting from the initial direct hydroxide attack at that atom centre.⁴⁵ The mechanistic and stereochemical details of this reaction were later reviewed by M^cEwen.⁴⁶ Alcoholysis of phosphonium ylides was postulated by Grayson and Keough in 1960,⁴⁷ to occur by a similar mechanism. The oxidation of phosphonium ylides results in the cleavage of the carbanion-phosphorus bond. Whilst the carbanion portion of the ylide is converted to a carbonyl or olefin group, the phosphorus portion, as in hydrolysis appears as a phosphine oxide, again due to the stability of the phosphorus-oxygen bond.

An alternative method for cleaving the phosphorus-ylidic carbon bond is by reduction. This method does not, however, produce the regiospecific products as seen in the aforementioned hydrolysis and oxidation reactions. Reduction of phosphonium salts or phosphonium ylides usually leads to an alkane (from the carbanion portion) and a tertiary phosphine which can be worked up to a phosphine oxide under certain conditions.

1.2.6 The Wittig reaction

The Wittig reaction first reported by George Wittig in 1953³ is one of the most important and useful of all the means of preparing alkenes. The general reaction proceeds via the condensation of a phosphonium ylide with a carbonyl compound to produce an alkene, with the elimination of a phosphine oxide (**Scheme 1.4**).



Scheme 1.4 The Wittig reaction.

The great advantages of the above reaction for synthetic organic chemists are that it can be performed under mild conditions (often -78°C) with short reaction times and high

⁴⁵ A. Blade-Font, K. F. Kumli, W. E. M^cEwen, C. A. Vanderwerf and M. Zanger, *J. Am. Chem. Soc.*, **86**, 2378 (1964).

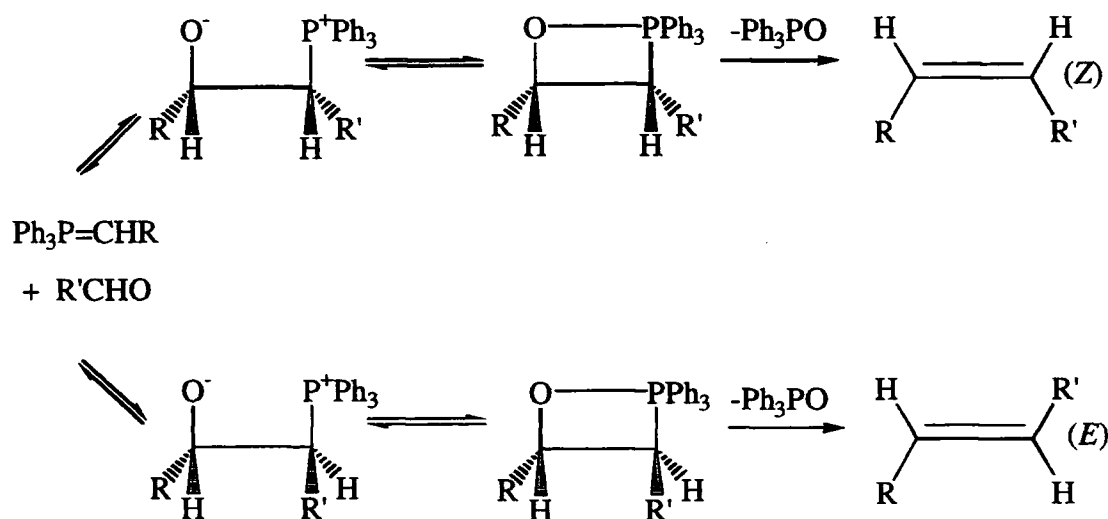
⁴⁶ W. E. M^cEwen, 'Topics in phosphorus chemistry', M. Grayson and E. J. Griffith (Eds.), Interscience, New York, Vol. 2 (1965).

⁴⁷ M. Grayson and P. T. Keough, *J. Am. Chem. Soc.*, **82**, 3919 (1960).

yields. The starting materials are usually easily prepared and the phosphine oxide can be removed fairly easily once the reaction is complete.

Like Grignard reactions⁴⁸ the Wittig reaction is regiospecific, however with careful choice of ylide the reaction can also be highly stereospecific. The degree of selectivity is dependant on the carbanion substituents in general, stabilised ylides afford the *E* or trans alkenes, non-stabilised ylides afford the *Z* or cis alkenes whereas semi-stabilised ylides afford a mixture. Reaction conditions, solvent, carbonyl substituents, temperature and pressure also affect the *E/Z* ratio.

The Wittig reaction has generally been considered to proceed via nucleophilic attack of the ylide carbanion on the carbonyl carbon to give the betaine intermediates. Wittig proposed that these intermediates then cyclised to their respective transient oxaphosphetanes which in turn disassociated, leaving a phosphine oxide and the cis or trans alkene (**Scheme 1.5**).



Scheme 1.5 Proposed mechanism of the Wittig reaction.

Since the initial postulation of the Wittig reaction mechanism, many modifications have been suggested (see Chapter 9 of reference 5). Current thinking suggests that the oxaphosphetanes are in fact the intermediates in the mechanism with the betaines as a model for the transition state.

⁴⁸ P. E. Rakita and G. S. Silverman (Eds.), 'Handbook of Grignard Reagents', Marcel Dekker. Inc., Monticello (1996).

There are many alternative reactions based on a similar theme and one of the most important is the Wittig-Schlosser reaction.⁴⁹ This reaction causes a complete reversal of the Wittig reaction stereochemistry i.e. non-stabilised ylides give predominantly trans alkenes. Schlosser reported that by allowing the betaine isomers to equilibrate, the ratio of the betaine isomers could be altered in favour of the threo betaine leading inevitably to increased formation of the *E* alkene. This was achieved by using an organolithium compound in the presence of a proton source.

However, as already mentioned, Wittig originally found that lithium halides complexed to ylides and their corresponding Wittig intermediate. Lithium salts are known to have a marked effect on the stereochemistry when present in Wittig reactions which resulted in the use of sodium and potassium bases in the production of ylides.

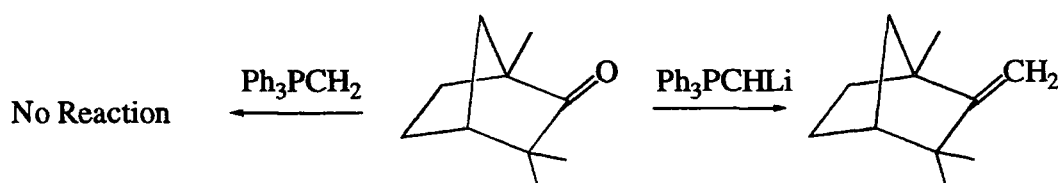
1.2.7 Lithium metallated phosphonium ylides

Although phosphorus ylides have been shown to play an important part as reagents in organic synthesis, they are only moderately nucleophilic, especially in the case of stabilised ylides. This means that their reactions are limited to those with the most electrophilic carbonyl compounds, for example aldehydes and ketones.

Metallation of phosphorus ylides has led to the development of a new group of nucleophilic organophosphorus reagents. Phosphorus ylides can complex with a variety of metals (see 1.2.8), but the most synthetically useful are those containing lithium. Corey and Kang⁵⁰ postulated that triphenylphosphonium methyllide Ph_3PCH_2 , reacts with *tert*-butyl lithium in thf solution to form the α -lithiated species Ph_3PCHLi , which unlike the free ylide, known to be unreactive with epoxides or hindered ketones, is active with fenchone, a hindered ketone (Scheme 1.6). This leads to the idea that α -lithioylides can be thought of as 'activated' phosphorus ylides.

⁴⁹ M. Schlosser, *Topics Stereochem.*, **5**, 1 (1970).

⁵⁰ E. J. Corey and J. Lang, *J. Am. Chem. Soc.*, **104**, 4724 (1982); E. J. Corey, J. Kang and K. Kyler, *Tetrahedron. Lett.*, **26**, 555 (1985).



Scheme 1.6

There is, however much debate as to whether the α -lithiated species $\text{Ph}_3\text{P}=\text{CHLi}$ is produced at all. Schlosser et al⁵¹ disagreed with this finding and, on the basis of NMR experiments and quenching reactions, proposed an alternative structure in which the ortho position of one of the phenyl groups is lithiated. It is also proposed that above 25°C the 'ortho-lithiated' species decomposes to a lithiated phosphine species $\text{Ph}_2\text{PCH}_2\text{Li}$.

Grützmacher et al⁵² recently reported the synthesis of an α -zincated phosphonium ylide, which upon heating converts to an ortho-zincated species. Given this evidence, and the postulations of Corey and Schlosser, it is quite possible that both proposals are correct. The α -lithio species proposed by Corey is a kinetic product, which upon heating reverts to the more stable ortho-lithiated species (thermodynamic product).

There are a few other lithiated phosphonium ylides reported in the literature. The single crystal XRD structure of $\text{Ph}_2\text{P}(\text{CH}_2)_2\text{Li}$ has been determined⁵³ and found to perform the same activation of fenchone⁵⁴ (Scheme 1.6).

However, as previously mentioned, lithium salts are known to have a marked effect on the stereochemistry when present in Wittig reactions. Ester ylides (stabilised) and aldehydes react to form an approximate *E/Z* ratio of 94:6 in 'lithium salt free' conditions, whilst it is a 78:22 ratio with a lithium halide present.

⁵¹ T. Jenny, B. Schaub and M. Schlosser, *Tetrahedron. Lett.*, 25, 4097 (1984); B. Schaub and M. Schlosser, *Tetrahedron. Lett.*, 26, 1623 (1985).

⁵² H. Grützmacher, L. Ksolnai, H. Pritzkow and M. Steiner, *J. Chem. Soc., Chem. Commun.*, 285 (1998).

⁵³ M. A. Bruck, R. E. Cramer and J. W. Gilje, *Organometallics.*, 5, 1497 (1986).

⁵⁴ H.-J. Cristau, *J. Organomet. Chem.*, 352, C47 (1988).

1.2.8 Co-ordination chemistry of phosphonium ylides

1.2.8.1. Main group metals

The vast amount of co-ordination chemistry known for phosphorus ylides is concerned with transition metal complexes. Recently, though examples of s-block metal and main group co-ordinated ylides have been isolated and characterised (Figure 1.12).^{52,55,56}

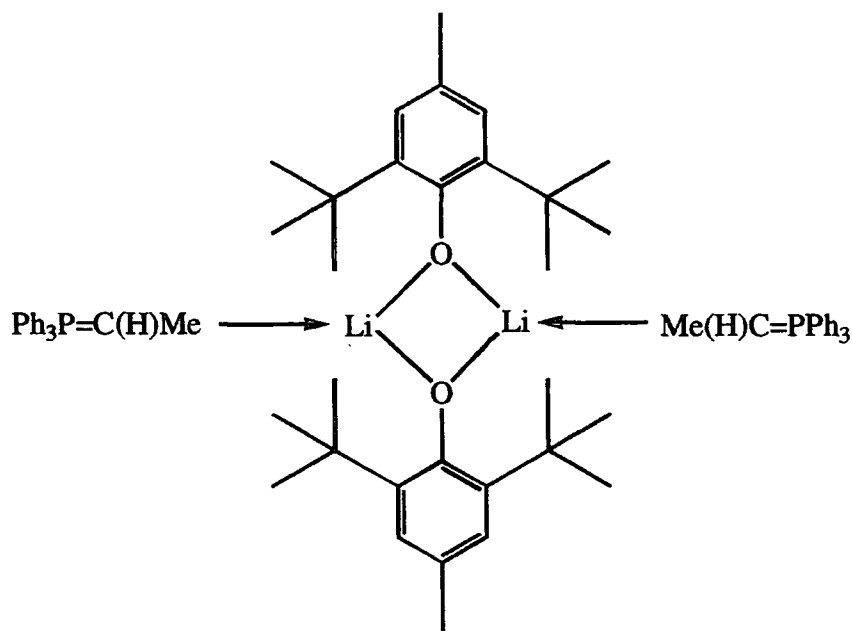


Figure 1.12 A phosphonium ylide lithium aryloxide complex

It is possible for metals to interact with the ylidic carbanion in two ways (Figure 1.13).

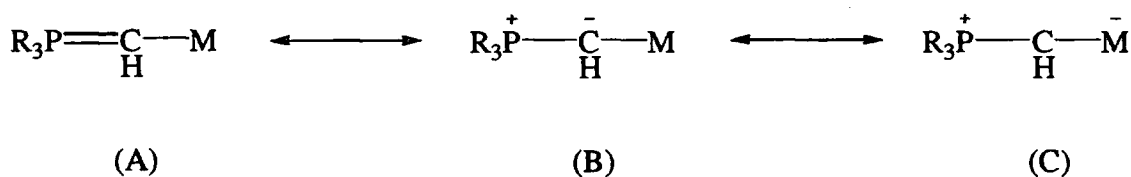


Figure 1.13 Interactions of metals with phosphonium ylides

⁵⁵ R. D. Price, *Ph.D. Thesis*, University of Durham (1999).

⁵⁶ D. R. Armstrong, M. G. Davidson and D. Moncrieff, *Angew. Chem., Int. Ed. Engl.*, **34**, 478 (1995).

(1). Metals which have σ -acceptor properties can increase the electron-density at the ylidic carbon (B) thereby increasing its nucleophilicity and leading to increased reactivity e.g. Ph_3PCHLi .⁵¹

(2). Main group metals with suitable acceptor orbitals, such as metals of the silicon group, can interact with the filled carbon centred p-orbitals of the ylide (C). This results in a M-C bond and subsequent π -back donation, leading to decreased electron density on the ylide carbon and reduced ylide nucleophilicity. The greater the π -acceptor capacity of the metal, the more stabilised the ylidic carbanion and the more likely the formation of oligomeric complexes.

The overall contribution from these two opposing effects is dependent on both the ligands and the metal centre itself.⁵⁷

1.2.8.2. Transition metals

Complexes of ylides with most of the transition metals are known (see chapter 14 of reference 5), all with diverse structures dependent on the metal and the particular ylide used. Transition metals possessing a high π -acceptor capacity have the ability to stabilise ylidic carbanions and due to their natural desire for high co-ordination numbers tend to form dimers and higher oligomers with ylides.

The reactions of Cu^{I} , Ag^{I} and Au^{I} (Group 1b metals) compounds with phosphonium ylides proceed in a 2:1 ratio resulting in complexes that are particularly stable to hydrolysis, oxidation and heat (**Scheme 1.7**).^{58,59,60,61,62}

⁵⁷ O. I. Kolodiaznyi, 'Phosphorus Ylides', Wiley-VCH, Weinheim and New York, (1999) and references cited therein.

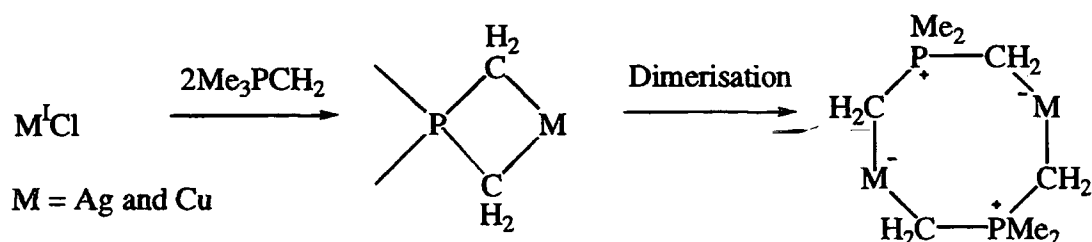
⁵⁸ R. Franke and H. Schmidbaur, *Chem. Ber.*, **108**, 1321 (1975).

⁵⁹ R. Franke and H. Schmidbaur, *Angew. Chem.*, **85**, 449 (1973).

⁶⁰ H. Schmidbaur and Y. Yamamoto, *J. Organomet. Chem.*, **96**, 133 (1975).

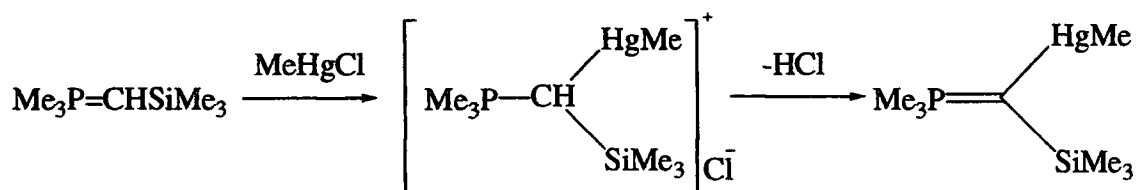
⁶¹ H. Schmidbaur and Y. Yamamoto, *J. Organomet. Chem.*, **97**, 479 (1975).

⁶² Y. Yamamoto, *Chem. Lett.*, **11**, 311 (1980).



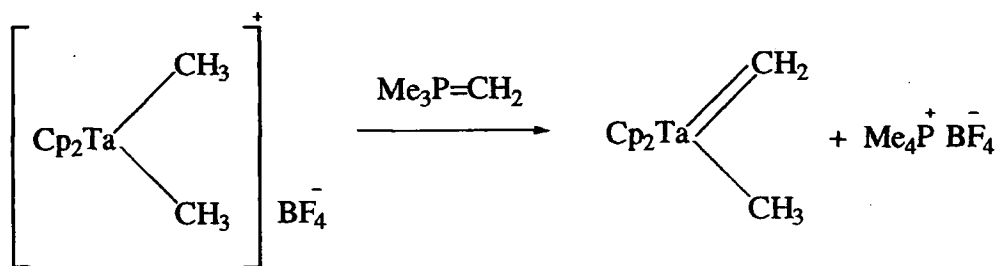
Scheme 1.7 Co-ordination of group 1b metals to phosphonium ylides

Mercury compounds, due to their tendency to form σ -bonds with a low co-ordination number for the metal centre, give non-associated monomeric complexes, co-ordinated via the α -carbon (Scheme 1.8).⁶³



Scheme 1.8 Co-ordination of mercury compounds to phosphonium ylides

A chemical analogy between group V transition metal complexes and main group V ylides became apparent when ylides were used to synthesise the first coordinated alkylidene by the deprotonation of the coordinated alkyl group (Scheme 1.9).⁶⁴

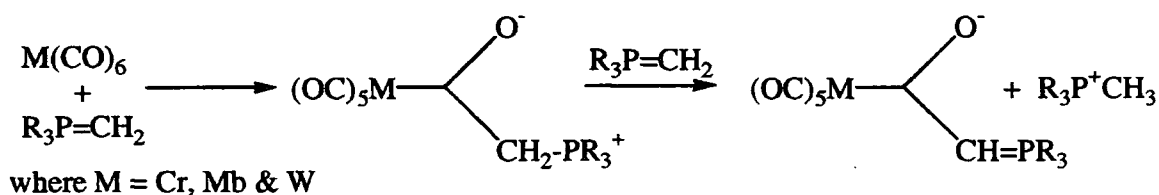


Scheme 1.9 Formation of alkylidenes via phosphonium ylides

⁶³ R. H. Rothlein and H. Schmidbaur, *Chem. Ber.*, **107**, 102 (1974).

⁶⁴ R. R. Schrock and P. R. Sharp, *J. Am. Chem. Soc.*, **100**, 2389 (1978); R. R. Schrock, *Acc. Chem. Res.*, **12**, 98 (1979).

Phosphonium ylides that do not contain electron withdrawing groups in the alkylidene moiety are nucleophilic enough to add across the carbonyl group of $M(CO)_6$ complexes (Scheme 1.10).⁶⁵



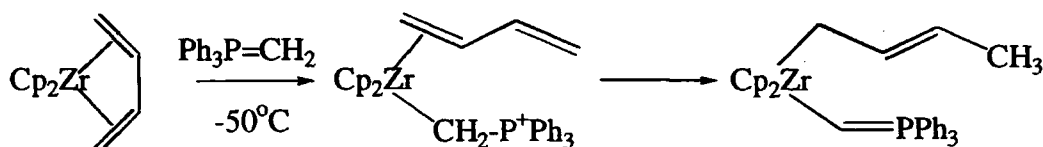
Scheme 1.10 Nucleophilic addition of a phosphonium ylide to a carbonyl group

However, in some cases ylides do not add to the carbonyl group of metal carbonyls, but effect substitution reactions instead (Scheme 1.11).



Scheme 1.11 Substitution of a bromine for a phosphonium ylide

Erker⁶⁶ has observed the displacement of butadiene from a divalent zirconocene complex, in much the same way as a trivalent phosphine is displaced to form an alkylidene. This has potential uses in catalysis (Scheme 1.12) ;



Scheme 1.12 Displacement of butadiene by a phosphonium ylide

⁶⁵ W. C. Kaska, W. D. Korte, K. D. Mitchell and R. F. Reichelderfer, *J. Am. Chem. Soc.*, **96**, 2847 (1974); C. Creaser and W. C. Kaska, *Transition. Met. Chem.*, **3**, 360 (1978); H. Blah, W. Malisch and S. Voran, *Angew. Chem., Int. Ed. Engl.*, **31**, 850 (1992).

⁶⁶ P. Czisch, G. Erker and R. Mynott, *Z. Naturforsch.*, **405**, 1177 (1985).

1.2.8.3. Lanthanides and Actinides

There are very few reported complexes of phosphonium ylides with the lanthanides in the literature, with only one structurally characterised reported samarium complex known (Figure 1.14).⁶⁷

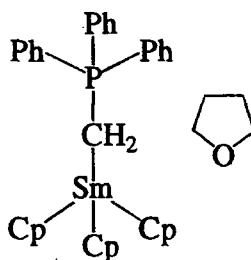
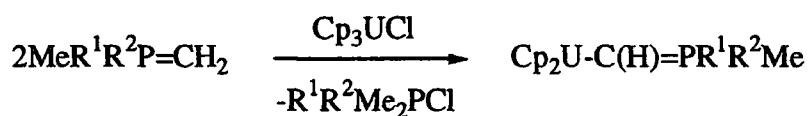


Figure 1.14 Samarium-phosphonium ylide complex

The co-ordination of phosphonium ylides to actinide metals is also possible. There is a handful of reported complexes in the literature most of which contain uranium (Scheme 1.13);



where $\text{R}^1 = \text{Me}$, $\text{R}^2 = \text{Ph}$ ^{68,69}

& $\text{R}^1 = \text{Me}$, $\text{R}^2 = \text{Me}$ ^{70,71}

Scheme 1.13 Formation of uranium-phosphonium ylide complexes

⁶⁷ J. Guan, J. Ren, Q. Shen, W-K. Wong, W-T. Wong, *Polyhedron.*, **12**, 2749 (1993).

⁶⁸ R. E. Cramer, J. W. Gilje, R. B. Maynard and J. C. Paw, *J. Am. Chem. Soc.*, **103**, 3589 (1981).

⁶⁹ R. E. Cramer, J. W. Gilje, R. B. Maynard and J. C. Paw, *Organometallics.*, **2**, 1336 (1983).

⁷⁰ D. Afzal, M. A. Bruck, R. E. Cramer, F. Edelmann, J. W. Gilje and H. Schmidbaur, *Chem. Ber.*, **121**, 417 (1988).

⁷¹ D. Afzal, R. Bau, R. E. Cramer, J. W. Gilje, T. F. Koetzle and R. C. Stevens, *Organometallics.*, **9**, 694 (1990).

1.3 Iminophosphoranes

1.3.1 Background

Iminophosphoranes or phosphinimines, are compounds of the general structure $R_3P=NR'$. They are isoelectronic with ylides and exhibit broadly similar chemistry. As with the analogous phosphorus-carbon bond in ylides, iminophosphoranes can be considered essentially to contain a single phosphorus-nitrogen bond with a degree of electronic delocalisation (Figure 1.15).



Figure 1.15 Two resonance canonical forms of an iminophosphorane

The phosphorus-nitrogen bond is considerably less dipolar in character, and has greater delocalisation of electron density from the nitrogen to the phosphorus than is seen from the carbon to the phosphorus in the corresponding ylide bond. This is believed to be the reason why iminophosphoranes are more air and moisture stable than the corresponding ylides.

Iminophosphoranes were first reported in 1919 by Staudinger et al.,⁷² but investigations into these compounds only began in the late 1950s. They are basic compounds with nitrogen being the site of attack⁷² - $[(Me_2N)_3P=N]_3P=NBu^t$, for example being the strongest known neutral base.⁷³ They have found much use in organic synthesis,⁷⁴ most importantly in the formation of C-N bonds via the aza-Wittig reaction.

⁷² R. Bau and R. D. Wilson, *J. Am. Chem. Soc.*, **96**, 7601 (1974)

⁷³ H. Schlemper and R. Schwesinger, *Angew. Chem., Int. Ed. Engl.*, **26**, 1167 (1987); R. Link and R. Schwesinger, *Angew. Chem., Int. Ed. Engl.*, **31**, 850 (1992).

⁷⁴ Ref 5 (Chp.13) and references cited therein; H-J. Cristau, *Chem. Rev.*, **94**, 1299 (1994).

1.3.2 Structure and bonding

The bonding in iminophosphoranes is analogous to that in ylides due to the isolobality of the frontier orbitals of the CH_2 and NH moieties (Figure 1.16).²⁵

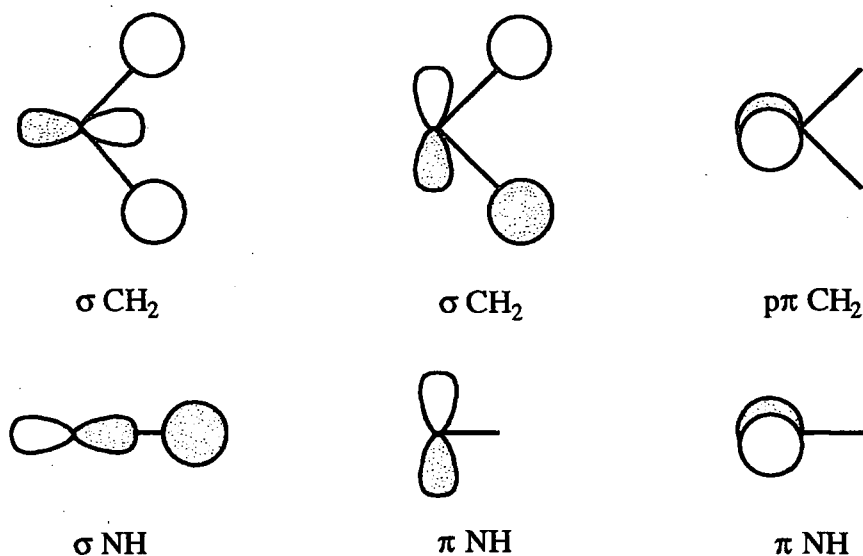


Figure 1.16 Isolobality of frontier orbitals in CH_2 and NH moieties

As with ylides the bonding may again be described using the following different models: either $d\pi$ - $p\pi$ bonding due to back donation from the two singly occupied $2p$ orbitals on nitrogen into a vacant $3d$ orbital on phosphorus, by electrostatic shortening,⁶ or by the most widely accepted model that describes the bonding in terms of negative hyperconjugation (c.f. ylides). This again involves π - σ^* donation which in the case of iminophosphoranes has the possibilities shown by the theoretical iminophosphorane H_3PNH (Figure 1.17).²⁵

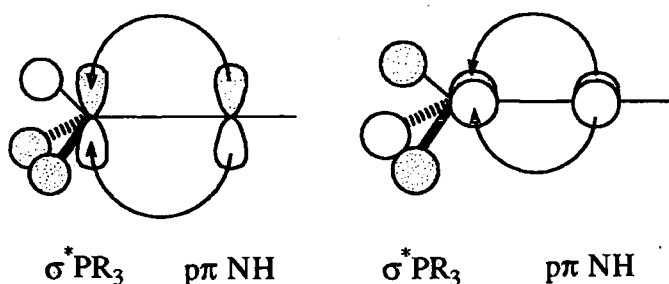


Figure 1.17 Negative hyperconjugation in iminophosphoranes

Considering the molecular geometry of an iminophosphorane (**Figure 1.18**), it can be seen that it is based around a tetrahedral phosphorus environment bound to a trigonal nitrogen.

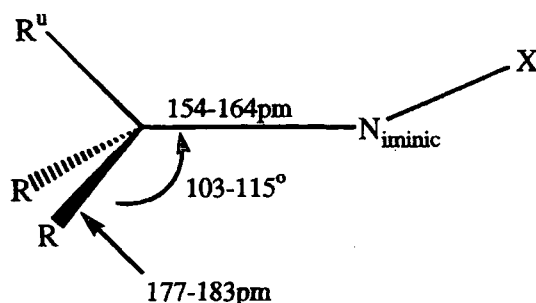


Figure 1.18 Molecular geometry of an iminophosphorane

The P-N_{iminic} bond is considered to be almost a double bond, the range of known lengths (1.54-1.64 Å) comparing well with the sum of the covalent radii for a P-N double bond.⁷⁵ It is worth noting at this point that the reported P-N bond lengths for the following aminophosphonium cations Ph₂(PhCH₂)P⁺NEt₂, Ph₃P⁺NH₂ and Ph₃P⁺(NHC₁₀H₇) are 1.63,⁷⁶ 1.615⁷⁷ and 1.63 Å⁷⁸ respectively, which are all in the range expected for iminophosphoranes. This would suggest that the major shortening of the P-N bond occurs upon quaternisation of the phosphorus atom with only a very small further shortening of the bond occurring upon formation of the imine. It is postulated that this may be due to the overlap of the nitrogen's lone pair with a suitable phosphorus acceptor orbital.

The existence of a unique phosphorus substituent R^u, again a feature seen in phosphonium ylides (**Figure 1.2**), is caused by the interaction between the π orbital on the nitrogen and the unique σ^* orbital of the R₃P. Consequently the P-R^u bond vector is more elongated and has a wider NPR^u angle than the other two P-R vectors.

⁷⁵ L. Pauling, *The Nature of the Chemical Bond*, 3rd Ed., Cornell University Press, Ithaca, NY, pp224&228 (1960).

⁷⁶ J. C. J. Bart, I. W. Bassi and M. Calcaterra, *Acta Cryst.*, **38B**, 1932 (1982).

⁷⁷ M. B. Hursthouse, N. P. C. Walker, C. P. Warrens and J. D. Woolins, *J. Chem. Soc., Dalton Trans.*, 1043 (1985).

⁷⁸ M. Alajarin, J. Elguero, C. Foces-Foces, A. L. Llamas-Saiz, P. Molina and A. Vidal, *J. Chem. Soc., Perkin Trans 2.*, 1667 (1991).

Theoretical calculations and ^{31}P NMR spectroscopy have been utilised to study the ease of rotation about the $\text{P-N}_{\text{imino}}$ bond. A barrier to rotation of approximately 2kcal mol^{-1} has been calculated for $\text{Ph}_3\text{P}=\text{NCH}=\text{CH}_2$,⁷⁹ and whilst larger than was seen for phosphonium ylides^{19,20} due to a greater degree of electronic delocalisation, is still low enough to suggest that rotation could occur. NMR studies of $\text{Ph}_3\text{P}=\text{NPh}$ produced only one set of resonances indicating rapid rotation about the $\text{P-N}_{\text{imino}}$ bond.⁸⁰

1.3.3 Preparation of Iminophosphoranes

Iminophosphoranes have been prepared by two different approaches, the direct union of nitrogen and phosphorus fragments, or the indirect approach of substitution of a simple (previously prepared) iminophosphorane.

The Staudinger² reaction uses the first approach of direct combination and is the nucleophilic attack of the phosphorus atom of a tertiary phosphine on the terminal nitrogen atom of an azide. It proceeds through a 4-centred transition state to yield a linear phosphazide, which then loses nitrogen gas to generate the iminophosphorane (**Scheme 1.14**).



Scheme 1.14 The Staudinger reaction

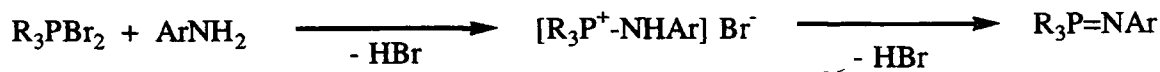
Due to the explosive nature of azides, a safer method of producing iminophosphoranes was developed and is based on a principle used by Kirsanov in 1950.⁸¹ Horner et al⁸² found that conversion of triphenylphosphine to its dibromide in solution, followed by reaction with an arylamine, in the presence of two equivalents of triethylamine gave high yields of N-aryliminophosphoranes (**Scheme 1.15**).

⁷⁹ J. Bragin, S. Chan, H. Goldwhite and E. Mazzola, *J. Phys. Chem.*, **77**, 1506 (1973).

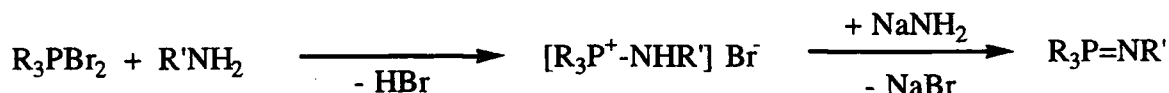
⁸⁰ T. A. Albright, W. J. Freeman and E. E. Schweizer, *J. Org. Chem.*, **41**, 2716 (1976).

⁸¹ A. V. Kirsanov, *Isv. Akad. Nauk. SSSR.*, 426 (1950); *Chem. Abstr.*, **45**, 1503 (1951); *Zh. Obshch. Khim.*, **22**, 269 (1952); *Chem. Abstr.*, **46**, 11135 (1952).

⁸² L. Horner and H. Oedingen, *Liebigs Ann. Chem.*, **627**, 142 (1959).

**Scheme 1.15 Kirsanov reaction using arylamines**

Singh and Zimmer⁸³ later applied the same process to aliphatic amines, but found that the reaction stopped at the salt. However, separate deprotonation with a strong base such as sodamide produced the required imine (Scheme 1.16).

**Scheme 1.16 Kirsanov reaction using aliphatic amines**

There are other reported syntheses of iminophosphoranes, but as with certain syntheses of phosphonium ylides, they are very specific and not used generally e.g. the reaction of chloroamines or azocarboxylates⁷⁴ with tertiary phosphines.

1.3.4 Reactions of iminophosphoranes

Analogous to phosphonium ylides, iminophosphoranes undergo hydrolysis to form amines and phosphine oxides. The driving force behind this reaction is again the formation of a phosphorus-oxygen bond. The nitrogen atom in place of the carbon means that iminophosphoranes are inherently more stable and less prone to hydrolysis, as can be seen in the higher reactivity of triphenylphosphonium methyllide with respect to triphenyliminophosphorane. Aryl iminophosphoranes are the most resilient being stable to air and often water, but readily hydrolysed in dilute acid/base conditions.

Iminophosphoranes can undergo both oxidation and reduction reactions, as is the case with the analogous ylides. Imines with more electron-withdrawing substituents, such as

⁸³ G. Singh and H. Zimmer, *J. Org. Chem.*, **28**, 483 (1963).

carbonyl or sulphonyl groups are more difficult to oxidise, again reflecting their greater stability over ylides.

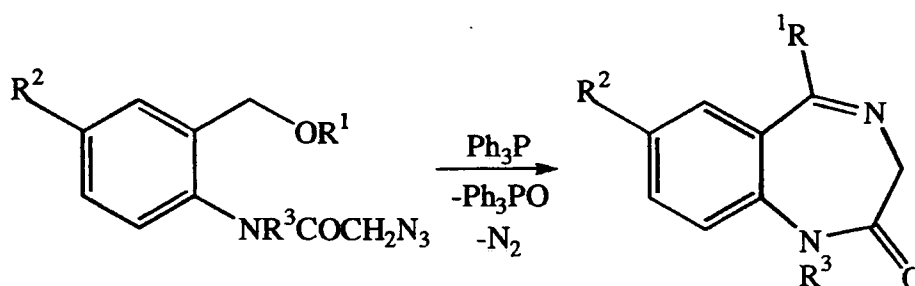
However, as with the Wittig reaction for ylides, the most synthetically useful reaction of iminophosphoranes is called the aza-Wittig reaction.⁸⁴ Discovered by Staudinger, it is the reaction of aldehydes and ketones with iminophosphoranes (Scheme 1.17).



Scheme 1.17 The aza-Wittig reaction

Again, this reaction occurs under mild conditions in a neutral solvent, and in high yields. It is thought to proceed through the nucleophilic attack of the iminic nitrogen at the carbonyl carbon, although no evidence of any betaine or oxaphosphetane type intermediates has been seen.

Intramolecular aza-Wittig reactions imparting cyclisations have been reported (Scheme 1.18).⁸⁵



Scheme 1.18 Intramolecular aza-Wittig reaction

1.3.5 S-block metallated iminophosphoranes

The use of metallated iminophosphoranes in organic synthesis, particularly those containing s-block metals,^{86,87} has so far been much less studied than other aspects of the

⁸⁴ Ref 5 (Chp.13) p423.

⁸⁵ J. Ackrell, E. Galeazzi, J. M. Muchowski and L. Tokes, *Can. J. Chem.*, **57**, 2696 (1979).

chemistry of iminophosphoranes. As with the analogous phosphonium ylides, it is their potential for increased reactivity that is attracting much interest.

There are several s-block metallated iminophosphoranes reported in the literature containing neutral and anionic iminophosphorane moieties. The single crystal x-ray diffraction structures of $(\text{LiNPPH}_3)_6$ and $(\text{KNPPH}_3)_6$ have recently been reported (Figure 1.19).^{88,89}

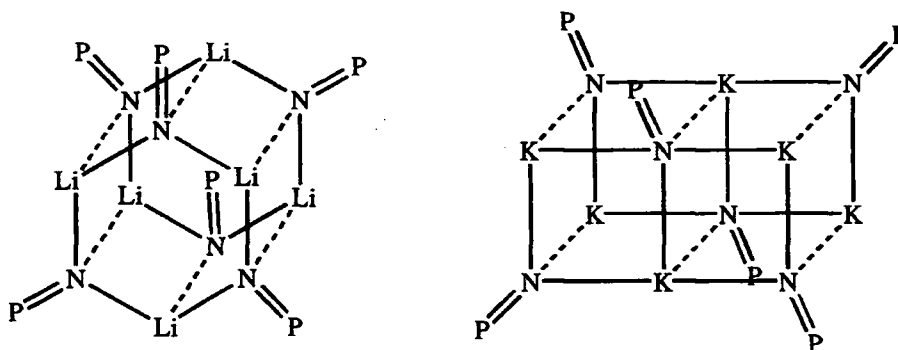


Figure 1.19 Structure of $(\text{LiNPPH}_3)_6$ and $(\text{KNPPH}_3)_6$ with the Ph_3 groups omitted for clarity

Other N-metallated structures have recently been determined in our group such as $\text{Ph}_3\text{PNLi} \cdot \text{LiBr} \cdot 2\text{thf}$ ⁹⁰ and $(\text{Me}_2\text{N})_3\text{PNLi}$.⁵⁵ The majority of the complexes in the literature involve co-ordination of an alkali metal to an iminophosphorane through both the iminic nitrogen and the carbanion bound to the phosphorus i.e. α -metallation (Figure 1.20)^{87,91,92}

⁸⁶ L. Chiche, H-J. Cristau, J. Kadoura and E. Toreilles, *Bull. Soc. Chim. Fr.*, **4**, 515 (1989).

⁸⁷ S. García-Granda, F. López-Ortiz, E. Paláez-Arango, E. Pérez-Carreño and B. Tejerina, *J. Am. Chem. Soc.*, **117**, 9972 (1995).

⁸⁸ S. Anfang, K. Dehnicke, G. Geisler, K. Harris, W. Massa and G. Seybert, *Z. Anorg. Allg. Chem.*, **624**, 1187 (1998).

⁸⁹ S. Chitsaz, K. Dehnicke and B. Neumuller, *Z. Anorg. Allg. Chem.*, **625**, 9 (1999).

⁹⁰ A. S. Batsanov, M. G. Davidson, J. A. K. Howard, S. Lamb, C. Lustig and R. D. Price., *J. Chem. Soc., Chem. Commun.*, 1211 (1997).

⁹¹ K. Dehnicke, A. Muller and B. Neumuller, *Chem. Ber.*, **129**, 253 (1996).

⁹² D. Stalke and A. Steiner, *Inorg. Chem.*, **32**, 1977 (1993).

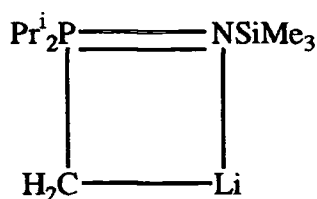


Figure 1.20 An α -lithiated iminophosphorane

Analogous complexes containing heavier alkali metals are known (Figure 1.21).⁹²

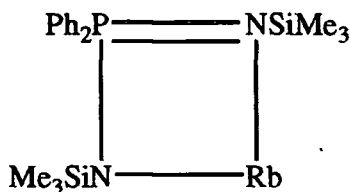


Figure 1.21 An example of a heavier alkali metal iminophosphorane complex

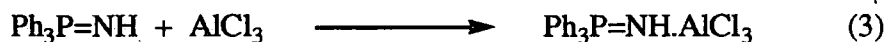
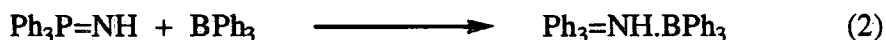
Group 2 (alkaline earth metal) iminophosphorane complexes are more scarce in the literature and a more thorough discussion of these complexes will be given in **Chapter 5** of this thesis.

1.3.6 Co-ordination chemistry of Iminophosphoranes

Early co-ordination complexes of iminophosphoranes were very poorly characterised and considered of little importance. Recently however, there has been much interest in this area with complexes finding use in catalysis for example $[(^t\text{Bu}_3\text{PN})_2\text{TiMe}_2]$.⁹³ With metals, iminophosphoranes can interact as neutral Lewis bases e.g. Ph_3PNH or as the counter anionic ligand Ph_3PN^- , which can act as a 1,2 or 4 electron donor and is isoelectronic with the analogous phosphine oxide ($\text{Ph}_3\text{P}=\text{O}$).

⁹³ S. J. Brown, X. Gao, F. Guérin, D. G. Harrison, L. Koch, R. E. v. H. Spence, D. W. Stephan, J. W. Swabey, Q. Wang, W. Xu and P. Zoricak, *Organometallics.*, **18**, 2046 (1999).

Iminophosphoranes are able to form 1:1 adducts with Lewis acids especially with boron halides (1),⁹⁴ boranes (2)⁹⁵ and Gp 3 metal alkyls/halides (3)⁹⁶ (Scheme 1.19).



Scheme 1.19 Iminophosphorane-Lewis acid adduct formation

Iminophosphorane complexes with transition metals are more widely known⁹⁷ and there are many different synthetic routes available to achieve these complexes. There are generally 3 modes of co-ordination by which the iminophosphorane (neutral or anionic) can bind to a metal centre (Figure 1.22).

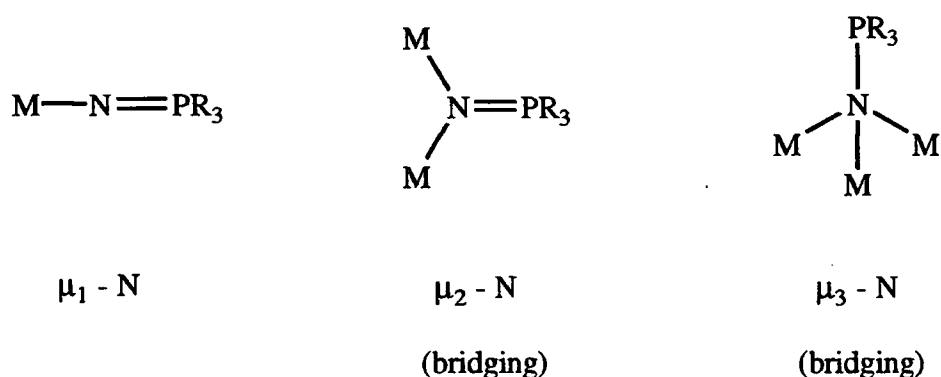


Figure 1.22 Different modes of co-ordination to a metal centre by Ph_3PN^-

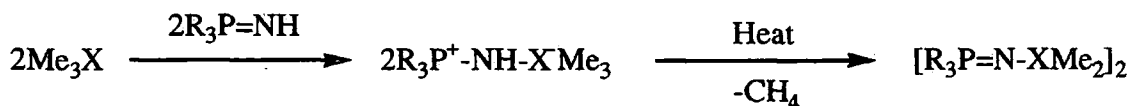
As with the corresponding phosphonium ylides, the mode of co-ordination depends upon the metal centre and the ligand substituents on the phosphorus. The reaction of Gp IIIb metal trialkyls with an unsubstituted imine afforded isolable complexes which upon heating evolved methane to form dimers (Scheme 1.20).⁹⁵

⁹⁴ E. W. Abel and S. A. Muckeljohn, *Phosphorus Sulphur*, **9**, 235 (1981).

⁹⁵ G. Jonas and H. Schmidbaur, *Angew. Chem.*, **6**, 449 (1967); *Chem. Ber.*, **101**, 1271 (1968).

⁹⁶ U. Kruger, G. Kuhn and H. Schmidbaur, *Angew. Chem.*, **4**, 877 (1965).

⁹⁷ K. Dehnicke, M. Krieger and W. Massa, *Coord. Chem. Rev.*, **182**, 19 (1999).

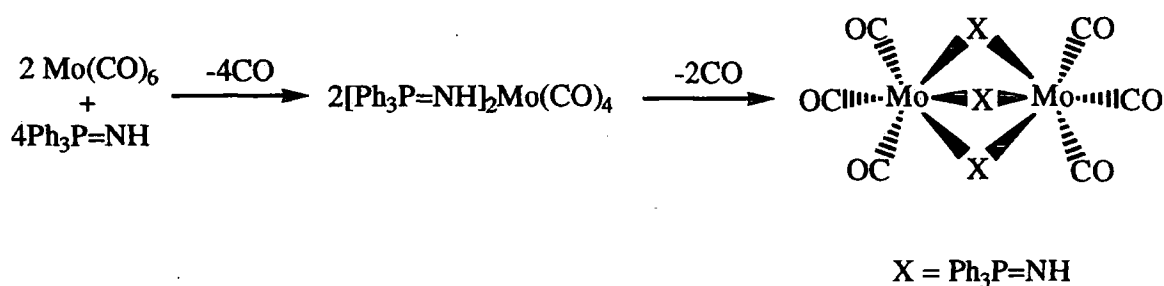


where X = Al, Ga & In

Scheme 1.20 Reaction of iminophosphoranes with group IIIb metal trialkyls

With nickel and cobalt dihalides, imines (X) formed monomeric complexes X_2MCl_2 containing tetrahedral metal atoms,^{98,99} whereas platinum and palladium formed square planar complexes.¹⁰⁰

A number of complexes have been formed by the reaction of metal carbonyls and iminophosphoranes (**Scheme 1.21**).^{101,102}



Scheme 1.21 Formation of a molybdenum carbonyl-iminophosphorane complex

Many more iminophosphorane complexes incorporating transition metals are known including manganese¹⁰³ and zinc.^{104,105}

⁹⁸ R. Appel and P. Z. Volz, *Anorg. Allg. Chem.*, **45**, 413 (1975).

⁹⁹ R. Appel and R. Schaaff, *Z. Naturforsch.*, **6b**, 405 (1961).

¹⁰⁰ J. F. Baeza, M. T. Chicote, F. J. Lahoz, J. A. Lopez and J. Vicente, *Inorg. Chem.*, **30**, 3617 (1991).

¹⁰¹ H. Bock and H. T. Dieck, *Z. Naturforsch.*, **21b**, 739 (1966).

¹⁰² K. G. Caulton, J. S. Miller and M. O. Visscher, *Inorg. Chem.*, **13**, 1632 (1974).

¹⁰³ M. A. Leeson, B. K. Nicholson and M. R. Olsen, *J. Organomet. Chem.*, **579**, 243 (1999).

¹⁰⁴ E. W. Abel and S. A. Mucklejohn, *Inorg. Chim. Acta.*, **37**, 107 (1979).

¹⁰⁵ H. Ackermann, K. Dehnicke, B. Neumuller and F. Weller, *Z. Anorg. Allg. Chem.*, **625**, 147 (1999).

1.4 Hydrogen Bonding

For many of the compounds and complexes detailed throughout this thesis the structural phenomenon of hydrogen bonding is important in determining their molecular structure, as has been previously noted in other phosphonium salts.¹⁰⁶ Hydrogen bonding was defined in 1940 by Pauling¹⁰⁷ as follows:

“It has been recognised in recent years that under certain conditions an atom of hydrogen is attracted by rather strong forces to two atoms, instead of only one, so that it may be considered to be acting as a bond between them. This is called the hydrogen bond. It is not recognised that [...] the hydrogen bond is largely ionic in character, and is formed only between the most electronegative atoms [...]. Although the hydrogen bond is not a strong bond [...] it has great significance in determining the properties of substances”.

With the discoveries made since 1940, it is now recognised that a hydrogen bond cannot simply be defined in terms of the elements which are involved in it. Certain elements such as the most electronegative ones e.g. F or O exhibit a higher propensity to form these bonds. These were amongst the earliest recognised and hence referred to by Pauling. Although there is no one definitive description of a hydrogen bond it is generally regarded as a weak association occurring between atoms, molecules or ions (positive or negative) in the gas, liquid or solid state, where an interaction between a donor D-H and an acceptor A specifically involves the H atom. This interaction is predominantly an electrostatic one between the centre of high electron density of A (e.g. a lone pair) and the positive end of the polar covalent bond $D^{\delta-}-H^{\delta+}$. The accepted notation is D-H...A, for which the term ‘hydrogen bond’ is used and it refers to the H...A interaction. The distance $r(D-H)$ is shorter than the $r(H...A)$ distance assuming this description. Hydrogen bonds may be classed as simple (which involves just one acceptor and one donor) or three centred, four centred etc (Figure 1.23).

¹⁰⁶ M. G. Davidson and S. Lamb, *Polyhedron.*, **16**, 4393 (1997).

¹⁰⁷ L. Pauling, *The Nature of the Chemical Bond and the Structure of Molecules and Crystals – An Introduction to Modern Structural Chemistry.* 2nd Edn, Oxford University Press, London (1940).

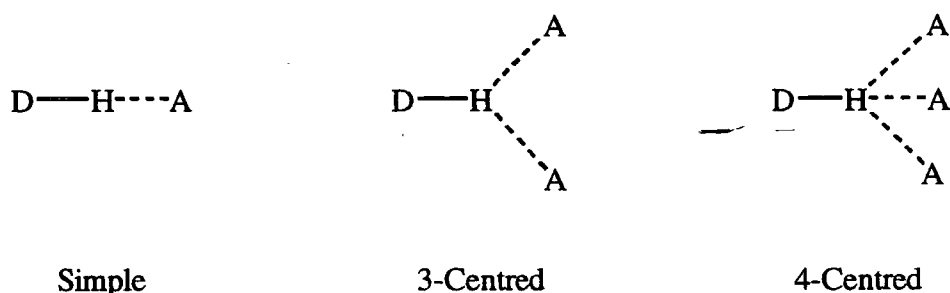


Figure 1.23 Different classifications of a hydrogen bond

Further to the above description, it is also widely accepted that not all hydrogen bonds have this in character. In some hydrogen bonds it is clear that the proton is not bonded covalently to either the donor or acceptor but is equally attracted to both. Referred to as ‘strong’ or ‘very strong’ hydrogen bonds the name refers to the whole system and is written as $D \dots H \dots A$ or $D-H-A$.¹⁰⁸ More recently there has been agreement in the literature¹⁰⁹ that weaker $C-H \dots O$ interactions such as those involved in acidic $C-H$ groups also warrant the label hydrogen bonds. This was not always the case as despite the wide range of experimental and theoretical work supporting their existence, the concept of ‘weak’ hydrogen bonds has been repeatedly questioned. As early as the 1960’s Sutor had concluded that weak hydrogen bonds existed in caffeine, theophylline and other related compounds^{110,111} but his work was disregarded by Donohue,¹¹² who claimed in his book that they did not exist.

Crystal structures of molecules are mediated by intermolecular interactions such as hydrogen bonding. $C-H \dots X$ ($X = O, N, Cl$ and S) hydrogen bonds are relatively long with definite orientations directed by electrostatic interactions, however the ‘weaker’ bonds such as $C-H \dots O$ can be easily bent if steric hindrance or competition with other stronger hydrogen bonding groups plays a part.

¹⁰⁸ J. Emsley, *Chem. Soc. Rev.*, **9**, 91 (1980).

¹⁰⁹ R. Taylor and O. Kennard, *J. Am. Chem. Soc.*, **104**, 5063 (1982).

¹¹⁰ D. J. Sutor, *Nature.*, **68**, 195 (1962).

¹¹¹ D. J. Sutor, *J. Chem. Soc.*, 1105 (1963).

¹¹² J. Donohue, ‘*Structural Chemistry and Molecular Biology*’, W.H.Freeman, San Francisco, 459 (1968).

2. General Experimental Techniques

2.1 Inert Atmosphere Techniques

Due to the hygroscopic and air-sensitive nature of the compounds and complexes studied in this work, it was necessary to undertake all reactions and subsequent analysis using inert atmosphere techniques. Syntheses were therefore carried out using standard vacuum line techniques¹ (Figure 2.1), under an atmosphere of dry argon or nitrogen from a manifold supply. Pre-dried, and where required degassed² solvents were used at all times, along with pre-dried starting materials when necessary.

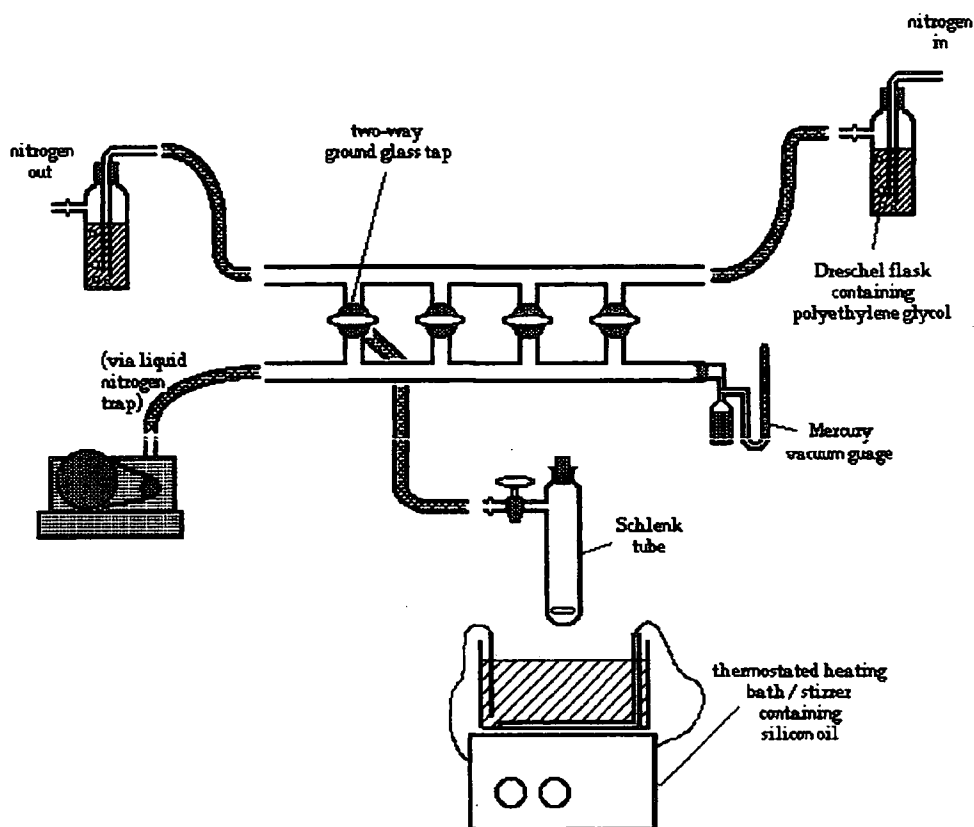


Figure 2.1 Schematic representation of a vacuum line

¹ D. F. Schriver and M. A. Drezdon, *The Manipulation of Air Sensitive Compounds*, 2nd Edn., Wiley, New York (1986).

² Using standard freeze-thaw procedures where appropriate, bubbling argon/nitrogen through the solvent for those where it was not.

Reactions were carried out in Schlenk tubes (or different vessels depending on volume required), dried in a hot (@130°C) oven, evacuated to 10^{-2} Torr three times and flushed with dry argon or nitrogen from the manifold supply after each evacuation. Solids were pre-weighed in a dry, oxygen free glovebox (Figure 2.2) either into an airtight sample bottle (then being introduced to the reaction vessel under a positive pressure of inert gas) or directly into the reaction vessel itself. Hygroscopic and air-sensitive liquid reagents and solvents were introduced by a dry syringe.

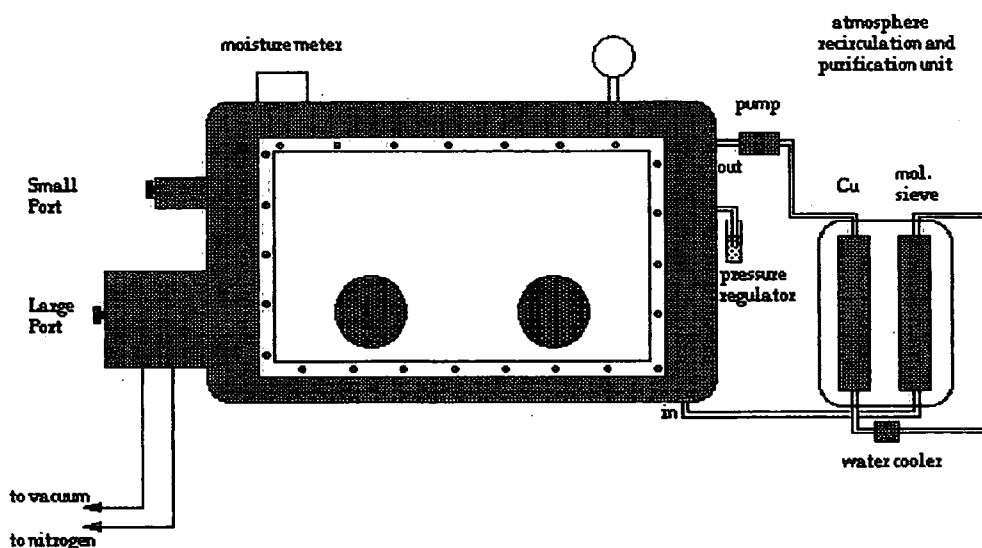


Figure 2.2 Schematic representation of a glove box.

Products were isolated from the reaction vessels using filter sticks of varying porosities. These had previously been evacuated and flushed with inert gas via attachment to the vacuum line. Attachment to the reaction vessel and inversion allowed the separation of the product from the mother liquor, then removal of the reaction vessel followed by drying of the product *in vacuo* allowed the subsequent isolation of the product in the glove box.

Introduction of products into the glove box was via one of its two ports, which are evacuated and flushed with inert gas at least three times to maintain the inert atmosphere inside the glove box. The moisture and oxygen levels are monitored by meters and maintained by a recirculation system which uses a copper catalyst (BASF Cu catalyst R11) at 200°C to remove oxygen as copper oxide and molecular sieves (BDH 3,16") to

remove moisture. Typical acceptable levels are moisture levels between 2 and 4ppm and oxygen levels kept below 10ppm.

When the oxygen and moisture levels become too high the purification columns have to be regenerated. To do this, the copper column is heated to 180°C and reforming gas (80% N₂, 20% H₂) passed through the column. The molecular sieve column is heated and evacuated using a rotary pump, the steam removed being condensed into a cold trap.

2.2 Starting Materials and Solvents

Starting materials were of the highest quality available or were purified upon arrival. Solvents used (e.g. hexane, toluene, thf, diethyl ether, acetonitrile, chloroform and benzene) were freshly distilled over the appropriate drying agents under a nitrogen atmosphere. Deuterated solvents, for use in NMR spectroscopy, were stored in the glove box over molecular sieves or supplied in glass ampoules, which were subsequently opened in a glove box as required.

Hygroscopic and air-sensitive reagents such as n-butyllithium and benzylmagnesium chloride, were purchased as standard solutions in Sure-SealTM bottles and manipulated using standard inert atmosphere techniques. Certain starting materials [e.g. tris(dimethylamino)iminophosphorane] were stored over the appropriate grade of molecular sieve (4A or 13X), since they could not be purchased as anhydrous liquids.

2.3 Melting Point Determination

Melting points were determined by Differential Scanning Calorimetry (DSC) using a Mettler FP80 control unit coupled to a Mettler FP85 thermal analysis cell, or a Mettler Toledo TC15 TA controller coupled to a Mettler DSC 25 thermal analysis cell run by a Dell P.C. DSC capsules were prepared in the glove box by loading between 5 and 10mg of sample into an aluminium capsule, which was then sealed and placed in the furnace, which itself is under a nitrogen atmosphere.

Some of the melting points were determined by an Electrothermal 9200 melting point determination machine using glass tubes prepared and sealed in the glove box under an inert atmosphere.

2.4 Infra-Red Spectroscopy (IR)

The IR spectra of isolated products were obtained as nujol mulls on NaCl plates using a Perkin Elmer 1720x Fourier Transform spectrometer. These were prepared, where necessary in a glove box with the nujol mull stored over molecular sieves. The spectra were run as soon as the sample was removed from the glove box. In some cases the plates were then separated to expose the mull to air, and then another spectrum was recorded to observe the effect of air and moisture on the compound.

2.5 Nuclear Magnetic Resonance Spectroscopy (NMR)

The presence of phosphorus in most of the complexes synthesised has facilitated the use of ^{31}P NMR, as well as ^1H and ^{13}C NMR studies. Samples were prepared by dissolving approximately 5mg of product in a deuterated solvent (most commonly CDCl_3 or C_6D_6 , see Chapter 3).

Standard ^1H NMR studies were performed at 200MHz on a Varian Mercury 200 or Varian VXR 200, at 250MHz on the Bruker AC 250 spectrometer or at 400MHz on a Varian 400. All chemical shifts (δ) are reported relative to TMS; all coupling constants are quoted in Hz.

^{31}P NMR spectroscopy was proton decoupled unless otherwise stated and performed at 81MHz using a Varian Mercury 200, at 101 MHz using a Bruker AC 250 spectrometer or at 162MHz using a Varian 400. All chemical shifts (δ) reported are relative to 85% H_3PO_4 , and all coupling constants are quoted in Hz.

^{13}C NMR spectroscopy was performed at 101MHz using a Varian Mercury 200. All chemical shifts (δ) are reported relative to TMS, and all coupling constants are quoted in Hz.

^1H - ^1H COSY and phosphorus decoupled ^1H spectra were carried out by the Durham University High Field NMR Service.

2.6 Elemental Analysis

Carbon, hydrogen and nitrogen content (% by mass) were determined for all fully characterized products. They were prepared in the glove box, with samples for CHN analysis containing between 1-2 mg of compound sealed in an aluminium capsule.

2.7 X-Ray Diffraction Studies

The most important analysis of a solid state structure involves X-ray diffraction studies. This technique requires single crystals no smaller in dimension than $0.1 \times 0.1 \times 0.1 \text{ mm}^3$ and no larger than $0.5 \times 0.5 \times 0.5 \text{ mm}^3$. Crystals were grown under an inert atmosphere in a Schlenk tube at temperatures from room temperature ($+25^\circ\text{C}$), through refrigerator ($+5^\circ\text{C}$), freezer (-18 or -30°C) and finally cold freezer (-80°C). Products were all characterised by IR and NMR spectroscopy before X-ray analysis was performed.

As the compounds and complexes are generally air and moisture sensitive, extreme care must be taken with the preparation of the crystals for diffraction study. The usual method is to coat the crystal with a perfluorinated ether oil that is inert to reaction, and is transparent to X-rays. The crystal is then mounted by gluing the crystal to the top of a glass fibre which is then attached to the goniometer head. Finally the oil is frozen by the introduction of cold nitrogen gas which fixes the orientation of the crystal and also prevents decomposition.

The data collection takes place at low temperatures (at 153K in Durham) in order to reduce lattice vibrations and the likelihood of decomposition. The data were collected on

Chapter 2 – General Experimental Techniques

a 3-circle diffractometer equipped with a Siemens CCD Area Detector using graphite monochromated Mo - K α radiation ($\lambda = 0.71073\text{\AA}$).

For structures where the data were collected at the University of Bath Chemistry Department, a Nonius Kappa diffractometer equipped with a CCD Area Detector using graphite monochromated Mo-K α radiation ($\lambda = 0.71069\text{\AA}$) was used at a collection temperature of 170K.

3. Experimental

This chapter details the preparation of all the starting materials, along with the synthesis of complexes formed in subsequent reactions. For the complexes where single crystal X-ray diffraction was possible the relevant information is discussed in the following chapters, accompanied by a condensed summary of the crystallographic data in Appendix A. This chapter is divided into five sections: the first details the synthesis of the starting materials **I-VIIa-c**, and the next four with the preparation of complexes **1-50** separated according to their respective discussion chapters, see **Table 3.1**.

Unless otherwise stated, all syntheses were carried out using inert atmosphere techniques, using either a nitrogen or an argon gas supply. All subsequent products were then isolated and stored in an argon filled glove box.

Chapter 3 - Experimental

Number Used In Text	Empirical Formula	Discussion Chapter
I	Ph_3PCH_2	-
II	$(\text{Me}_2\text{N})_3\text{PCH}_2$	-
III	Ph_3PNH	-
IV	$(\text{Me}_2\text{N})_3\text{PNH}$	-
V	$(\text{Ph}_2\text{PS})_2\text{NH}$	-
VI	Ph_3PO	-
VIIa-c	$\text{M}[\text{N}(\text{SiMe}_3)_2]_2$ where M = Ca, Sr & Ba for a, b & c respectively.	-
1	$(\text{Ph}_3\text{PCH}_2)_2 \cdot \text{Ca}[\text{N}(\text{SiMe}_3)_2]_2$	4
2	$(\text{Ph}_3\text{PCH}_2)_2 \cdot \text{Sr}[\text{N}(\text{SiMe}_3)_2]_2$	4
3	$(\text{Ph}_3\text{PCH}_2)_2 \cdot \text{Ba}[\text{N}(\text{SiMe}_3)_2]_2$	4
4	$[(\text{Me}_2\text{N})_3\text{PCH}_2]_2 \cdot \text{Ca}[\text{N}(\text{SiMe}_3)_2]_2$	4
5	$[(\text{Me}_2\text{N})_3\text{PCH}_2]_2 \cdot \text{Sr}[\text{N}(\text{SiMe}_3)_2]_2$	4
6	$(\text{Ph}_3\text{PCH}_2)_2 \cdot \text{Mg}\{\text{N}[\text{PPh}_2(\text{S})]_2\}_2$	4
7	$(\text{Ph}_3\text{PCH}_2)_2 \cdot \text{Ca}\{\text{N}[\text{PPh}_2(\text{S})]_2\}_2$	4
8	$(\text{Ph}_3\text{PCH}_2)_2 \cdot \text{Sr}[\text{OC}_6\text{H}_2(\text{Me})^t\text{Bu}_2]_2$	4
9	$(\text{Ph}_3\text{PNH})_2 \cdot \text{Ca}[\text{OC}_6\text{H}_2(\text{Me})^t\text{Bu}_2]_2$	5
10	$(\text{Ph}_3\text{PNH})_2 \cdot \text{Sr}[\text{OC}_6\text{H}_2(\text{Me})^t\text{Bu}_2]_2$	5
11	$(\text{Ph}_3\text{PNH})_2 \cdot \text{Ba}[\text{OC}_6\text{H}_2(\text{Me})^t\text{Bu}_2]_2$	5
12	$[(\text{Me}_2\text{N})_3\text{PNH}]_2 \cdot \text{Sr}[\text{OC}_6\text{H}_2(\text{Me})^t\text{Bu}_2]_2$	5
13	$(\text{Ph}_3\text{PNH})_2 \cdot \text{Sr}\{\text{N}[\text{PPh}_2(\text{S})]_2\}_2$	5
14	$(\text{Ph}_3\text{PNH})_2 \cdot \text{Sr}(\text{OCPh}_3)_2$	5
15	$(\text{Ph}_2\text{MePNH})_2 \cdot \text{Sr}[\text{OC}_6\text{H}_2(\text{Me})^t\text{Bu}_2]_2$	5
16	$(\text{Ph}_3\text{PO})_2 \cdot \text{Ca}[\text{N}(\text{SiMe}_3)_2]_2$	5
17	$(\text{Ph}_3\text{PO})_2 \cdot \text{Sr}[\text{N}(\text{SiMe}_3)_2]_2$	5
18	$(\text{Ph}_3\text{PO})_2 \cdot \text{Ba}[\text{N}(\text{SiMe}_3)_2]_2$	5
19	$(\text{Ph}_3\text{PO})_2 \cdot \text{Ca}[\text{OC}_6\text{H}_2(\text{Me})^t\text{Bu}_2]_2$	5
20	$(\text{Ph}_3\text{PO})_2 \cdot \text{Sr}[\text{OC}_6\text{H}_2(\text{Me})^t\text{Bu}_2]_2$	5
21	$(\text{Ph}_3\text{PO})_2 \cdot \text{Ba}[\text{OC}_6\text{H}_2(\text{Me})^t\text{Bu}_2]_2$	5
22	$\text{Ph}_3\text{PNH} \cdot \text{LiN}[\text{PPh}_2(\text{S})]_2$	6

Chapter 3 - Experimental

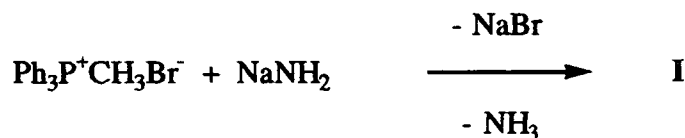
23	$(\text{Ph}_2\text{MePN}^-)_2\text{Li}_3[\text{OC}_6\text{H}_2(\text{Me})^t\text{Bu}_2]$	6
24	$\text{Ph}_2\text{MePNH}\cdot\text{LiOS}(\text{O})(\text{CF}_3)\text{NSO}_2\text{CF}_3$	6
25	$\text{Ph}_3\text{PNH}\cdot\text{LiOS}(\text{O})(\text{CF}_3)\text{NSO}_2\text{CF}_3$	6
26	$\text{TMEDA}\cdot\text{LiOS}(\text{O})(\text{CF}_3)\text{NSO}_2\text{CF}_3$	6
27	$\text{Ph}_2[\text{C}(\text{H})(\text{Ph})\text{CO}_2\text{Me}]\text{PNC}_2\text{O}_2\text{Me}$	6
28	$\text{Ph}_2(\text{o}-\text{C}_6\text{H}_4\text{OMe})\text{P}^+\text{CH}_3\text{Br}^-$	7
29	$\text{Ph}_2(\text{o}-\text{C}_6\text{H}_4\text{OMe})\text{P}^+\text{CH}_2\text{PhBr}^-$	7
30	$\text{Ph}_2(\text{o}-\text{C}_5\text{H}_5\text{N})\text{P}^+\text{CH}_2\text{PhBr}^-$	7
31	$\text{Ph}_2(\text{o}-\text{C}_6\text{H}_4\text{CH}_2\text{NMe}_2)\text{P}^+\text{CH}_2\text{PhBr}^-$	7
32	$[\text{C}_6\text{H}_4(\text{o}-\text{CH}_2\text{P}^+\text{Ph}_3\text{Br}^-)]_2$	7
33	$\text{Ph}_2\text{P}^+(\text{CH}_3\text{Br}^-)\text{C}_4\text{H}_8\text{P}^+(\text{CH}_3\text{Br}^-)\text{Ph}_2$	7
34	$\text{Ph}_2(\text{o}-\text{C}_6\text{H}_4\text{OMe})\text{PCH}_2$	7
35	$\text{Ph}_2(\text{o}-\text{C}_6\text{H}_4\text{OMe})\text{PCHPh}$	7
36	$\text{Ph}_2(\text{o}-\text{C}_5\text{H}_5\text{N})\text{PCHPh}$	7
37	$\text{Ph}_2(\text{o}-\text{C}_6\text{H}_4\text{CH}_2\text{NMe}_2)\text{PCHPh}$	7
38	$\text{Ph}_2\text{MePCHPh}$	7
39	Ph_3AsCHPh	7
40	$\{\text{C}_6\text{H}_4[\text{o}-\text{C}(\text{H})\text{PPh}_3]\}_2$	7
41	$\text{C}_6\text{H}_4[\text{C}(\text{H})\text{PPh}_3]_2$	7
42	$\text{Ph}_2\text{P}(\text{CH}_2)\text{C}_4\text{H}_8\text{P}(\text{CH}_2)\text{Ph}_2$	7
43	$\text{Ph}_3\text{P}(\text{H})\text{CC}_3\text{H}_6\text{C}(\text{H})\text{PPh}_3$	7
44	$\text{Ph}_2\text{P}^+(\text{CH}_2\text{Ph})\text{NH}_2\text{Br}^-$	7
45	Ph_2MePNH	7
46	Ph_2EtPNH	7
47	$\text{Ph}_3\text{PNH}_2^+\cdot\text{N}[\text{PPh}_2(\text{S})]_2$	7
48	$\text{Ph}_3\text{PCH}_2\cdot\text{HOCPh}_3$	7
49	$\text{Ph}_3\text{PNH}\cdot\text{HOCPh}_3$	7
50	$\text{Ph}_3\text{PO}\cdot\text{HOCPh}_3$	7

Table 3.1 List of compounds and complexes produced.

3.1 Preparation of Ligands I-VII.

Preparation of the ylides (I & II) was performed using the standard 'salt-free' method of preparation.¹ The phosphonium salt for the production of I was purchased from *Lancaster* and used as supplied, the salt for II was synthesized by the standard quaternisation reaction described in **Chapter 1**. The preparation of II was carried out according to the literature procedure.² The preparation of iminotriphenylphosphorane III was modified from syntheses found in the literature.^{3,4} Compound IV was purchased from *Fluka Synthesis* and stored over molecular sieve 13X. Compound V was prepared via a literature procedure.⁵ Compound VI was purchased from *Aldrich* and used as supplied. Compounds VIIa-c were produced according to the literature procedure.⁶

3.1.1 Preparation of Triphenylphosphonium methyllide (I).



Dry thf (150ml) was added to a round bottomed flask containing methyl(triphenyl)phosphonium bromide (35.6g, 100mmol) and sodium amide (4.2g, 108mmol) under an inert atmosphere. The resulting solution was stirred overnight affording a yellow solution after 24 hours. Filtration, to remove sodium bromide and any unreacted sodium amide followed, and the majority of the thf was removed *in vacuo* to leave a yellow slurry. This dissolved in approximately 80ml of hexane and 8ml of toluene with heating. On cooling to room temperature this yielded a crop of yellow crystals.

Yield : 12.9g (47%)

¹ R. Koster, D. Simic and M. Grassberger, *Liebigs Ann. Chem.*, **739**, 281 (1970); H. Schmidbaur, H. Stuhler and W. Vornberger, *Chem. Ber.*, **116**, 1393 (1972).

² H. J. Bestmann and S. Pfohl, *Justus Liebigs Ann. Chem.*, 1688 (1974).

³ H. Staudinger and J. Meyer, *Helv. Chim. Acta.*, **2**, 635 (1919); L. Bickofer and S. M. Kim, *Chem. Ber.*, **96**, 3099 (1963); H-J. Cristau, J. Kadoura, L. Chiche and E. Toreilles, *Bull. Soc. Chim. Fr.*, **4**, 515 (1989).

⁴ R. Appel and A. Hauss, *Chem. Ber.*, **93**, 405 (1960).

⁵ F. T. Wang, *Synth. React. Inorg. Met. Chem.*, **8**, 120 (1978).

⁶ M. Westerhausen, *Coord. Chem. Rev.*, **176**, pp157 – 210 (1998) and references cited therein.

Melting Point : 100°C

IR Spectrum : ν 2920cm⁻¹, 2850cm⁻¹ and 1460cm⁻¹ C-H stretches of the nujol mull,
 ν 880cm⁻¹ P-C stretch of ylide.

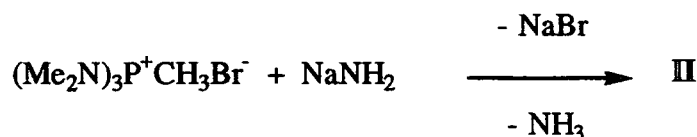
¹H NMR spectrum : 200MHz, solvent C₆D₆

δ (ppm)	Multiplicity	Integral	Coupling (Hz)	Assignment
0.9	doublet	2H	$^2J_{PH} = 7.6$	Ph ₃ PCH ₂
7.2 - 7.8	multiplet	15H	-	Ph ¹ Hs

³¹P NMR spectrum : 101.2MHz, solvent C₆D₆

δ (ppm)	Multiplicity	Assignment
20.7	singlet	Ph ₃ PCH ₂

3.1.2 Preparation of Tris(dimethylamino) phosphonium methyllide (II).



Dry thf (150mL) was added to a mixture of methyltris(dimethylamino)phosphonium bromide (24.3g, 100mmol) and sodium amide (4.2g, 108mmol) under an inert atmosphere. The solution was vigorously stirred at room temperature for 24 hours, before filtration to remove the solid residues. The solvent was removed *in vacuo* and the product distilled (39°C, 10⁻³ Torr).

Yield : 12.5g (75%)

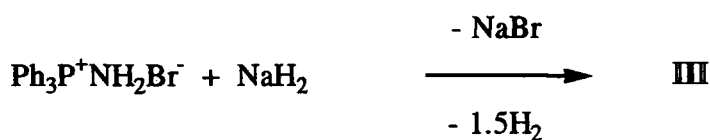
¹H NMR spectrum : 200 MHz, solvent C₆D₆

δ (ppm)	Multiplicity	Integral	Coupling (Hz)	Assignment
0.1	broad singlet	2H		(Me ₂ N) ₃ PCH ₂
2.4	doublet	18H	² J _{PH} = 8.8	(Me ₂ N) ₃ PCH ₂

³¹P NMR spectrum : 101.2 MHz, solvent C₆D₆

δ (ppm)	Multiplicity	Assignment
71.3	singlet	(Me ₂ N) ₃ PCH ₂

3.1.3 Preparation of Iminotriphenylphosphorane (III).



Dry toluene (15 mL) was added to amino(triphenyl)phosphonium bromide (17.9g, 50 mmol) and sodium hydride (2.0g, 50 mmol). Stirring of the solution at 100°C for 48 hours, was followed by filtration and reduction of the solvent *in vacuo* to approximately 10mL. Storage of this solution at -40°C for 24 hours yielded a crop of colourless crystals.

Yield : 10g (72%)

Melting point : 128°C

IR Spectrum: ν 1189 cm⁻¹ P-N stretch of imine

ν 3349 cm⁻¹ N-H stretch

¹H NMR spectrum : 200 MHz, solvent C₆D₆

δ (ppm)	Multiplicity	Integral	Assignment
1.1	broad singlet	1H	Ph ₃ PNH

7.1 – 7.3	multiplet	9H	m & p Ph <u>¹H</u>
7.3	multiplet	6H	o Ph <u>¹H</u>

³¹P NMR spectrum : 101.2 MHz, solvent C₆D₆

δ (ppm)	Multiplicity	Assignment
17.5	singlet	Ph ₃ <u>P</u> NH

3.1.4 Data for tris(dimethylamino)iminophosphorane (IV).

¹H NMR spectrum : 200 MHz, solvent C₆D₆

δ (ppm)	Multiplicity	Integral	Assignment
0.3	multiplet	1H	<u>NH</u>
2.3 – 2.5	multiplet	18H	<u>Me</u> ₂ N

³¹P NMR spectrum : 101.2 MHz, solvent C₆D₆

δ (ppm)	Multiplicity	Assignment
40.0	singlet	(Me ₂ N) ₃ <u>P</u> NH

3.1.5 Preparation of tetraphenyldithiodiphosphinylimide (V).⁶



A solution of hexamethyldisilazane (4.2g, 26mmol) in 70ml of toluene was prepared, and placed in a two necked round bottomed flask equipped with a pressure equalising

⁶ F. T. Wang, *Synth. React. Inorg. Met. Chem.*, 8, 120 (1978).

dropping funnel on one neck and a condenser set up for distillation on the other. The system was closed with a calcium chloride drying tube on the receiver flask. The reaction flask was then heated with an oil bath to 90°C. A solution of chlorodiphenylphosphine (11.5g, 52mmol) in toluene (70ml) was placed in the dropping funnel and added dropwise over 20 minutes to the solution of hexamethyldisilazane. As the reaction proceeded the chlorotrimethylsilane which was formed distilled over. After addition the flask was heated for a further 1.5 hours, after which time the temperature of the oil bath was raised to enable removal of about half the toluene. The mixture was then cooled to room temperature, sulphur (1.65g, 52mmol) added and the reactants heated to 100°C for 2 hours. The system was then cooled to room temperature and the solid removed by filtration, washed thoroughly with cold toluene and then carbon disulphide (to remove unreacted sulphur), then finally dried in air.

Yield : 9g (77%)

Melting point : 213°C

¹H NMR spectrum : 200 MHz, solvent C₆D₆

δ (ppm)	Multiplicity	Integral	Assignment
4.5 – 4.7	br singlet	1H	PN(<u>H</u>)P
6.8 – 7.1	multiplet	12H	m & p Ph ¹ <u>H</u>
8.0 – 8.3	multiplet	8H	o Ph ¹ <u>H</u>

³¹P NMR spectrum : 101.2 MHz, solvent C₆D₆

δ (ppm)	Multiplicity	Assignment
57.7	singlet	Ph ₂ <u>P</u> N(H) <u>P</u> Ph ₂

3.1.6 Data for triphenylphosphine oxide (VI).

Melting point : 156-7°C

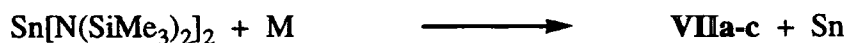
¹H NMR spectrum : 200 MHz, solvent C₆D₆

δ (ppm)	Multiplicity	Integral	Assignment
7.0 – 7.1	multiplet	9H	m & p <u>Ph</u> ₃ PO
7.8 – 7.9	multiplet	6H	o <u>Ph</u> ₃ PO

³¹P NMR spectrum : 101.2 MHz, solvent C₆D₆

δ (ppm)	Multiplicity	Assignment
25.9	singlet	Ph ₃ <u>P</u> O

3.1.7 Preparation of M[N(SiMe₃)₂]₂ where M = Ca, Sr & Ba for a, b and c respectively (VIIa-c).



Lithium bis[(trimethylsilyl)amide] (16.8g, 100 mmol) was added to a stirred suspension of tin (II) chloride (9.5g, 50 mmol) in 140 ml of Et₂O. An immediate reaction was observed with the formation of an orange solution and the precipitation of lithium chloride. After stirring for 2 hours, the ether was removed in vacuo. The tin amide was extracted with dry benzene and filtered to remove the lithium chloride. The benzene was then removed in vacuo to leave a dark red liquid. This was purified by distillation; 80°C at 10⁻¹ Torr. The resulting orange liquid was then frozen at -70°C to give a yellow solid. This solid was then purged into the glove box for final isolation.

The metal (calcium, strontium or barium) and bis[bis(trimethylsilyl)amido] tin(II) were combined in toluene (100ml) and the solution was stirred at room temperature for 2/4/5 days (Ca, Sr & Ba respectively) under nitrogen. The resulting reaction mixture was in each case reddish brown in colour. After separation of the metal, (achieved through cannulating the solution through a celite covered filter), approximately half of the volume of the toluene was removed in vacuo, and the solution was stored at -70°C. After 24 hours

a crop of light orange-brown colour crystals was obtained. In the case of the barium compound it was recrystallised from pentane.

Yield : Ca = 8g(69%), Sr = 10g(77%), Ba = 7g(48%).

3.2 Preparation of complexes 1-8.

These complexes will be discussed in further detail in Chapter 4.

3.2.1 Preparation of 1.



Triphenylphosphonium methylide (0.552g, 2 mmol) was added to calcium bis[bis(trimethylsilyl)amide] (0.361g, 1mmol) in an evacuated Schlenk tube. Under argon, 4 ml of toluene was added and the mixture was stirred for 2 hours, upon which there was a yellow solution. The resulting solution was stored at -40°C for 48 hours to yield a crop of crystals suitable for X-ray diffraction.

Yield : 0.76g (83%)

Melting Point : 65-67°C

IR Spectrum : ν 2920cm⁻¹, 2851cm⁻¹ and 1461cm⁻¹ C-H stretches of the Nujol mull.

ν 1575cm⁻¹ Aromatic hydrocarbon ring vibration.

ν 1109cm⁻¹ SiNSi stretch.

ν 881cm⁻¹ P=C ylide stretch.

¹H NMR spectrum : 200MHz, solvent C₆D₆

δ (ppm)	Multiplicity	Integral	Assignment
0.1 - 0.7	multiplet	40H	[(<u>Me</u> ₃ Si) ₂ N] ₂ & Ph ₃ P <u>CH</u> ₂
7.0 - 7.6	multiplet	30H	<u>Ph</u> ₃ PCH ₂

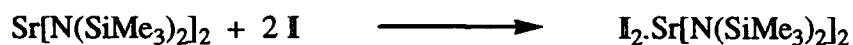
³¹P NMR spectrum : 81MHz, solvent C₆D₆

δ (ppm)	Multiplicity	Assignment
29.3	singlet	Ph ₃ <u>P</u> CH ₂

Elemental Analysis : C₅₀H₇₀Si₄P₂N₂Ca, M_r = 913.49

	C	H	N
% Mass by Calculation	65.74	7.72	3.07
% Mass by Analysis	63.99	6.75	1.78

3.2.2 Preparation of 2.



Triphenylphosphonium methyllide (0.552g, 2 mmol) was added to strontium bis[bis(trimethylsilyl)amide] (0.407g, 1mmol) in an evacuated Schlenk tube. Under argon, 5 ml of toluene was added and the mixture was stirred for 2 hours, upon which there was a yellow solution. The resulting solution was stored at -40°C for 48 hours to yield a crop of crystals suitable for X-ray diffraction.

Yield : 0.8g (78%)Melting Point : 128-129°CIR Spectrum : ν 2920cm⁻¹, 2851cm⁻¹ and 1461cm⁻¹ C-H stretches of the Nujol mull.

ν 1575 cm^{-1} Aromatic hydrocarbon ring vibration.

ν 1109 cm^{-1} SiNSi stretch.

ν 881 cm^{-1} P=C ylide stretch

^1H NMR spectrum : 200MHz, solvent C_6D_6

δ (ppm)	Multiplicity	Integral	Assignment
0.1 - 0.8	multiplet	40H	$[(\text{Me}_3\text{Si})_2\text{N}]_2$ & Ph_3PCH_2
7.0 - 7.6	multiplet	30H	Ph_3PCH_2

^{31}P NMR spectrum : 81MHz, solvent C_6D_6

δ (ppm)	Multiplicity	Assignment
29.8	singlet	Ph_3PCH_2

^{13}C NMR spectrum : 100.6 MHz, solvent C_6D_6

δ (ppm)	Multiplicity	Coupling (Hz)	Assignment
2.0	triplet	$^1J_{\text{CH}} = 117.1$	PCH_2
6.7	quartet	$^1J_{\text{CH}} = 115.2$	SiMe_3
129.6	multiplet	-	$\text{Ph } \underline{\text{C}}$
130.7	multiplet	-	$\text{Ph } \underline{\text{C}}$
131.3	multiplet	-	$\text{Ph } \underline{\text{C}}$
132.3	multiplet	-	$\text{Ph } \underline{\text{C}}$
133.5	multiplet	-	$\text{Ph } \underline{\text{C}}$

Also obtained was a ^{13}C DEPT NMR spectrum which indicated the presence of 8 different types of protonated carbon atom comprising of 6 CHs, 1 CH_2 and 1 CH_3 as follows :

δ (ppm)	Multiplicity	Moiety	Coupling (Hz)	Assignment
2.5	singlet	CH_2	-	Ph_3PCH_2
6.6	singlet	CH_3	-	SiMe_3
128.2	singlet	CH	-	C_6D_6
128.8	doublet	CH	$^1J_{\text{CH}} = 11.5$	m $\text{Ph } \underline{\text{C}}$

131.4	doublet	CH	$^1J_{\text{CH}} = 2.4$	p Ph <u>C</u>
132.6	doublet	CH	$^1J_{\text{CH}} = 9.7$	o Ph <u>C</u>

Elemental Analysis : $\text{C}_{50}\text{H}_{70}\text{Si}_4\text{P}_2\text{N}_2\text{Sr}$, $M_r = 961.03$

	C	H	N
% Mass by Calculation	62.49	7.34	2.91
% Mass by Analysis	58.09	7.22	3.43

3.2.3 Preparation of 3.



Triphenylphosphonium methyllide (0.552g, 2 mmol) was added to barium bis[bis(trimethylsilyl)amide] (0.457g, 1mmol) in an evacuated Schlenk tube. Under argon, 2 ml of toluene was added and the mixture was stirred for 1 hour, upon which there was a yellow solution. The resulting solution was stored at -40°C for 48 hours to yield a crop of crystals suitable for X-ray diffraction.

Yield : 0.60g (59%)

Melting Point : $107-108^\circ\text{C}$

IR Spectrum : ν 2920cm^{-1} , 2851cm^{-1} and 1461cm^{-1} C-H stretches of the Nujol mull.

ν 1575cm^{-1} Aromatic hydrocarbon ring vibration.

ν 1109cm^{-1} SiNSi stretch.

ν 881cm^{-1} P=C ylide stretch.

^1H NMR spectrum : 200MHz, solvent C_6D_6

δ (ppm)	Multiplicity	Integral	Assignment
0.1 - 0.5	multiplet	40H	$[(\text{Me}_3\text{Si})_2\text{N}]_2$

7.0 - 7.6	multiplet	30H	& Ph ₃ PCH ₂ Ph ₃ PCH ₂
-----------	-----------	-----	--

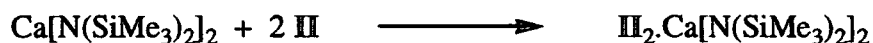
³¹P NMR spectrum : 81MHz, solvent C₆D₆

δ (ppm)	Multiplicity	Assignment
26.9	singlet	Ph ₃ PCH ₂

Elemental Analysis : C₅₀H₇₀Si₄P₂N₂Ba, M_r = 1010.75

	C	H	N
% Mass by Calculation	59.36	6.93	2.77
% Mass by Analysis	52.81	4.80	2.60

3.2.4 Preparation of 4.



Calcium bis[bis(trimethylsilyl)amide] (0.180g, 0.5mmol) was added to 2 equivalents of tris(dimethylamino)phosphonium methylide (0.177g, 1mmol) in an evacuated Schlenk tube. Under argon, toluene (1ml) and hexane (6ml) were added and the mixture was stirred for 1 hour. After stirring the suspension was heated to aid dissolution and left to cool at -30°C whereupon a crystalline material was obtained.

Yield : 0.30g (84%)

Melting Point : 148-150°C

¹H NMR spectrum : 200MHz, solvent C₆D₆

δ (ppm)	Multiplicity	Integral	Assignment
0.1 - 0.2	multiplet	2H	PCH ₂
0.5 - 0.7	multiplet	18H	[(Me ₃ Si) ₂ N] ₂

2.3 - 2.7	multiplet	18H	(<u>Me</u> ₂ N) ₃ P
-----------	-----------	-----	--

³¹P NMR spectrum : 81MHz, solvent C₆D₆

δ (ppm)	Multiplicity	Assignment
76.7	singlet	<u>P</u> CH ₂

Elemental Analysis : C₂₆H₇₆N₈Si₄P₂Ca, M_r = 715.328

	C	H	N
% Mass by Calculation	43.65	10.71	15.67
% Mass by Analysis	42.77	10.05	15.01

3.2.5 Preparation of 5.

Strontium bis[bis(trimethylsilyl)amide] (0.204g, 0.5mmol) was added to 2 equivalents of tris(dimethylamino)phosphonium methylide (0.177g, 1mmol) in an evacuated Schlenk tube. Under argon, toluene (1ml) and hexane (6ml) were added and the mixture was stirred for 1 hour. After stirring the suspension was heated to aid dissolution and left to cool at -30°C whereupon a crystalline material was obtained.

Yield : 0.34g (88%)Melting Point : 156-158°C¹H NMR spectrum : 200MHz, solvent C₆D₆

δ (ppm)	Multiplicity	Integral	Assignment
-0.4 - -0.2	multiplet	2H	<u>P</u> CH ₂
0.4 - 0.6	multiplet	18H	[(<u>Me</u> ₃ Si) ₂ N] ₂
2.1 - 2.4	multiplet	18H	(<u>Me</u> ₂ N) ₃ P

³¹P NMR spectrum : 81MHz, solvent C₆D₆

δ (ppm)	Multiplicity	Assignment
77.2	singlet	<u>P</u> CH ₂

Elemental Analysis : C₂₆H₇₂N₈Si₄P₂Sr, M_r = 762.868

	C	H	N
% Mass by Calculation	40.93	10.04	14.69
% Mass by Analysis	39.45	9.70	14.40

3.2.6 Preparation of 6.

Magnesium bis[bis(trimethylsilyl)amide] (0.173g, 0.5mmol) was added to 2 equivalents of triphenylphosphonium methyllide (0.276g, 1mmol) and two equivalents of tetraphenyldithiodiphosphinylimide (0.447g, 1mmol) in an evacuated Schlenk tube.

Under argon, toluene (30ml) was added and the mixture was stirred for 2 hours. After stirring the suspension was heated to aid dissolution and left to cool at room temperature whereupon a crystalline material was obtained.

Yield : 0.70g (94%)Melting Point : 320-322°C¹H NMR spectrum : 200MHz, solvent C₆D₆

δ (ppm)	Multiplicity	Integral	Coupling (Hz)	Assignment
2.6 - 2.8	doublet	2H	² J _{PH} = 13.2	<u>P</u> CH ₂
6.4 - 7.0	multiplet	28H	-	Ph <u>¹H</u>
8.2 - 8.4	multiplet	7H	-	Ph <u>¹H</u>

³¹P NMR spectrum : 81MHz, solvent C₆D₆

δ (ppm)	Multiplicity	Assignment
24.5	singlet	Ph ₃ <u>P</u> CH ₂
39.6	singlet	<u>P</u> [Ph ₂ (S)]NP

Elemental Analysis : C₈₆H₇₄P₆S₄N₂Mg, M_r = 1473.842

	C	H	N
% Mass by Calculation	70.08	5.06	1.90
% Mass by Analysis	68.88	4.93	1.85

3.2.7 Preparation of 7.

Calcium bis[bis(trimethylsilyl)amide] (0.180g, 0.5mmol) was added to 2 equivalents of triphenyl phosphonium methyllide (0.276g, 1mmol) and two equivalents of tetraphenyldithiodiphosphinyimide (0.449g, 1mmol) in an evacuated Schlenk tube.

Under an argon atmosphere, toluene (30ml) was added and the mixture was stirred for 2 hours. After stirring the suspension was heated to aid dissolution and left to cool at room temperature whereupon a crystalline material was obtained.

Yield : 0.50g (66%)Melting Point : 318-320°C¹H NMR spectrum : 200MHz, solvent C₆D₆

δ (ppm)	Multiplicity	Integral	Coupling (Hz)	Assignment
2.6 - 2.8	doublet	2H	² J _{PH} = 13.6	P <u>C</u> H ₂
6.5 - 7.1	multiplet	28H	-	Ph ¹ <u>H</u>
8.3 - 8.6	multiplet	7H	-	Ph ¹ <u>H</u>

³¹P NMR spectrum : 81MHz, solvent C₆D₆

δ (ppm)	Multiplicity	Assignment
24.5	singlet	Ph ₃ PCH ₂
39.6	singlet	P[Ph ₂ (S)]NP

Elemental Analysis : C₈₆H₇₄P₆S₄N₂Ca, M_r = 1488.872

	C	H	N
% Mass by Calculation	69.32	5.01	1.88
% Mass by Analysis	68.49	4.97	1.75

3.2.8 Preparation of 8.

Strontium bis[bis(trimethylsilyl)amide] (0.204g, 1mmol) was added to 2 equivalents of triphenylphosphonium methylide (0.276g, 2 mmol) and 2 equivalents of 2,6-di-tert-butyl 4-methyl phenol (0.221g, 1mmol) in an evacuated Schlenk tube. Under argon, toluene (5ml) was added and the mixture was stirred for 2 hours. After stirring the suspension was heated to aid dissolution and left to cool at room temperature whereupon a crystalline material was obtained.

Yield : 0.45g (78%)Melting Point : 70-72°C¹H NMR spectrum : 200MHz, solvent C₆D₆

δ (ppm)	Multiplicity	Integral	Coupling (Hz)	Assignment
0.4 - 0.5	doublet	2H	² J _{PH} = 9.6	Ph ₃ PCH ₂
1.7	singlet	18H	-	'Bu ¹ H
2.6	singlet	3H	-	Me ¹ H

6.8 - 7.0	multiplet	9H	-	m & p Ph ^1H
7.3	singlet	2H	-	phenol ring ^1H
7.4 - 7.5	multiplet	6H	-	o Ph ^1H

^{31}P NMR spectrum : 81MHz, solvent C_6D_6

δ (ppm)	Multiplicity	Assignment
30.2	singlet	Ph_3PCH_2

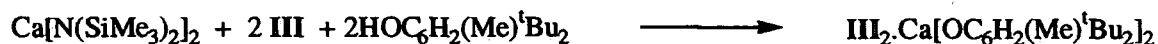
Elemental Analysis : $\text{C}_{68}\text{H}_{80}\text{P}_2\text{O}_2\text{Sr}$, $M_r = 1078.270$

	C	H
% Mass by Calculation	75.68	7.48
% Mass by Analysis	75.12	7.30

3.3 Preparation of complexes 9-21.

These complexes will be discussed further in Chapter 5.

3.3.1 Preparation of 9.



Calcium bis[bis(trimethylsilyl)amide] (0.361g, 1 mmol) was added to 2 equivalents of triphenyliminophosphorane (0.554g, 2 mmol) and 2 equivalents of 2,6-di-tert-butyl,4-methyl phenol (0.441g, 2 mmol). The reaction mixture was stirred under argon in 40ml toluene. The solution was then heated to aid dissolution, and then left to cool at room temperature whereupon crystals suitable for X-ray diffraction were obtained.

Yield : 0.60g (58%)

Melting Point : 316-318°C

¹H NMR spectrum : 200MHz, solvent C₆D₆

δ (ppm)	Multiplicity	Integral	Assignment
1.4	broad singlet	1H	PN <u>H</u>
1.7	singlet	18H	^t Bu ¹ <u>H</u> s
2.5	singlet	3H	Me ¹ <u>H</u>
6.8 – 7.0	multiplet	9H	Ph ¹ <u>H</u>
7.3	singlet	2H	phenol ring ¹ <u>H</u>
7.5	multiplet	6H	Ph ¹ <u>H</u>

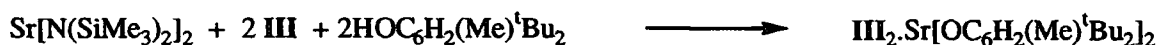
³¹P NMR spectrum : 81MHz, solvent C₆D₆

δ (ppm)	Multiplicity	Assignment
30.8	singlet	Ph ₃ PN <u>H</u>

Elemental Analysis : C₆₆H₇₈O₂P₂N₂Ca, M_r = 1032.723

	C	H	N
% Mass by Calculation	76.70	7.61	2.71
% Mass by Analysis	76.29	7.39	2.54

3.3.2 Preparation of 10.



Strontium bis[bis(trimethylsilyl)amide] (0.407g, 1 mmol) was added to 2 equivalents of triphenyliminophosphorane (0.554g, 2 mmol) and 2 equivalents of 2,6-di-tert-butyl,4-methyl phenol (0.441g, 2 mmol). The reaction mixture was stirred under argon in 30ml toluene. The solution was then heated to aid dissolution, and then left to cool at room temperature whereupon crystals of X-ray quality were obtained.

Yield : 0.70g (66%)

Melting Point : 296-298°C¹H NMR spectrum : 200MHz, solvent C₆D₆

δ (ppm)	Multiplicity	Integral	Coupling (Hz)	Assignment
1.2	doublet	1H	² J _{PH} = 9.8	P=NH
1.7	singlet	18H	-	^t Bu ¹ Hs
2.6	singlet	3H	-	Me ¹ H
6.8 - 7.0	multiplet	9H	-	Ph ¹ H
7.3	singlet	2H	-	phenol ring ¹ H
7.4 - 7.5	multiplet	6H	-	Ph ¹ H

³¹P NMR spectrum : 81MHz, solvent C₆D₆

δ (ppm)	Multiplicity	Assignment
30.8	singlet	Ph ₃ PNH

Elemental Analysis : C₆₆H₇₈O₂P₂N₂Sr, M_r = 1080.864

	C	H	N
% Mass by Calculation	73.34	7.27	2.59
% Mass by Analysis	71.47	7.10	2.42

3.3.3 Preparation of 11.



Barium bis[bis(trimethylsilyl)amide] (0.457g, 1 mmol) was added to 2 equivalents of triphenyliminophosphorane (0.554g, 2 mmol) and 2 equivalents of 2,6-di-tert-butyl,4-methyl phenol (0.441g, 2 mmol). The reaction mixture was stirred under argon in 8ml toluene. The solution was then heated to aid dissolution, and then left to cool at room temperature whereupon crystals suitable for X-ray diffraction were obtained.

Yield : 1.0g (90%)

Melting Point : 281-283°C

¹H NMR spectrum : 200MHz, solvent C₆D₆

δ (ppm)	Multiplicity	Integral	Coupling (Hz)	Assignment
1.2	doublet	1H	² J _{PH} = 9.4	PN <u>H</u>
1.7	singlet	9H	-	^t Bu ¹ <u>H</u> s
2.5	singlet	3H	-	Me ¹ <u>H</u>
6.9 - 7.0	multiplet	9H	-	Ph ¹ <u>H</u>
7.3	singlet	2H	-	phenol ring ¹ <u>H</u>
7.4 - 7.5	multiplet	6H	-	Ph ¹ <u>H</u>

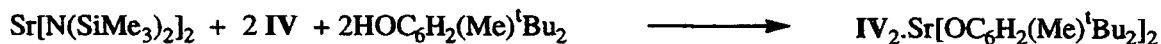
³¹P NMR spectrum : 81MHz, solvent C₆D₆

δ (ppm)	Multiplicity	Assignment
30.0	singlet	Ph ₃ <u>P</u> NH

Elemental Analysis : C₆₆H₇₈O₂P₂N₂Ba, M_r = 1130.584

	C	H	N
% Mass by Calculation	70.11	6.95	2.48
% Mass by Analysis	69.38	6.91	1.99

3.3.4 Preparation of 12.



Strontium bis[bis(trimethylsilyl)amide] (0.407g, 1 mmol) was added to 2 equivalents of tris(dimethylamino)iminophosphorane (0.36ml, 2 mmol) and 2 equivalents of 2,6-di-tert-butyl,4-methyl phenol (0.441g, 2 mmol). The reaction mixture was stirred under argon in

20ml toluene. The reaction was then heated to aid dissolution, and then left to cool at -40°C whereupon crystalline material was obtained.

Yield : 0.60g (68%)

Melting Point : 108-110°C

¹H NMR spectrum : 200MHz, solvent C₆D₆

δ (ppm)	Multiplicity	Integral	Assignment
1.4	singlet	1H	(Me ₂ N) ₃ PN <u>H</u>
1.8	singlet	18H	^t Bu ¹ H <u>s</u>
2.2	multiplet	18H	(<u>Me</u> ₂ N) ₃
2.5	singlet	3H	Me ¹ H <u></u>
7.3	multiplet	2H	phenol ring ¹ H <u></u>

³¹P NMR spectrum : 81MHz, solvent C₆D₆

δ (ppm)	Multiplicity	Assignment
45.6	singlet	(Me ₂ N) ₃ PN <u>H</u>

Elemental Analysis : C₄₂H₈₆O₂P₂N₈Sr, M_r = 884.748

	C	H	N
% Mass by Calculation	57.01	9.80	12.67
% Mass by Analysis	55.00	9.01	11.88

3.3.5 Preparation of 13.



Strontium bis[bis(trimethylsilyl)amide] (0.204g, 0.5 mmol) was added to 2 equivalents of triphenyliminophosphorane (0.277g, 1 mmol) and 2 equivalents of tetraphenyldithiodiphosphinylimide (0.449g, 1 mmol). The reaction mixture was stirred

under argon in 15ml toluene. The reaction was then heated to aid dissolution, and then left to cool at room temperature whereupon crystalline material was obtained.

Yield : 0.57g (74%)

Melting Point : 224-225°C

¹H NMR spectrum : 200MHz, solvent C₆D₆

δ (ppm)	Multiplicity	Integral	Assignment
1.8	singlet	1H	Ph ₃ P <u>NH</u>
6.9	multiplet	21H	Ph ¹ <u>H</u>
7.6	multiplet	6H	Ph ¹ <u>H</u>
8.0	multiplet	8H	Ph ¹ <u>H</u>

³¹P NMR spectrum : 81MHz, solvent C₆D₆

δ (ppm)	Multiplicity	Assignment
27.0	singlet	Ph ₃ <u>P</u> NH
39.6	singlet	<u>P</u> [Ph ₂ (S)] <u>N</u> <u>P</u>

Elemental Analysis : C₈₄H₇₂P₆S₄N₄Sr, M_r = 1539.136

	C	H	N
% Mass by Calculation	65.55	4.72	3.64
% Mass by Analysis	64.05	4.57	3.59

3.3.6 Preparation of 14.



Strontium bis[bis(trimethylsilyl)amide] (0.204g, 1mmol) was added to 2 equivalents of triphenyliminophosphorane (0.277g, 1mmol) and 2 equivalents of triphenyl methanol

(0.260g, 1mmol) in an evacuated Schlenk tube. Under argon, toluene (3ml) was added and the mixture was stirred for 1 hour. After stirring the suspension was heated to aid dissolution and left to cool at room temperature whereupon a crystalline material was obtained.

Yield : 0.4g (65%)

Melting Point : 168-169°C

¹H NMR spectrum : 200MHz, solvent C₆D₆

δ (ppm)	Multiplicity	Integral	Assignment
0.6 - 1.0	broad singlet	1H	Ph ₃ P <u>NH</u>
7.0 - 7.2	multiplet	18H	m & p Ph ¹ <u>H</u>
7.5 - 7.8	multiplet	12H	o Ph ¹ <u>H</u>

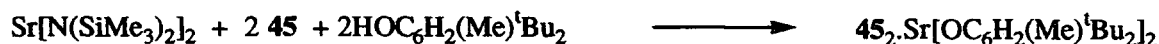
³¹P NMR spectrum : 81MHz, solvent C₆D₆

δ (ppm)	Multiplicity	Assignment
21.8	singlet	Ph ₃ <u>P</u> NH

Elemental Analysis : C₇₄H₆₄O₂N₂P₂Sr, M_r = 1162.832

	C	H	N
% Mass by Calculation	79.71	5.86	3.41
% Mass by Analysis	78.43	5.55	2.41

3.3.7 Preparation of 15.



Strontium bis[bis(trimethylsilyl)amide] (0.204g, 0.5mmol) was added to two equivalents of methyldiphenyliminophosphorane (0.215g, 1mmol) and two equivalents of 2,6-ditert

butyl,4-methyl phenol (0.221g, 1mmol) in a Schlenk tube under an argon atmosphere. To this mixture was added toluene (10ml) and the reaction mixture was allowed to stir at room temperature for one hour. The mixture was then heated to aid dissolution and left to cool at -30°C in the freezer, upon which a crystalline material was obtained.

Yield : 0.41g (89%)

Melting Point : $207-208^{\circ}\text{C}$

^1H NMR spectrum : 200MHz, solvent C_6D_6

δ (ppm)	Multiplicity	Integral	Assignment
1.0 - 1.7	multiplet	18H	$^t\text{Bu } ^1\text{H}$
2.0 - 2.1	singlet	3H	phenol Me ^1H
2.6 - 2.7	singlet	3H	Ph_2MeP
6.8 - 7.2	multiplet	12H	Ph ^1H

^{31}P NMR spectrum : 81MHz, solvent C_6D_6

δ (ppm)	Multiplicity	Assignment
35.6	singlet	$\text{Ph}_2\text{MeP}\text{NH}$

Elemental Analysis : $\text{C}_{61}\text{H}_{76}\text{O}_2\text{N}_2\text{P}_2\text{Sr}$, $M_r = 1018.244$

	C	H	N
% Mass by Calculation	71.89	7.52	2.75
% Mass by Analysis	71.18	7.29	2.51

3.3.8 Preparation of 16.



Calcium bis[bis(trimethylsilyl)amide] (0.181g, 0.5 mmol) was added to 2 equivalents of triphenylphosphine oxide (0.278, 1mmol) in toluene (5ml). The reaction mixture was stirred under argon for one hour and then heated to aid dissolution. The resulting solution was left to cool to room temperature upon which a crop of crystals was obtained.

Yield : 0.39g (81%)

Melting Point : 129-131°C

¹H NMR spectrum : 200MHz, solvent C₆D₆

δ (ppm)	Multiplicity	Integral	Assignment
-0.3 - 0.3	multiplet	18H	(CH ₃) ₃ Si
6.6 - 7.2	multiplet	15H	Ph ¹ H

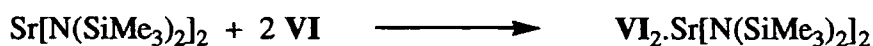
³¹P NMR spectrum : 81MHz, solvent C₆D₆

δ (ppm)	Multiplicity	Assignment
33.5	singlet	Ph ₃ P=O

Elemental Analysis : C₄₈H₆₆Si₄P₂O₂N₂Ca, M_r = 916.941

	C	H	N
% Mass by Calculation	62.82	7.25	3.06
% Mass by Analysis	62.23	7.01	2.88

3.3.9 Preparation of 17.



Strontium bis[bis(trimethylsilyl)amide] (0.204g, 0.5 mmol) was added to 2 equivalents of triphenylphosphine oxide (0.278, 1mmol) in toluene (5ml). The reaction mixture was

stirred under argon for one hour and then heated to aid dissolution. The resulting solution was left to cool to room temperature upon which a crop of crystals was obtained.

Yield : 0.42g (87%)

Melting Point : 140-141°C

¹H NMR spectrum : 200MHz, solvent C₆D₆

δ (ppm)	Multiplicity	Integral	Assignment
-0.3 - 0.3	multiplet	18H	(CH ₃) ₃ Si
6.6 - 7.2	multiplet	15H	Ph ¹ H

³¹P NMR spectrum : 81MHz, solvent C₆D₆

δ (ppm)	Multiplicity	Assignment
32.8	singlet	Ph ₃ P=O

Elemental Analysis : C₄₈H₆₆Si₄P₂O₂N₂Sr, M_r = 964.948

	C	H	N
% Mass by Calculation	59.74	6.89	3.32
% Mass by Analysis	58.17	6.31	3.14

3.3.10 Preparation of 18.



Barium bis[bis(trimethylsilyl)amide] (0.229g, 0.5 mmol) was added to 2 equivalents of triphenylphosphine oxide (0.278, 1mmol) in toluene (5ml). The reaction mixture was stirred under argon for one hour and then heated to aid dissolution. The resulting solution was left to cool to room temperature upon which a crop of crystals was obtained.

Yield : 0.45g (89%)

Melting Point : 110-112°C

¹H NMR spectrum : 200MHz, solvent C₆D₆

δ (ppm)	Multiplicity	Integral	Assignment
-0.3 - 0.3	multiplet	18H	(CH ₃) ₃ Si
6.6 - 7.2	multiplet	15H	Ph ¹ H

³¹P NMR spectrum : 81MHz, solvent C₆D₆

δ (ppm)	Multiplicity	Assignment
32.5	singlet	Ph ₃ P <u>O</u>

Elemental Analysis : C₄₈H₆₆Si₄P₂O₂N₂Ba, M_r = 1014.190

	C	H	N
% Mass by Calculation	56.80	6.56	2.76
% Mass by Analysis	56.12	6.38	2.48

3.3.11 Preparation of 19.



Calcium bis[bis(trimethylsilyl)amide] (0.181g, 0.5 mmol) was added to 2 equivalents of triphenylphosphine oxide (0.278, 1mmol) and 2 equivalents of 2,6-di-tert-butyl,4-methyl phenol (0.221g, 1mmol) in toluene (5ml). The reaction mixture was stirred under argon for one hour and then heated to aid dissolution. The resulting solution was left to cool to room temperature upon which a crop of crystals was obtained.

Yield : 0.47g (81%)

Melting Point : 275-277°C¹H NMR spectrum : 200MHz, solvent C₆D₆

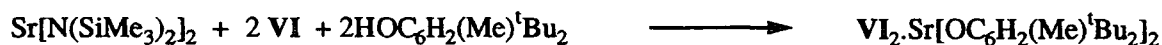
δ (ppm)	Multiplicity	Integral	Assignment
1.5 - 1.6	singlet	18H	^t Bu ¹ H
2.4	singlet	3H	Me ¹ H
6.6 - 6.8	multiplet	9H	m & p Ph ¹ H
7.0	singlet	2H	phenol ring ¹ H
7.3 - 7.4	multiplet	6H	o Ph ¹ H

³¹P NMR spectrum : 81MHz, solvent C₆D₆

δ (ppm)	Multiplicity	Assignment
33.7	singlet	Ph ₃ P=O

Elemental Analysis : C₆₆H₇₆O₄P₂Ca, M_r = 1035.288

	C	H
% Mass by Calculation	76.56	7.40
% Mass by Analysis	76.60	7.41

3.3.12 Preparation of 20.

Strontium bis[bis(trimethylsilyl)amide] (0.204g, 0.5 mmol) was added to 2 equivalents of triphenylphosphine oxide (0.278, 1mmol) and 2 equivalents of 2,6-di-tert-butyl,4-methyl phenol (0.221g, 1mmol) in toluene (5ml). The reaction mixture was stirred under argon for one hour and then heated to aid dissolution. The resulting solution was left to cool to room temperature upon which a crop of crystals was obtained.

Yield : 0.52g (89%)

Melting Point : 280-282°C¹H NMR spectrum : 200MHz, solvent C₆D₆

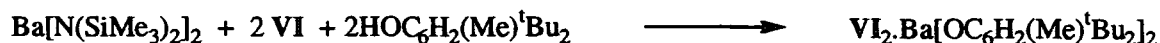
δ (ppm)	Multiplicity	Integral	Assignment
1.5 - 1.6	singlet	18H	^t Bu ¹ H
2.4	singlet	3H	Me ¹ H
6.6 - 6.8	multiplet	9H	m & p Ph ¹ H
7.0	singlet	2H	phenol ring ¹ H
7.3 - 7.4	multiplet	6H	o Ph ¹ H

³¹P NMR spectrum : 81MHz, solvent C₆D₆

δ (ppm)	Multiplicity	Assignment
33.7	singlet	Ph ₃ P=O

Elemental Analysis : C₆₆H₇₆O₄P₂Sr, M_r = 1082.828

	C	H
% Mass by Calculation	73.20	7.07
% Mass by Analysis	72.05	7.00

3.3.13 Preparation of 21.

Barium bis[bis(trimethylsilyl)amide] (0.229g, 0.5 mmol) was added to 2 equivalents of triphenylphosphine oxide (0.278, 1mmol) and 2 equivalents of 2,6-di-tert-butyl,4-methyl phenol (0.221g, 1mmol) in toluene (5ml). The reaction mixture was stirred under argon for one hour and then heated to aid dissolution. The resulting solution was left to cool to room temperature upon which a crop of crystals was obtained.

Yield : 0.55g (87%)

Melting Point : 299-301°C

¹H NMR spectrum : 200MHz, solvent C₆D₆

δ (ppm)	Multiplicity	Integral	Assignment
1.5 - 1.6	singlet	18H	^t Bu ¹ H
2.4	singlet	3H	Me ¹ H
6.6 - 6.8	multiplet	9H	m & p Ph ¹ H
7.0	singlet	2H	phenol ring ¹ H
7.3 - 7.4	multiplet	6H	o Ph ¹ H

³¹P NMR spectrum : 81MHz, solvent C₆D₆

δ (ppm)	Multiplicity	Assignment
32.5	singlet	Ph ₃ P=O

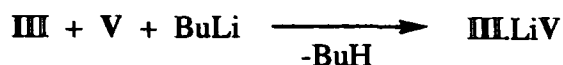
Elemental Analysis : C₆₆H₇₆O₄P₂Ba, M_r = 1132.535

	C	H
% Mass by Calculation	69.94	6.76
% Mass by Analysis	69.87	6.72

3.4 Preparation of compounds 22-27.

These compounds will be discussed in further detail in Chapter 6.

3.4.1 Preparation of 22.



Triphenyliminophosphorane (0.277g, 1mmol) and tetraphenyldithiodiphosphinylimide (0.449g, 1mmol) were added together in a Schlenk tube under an inert argon atmosphere. Toluene (10ml) was added and the Schlenk was cooled in a liquid nitrogen bath. "Butyl

Chapter 3 - Experimental

lithium (0.7ml, 1.1mmol) was then added and the reaction mixture was allowed to stir for one hour at room temperature, after which time a further 20ml of toluene was added and the mixture was heated to aid dissolution. Upon standing overnight at room temperature a crop of colourless crystals was obtained.

Yield : 0.65g (89%)

Melting Point : 160-162°C

¹H NMR spectrum : 200MHz, solvent C₆D₆

δ (ppm)	Multiplicity	Integral	Assignment
0.9 - 1.0	br singlet	1H	Ph ₃ P= <u>NH</u>
6.9 - 7.1	multiplet	21H	Ph ¹ <u>H</u>
7.4 - 7.6	multiplet	6H	Ph ¹ <u>H</u>
8.2 - 8.4	multiplet	8H	Ph ¹ <u>H</u>

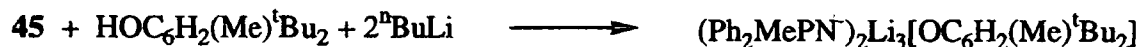
³¹P NMR spectrum : 81MHz, solvent C₆D₆

δ (ppm)	Multiplicity	Assignment
31.5	singlet	Ph ₃ <u>P</u> =NH
39.1	singlet	<u>P</u> [Ph ₂ (S)] <u>NP</u>

Elemental Analysis : C₄₂H₃₆P₃S₂N₂Li, M_r = 732.698

	C	H	N
% Mass by Calculation	68.84	4.95	3.82
% Mass by Analysis	67.29	4.76	3.66

3.4.2 Preparation of 23.



To a mixture of methyldiphenyliminophosphorane (0.215g, 1mmol) and 2,6-ditert butyl 4-methyl phenol (0.221g, 1mmol) in toluene (5ml) was added ⁿbutyl lithium (1.3ml, 2mmol) at -78°C. After stirring for one hour the reaction mixture was allowed to warm to room temperature. The mixture was then heated to aid dissolution and left to cool to room temperature whereupon a crystalline material was obtained.

Yield : 0.13g (19%) Product not expected hence low yield.

Melting Point : 130°C (decomposes)

¹H NMR spectrum : 200MHz, solvent C₆D₆

δ (ppm)	Multiplicity	Integral	Coupling (Hz)	Assignment
1.0 – 1.1	doublet	6H	² J _{PH} = 12.0	Ph ₂ <u>Me</u> P
1.6 – 1.7	multiplet	18H	-	^t <u>Bu</u> ¹ H
2.2 – 2.3	singlet	3H	-	Ar – <u>CH</u> ₃
6.6 – 7.0	multiplet	22H	-	Ph ¹ <u>H</u> & ArOH ¹ <u>H</u>

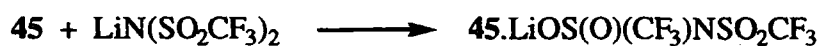
³¹P NMR spectrum : 81MHz, solvent C₆D₆

δ (ppm)	Multiplicity	Assignment
-1.8	singlet	Ph ₂ Me <u>P</u> N ⁻

Elemental Analysis : C₄₁H₄₆P₂N₂Li₃O, M_r = 665.605

	C	H	N
% Mass by Calculation	73.99	6.97	4.22
% Mass by Analysis	72.92	6.77	4.46

3.4.3 Preparation of 24.



To a sample of methyldiphenyliminophosphorane (0.215g, 1mmol) was added N-lithiotrifluoromethanesulphonimide (0.289g, 1mmol) in 2ml of toluene. The reaction was stirred for one hour under an argon atmosphere and a further 3ml of toluene was added. The mixture was then heated to aid dissolution and the solution left to crystallise at room temperature to yield a crop of crystals suitable for x-ray analysis.

Yield : 0.36g (71%)

Melting Point : 120-122°C

¹H NMR spectrum : 400MHz, solvent C₆D₆

δ (ppm)	Multiplicity	Integral	Coupling (Hz)	Assignment
0.0 – 0.1	singlet	1H	-	N <u>H</u>
1.4 – 1.5	doublet	3H	² J _{PH} = 13.2	P <u>CH</u> ₃
6.8 – 7.0	multiplet	6H	-	m & p Ph ¹ <u>H</u>
7.1 – 7.3	multiplet	4H	-	o Ph ¹ <u>H</u>

¹⁹F NMR spectrum : 376MHz, solvent C₆D₆

δ (ppm)	Multiplicity	Assignment
-79.9	singlet	C <u>F</u> ₃

³¹P NMR spectrum : 162MHz, solvent C₆D₆

δ (ppm)	Multiplicity	Assignment
33.7	singlet	Ph ₂ MeP <u>N</u> H

Elemental Analysis : C₁₅H₁₄F₆O₄S₂N₂PLi, M_r = 502.174

	C	H	N
% Mass by Calculation	35.85	2.81	5.58
% Mass by Analysis	36.20	3.23	4.87

3.4.4 Preparation of 25.



To a sample of triphenyliminophosphorane (0.277g, 1mmol) was added N-lithiotrifluoromethanesulphonimide (0.289g, 1mmol) in 2ml of toluene. The reaction was stirred for one hour under an argon atmosphere and a further 3ml of toluene was added. The mixture was then heated to aid dissolution and then left to crystallise at room temperature.

Yield : 0.37g (73%)

Melting Point : 85-87°C

¹H NMR spectrum : 400MHz, solvent C₆D₆

δ (ppm)	Multiplicity	Integral	Assignment
1.3 – 1.4	singlet	1H	<u>NH</u>
7.0 – 7.2	multiplet	9H	m & p Ph <u>¹H</u>
7.4 – 7.6	multiplet	6H	o Ph <u>¹H</u>

¹⁹F NMR spectrum : 376MHz, solvent C₆D₆

δ (ppm)	Multiplicity	Assignment
-79.7	singlet	<u>CF₃</u>

³¹P NMR spectrum : 81MHz, solvent C₆D₆

δ (ppm)	Multiplicity	Assignment
33.0	singlet	Ph ₃ <u>P</u> NH

Elemental Analysis : C₂₀H₁₆F₆O₄S₂N₂PLi, M_r = 564.195

	C	H	N
% Mass by Calculation	42.54	2.86	4.97
% Mass by Analysis	43.2	3.34	4.77

3.4.5 Preparation of 26.



To a sample of N-lithotrifluoromethanesulphonimide (0.289g, 1mmol) in 5ml of toluene was added N, N, N', N',-tetramethylethylenediamine (0.22ml, 0.172g, 1mmol). The mixture was stirred for one hour at room temperature upon which there was a white precipitate. The precipitate was redissolved with heating and the solution was left to cool at room temperature to yield a crystalline material.

Yield : 0.4g (85%)

Melting Point : 110-112°C

¹H NMR spectrum : 400MHz, solvent C₆D₆

δ (ppm)	Multiplicity	Integral	Assignment
1.8	br singlet	2H	TMEDA <u>¹H</u>
1.9	br singlet	6H	TMEDA <u>¹H</u>

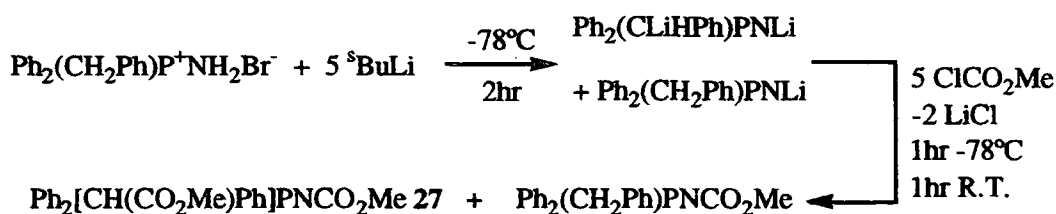
¹⁹F NMR spectrum : 376MHz, solvent C₆D₆

δ (ppm)	Multiplicity	Assignment
-80.0	singlet	<u>CF₃</u>

Elemental Analysis : C₄H₈F₆O₄N₃S₂Li, M_r = 347.149

	C	H	N
% Mass by Calculation	13.83	2.32	12.10
% Mass by Analysis	13.64	2.30	11.90

3.4.6 Preparation of 27.



To one equivalent of benzyldiphenylphosphonio ammonium bromide (0.371g, 1mmol) in 30ml of thf were added 5 equivalents of sec-Butyl lithium (3.9ml, 5mmol, 1.3M in cyclohexane/hexane) and the mixture was allowed to stir for 2 hours at -78°C upon which time there was an intense orange colour. 5 equivalents of methyl chloroformate (0.39ml, 5mmol) were then added and the intense orange colour was replaced by a pale yellow. The solution was stirred for 1 hour at -78°C and then for a further hour at room temperature. The reaction was quenched with methanol and high purity water was added. The product was extracted thoroughly using dichloromethane and the organic layer was then dried over magnesium sulphate. Removal of the solvent using a rotary evaporator left a solid white product, which was then dried fully *in vacuo*.

^1H NMR spectrum : 400MHz, solvent C_6D_6

δ (ppm)	Multiplicity	Coupling (Hz)	Assignment	Product
3.53	singlet		<u>PNCO₂Me</u>	Di-addition
3.54	singlet		<u>PNCO₂Me</u>	Mono-addition
4.10	doublet	$^2J_{\text{PH}} = 13.2$	[<u>CH</u> (CO ₂ Me)]	Di-addition
5.82	doublet	$^2J_{\text{CH}} = 12.8$	<u>Ph₂(CH₂Ph)P</u>	Mono-addition
6.90 – 8.00	multiplets		<u>Ph ¹H</u>	Mono & Di

$^1\text{H}\{^{31}\text{P}\}$ NMR spectrum : 400MHz, solvent C_6D_6

δ (ppm)	Multiplicity	Coupling (Hz)	Assignment	Product
3.53	singlet	-	<u>CH(CO₂Me)</u>	Di-addition
3.54	singlet	-	<u>PNCO₂Me</u>	Mono-addition
4.10	singlet	-	<u>CH</u> (CO ₂ Me)	Di-addition
5.82	singlet	-	<u>Ph₂(CH₂Ph)P</u>	Mono-addition

6.8 – 7.5	multiplets	-	Ph $\underline{\underline{^1\text{H}}}$	Mono & Di
7.65	Doublet	$^3J_{\text{HH}} = 8.0$	Ph $\underline{\underline{^1\text{H}}}$	Mono-addition
7.72	doublet of doublets	$^3J_{\text{HH}} = 15.2$ $^3J_{\text{HH}} = 7.9$	Ph $\underline{\underline{^1\text{H}}}$	Di-addition

^{31}P NMR spectrum : 162MHz, solvent C_6D_6

δ (ppm)	Multiplicity	Integral	Assignment
24.8	singlet	0.29P	$\text{Ph}_2(\text{CH}_2\text{Ph})\underline{\underline{\text{P}}}\text{NCO}_2\text{Me}$
25.4	singlet	0.71P	$\text{Ph}_2[\text{C}(\text{H})(\text{Ph})\text{CO}_2\text{Me}]\underline{\underline{\text{P}}}\text{NCO}_2\text{Me}$ 27

3.5 Preparation of compounds 28-50.

These compounds will be discussed in further detail in **Chapter 7**.

3.5.1 Preparation of compound 28.



To a solution of $\text{Ph}_2\text{P}(\text{o-C}_6\text{H}_4\text{OMe})$ (9g, 31 mmol) (previous prepared via the literature method)⁷ in toluene (80 ml) was added methyl bromide (16ml, 3.04g, 2M in Et_2O). The solution was then stirred for 4 hours and the resulting precipitate was filtered and dried in vacuo. A sample of the solid was recrystallised from hot acetonitrile to yield crystal suitable for X-ray analysis.

Yield : 10.1g (85%)

Melting Point : 148-149°C

IR Spectrum : ν 2966 cm^{-1} , 2850 cm^{-1} and 1463 cm^{-1} C-H stretches of the Nujol mull.

⁷ W. E. McEwen, W. Shiao, Y. Yeh, D. N. Schulz, R. U. Pagilagan, J. B. Levy, C. Symmes Jr, G. O. Nelson and I. Granoth, *J. Am. Chem. Soc.*, **97**, pp.1787-1794 (1975).

Chapter 3 - Experimental

ν 1587cm⁻¹ Aromatic hydrocarbon ring vibration

ν 916cm⁻¹ P-C salt stretch

ν 742cm⁻¹ 1,2 disubstituted benzene derivative

¹H NMR spectrum : 200MHz, solvent CDCl₃

δ (ppm)	Multiplicity	Integral	Coupling (Hz)	Assignment
3.2	doublet	3H	$^2J_{PH} = 13.6$	$P^+CH_3Br^-$
3.8	singlet	3H	-	Ph ₂ P(PhOMe)
7.0 - 7.8	multiplet	14H	-	Ph ¹ Hs

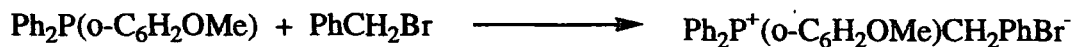
³¹P NMR spectrum : 81MHz, solvent CDCl₃

δ (ppm)	Multiplicity	Assignment
21.1	singlet	$P^+CH_3Br^-$

Elemental Analysis : C₂₀H₂₀POBr, M_r = 387.26

	C	H
% Mass by Calculation	62.03	5.21
% Mass by Analysis	61.88	5.07

3.5.2 Preparation of 29.



o-Anisyl diphenyl phosphine (6g, 21mmol) was dissolved in 100ml of toluene. To the above solution was added benzyl bromide (2.7ml, 3.93g, 23mmol). The reaction mixture was stirred for 24 hours upon which there was a white precipitate. The precipitate was filtered off and dried under vacuum. A small amount of the salt was recrystallised from hot acetonitrile, to yield a sample of crystals suitable for X-ray diffraction.

Yield : 7.8g (82%)

Melting Point : 240-242°C¹H NMR spectrum : 200MHz, solvent CDCl₃

δ (ppm)	Multiplicity	Integral	Coupling (Hz)	Assignment
3.8	singlet	3H	-	<u>OMe</u>
5.1	doublet	2H	² J _{PH} = 15.2	P ⁺ <u>CH</u> ₂ Ph
7.0 – 7.9	multiplet	19H	-	Ph ¹ <u>H</u>

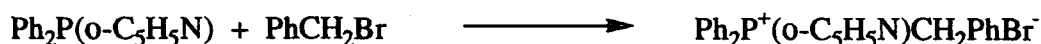
³¹P NMR spectrum : 81MHz, solvent CDCl₃

δ (ppm)	Multiplicity	Coupling (Hz)	Assignment
22.6	singlet (with visible coupling)	¹ J _{PC} = 82.8	<u>P</u> ⁺ CH ₂ Ph

Elemental Analysis : C₂₆H₂₄POBr, M_r = 463.094

	C	H
% Mass by Calculation	67.38	5.22
% Mass by Analysis	67.11	5.17

3.5.3 Preparation of 30.



Diphenyl-2-pyridyl phosphine (5g, 19mmol) was dissolved in 100ml of toluene. To the above solution was added benzyl bromide (2.5ml, 3.59g, 21mmol). The reaction mixture was stirred for 24 after which a white precipitate was filtered off and dried under vacuum. A small amount of the salt was recrystallised from a minimal amount of hot acetonitrile to yield a sample of crystals suitable for X-ray diffraction.

Yield : 4.1g (50%)

Melting Point : 196-197°C¹H NMR spectrum : 200MHz, solvent CDCl₃

δ (ppm)	Multiplicity	Integral	Coupling (Hz)	Assignment
5.2	doublet	2H	² J _{PH} = 15.0	P ⁺ CH ₂
6.9 – 7.2	multiplet	6H	-	Ph ¹ H
7.5 – 7.7	multiplet	10H	-	Ph + 2-Py ¹ H
7.9 – 8.1	multiplet	1H	-	2-Py ¹ H
8.2 – 8.3	multiplet	1H	-	2-Py ¹ H
8.8 – 8.9	multiplet	1H	-	2-Py ¹ H

³¹P NMR spectrum : 81MHz, solvent CDCl₃

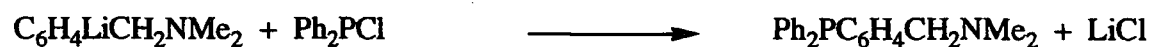
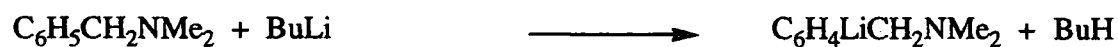
δ (ppm)	Multiplicity	Assignment
20.6	singlet	P ⁺ CH ₂ Ph

Elemental Analysis : C₂₄H₂₁NPBr, M_r = 434.288

	C	H	N
% Mass by Calculation	66.37	4.87	3.23
% Mass by Analysis	64.93	4.63	3.02

3.5.4 Preparation of 31

Production of o-diphenylphosphino-N,N'-dimethylbenzylamine



The following phosphine was produced by modifying a literature procedure⁸ and thus improving the yield by 20%. N,N'-dimethylbenzylamine (11.3ml, 75mmol) was added to

⁸ F. T. Patino, T. B. Rauchfuss and D. M. Roundhill, *Inorg. Chem.*, **14**, 652 (1975).

ether (100ml) containing butyllithium (50ml, 80mmol). After stirring of the solution overnight a yellow precipitate was afforded and subsequently isolated and dried *in vacuo*. The solid was added to 100ml of fresh ether and cooled to -78°C , chlorodiphenylphosphine was added dropwise and the reaction mixture was allowed to warm to room temperature. After filtration to remove the lithium chloride, the ether was removed *in vacuo* and the remaining brown slurry vacuum distilled to yield a colourless viscous liquid (160° , 10^{-1} torr).

Yield : 13.8g (58%)

Melting Point : $54-56^{\circ}\text{C}$

^1H NMR spectrum : 400MHz, solvent CDCl_3

δ (ppm)	Multiplicity	Integral	Assignment
2.1	singlet	6H	CH_2NMe_2
3.6	singlet	2H	CH_2NMe_2
6.9 – 7.5	multiplet	14H	Ph ^1H

^{31}P NMR spectrum : 162MHz, solvent CDCl_3

δ (ppm)	Multiplicity	Assignment
-14.2	singlet	$\text{Ph}_2\text{PC}_6\text{H}_4$

Production of o-diphenylphosphonium-(N,N'-dimethylbenzylamine) benzyl bromide.



To o-diphenylphosphino-N,N'-dimethylbenzylamine (6.9g, 22mmol) in 100ml of toluene was added benzyl bromide (3ml, 24mmol) and the mixture was allowed to stir at room temperature for 4hours. After this time dry diethyl ether was added and the ensuing white precipitate was isolated and dried *in vacuo*. A small amount of this salt was recrystallised from hot acetonitrile.

Yield : 2.2g (21%)

Melting Point : 188-190°C¹H NMR spectrum : 400MHz, solvent CDCl₃

δ (ppm)	Multiplicity	Integral	Coupling (Hz)	Assignment
1.7	singlet	6H	-	CH ₂ NMe ₂
3.3	singlet	2H	-	<u>CH</u> ₂ NMe ₂
5.2	doublet	2H	² J _{PH} = 15.1	P ⁺ CH ₂ Ph
7.0 – 7.6	multiplet	14H	-	Ph ¹ H

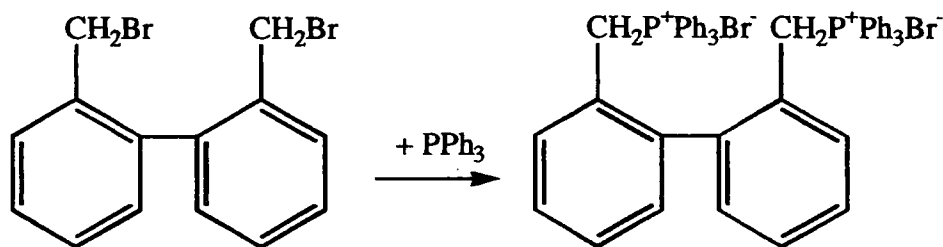
³¹P NMR spectrum : 162MHz, solvent CDCl₃

δ (ppm)	Multiplicity	Assignment
23.9	singlet	Ph ₂ <u>P</u> C ₆ H ₄

Elemental Analysis : C₂₈H₂₉NPBr, M_r = 490.41

	C	H	N
% Mass by Calculation	68.58	5.96	2.85
% Mass by Analysis	67.80	5.90	2.78

3.5.5 Preparation of 32.



2,2'-bis(bromomethyl)-1,1'-biphenyl (10.2g, 30 mmol) was added to triphenylphosphine (16.2g, 62 mmol) in 180ml of acetonitrile. The solution was stirred for 24 hours in an oil bath at 35°C. The resulting precipitate was filtered and then dried in vacuo. A small sample was recrystallized from a minimal amount of hot acetonitrile to yield a crop of crystals suitable for X-ray diffraction.

Yield : 24.5g (94%)

Melting Point : 350-351°C

IR Spectrum : ν 2920 cm^{-1} , 2849 cm^{-1} and 1461 cm^{-1} C-H stretches of the Nujol mull.

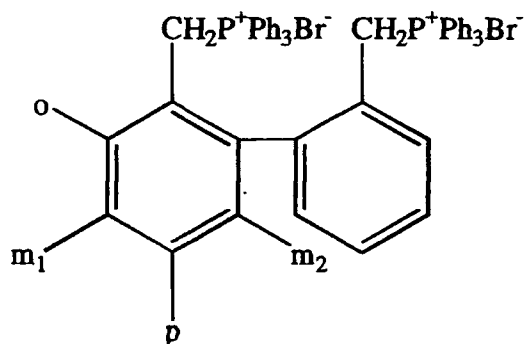
ν 1583 cm^{-1} Aromatic hydrocarbon ring vibration.

ν 994 cm^{-1} P-C salt stretch.

^1H NMR spectrum : 200MHz, solvent CDCl_3

δ (ppm)	Multiplicity	Integral	Coupling (Hz)	Assignment
4.1	triplet	2H	$^2J_{\text{PH}} = 15.0$ $^2J_{\text{HH}} = 15.5^*$ <small>*From ^{31}P decoupled ^1H</small>	<u>CH_2</u>
5.6	doublet	2H	$^3J_{\text{HH}} = 7.8$	o bpap
5.9	triplet	2H	$^2J_{\text{PH}} = 15.0$ $^2J_{\text{HH}} = 15.5^*$ <small>*From ^{31}P decoupled ^1H</small>	<u>CH_2</u>
7.0	multiplet	2H	-	m1 bpap
7.2	multiplet	2H	-	m2 bpap
7.3	multiplet	2H	-	p bpap
7.4 - 7.8	multiplet	30H	-	$\text{P}^+ \text{Ph}_3\text{Br}^-$

bpap = biphenyl aromatic protons



Assignments of ortho, meta and para came from a ^1H - ^1H COSY spectrum

³¹P NMR spectrum : 81MHz, solvent CDCl₃

δ (ppm)	Multiplicity	Assignment
23.8	singlet	<u>P</u> ⁺ Ph ₃ Br ⁻

Elemental Analysis : C₅₀H₄₂P₂Br₂, M_r = 864.64

	C	H
% Mass by Calculation	69.46	4.90
% Mass by Analysis	69.22	4.79

3.5.6 Preparation of 33.

To a solution of 1,4 bis(diphenylphosphino) butane (6.53g, 15.3mmol) in 100ml of acetonitrile was added methyl bromide (16.5ml, 33mmol 2M in Et₂O). The reaction was stirred under an argon atmosphere for 24 hours, and then the salt was precipitated fully using dry diethyl ether. The salt was isolated and dried under vacuum.

Yield : 6.9g (73%)Melting Point : 350-351°C¹H NMR spectrum : 200MHz, solvent CDCl₃

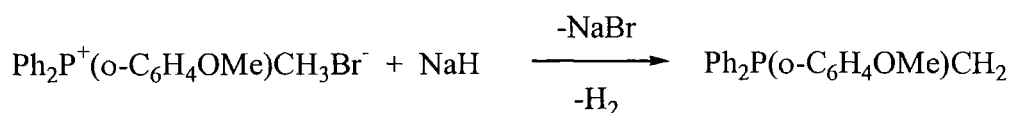
δ (ppm)	Multiplicity	Integral	Assignment
2.0 - 2.1	multiplet	4H	CH ₂ (C ₂ <u>H</u> ₄)C
2.7 - 2.8	multiplet	6H	P ⁺ <u>CH</u> ₃ Br ⁻
3.5 - 3.6	multiplet	4H	<u>CH</u> ₂ (C ₂ H ₄) <u>CH</u> ₂
7.6 - 7.7	multiplet	12H	m & p Ph <u>H</u>
7.9 - 8.0	multiplet	8H	o Ph <u>H</u>

³¹P NMR spectrum : 81MHz, solvent CDCl₃

δ (ppm)	Multiplicity	Assignment
25.6	singlet	<u>P</u> ⁺ CH ₃ Br ⁻

Elemental Analysis : C₃₀H₃₄P₂Br₂, M_r = 616.055

	C	H
% Mass by Calculation	58.44	5.56
% Mass by Analysis	58.39	5.50

3.5.7 Preparation of 34.

NaH (0.24g, 10 mmol) was added to the anisyl methyl bromide salt (3.87g, 10 mmol) in an evacuated round bottomed flask. To it was added 100ml of dry thf and the mixture was heated externally by an oil bath at 55°C. After 24 hours, the resulting bright yellow suspension was cooled to room temperature and filtered to remove the NaBr and any unreacted NaH. Nearly all the remaining thf was removed in vacuo, and the resulting slurry was warmed to redissolve the ylide. It was then placed in a freezer whereupon it yielded a bright yellow solid.

Yield : 0.9g (29%)Melting Point : 80-81°C¹H NMR spectrum : 200MHz, solvent C₆D₆

δ (ppm)	Multiplicity	Integral	Coupling (Hz)	Assignment
1.0	doublet	2H	² J _{PH} = 6.2	P <u>CH</u> ₂
3.0	singlet	3H	-	P(C ₆ H ₄ <u>OMe</u>)

6.4 - 8.0	multiplet	14H	-	aromatic <u>¹H</u> s
-----------	-----------	-----	---	---------------------------------

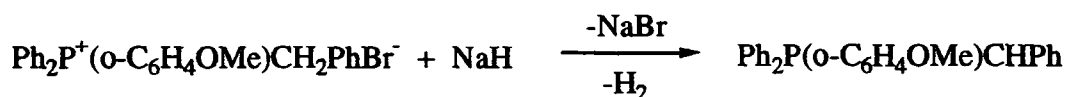
³¹P NMR spectrum : 81MHz, solvent C₆D₆

δ (ppm)	Multiplicity	Assignment
19.5	singlet	<u>P</u> CH ₂

Elemental Analysis : C₂₀H₁₉PO, M_r = 306.144

	C	H
% Mass by Calculation	78.40	6.26
% Mass by Analysis	78.02	6.18

3.5.8 Preparation of 35.



o-Anisyl diphenyl phosphonium benzyl bromide (7.8g, 16.9mmol) and sodium hydride (0.432g, 18mmol) were stirred in 150ml of thf for a period of 24 hours. After this time the sodium bromide and any unreacted sodium hydride were filtered off and the remaining THF was reduced under vacuum to leave a dark red slurry. 15ml of toluene was then added and the solid heated back into solution. This solution was then left at room temperature whereupon crystals suitable for X-ray diffraction were obtained.

Yield : 3.7g (58%)

Melting Point : 186-187°C

¹H NMR spectrum : 200MHz, solvent C₆D₆

δ (ppm)	Multiplicity	Integral	Assignment
2.8	singlet	3H	<u>Me</u>

Chapter 3 - Experimental

3.0	broad singlet	1H	PCHPh
6.3 – 8.2	multiplet	19H	Ph ¹ H

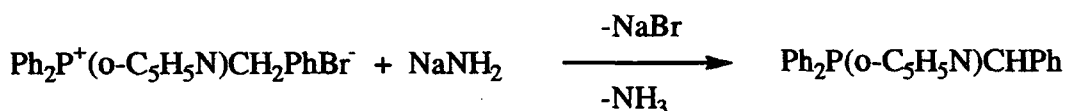
³¹P NMR spectrum : 81MHz, solvent C₆D₆

δ (ppm)	Multiplicity	Assignment
8.3	singlet	<u>P</u> C(H)Ph

Elemental Analysis : C₂₆H₂₃PO, M_r = 382.182

	C	H
% Mass by Calculation	81.64	6.07
% Mass by Analysis	81.33	5.98

3.5.9 Preparation of 36.



Diphenyl-2-pyridyl phosphonium benzyl bromide (5.5g, 12.67mmol) and sodium amide (0.546g, 14mmol) were stirred in 150ml of thf for a period of 24 hours. After this time the sodium bromide and any unreacted sodium amide were filtered off and the remaining thf was reduced under vacuum to leave a dark red slurry. Toluene (20ml) was then added and the solid heated back into solution. This solution was then left at room temperature whereupon crystals suitable for X-ray diffraction were obtained.

Yield : 3.2g (71%)

Melting Point : 190-191°C

¹H NMR spectrum : 200MHz, solvent C₆D₆

δ (ppm)	Multiplicity	Integral	Coupling (Hz)	Assignment
---------	--------------	----------	---------------	------------

Chapter 3 - Experimental

2.4	doublet	2H	$^2J_{PH} = 17.0$	PC(<u>H</u>)Ph
6.0 – 7.8	multiplet	19H	-	2-Py & Ph 1H

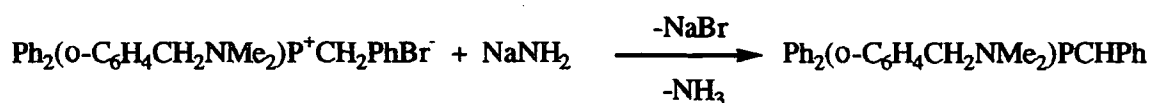
^{31}P NMR spectrum : 81MHz, solvent C_6D_6

δ (ppm)	Multiplicity	Assignment
3.7	singlet	<u>PC</u> (H)Ph

Elemental Analysis : $C_{26}H_{20}NP$, $M_r = 353.38$

	C	H	N
% Mass by Calculation	81.57	5.70	3.96
% Mass by Analysis	79.14	5.60	3.85

3.5.10 Preparation of 37.



o-diphenylphosphonium-(N,N'-dimethylbenzylamine) benzyl bromide (0.490g, 1mmol) was added to sodium amide (0.042g, 1mmol) in 30ml of thf. The reaction mixture was stirred overnight and then filtered to remove sodium bromide and any unreacted sodium amide. The thf was reduced to a minimum *in vacuo* and toluene added. The suspension was heated to aid dissolution and left to stand at room temperature whereupon an orange solid was obtained.

Yield : 0.2g (49%)

Melting Point : 178-180°C

1H NMR spectrum : 400MHz, solvent C_6D_6

δ (ppm)	Multiplicity	Integral	Coupling (Hz)	Assignment
1.7	singlet	6H	-	CH_2NMe_2

2.8	doublet	1H	$^2J_{PH} = 16.8$	P <u>C</u> HPh
3.3	singlet	2H	-	<u>CH</u> ₂ NMe ₂
7.0 – 7.6	multiplet	19H	-	Ph ¹ <u>H</u>

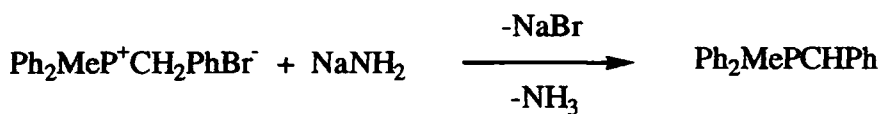
^{31}P NMR spectrum : 162MHz, solvent C_6D_6

δ (ppm)	Multiplicity	Assignment
7.1	singlet	Ph ₂ <u>P</u> C ₆ H ₄

Elemental Analysis : $\text{C}_{28}\text{H}_{28}\text{NP}$, $M_r = 409.50$

	C	H	N
% Mass by Calculation	82.13	6.89	3.42
% Mass by Analysis	81.76	6.70	3.28

3.5.11 Preparation of 38.



Methyldiphenyl phosphonium benzyl bromide (15g, 40.4mmol) and sodium amide (1.64g, 42mmol) were stirred under an argon atmosphere in dry thf (150ml) for 24 hours. Upon completion the reaction mixture was filtered to remove sodium bromide and any unreacted sodium amide. The thf was removed in vacuo to leave a bright orange slurry which was then dissolved in 5ml of toluene with heating. Upon standing at room temperature for a few hours a crystalline material was obtained.

Yield : 7.9g (68%)

Melting Point : 122-123°C (This is in agreement with the literature value)⁹

⁹ W. J. Ward and W. E. M^cEwen, *J. Org. Chem.*, **55**, 2, 493, (1990).

¹H NMR spectrum : 200MHz, solvent C₆D₆

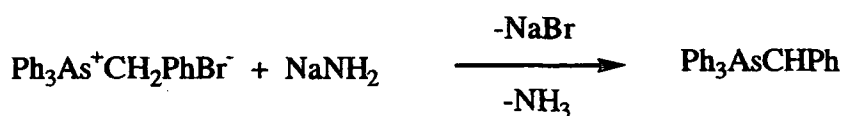
δ (ppm)	Multiplicity	Integral	Coupling (Hz)	Assignment
1.3 - 1.5	doublet	3H	² J _{PH} = 14.6	Ph ₂ <u>Me</u> P
2.4 - 2.5	singlet	1H	-	P <u>CH</u> Ph
6.6 - 7.6	multiplet	15H	-	Ph ¹ <u>H</u>

³¹P NMR spectrum : 81MHz, solvent C₆D₆

δ (ppm)	Multiplicity	Assignment
0.4	singlet	Ph ₂ MeP <u>CH</u> Ph

Elemental Analysis : C₂₀H₁₉P, M_r = 290.322

	C	H
% Mass by Calculation	82.74	6.60
% Mass by Analysis	82.25	6.57

3.5.12 Preparation of 39.

Triphenyl arsonium benzybromide (9g, 18.85mmol) and sodium amide (0.78g, 20mmol) were combined in a round bottomed flask containing 100ml of dry thf. This mixture was allowed to stir under nitrogen at room temperature for 72 hours resulting in a bright orange solution. After filtration to remove sodium bromide and any unreacted sodium amide the thf was removed in vacuo to leave a dark red slurry. Toluene (20ml) was added and the reaction heated to aid dissolution. Refrigeration of the red solution at -20°C yielded orange crystals, and recrystallisation in toluene followed by storage at 5°C for a week yielded crystals suitable for X-ray analysis.

Yield : 4.5g (60%)

Melting Point : 215-216°C

IR Spectrum : ν 2920 cm^{-1} , 2851 cm^{-1} and 1461 cm^{-1} C-H stretches of the Nujol mull.

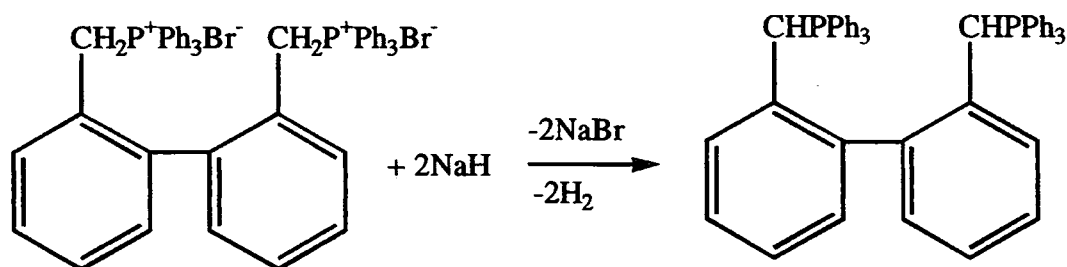
ν 1575 cm^{-1} Aromatic hydrocarbon ring vibration.

ν 692 cm^{-1} Arsenic-Carbon stretch

^1H NMR spectrum : 200MHz, solvent C_6D_6

δ (ppm)	Multiplicity	Integral	Assignment
3.9	singlet	1H	AsCH $\underline{\text{H}}$ PhBr
6.8-7.8	multiplet	20H	Ph $\underline{\text{H}}$

3.5.13 Preparation of 40.



2,2'-bis(methyl(triphenylphosphonium bromide))-1,1'-biphenyl (4.32g, 5 mmol) was added to NaH (0.27g, 0.11 mmol) in 150ml of thf. The suspension was then stirred under argon for 24 hours at 55°C. The resulting dark red mixture was then filtered to remove the NaBr and any unreacted NaH to leave a clear dark red solution. The thf was removed in vacuo until a solid precipitate was visible. This was then heated back into the remaining thf, and placed in the freezer (-30°C) where upon a bright red solid formed.

Yield : 2.4g (68%)

Melting Point : 238-240°C

^1H NMR spectrum : 200MHz, solvent C_6D_6

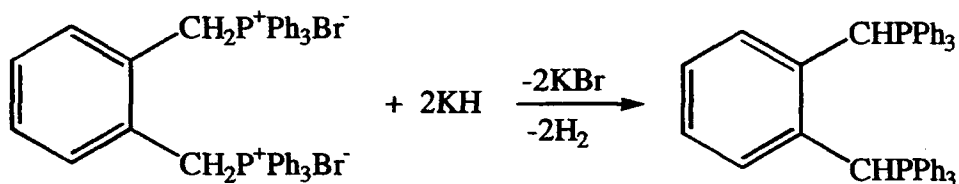
δ (ppm)	Multiplicity	Integral	Coupling (Hz)	Assignment
3.2	doublet	2H	$^2J_{\text{PH}} = 20.4$	$\text{C}(\underline{\text{H}})\text{PPh}_3$
6.8 - 7.7	multiplet	38H	-	aromatic ^1H s

 ^{31}P NMR spectrum : 81MHz, solvent C_6D_6

δ (ppm)	Multiplicity	Assignment
7.8	singlet	$\text{CH}\underline{\text{P}}\text{Ph}_3$

Elemental Analysis : $\text{C}_{50}\text{H}_{40}\text{P}_2$, $M_r = 706.76$

	C	H
% Mass by Calculation	85.45	5.74
% Mass by Analysis	85.08	5.72

3.5.14 Preparation of 41.

α,α' -bis(triphenylphosphonium methyl bromide)- σ -xylene (7.88g, 10 mmol) as supplied by Aldrich, and potassium hydride (1.0g, 25mmol) were stirred in 100ml of dry thf for 12 hours at room temperature. The resulting dark red solution was filtered to remove the KBr and any unreacted KH. The thf was then removed in vacuo and the resulting red solid dissolved in a 3:2 mixture of toluene:hexane (50ml). The solution was then stored in the freezer at -30°C to yield a very small amount of solid ylide.

Yield : 0.3g (5%)Melting Point : $190\text{-}192^\circ\text{C}$

¹H NMR spectrum : 200MHz, solvent C₆D₆

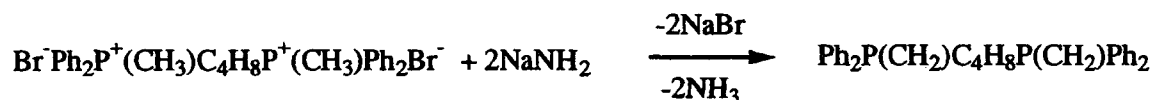
δ (ppm)	Multiplicity	Integral	Assignment
3.1	broad singlet	2H	C(<u>H</u>)PPh ₃
6.9 - 7.9	multiplet	34H	aromatic ¹ <u>H</u> s

³¹P NMR spectrum : 101MHz, solvent C₆D₆

δ (ppm)	Multiplicity	Assignment
8.3	Singlet	C(H) <u>P</u> Ph ₃

Elemental Analysis : C₄₄H₃₆P₂, M_r = 626.28

	C	H
% Mass by Calculation	84.31	5.79
% Mass by Analysis	84.01	5.49

3.5.15 Preparation of 42.

To a solution of 1,4-(bisdiphenylmethyl phosphonium) butane dibromide (5.5g, 8.9mmol) in 150 ml of thf was added sodium amide (0.759g, 19.5mmol) and the reaction mixture was then stirred under an argon atmosphere at room temperature for 24hours, whereupon a yellow colour was present. The mixture was filtered to remove the sodium bromide and any unreacted sodium amide. The thf was then reduced to a minimal amount (ca.15ml) and the resulting suspension was dissolved in toluene with heating and left to crystallise at room temperature.

Yield : 2.1g (52%)Melting Point : 168-169°C

¹H NMR spectrum : 200MHz, solvent C₆D₆.

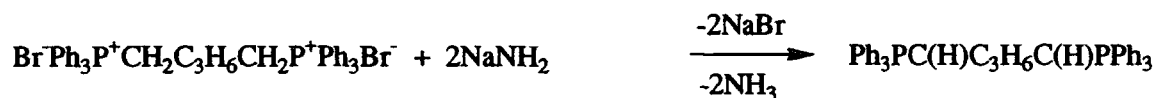
δ (ppm)	Multiplicity	Integral	Assignment
1.0 - 2.0	multiplet	12H	PCH ₂ & (CH ₂) ₄
6.8 - 6.9	multiplet	12H	m & p Ph ¹ Hs
7.4 - 7.5	multiplet	8H	o Ph ¹ Hs

³¹P NMR spectrum : 81MHz, solvent C₆D₆

δ (ppm)	Multiplicity	Assignment
17.9	singlet	Ph ₂ PCH ₂

Elemental Analysis : C₃₀H₃₂P₂, M_r = 454.496

	C	H
% Mass by Calculation	79.27	7.10
% Mass by Analysis	78.79	6.87

3.5.16 Preparation of 43.

To a round bottomed flask containing 1,5-(bistriphenyl phosphonium) pentane dibromide (9.8g, 13 mmol) was added sodium amide (1.2g, 30 mmol). The mixture was stirred, under argon in a 1:1 mixture of toluene:thf (40 ml) for 24 hours resulting in a dark red solution with a precipitate of sodium bromide. After filtration to remove any sodium bromide and unreacted sodium amide, the toluene:thf solution was reduced in vacuo. The resulting dark red slurry was heated until it redissolved and left to crystallise at room temperature.

Yield : 5.2g (67%)

Melting Point : 118-119°C

IR Spectrum : ν 2960 cm^{-1} , 2850 cm^{-1} and 1463 cm^{-1} C-H stretches of the Nujol mull.
 ν 1568 cm^{-1} Aromatic hydrocarbon ring vibration.
 ν 865 cm^{-1} P=C ylide stretch.

^1H NMR spectrum : 200MHz, solvent C_6D_6

δ (ppm)	Multiplicity	Integral	Coupling (Hz)	Assignment
1.2	doublet of triplets	2H	$^2J_{\text{PH}} = 17.8$ $^3J_{\text{HH}} = 7.7$	$\text{Ph}_3\text{PC}(\underline{\text{H}})$
2.2	quintet	2H	$^3J_{\text{HH}} = 7.1$	$\text{CH}_2\text{CH}_2\text{CH}_2$
2.6	doublet of triplets	4H	$^3J_{\text{HH}} = 8.0$ $^3J_{\text{HH}} = 7.6$	$\underline{\text{CH}}_2\text{CH}_2\underline{\text{CH}}_2$
7.0 - 7.8	multiplet	30H	-	aromatic ^1H s

^{31}P NMR spectrum : 81MHz, solvent C_6D_6

δ (ppm)	Multiplicity	Assignment
12.0	singlet	$\text{Ph}_3\underline{\text{P}}\text{C}(\text{H})$

Elemental Analysis : $\text{C}_{41}\text{H}_{38}\text{P}_2$, $M_r = 592.70$

	C	H
% Mass by Calculation	83.09	6.46
% Mass by Analysis	81.94	5.95

3.5.17 Preparation of 44.

Preparation of benzyldiphenyl phosphine



Chapter 3 - Experimental

To benzyl magnesium chloride (40ml, 1M solⁿ in Et₂O) in 150ml of toluene was added chlorodiphenylphosphine (7.2ml, 40mmol) dropwise over a period of one hour. The reaction mixture was stirred for a further 30 minutes and then filtered to remove magnesium chloride. The ether was removed *in vacuo* and the phosphine recovered.

Yield : 8.5g (77%)

Melting Point : 142-143°C

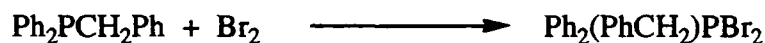
¹H NMR spectrum : 200MHz, solvent CDCl₃

δ (ppm)	Multiplicity	Integral	Assignment
2.9	singlet	2H	PCH ₂ Ph
6.7 – 6.9	multiplet	9H	m & p Ph ¹ H
7.0 – 7.1	multiplet	6H	o Ph ¹ H

³¹P NMR spectrum : 81MHz, solvent CDCl₃

δ (ppm)	Multiplicity	Assignment
-9.1	singlet	Ph ₂ PCH ₂ Ph

Preparation of benzyldiphenyl phosphorus dibromide



To a sample of benzyldiphenyl phosphine (3.5g, 12.7mmol) in acetonitrile (100ml) was added bromine (0.67ml, 2.08g, 13mmol) dropwise over 30 minutes. Upon addition the reaction mixture was allowed to stir for 4 hours whereupon a small amount of precipitate had formed. This was isolated for NMR analysis and then added back to the acetonitrile.

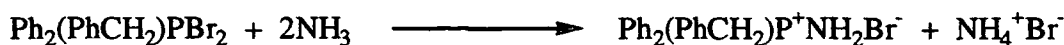
¹H NMR spectrum : 200MHz, solvent CDCl₃

δ (ppm)	Multiplicity	Integral	Assignment
0.0 – 0.1	singlet	2H	Ph ₂ PCH ₂ Ph
7.0 – 8.0	multiplet	15H	Ph ¹ H

³¹P NMR spectrum : 81MHz, solvent CDCl₃

δ (ppm)	Multiplicity	Assignment
64.8	singlet	Ph ₂ Bz <u>P</u> Br ₂

Preparation of benzyldiphenyl phosphonioammonium bromide



To the acetonitrile solution obtained in the previous part of the reaction was added gaseous ammonia over a period of 2 hours. Upon addition the reaction was allowed to stir at room temperature for 1 hour after which time the acetonitrile was removed *in vacuo*. Chloroform (50ml) was added and the undissolved ammonium bromide filtered off, the salt was then fully precipitated with diethyl ether, filtered and dried *in vacuo*.

Yield : 1.1g (24%)Melting Point : 157-159°C¹H NMR spectrum : 200MHz, solvent CDCl₃

δ (ppm)	Multiplicity	Integral	Coupling (Hz)	Assignment
4.2 – 4.3	doublet	2H	² J _{PH} = 15.6	Ph ₂ P <u>CH</u> ₂ Ph
6.1	singlet	2H	-	P ⁺ <u>NH</u> ₂ Br ⁻
7.0 – 7.2	multiplet	5H	-	Ph ¹ <u>H</u>
7.4 – 7.7	multiplet	10H	-	Ph ¹ <u>H</u>

³¹P NMR spectrum : 81MHz, solvent CDCl₃

δ (ppm)	Multiplicity	Assignment
40.1	singlet	<u>P</u> ⁺ NH ₂ Br ⁻

Elemental Analysis C₁₉H₁₉PNBr, Mr = 372.231

	C	H	N
% Mass by Calculation	61.31	5.15	3.76
% Mass by Analysis	60.90	4.99	3.70

3.5.18 Preparation of 45.

Preparation of methyldiphenylphosphorus dichloride¹⁰

Methyldiphenylphosphine (10g, 50mmol) was placed in a round bottomed flask containing dry acetonitrile (100ml). Hexachloroethane (12.3g, 52mmol) was added and the reaction mixture was refluxed for 1 hour under an argon atmosphere. The solution was allowed to cool to room temperature and then the acetonitrile and tetrachloroethene were removed in vacuo. The compound was recrystallised from acetonitrile/ pet ether (1:1, 40ml) and then dried in vacuo.

Yield : 11.1g (82%)

Melting Point : 115-116°C

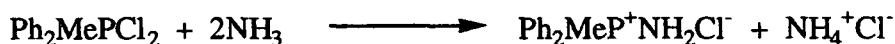
¹H NMR spectrum : 200MHz, solvent CDCl₃

δ (ppm)	Multiplicity	Integral	Coupling (Hz)	Assignment
2.5 – 2.6	doublet	3H	² J _{PH} = 14.0	Ph ₂ <u>Me</u> PCl ₂
7.6 – 7.8	multiplet	6H	-	m & p Ph ¹ <u>H</u>
7.9 – 8.1	multiplet	4H	-	o Ph ¹ <u>H</u>

³¹P NMR spectrum : 81MHz, solvent CDCl₃

δ (ppm)	Multiplicity	Assignment
71.0	singlet	Ph ₂ Me <u>P</u> Cl ₂

Preparation of methyldiphenylphosphorus ammonium chloride



¹⁰ R. Appel and H. Scholer, *Chem. Ber.*, **110**, 2382 (1977).

Chapter 3 - Experimental

Methyldiphenyl phosphorus dichloride (11.1g, 41mmol) was placed in a round bottomed flask and acetonitrile (150ml) was added. Gaseous ammonia was bubbled through the solution for 4 hours at room temperature under a nitrogen atmosphere. The reaction mixture was stirred overnight, acetonitrile was removed in vacuo and the solid product dissolved in dry chloroform. The suspension was then filtered to remove the ammonium chloride, and the phosphonium salt was then precipitated fully using dry ether. The product was then dried in vacuo and isolated.

Yield : 8g (77%)

Melting Point : 165-166°C (This is in agreement with the literature value).¹¹

¹H NMR spectrum : 200MHz, solvent CDCl₃

δ (ppm)	Multiplicity	Integral	Coupling (Hz)	Assignment
2.5 – 2.6	doublet	3H	² J _{PH} = 14.0	Ph ₂ <u>Me</u> PNH ₂
6.9 – 7.0	br singlet	2H	-	<u>NH</u> ₂
7.5 – 7.7	multiplet	6H	-	m & p Ph ¹ <u>H</u>
7.8 – 8.0	multiplet	4H	-	o Ph ¹ <u>H</u>

³¹P NMR spectrum : 81MHz, solvent CDCl₃

δ (ppm)	Multiplicity	Assignment
24.2	singlet	Ph ₂ Me <u>P</u> N

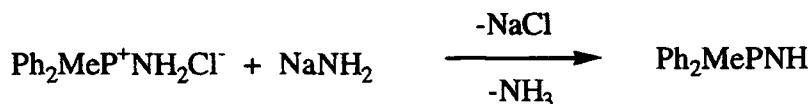
Elemental Analysis : C₁₃H₁₅PNCl, M_r = 251.566

	C	H	N
% Mass by Calculation	62.02	6.01	5.57
% Mass by Analysis	61.88	5.89	5.50

¹¹ W. S. Brey, S. R. Jain and H. H. Sisler, *Inorg. Chem.*, 6, 515 (1967).

Chapter 3 - Experimental

Preparation of methyldiphenyliminophosphorane



Methyldiphenylphosphonio ammonium chloride (8g, 32mmol) and sodium amide (1.37g, 35mmol) were stirred together in thf (100ml) under an argon atmosphere. After stirring for 24 hours, the reaction mixture was filtered to remove sodium bromide and any unreacted sodium amide. The thf was then reduced in vacuo until a slurry was obtained, after which toluene/hexane (1:8, 18ml) was added. The mixture was heated to aid dissolution and then left to cool to room temperature whereupon a crystalline material was obtained.

Yield : 5.5g (79%)

Melting Point : 62-63°C

¹H NMR spectrum : 200MHz, solvent C₆D₆

δ (ppm)	Multiplicity	Integral	Coupling (Hz)	Assignment
0.2 – 0.4	br singlet	1H	-	<u>NH</u>
1.2 - 1.3	doublet	3H	² J _{PH} = 13.0	Ph ₂ <u>Me</u> P
6.7 - 6.9	multiplet	6H	-	m & p Ph ¹ <u>H</u>
7.3 - 7.4	multiplet	4H	-	o Ph ¹ <u>H</u>

³¹P NMR spectrum : 81MHz, solvent CDCl₃

δ (ppm)	Multiplicity	Assignment
14.7	singlet	Ph ₂ Me <u>P</u> NH

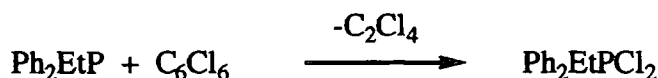
Elemental Analysis : C₁₃H₁₄PN, M_r = 215.22

	C	H	N
% Mass by Calculation	72.54	6.56	6.51
% Mass by Analysis	71.55	6.47	6.31



3.5.19 Preparation of 46.

Preparation of ethyldiphenylphosphorus dichloride



Ethyldiphenylphosphine (10g, 46.7mmol) and hexachloroethane (11.9g, 50mmol) were refluxed together in 100ml of dry acetonitrile under an inert argon atmosphere for 1 hour. After refluxing the solvent and tetrachloroethene were removed by distillation and the product recrystallised from acetonitrile/petrol ether 60/40 (1:1).

Yield : 4g (30%)

Melting Point : 165-167°C (This is in agreement with the literature value).⁹

¹H NMR spectrum ; 200MHz, solvent CDCl₃

δ (ppm)	Multiplicity	Integral	Assignment
1.3 - 1.5	multiplet	3H	Et CH ₃
4.1 - 4.4	multiplet	2H	Et CH ₂
7.6 - 8.3	multiplet	10H	Ph ¹ H _s

³¹P NMR spectrum ; 81MHz, solvent CDCl₃

δ (ppm)	Multiplicity	Assignment
81.4	singlet	Ph ₂ EtP <u>Cl</u> ₂

Preparation of ethyldiphenyl phosphorus ammonium chloride



To a solution of ethyldiphenyl phosphorus dichloride (4g, 14mmol) in dry acetonitrile (100ml), hexamethyldisilazane (2.42g, 15mmol, 3.16ml) was added dropwise to cause a steady reflux. After addition the mixture was refluxed for a further 6 hours and the

Chapter 3 - Experimental

acetonitrile was removed in vacuo. Ethyldiphenyl trimethylsilylimine was then extracted using petrol ether 60/40, and the required salt was separated and dried in vacuo.

Yield : 3.6g (97%)

Melting Point : 164-166°C

¹H NMR spectrum : 200MHz, solvent CDCl₃

δ (ppm)	Multiplicity	Integral	Assignment
1.0 - 1.4	multiplet	3H	Et <u>CH</u> ₃
2.1 - 2.4	multiplet	1H	1 Et <u>CH</u> ₂
2.7 - 3.0	multiplet	1H	1 Et <u>CH</u> ₂
6.6 - 7.0	br singlet	2H	<u>NH</u> ₂
7.4 - 8.0	multiplet	10H	Ph ¹ <u>H</u> s

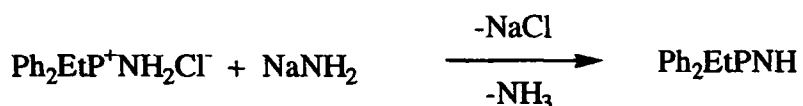
³¹P NMR spectrum : 81MHz, solvent CDCl₃

δ (ppm)	Multiplicity	Assignment
42.6	singlet	Ph ₂ Et <u>P</u> ⁺ NH ₂ Cl

Elemental Analysis : C₁₄H₁₇PNCl, M_r = 265.582

	C	H	N
% Mass by Calculation	63.26	6.45	5.27
% Mass by Analysis	63.21	6.40	5.22

Preparation of ethyldiphenyliminophosphorane



Ethyldiphenyl phosphorus ammonium chloride (3.6g, 13.6mmol) and sodium amide (0.59g, 15mmol) were stirred together in dry thf (100ml) under an inert argon atmosphere for 24hrs. After this time the suspension was filtered to remove sodium chloride and any

unreacted sodium amide and the thf removed in vacuo. The resulting solid was dissolved in toluene/hexane (1:1, 10ml) and left to crystallise at room temperature.

Yield : 1.9g (59%)

Melting Point : 74-75°C (this is in agreement with the literature value).¹²

¹H NMR spectrum : 200MHz, solvent C₆D₆

δ (ppm)	Multiplicity	Integral	Assignment
0.6 - 0.8	multiplet	3H	Et <u>CH</u> ₃
1.4 - 1.6	multiplet	2H	Et <u>CH</u> ₂
6.6 - 6.9	multiplet	6H	Ph ¹ <u>H</u> s
7.3 - 7.6	multiplet	4H	Ph ¹ <u>H</u> s

³¹P NMR spectrum : 81MHz, solvent C₆D₆

δ (ppm)	Multiplicity	Assignment
15.2	singlet	Ph ₂ Et <u>P</u> NH

Elemental Analysis : C₁₄H₁₆NP, M_r = 229.248

	C	H	N
% Mass by Calculation	73.34	7.04	6.11
% Mass by Analysis	72.44	6.51	6.06

3.5.20 Preparation of 47.



To a sample of triphenyliminophosphorane (0.277g, 1mmol) and tetraphenyldithiodiphosphinylimide (0.449g, 1mmol) was added toluene (5ml). The mixture was stirred at room temperature for 2 hours whereupon a white precipitate had

¹² R. Appel, *Chem. Ber.*, **98**, 1355 (1965).

formed. The mixture was then heated to aid dissolution and then left to cool to room temperature whereupon crystals were obtained.

Yield : 0.63g (87%)

Melting Point : 196-198°C

¹H NMR spectrum : 200MHz, solvent C₆D₆

δ (ppm)	Multiplicity	Integral	Assignment
7.0 – 7.2	multiplet	21H	m & p Ph ¹ H
7.4 – 7.8	multiplet	14H	o Ph ¹ H

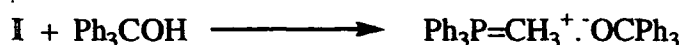
³¹P NMR spectrum : 81MHz, solvent C₆D₆

δ (ppm)	Multiplicity	Assignment
34.3	singlet	Ph ₃ P ⁺ NH ₂
37.3	singlet	Ph ₂ P(S)N

Elemental Analysis : C₄₂H₃₇P₃S₂N₂, M_r = 726.403

	C	H	N
% Mass by Calculation	69.39	5.13	3.86
% Mass by Analysis	69.27	5.10	3.77

3.5.21 Preparation of 48.



Triphenyl phosphonium methyllide (0.139g, 0.5mmol) was added to a Schlenk tube containing triphenyl methanol (0.130g, 0.5mmol). To the mixture was added 2ml of toluene and a clear yellow solution was obtained upon heating. Upon standing at -30°C for 24 hours a crystalline material was obtained.

Yield : 0.25g (93%)

Melting Point : 76-78°C

$\text{Ph}_3\text{P}=\text{CH}_2$ = 96°C

Ph_3COH = 160-163°C

^1H NMR spectrum : 200MHz, solvent C_6D_6

δ (ppm)	Multiplicity	Integral	Assignment
1.8	multiplet	3H	CH_3
7.0 - 7.1	multiplet	18H	m & p Ph ^1H
7.2 - 7.3	multiplet	6H	o Ph ^1H
7.6 - 7.7	multiplet	6H	o Ph ^1H

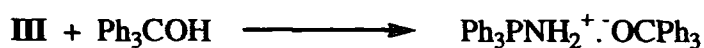
^{31}P NMR spectrum : 81MHz, solvent C_6D_6

δ (ppm)	Multiplicity	Assignment
22.3	singlet	Ph_3PCH_2

Elemental Analysis : $\text{C}_{38}\text{H}_{33}\text{OP}$, $M_r = 536.273$

	C	H
% Mass by Calculation	85.04	6.20
% Mass by Analysis	84.98	6.18

3.5.22 Preparation of 49.



Triphenyl iminophosphorane (0.140g, 0.5mmol) was added to a Schlenk tube containing triphenyl methanol (0.130g, 0.5mmol). To the mixture was added 2ml of toluene and a

clear solution was obtained upon heating. Upon standing at room temperature for one hour, needle-like crystals suitable for x-ray diffraction were obtained.

Yield : 0.25g (90%)

Melting Point : 173-175°C

$\text{Ph}_3\text{P}=\text{NH}$ = 128°C

Ph_3COH = 160-163°C

^1H NMR spectrum : 200MHz, solvent C_6D_6

δ (ppm)	Multiplicity	Integral	Assignment
6.7 - 6.9	multiplet	18H	m & p Ph ^1H
7.1 - 7.2	multiplet	6H	o Ph ^1H
7.3 - 7.4	multiplet	6H	o Ph ^1H

^{31}P NMR spectrum : 81MHz, solvent C_6D_6

δ (ppm)	Multiplicity	Assignment
20.5	singlet	$\text{Ph}_3\text{P}\underline{\text{N}}\text{H}$

Elemental Analysis : $\text{C}_{37}\text{H}_{32}\text{OPN}$, $M_r = 537.606$

	C	H	N
% Mass by Calculation	82.66	6.00	2.61
% Mass by Analysis	82.11	5.75	2.50

3.5.23 Preparation of 50.



Triphenyl phosphine oxide (0.139g, 0.5mmol) was added to a Schlenk tube containing triphenyl methanol (0.130g, 0.5mmol). To the mixture was added 2ml of toluene and a clear solution was obtained upon heating. Upon standing at room temperature for one hour, crystals suitable for x-ray diffraction were obtained.

Yield : 0.26g (95%)

Melting Point : 168-170°C

$\text{Ph}_3\text{P}=\text{O}$ = 156-158°C

Ph_3COH = 160-163°C

^1H NMR spectrum : 200MHz, solvent C_6D_6

δ (ppm)	Multiplicity	Integral	Assignment
3.4 - 3.6	multiplet	1H	COH
7.0 - 7.2	multiplet	18H	m & p Ph ^1H
7.3 - 7.4	multiplet	6H	o Ph ^1H
7.6 - 7.7	multiplet	6H	o Ph ^1H

^{31}P NMR spectrum : 81MHz, solvent C_6D_6

δ (ppm)	Multiplicity	Assignment
26.4	singlet	$\text{Ph}_3\text{P}=\text{O}$

Elemental Analysis : $\text{C}_{37}\text{H}_{31}\text{O}_2\text{P}$, $M_r = 538.588$

	C	H
% Mass by Calculation	82.51	5.80
% Mass by Analysis	81.65	5.72

4. Group 2 Metal Complexes of Phosphonium Ylides.

This chapter deals with the investigation of complexes 1-8. These complexes were synthesised according to the procedures outlined in **Chapter 3** and are listed in **Table 4.1**.

Complex Number	Chemical Formula
1	$(\text{Ph}_3\text{PCH}_2)_2 \cdot \text{Ca}[\text{N}(\text{SiMe}_3)_2]_2$
2	$(\text{Ph}_3\text{PCH}_2)_2 \cdot \text{Sr}[\text{N}(\text{SiMe}_3)_2]_2$
3	$(\text{Ph}_3\text{PCH}_2)_2 \cdot \text{Ba}[\text{N}(\text{SiMe}_3)_2]_2$
4	$[(\text{Me}_2\text{N})_3\text{PCH}_2]_2 \cdot \text{Ca}[\text{N}(\text{SiMe}_3)_2]_2$
5	$[(\text{Me}_2\text{N})_3\text{PCH}_2]_2 \cdot \text{Sr}[\text{N}(\text{SiMe}_3)_2]_2$
6	$(\text{Ph}_3\text{PCH}_2)_2 \cdot \text{MgN}[\text{PPh}_2(\text{S})]_2$
7	$(\text{Ph}_3\text{PCH}_2)_2 \cdot \text{CaN}[\text{PPh}_2(\text{S})]_2$
8	$(\text{Ph}_3\text{PCH}_2)_2 \cdot \text{Sr}[\text{OC}_6\text{H}_2(\text{Me})^t\text{Bu}_2]_2$

Table 4.1 Table of complexes discussed in Chapter 4.

4.1 Background.

In spite of the extensive organometallic chemistry displayed by magnesium,¹ and, to a lesser extent, beryllium,² the organometallic chemistry of the heavier alkaline earth metals is very sparse.³ In part, this is due to the highly ionic nature of calcium, strontium and barium complexes in general which results in simple complexes such as MR_2 being insoluble, highly reactive polymeric solids which are difficult to prepare and purify and are consequently of limited use. In recent years, however, the quest for volatile metal precursors for MOCVD in particular has led to an interest in bulky cyclopentadienyl

¹ O. S. Akkerman, F. Bickelhaupt, P. R. Markies, W. J. J. Smeets and A. L. Spek, *Adv. Organomet. Chem.*, **32**, pp.147-226 (1991).

² N. A. Bell, *Comprehensive Organometallic Chemistry (A review of the literature 1982-1994)*. Volume 1, pp.35-55.

³ A. Earnshaw and N. N. Greenwood, *Chemistry of the Elements*, 2nd Ed., chp 5, pp.127-138 (1998).

complexes of calcium, strontium and barium and a significant number of examples of these π -bonded organometallics have now been well characterised for all the Group 2 metals.⁴

The ability of phosphorus ylides to stabilise M-C bonds is well documented⁵ and was first recognised by Schmidbaur who demonstrated the property by the synthesis of remarkably stable ylide complexes of copper, silver and gold.⁶ It seemed that, in the light of this ability of ylides to stabilise M-C bonds, and in the context of our group's recent work on lithium complexes of phosphorus ylides and related complexes,⁷ complexation of phosphorus ylides to alkaline earth metal salts would be a simple method of isolating and definitively characterising unsupported σ -bonded organometallics of the heavy alkaline earth metals. The first part of this chapter concerns the synthesis, isolation and X-ray characterisation of the first neutral ylide complexes of calcium, strontium and barium which contain unambiguously characterised examples of unsupported σ -bonding between the metal and the ylidic carbon. The second part of the chapter will include further complexes which also incorporate both a group 2 metal and a phosphonium ylide.

4.2 Structural investigation of I, II, V & VIIa-c.

The components used in the synthesis of complexes 1-8 were synthesised according to the procedures outlined in Chapter 3, and are listed in the table below (Table 4.2).

⁴ For review ; (a). T. P. Hanusa, *Polyhedron.*, **9**, pp.1345-1362 (1990). (b). T. P. Hanusa, *Chem. Rev.*, **93**, pp.1023-1036 (1993).

⁵ A. W. Johnson, *Ylides and Imines of Phosphorus.*, Wiley, (1993) and relevant chapters therein.

⁶ H. Schmidbaur, *Angew. Chem., Int. Ed. Engl.*, **22**, 12, pp.907-927 (1983).

⁷ (a). D. R. Armstrong, M. G. Davidson and D. Moncrieff, *Angew. Chem., Int. Ed. Engl.*, **34**, pp.478-481 (1995). (b). A. S. Batsanov, M. G. Davidson, J. A. K. Howard, S. Lamb, C. Lustig and R. D. Price, *J. Chem. Soc., Chem. Commun.*, pp.1211- 1212 (1997). (c). R. D. Price, *Ph.D. Thesis*, University of Durham (1999).

Component Number	Chemical Formula
I	Ph_3PCH_2
II	$(\text{Me}_2\text{N})_3\text{PCH}_2$
V	$\text{HN}[\text{PPh}_2(\text{S})]_2$
VIIa-c	$\text{M}[\text{N}(\text{SiMe}_3)_2]_2$ where M=Ca, Sr & Ba for a,b and c respectively

Table 4.2 Table of components used in complexes 1-8.

The solid state structures of components I, II, V & VIIa-c have been determined by single crystal X-ray diffraction studies.^{8, 9, 10, 11} A review of their salient structural features will precede a discussion of complexes 1-8.

I is typical of an unstabilised phosphonium ylide and as such exhibits all the expected features as described in Chapter 1. The phosphorus to carbon ylidic bond [1.693\AA (ave.)]⁸ is in the range expected for phosphonium ylides¹² and the sum of the angles around the phosphorus atom is 341° which is typical for a pyramidalised phosphorus centre. Considering the ylidic carbon it can be seen from the sum of the angles around it (353°) that it deviates slightly from planarity. Other features of Ph_3PCH_2 to note are that there is a unique $\text{C}_{\text{ipso}}\text{-P-C}_{\text{ylide}}$ bond which is both longer and has a greater $\text{C}_{\text{ipso}}\text{-P-C}_{\text{ylide}}$ angle in comparison to the other two $\text{C}_{\text{ipso}}\text{-P-C}_{\text{ylide}}$ bonds, and also that it has been observed to aggregate through $\text{C-H}\cdots\pi$ interactions unlike the $\text{C-H}\cdots\text{C}$ interactions observed for triphenylphosphonium benzylide.¹³

II is a liquid at room temperature, but its solid state structure has been determined recently using special techniques.⁹ The parent phosphine and subsequently the ylide have been shown by single crystal X-ray diffraction studies and also *ab initio* molecular orbital calculations to have a C_s symmetry around the phosphorus centre rather than the expected

⁸ W. Graf, J. Jeong, G. Muller, A. Schier, H. Schmidbaur and D. L. Wilkinson, *New J. Chem.*, **13**, pp.341-352 (1989).

⁹ K.-H. Dreihaupt, N. W. Mitzel, D. W. H. Rankin, H. Schmidbaur and A. Smart, *J. Am. Chem. Soc.*, **118**, 12673 (1996).

¹⁰ F. T. Wang, *Synth. React. Inorg. Met. Chem.*, **8**, 120 (1978).

¹¹ M. Westerhausen, *Coord. Chem. Rev.*, **176**, pp.157-210 (1998) and references cited therein.

¹² D. G. Gilheany, *Chem. Rev.*, **94**, 1339 (1994) and references cited therein.

¹³ A. S. Batsanov, M. G. Davidson, J. A. K. Howard, S. Lamb and C. Lustig, *J. Chem. Soc., Chem. Commun.*, 1791 (1996).

C_3 symmetry. It is thought that the CH_2 substituent on the phosphorus decreases the energy barrier to C_s - C_3 interconversion, however the barrier is then low enough to be overridden by the sum of weak lattice forces in the crystals which goes some way to explaining the observed symmetry deviations.¹⁴ The C_s geometry of the $(Me_2N)_3P$ part of ligand **II** can be described as follows, there are two planar, vertical dimethylamino groups (ave. sum of angles = 353°) and one pyramidal, horizontal dimethylamino group (sum of angles = 337°), see **Figure 4.1**.

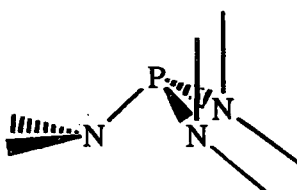


Figure 4.1 C_s symmetry for $P(NMe_2)_3$

Other salient structural features to note include a $P-C_{ylidic}$ bond length of $1.655(2)\text{\AA}$ and the sum of the angles around the phosphorus is 342° . It has been observed that the PCH_2 unit is planar.⁹ This would be in disagreement with many other known structures of unstabilised phosphonium ylides containing a pyramidalised ylide carbanion (e.g. Ligand **1**), although it must be noted that caution must be exercised when using XRD determined hydrogen positions.

V is related to both $Ph_2PN(H)PPh_2$ and $Ph_2C(O)CH_2C(O)Ph_2$, for which the transition metal chemistry is well known.^{15,16} **V** itself has been widely studied and a wealth of its transition metal co-ordination chemistry is presented in the literature.^{17a} Some of the salient structural features of **V** include an average $P=S$ bond length of 1.916\AA , a $N-H$ bond length of $0.812(2)\text{\AA}$, a $P-N$ bond length of $1.671(3)\text{\AA}$ and $P-N-P$ bond angle of $132.6(3)^\circ$.^{17b}

¹⁴ C. Lustig and N. W. Mitzel, *J. Chem. Soc., Dalton. Trans.*, pp3177-3183 (1999).

¹⁵ S. Kawaguchi, *Coord. Chem. Rev.*, **70**, 51 (1986).

¹⁶ See for example : (a). D. I. Arnold, F. A. Cotton and F. E. Kühn, *Inorg. Chem.*, **35**, 5764 (1996). (b). M. Knorr and C. Strohmann, *Eur. J. Inorg. Chem.*, 495 (1998).

^{17a} P. Bhattacharyya, A. M. Z. Slawin and M. B. Smith, *J. Chem. Soc., Dalton. Trans.*, pp2467-2475 (1998).

^{17b} H. Nöth, *Z. Naturforsch., Teil B.*, **37**, 1491 (1982).

Compounds **VIIa-c** $\{M[N(\text{SiMe}_3)_2]_2\}$ where $M=\text{Ca}$, Sr & Ba for a,b and c respectively} are valuable reagents for the incorporation of the alkaline earth metals into other molecules due to their inherent reactivity. The homoleptic alkaline earth metal bis[bis(trimethylsilyl)amides] of calcium, strontium and barium crystallize as dimeric molecules with a central M_2N_2 cycle¹¹ (**Figure 4.2**).

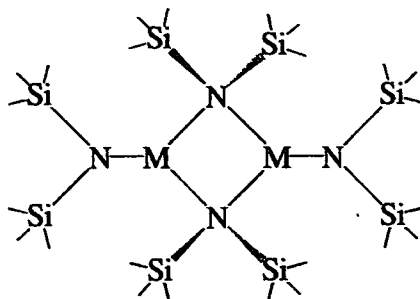


Figure 4.2 Group 2 metal amide dimer.

The molecules exhibit differing M-N bond lengths dependent upon whether the amide is bridging (N^b) or terminal (N^t) see **Table 4.3**.

M	M – N^b (Å)	M – N^t (Å)
Ca	2.47	2.27
Sr	2.64	2.44
Ba	2.82	2.58

Table 4.3 Metal to nitrogen distances in **VIIa-c**.

A similar difference, although to a lesser extent, is observed between the nitrogen to silicon distances of the bridging and terminal amides (**Table 4.4**).

M	N^b – Si (Å)	N^t – Si (Å)
Ca	1.73	1.70
Sr	1.71	1.69
Ba	1.70	1.69

Table 4.4 Nitrogen to silicon distances in **VIIa-c**.

One further structural feature to note is the large average Si – N – Si bond angle enforced by intra-ligand repulsion of the trimethylsilyl groups and even further stretched by agostic bonds between the coordinatively unsaturated metal centre and the trimethylsilyl substituent e.g. calcium 126.3°, strontium 132.3° and barium 131.7°.

Finally, in solution, the molecules remain dimeric as proven by cryoscopic measurements, although NMR studies show that there is evidence of exchange occurring between the bridging and terminal amide groups in solution.¹¹

4.3 NMR data of complexes 1-8.

All the complexes discussed in this chapter have been analysed by ³¹P and ¹H NMR spectroscopy (using d⁶-benzene as a solvent). All the complexes described herein contain at least one chemically unique phosphorus atom and as such ³¹P NMR is the most useful technique for analysis. Table 4.5 shows a ³¹P chemical shift comparison for the un-coordinated components I, II & V and the complexes 1-8.

Complex Number	Component(s) Used.	δ ³¹ P Complex (ppm)	δ ³¹ P Component (ppm)
1	I	29.3	20.7
2	I	29.8	20.7
3	I	26.9	20.7
4	II	76.7	71.3
5	II	77.2	71.3
6	I & V	24.5 & 39.6	20.7 & 57.7
7	I & V	24.5 & 39.6	20.7 & 57.7
8	I	30.2	20.7

Table 4.5 Table to show the ³¹P NMR chemical shift comparison between the starting components and the complexes.

In all cases, with the exception of V, the ^{31}P chemical shift of the complex moves to a lower field (i.e. the ^{31}P chemical shift and thus the frequency is higher) than the starting component. This can be explained simply in terms of electron density being drawn from the P-X bond to the electron deficient metal centre (i.e. deshielding of the phosphorus atom). The exception of V can be accounted for by the fact it is deprotonated in the formation of the complexes and as such has more electron density spread over and around the phosphorus atoms in the molecule giving an opposite effect to that described above.

4.4 Structural investigation of complexes 1-3.

Reaction of the metal bis(bis(trimethylsilyl)amides) VIIa-c with two equivalents of triphenylphosphonium methyllide I in toluene solution, followed by cooling at -40°C yielded a crop of yellow crystals of 1-3 in each case. Preliminary characterisation followed by X-ray crystallography revealed 1-2 to be monomeric bis-adducts of the metal amides of the general formula $(\text{Ph}_3\text{PCH}_2)_2\cdot\text{M}[\text{N}(\text{SiMe}_3)_2]_2\cdot 2\text{PhMe}$ (1-2 where M = Ca and Sr respectively). Complex 3 does not appear to contain any toluene in the crystal lattice and thus has the formula $(\text{Ph}_3\text{PCH}_2)_2\cdot\text{Ba}[\text{N}(\text{SiMe}_3)_2]_2$.

The solid state structure of complex 1 (Figure 4.3) contains a central calcium atom surrounded by two bis(trimethylsilyl)amide groups and two neutral triphenylphosphonium methyllide moieties. The angle between the calcium atom and the two ylidic carbon atoms [C1-Ca1-C1A] is $82.5(2)^\circ$ and the distance from the ylidic carbon atom to the calcium centre [Ca1-C1 & Ca1-C1A] is $2.646(4)\text{\AA}$. Comparison of the P-C_{ylidic} bond length in the free ylide [$1.693\text{\AA}(\text{ave.})$]⁸ with the coordinated ylide shows a slight lengthening to $1.717(3)\text{\AA}$ [P1-C1]. This lengthening may be explained as follows: in the free ylide there is a lone pair on the ylidic carbon which may be involved in backbonding (negative hyperconjugation) to the phosphorus atom and is thus capable of shortening the P-C ylidic bond. Complexation of the ylide to the metal centre localises this lone pair and will thus reduce any backbonding that it may have been involved in, causing elongation of the P-C bond. However, increased charge separation across the P-C bond upon complexation to the metal causes electrostatic shortening of the bond which

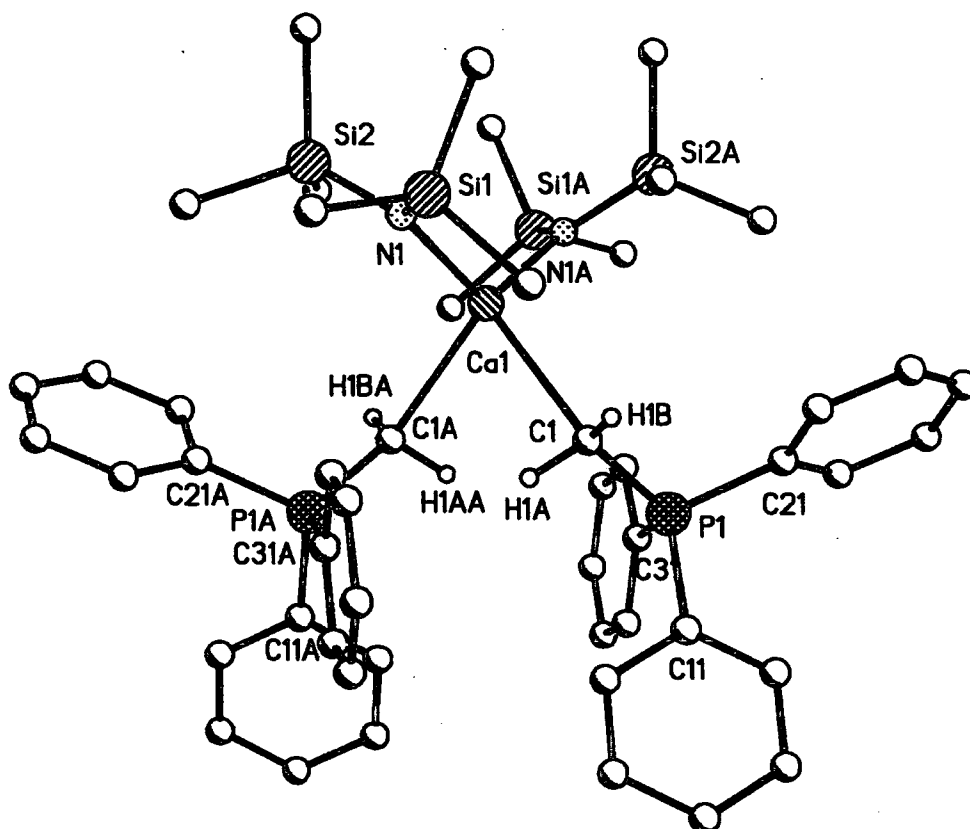


Figure 4.3 Single crystal X-ray structure of $(\text{Ph}_3\text{PCH}_2)_2 \cdot \text{Ca}[\text{N}(\text{SiMe}_3)_2]_2 \cdot 2\text{PhMe}$. All hydrogen atoms, except those bound to the ylidic carbon atoms, and the solvent molecules omitted for clarity.

in turn offsets the elongation and hence the overall effect on the change in bond length is minimal. The above lengthening ($\sim 0.02\text{\AA}$) is accompanied by a noticeable change in the geometry of the methylene unit in complex **1**, from close to trigonal planar geometry (sum of the angles in **1** = 353° , c.f. planar = 360°), to a distorted tetrahedral geometry (sum of angles in **1** = 325° , c.f. tetrahedral 328.5°). These data indicate a shift away from a sp^2 hybridised carbon atom towards a sp^3 hybridised carbon atom. Lastly, the P1-C1-Ca1 angle is $134.4(2)^\circ$ which is within the range known for other main group metal phosphonium ylide complexes.

Moving on to consider the PPh_3 unit of this particular complex there is one longer P-C_{ipso} bond of $1.823(3)\text{\AA}$ [P1-C11] compared to 1.833\AA (ave.) in ligand **I**, and also two shorter P-C_{ipso} bonds of $1.814(3)$ and $1.811(3)\text{\AA}$ [P1-C21 and P1-C31 respectively] comparing well with the starting ligand [1.818 and 1.821\AA (ave.) respectively]. A consideration of the C_{ipso}-P-C_{ylidic} angles again shows one larger and two smaller angles $116.5(2)$, $111.6(2)$ and $110.7(2)^\circ$ [C11-P1-C1, C21-P1-C1 & C31-P1-C1 respectively] in complex **1**, comparing favourably with those of ligand **I** [116 , 114 and 110° (ave.)]. These data serve to demonstrate that the geometry of the PPh_3 unit of the ylide is largely unchanged upon complexation, which implies an ionic nature of the $\text{P}^+\text{-C}^-$ ylidic bond in the ligand.

A further structural feature of this complex in the solid state is the pseudo-octahedral geometry about the calcium centre (Figure 4.4). The reason for this is that two carbon atoms, each one associated with a different trimethylsilyl moiety interact with the metal centre by what could be described as agostic interactions, although this is not in total agreement with Green's definition.¹⁸ Klinkhammer¹⁹ has studied in great detail similar interactions between alkali metal centres and tris(trimethylsilyl) silanides such as $\text{LiSi}(\text{SiMe}_3)_3$. His findings are in agreement with the assumption that the C-H of the SiMe_3 group acts as an electron donor to the electron deficient metal centre. Short intramolecular M...C distances observed by Klinkhammer range from $2.401(3)\text{\AA}$ for lithium complexes to $3.620(1)\text{\AA}$ for rubidium complexes, which are comparative to the observed distances of $3.151(4)\text{\AA}$ [C44-Ca1] in complex **1**.

¹⁸ M. Brookhart and M. L. H. Green, *J. Organomet. Chem.*, **250**, pp.395-408 (1983).

¹⁹ K. W. Klinkhammer, *Chem. Eur.*, **3**, 9, pp.1418-1431 (1997).

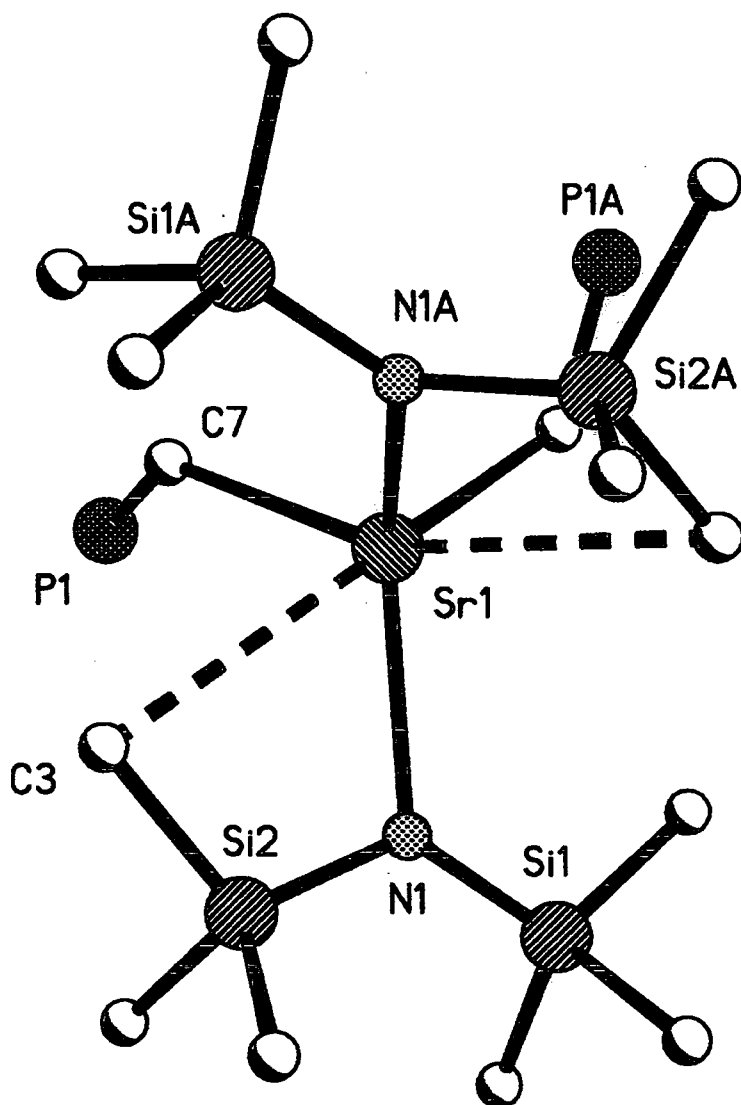


Figure 4.4 Diagram to show the interactions between the trimethylsilyl groups and the metal centre in complexes 1-3 (strontium complex shown). All hydrogen atoms and also the phenyl rings of the ylide omitted for clarity.

Consideration of the bond lengths and angles in the amide groups of **1** shows a Ca-N distance of 2.360(3) Å [Ca1-N1 & Ca1-N1A] which is approximately the average of the two lengths seen in the dimeric starting ligand **VIIa** (2.470 & 2.270 Å for terminal and bridging amides respectively). The N-Si bond length in **1** (both 1.699(3) Å, N1-Si1 & N1-Si2] is almost identical to that of the starting ligand (1.730 & 1.700 Å), whilst the Si1-N1-Si2 angle at 122.4(2)° has decreased in size (126.3°) due in part to the increased steric hindrance around the metal centre on addition of two neutral phosphonium ylide donors.

Searching the literature reveals that although complex **1** is not the first σ -bonded calcium carbon organometallic, it is one of only a few that are known and is as such, structurally interesting. There are many known calcium metallocenes⁴ which contain calcium-carbon π interactions, however the complexes of most interest are as follows.

The bis(1,4 dioxane) complex of bis[bis(trimethylsilyl)methyl]calcium reported by Lappert and co-workers²⁰ (Figure 4.5a).

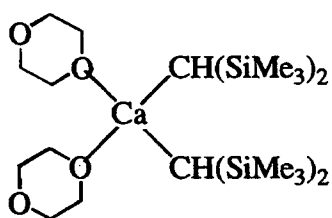


Figure 4.5a

and the solvent free bis[tris(trimethylsilyl)methyl] calcium²¹ (Figure 4.5b).



Figure 4.5b

Reaction of alkaline earth metal arenesulphonates with bis(trimethylsilyl) lithium or potassium yields alkali metal tris(alkyl) alkaline earth metalates²² (Figure 4.5c).

²⁰ F. G. N. Cloke, P. B. Hitchcock, M. F. Lappert, G. A. Lawless and B. Royo, *J. Chem. Soc., Chem. Commun.*, 724 (1991).

²¹ C. Eaborn, S. A. Hawkes, P. B. Hitchcock and J. D. Smith, *J. Chem. Soc., Chem. Commun.*, 1961 (1997).

²² A. D. Frankland and M. F. Lappert, *J. Chem. Soc., Dalton Trans.*, 4151 (1996).

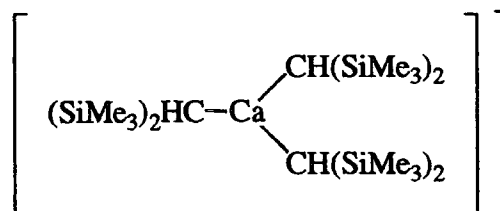


Figure 4.5c

Metallation of organic substrates with acidic protons, such as phenyl acetylene give rise to complexes such as Burkey and Hanusa's²³ (Figure 4.5d).

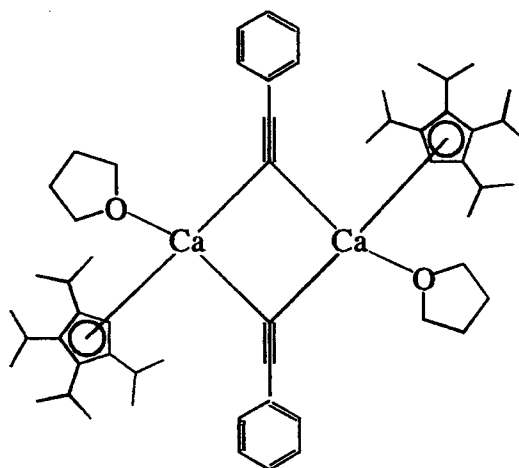


Figure 4.5d

Similar complexes containing crown ethers are known e.g. (Figure 4.5e).²⁴

²³ D. J. Burkey and T. P. Hanusa, *Organometallics.*, **15**, 4971 (1996).

²⁴ D. C. Green, U. English and K. Rutlandt-Senge, *Angew. Chem., Int. Ed. Engl.*, **38**, 354 (1999).

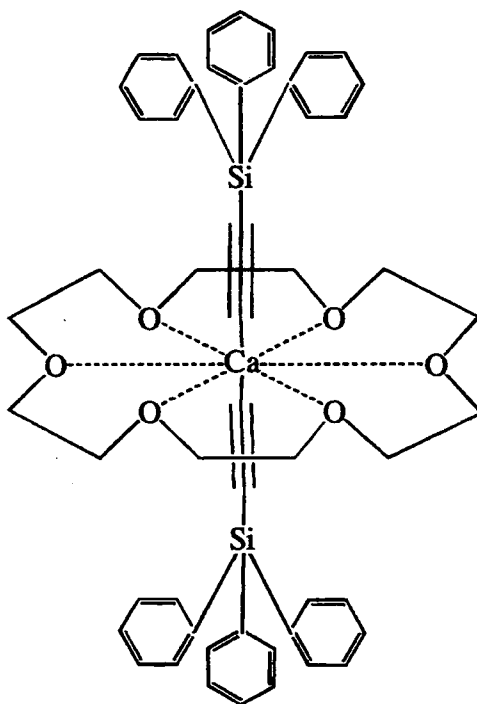


Figure 4.5e

Reaction of the tetrahydrofuran complex of trimethylaluminium with decamethylcalocene yields the complex shown in (Figure 4.5f).²⁵

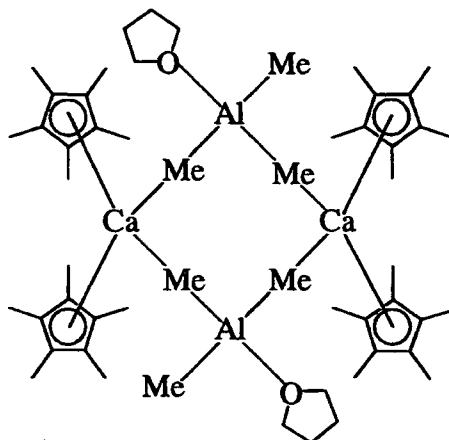


Figure 4.5f

Arduengo and co-workers²⁶ have recently published the structure of a calcium carbene complex (Figure 4.5g).

²⁵ P. S. Tanner, R. A. Williams and T. P. Hanusa, *Inorg. Chem.*, **32**, 2234 (1993).

²⁶ A. J. Arduengo, F. Davidson, R. Krafczyk, W. J. Marshall and M. Tamm, *Organometallics.*, **17**, 3375

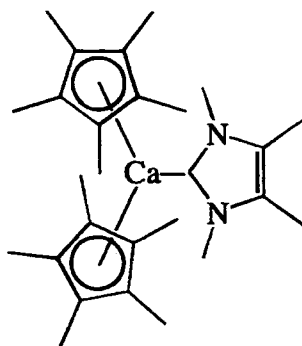


Figure 4.5g

Finally, Westerhausen et al²⁷ have published the structure of a calcium aluminate complex (Figure 4.5h).

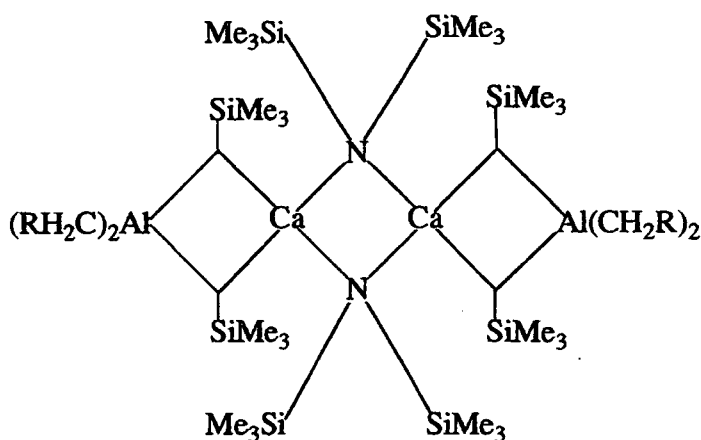


Figure 4.5h

A comparison of the calcium to carbon distances in each of the above with complex 1 (Table 4.6) shows good overall correlation, with the exception of complex f which has a rather extended calcium to carbon distance, for which the authors can find no reasonable explanation.

Complex	Ca-C (Å)
1	2.646(3)
a	2.483(4)

(1998).

²⁷ C. Birg, J. Knizek, H. Noth, T. Siefert and M. Westerhausen, *Eur. J. Inorg. Chem.*, 2209 (1999).

b	2.459(2)
c	No crystal structure.
d	2.521(2) & 2.551(2)
e	2.523(3) & 2.558(3)
f	2.948(2) & 2.999(1)
g	2.561(3)
h	2.638(2) & 2.678(3)

Table 4.6 Calcium-carbon bond lengths.

Complex **1** compares well with **g**, the only other example of neutral carbon Lewis base ligation to calcium. The other examples all contain a formal Ca-C σ bond, but in each case contain an anionic carbon interacting with the metal centre.

Complex **2** (Figure 4.6), the strontium analogue of **1**, crystallises in the space group C2/c as was the case for **1**. They are isostructural and isomorphous, displaying similar structural parameters e.g. consider the angle between the two ylidic carbon atoms and the metal centre, $1 = \text{C1-Ca-C1A} = 82.5(2)^\circ$ and $2 = \text{C7-Sr1-C7A} = 81.6(2)^\circ$. Consideration of other bond lengths and angles further substantiates the fact that these two complexes are almost identical in structure e.g. comparison of the P-C ylidic bond length in the uncoordinated ylide [1.693 Å (ave.)], with the co-ordinated ylide (1.686 Å) [P1-C7] again shows little difference. Similarly to **1**, complexation of **I** to **VIIIb** pyramidalises the ylidic carbon (sum of the angles = 329°). NMR studies on complex **2** further substantiate this structural phenomenon, by comparison of the $^1\text{J}_{\text{PC}}$ coupling constant obtained by ^{13}C NMR. The $^1\text{J}_{\text{PC}}$ coupling constant for the free ylide ($\text{Ph}_3\text{P}=\text{CH}_2$, sp^2 hybridised) is 100Hz,⁸ whereas for the conjugate acid ($\text{Ph}_3\text{P}^+-\text{CH}_3$, sp^3 hybridised) it is 57Hz.⁵ The value for complex **2** is 77Hz, which indicates that the ylidic carbon atom is tending more towards sp^3 type hybridisation and is thus bonding to the metal centre via a σ interaction. And, as expected, the Sr-C distance increases relative to **1** to 2.742(5) Å [Sr1-C7 & Sr1-C7A]. The P1-C7-Sr1 bond angle is $135.3(3)^\circ$ which again compares well with **1** and other known main group metal ylide complexes.

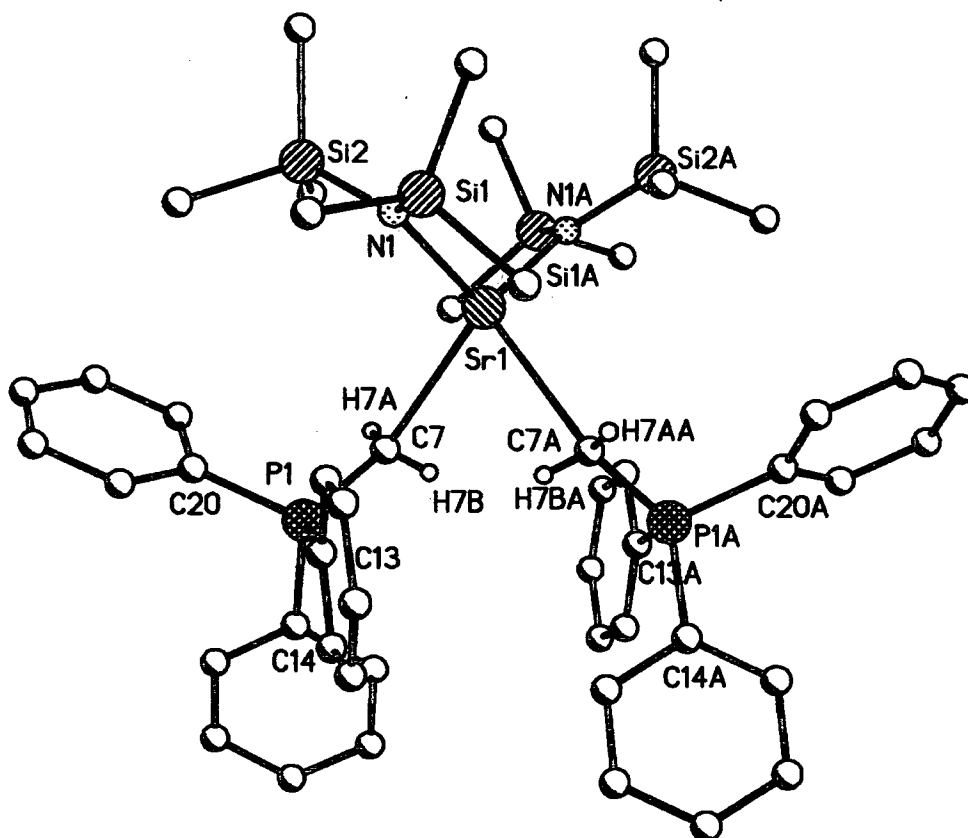


Figure 4.6 Single crystal X-ray structure of $(\text{Ph}_3\text{PCH}_2)_2\cdot\text{Sr}[\text{N}(\text{SiMe}_3)_2]_2\cdot 2\text{PhMe}$. All hydrogen atoms, except those bound to the ylidic carbon atoms, and the solvent molecules omitted for clarity.

Considering the PPh_3 unit of complex **2**, it is again evident that there is one longer P-C_{ipso} bond of $1.815(4)\text{\AA}$ [P1-C14] compared to 1.833\AA (ave.) in ligand **I**, and also two shorter P-C_{ipso} bonds of $1.804(4)$ and $1.809(4)\text{\AA}$ [P1-C13 and P1-C20 respectively] compared to the starting ligand [1.818 and 1.821\AA (ave.) respectively]. A consideration of the $\text{C}_{\text{ipso}}\text{-P-C}_{\text{ylidic}}$ angles again shows one large and two smaller angles $117.2(2)$, $110.5(2)$ and $110.2(2)^\circ$ [P1-C7-C14, P1-C7-C13 & P1-C7-C20 respectively] in complex **2**, comparing favourably with those of ligand **I** [116 , 114 and 110° (ave.)]. These measurements serve to demonstrate that the PPh_3 unit of the ylide is again unchanged upon complexation due in part to the ionic nature of the $\text{P}^+\text{-C}^-$ ylidic bond and its subsequent complexation to the metal centre.

A consideration of the bond lengths and angles in the amide groups of **2** shows a Sr1-N1 distance of $2.502(3)\text{\AA}$ which again is close to the average found in the dimeric starting ligand **VIIIb** (2.640 & 2.440\AA for terminal and bridging amides respectively). The N1-Si2 bond length in **2** [$1.693(3)\text{\AA}$] is almost identical to that of **1** (1.699\AA) and also the starting ligand **VIIIb** (1.710 & 1.690\AA), whilst the Si1-N1-Si2 angle at $125.5(2)^\circ$ has decreased markedly in size [$132.3(2)^\circ$]. The Si-N-Si angle is smaller than in **VIIIb**, but not as contracted as in **1** supporting the view that this feature is caused by steric crowding of the metal centre ; Sr is bigger than Ca so there is less steric strain on the amide.

Searching the literature again reveals **2** to be one of only a few complexes in which there is evidence of a neutral carbon-strontium σ -bonded organometallic. Whilst there are examples of π interactions between carbon and strontium such as an alkyne,²⁸ a carborane,²⁹ a diene,³⁰ a phosphapropenide complex,³¹ an indenyl complex³² and a bis(trimethylsilyl)cyclopentadienyl³³ complex, the complexes of most interest are as follows, a crown ether complex as published by Ruhlandt-Senge²⁴ (**Figure 4.7a**) which includes a strontium-carbon σ bond but is not neutral.

²⁸ (a). M. A. Coles and F. A. Hart, *J. Organomet. Chem.*, **32**, pp.279-284 (1971). (b). S. R. Drake and D. J. Otway, *J. Chem. Soc., Chem. Commun.*, pp.517-519 (1990).

²⁹ M. F. Hawthorne, R. Khattar and C. B. Knobler, *Inorg. Chem.*, **29**, pp.2191-2192 (1990).

³⁰ Y. Kai, N. Kanehisa, K. Mashima, A. Nakamura, H. Sugiyama and H. Yasuda, *J. Am. Chem. Soc.*, **116**, pp.6977-6978 (1994).

³¹ M. H. Digeser, W. Schwarz and M. Westerhausen, *Inorg. Chem.*, **36**, pp.521-527 (1997).

³² T. P. Hanusa and J. S. Overby, *Organometallics.*, **15**, pp.2205-2212 (1996).

³³ L. M. Engelhardt, P. C. Junk, C. L. Raston and A. H. White, *J. Chem. Soc., Chem. Commun.*, pp.1500-1501 (1988).

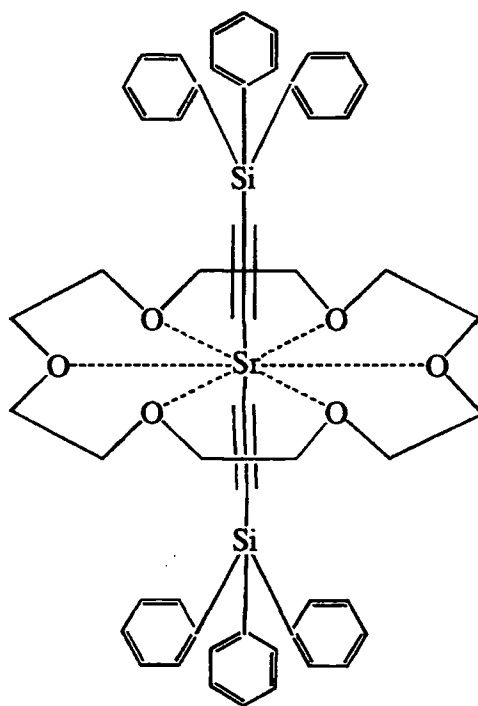


Figure 4.7a.

and a strontium carbene complex reported by Arduengo et al²⁶ (Figure 4.7b).

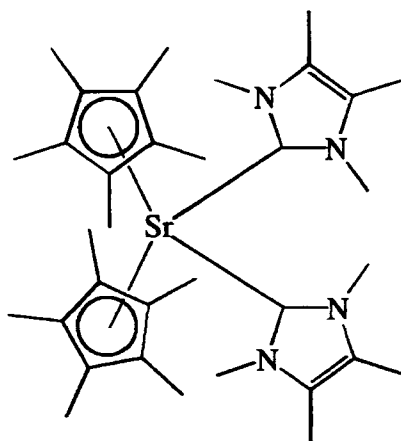


Figure 4.7b

Comparison of the strontium to carbon distance in each of these complexes with respect to complex **2** (Table 4.7) shows that the strontium to carbon bond length of **2** falls between the two sets of observed bond lengths for the reported complexes.^{24,26}

Complex	Sr-C (Å)
2	2.742(3)
a	2.692(2) & 2.723(3)
b	2.854(4) & 2.868(3)

Table 4.7 Strontium-carbon bond lengths.

Again, the most useful comparison is with the carbene complex (**Figure 4.7b**) as this complex contains neutral carbene Lewis base donors to the strontium centre. Unlike the comparison of the calcium carbene complex with **1**, this time the Sr-C distance in our complex is shorter. This could be attributed to the fact that Ardeungo was able to crystallise only the strontium bis carbene complex, and thus the strontium bonding to two carbenes would undoubtedly have longer bond lengths than a strontium bonding to one carbene.

Complex **3** (**Figure 4.8**), the barium analogue of complexes **1** & **2**, crystallises in space group $P(2)1/n$ which whilst similar in structure to **1** & **2** exhibits some notable differences such as non centrosymmetry i.e. differing orientation of the two coordinated ylides around the barium. Second, the angle between the two ylidic carbon atoms and the metal centre is significantly greater [**1** = C1-Ca1-C1A = 82.5(2)°, **2** = C7-Sr1-C7A = 81.6(2)°, **3** = C1-Ba1-C2 = 92.7(2)°]. This effect could be caused by the increased ionic radius of the barium enabling the co-ordinating ylides to move away from each other and thus allowing them to adopt different positions relative to the metal.

However, comparison of the P-C ylidic bond length in the un-coordinated ylide [1.693Å (ave.)] with the co-ordinated ylide again shows little difference [1.704(8)Å, P1-C1]. There is a similarly pyramidalised ylidic carbon atom with a sum of angles equal to 329°(ave.). The Ba-C_{ylidic} bond length is 3.002Å(ave.) [Ba1-C1 & Ba1-C2] which again is elongated compared to **1** and **2** as is to be expected given the increased atomic radius of barium and also a P-C_{ylidic}-Ba angle of 131°(ave.) [P1-C1-Ba1 & P2-C2-Ba1] which is smaller than **1** & **2** [134.2(2) & 135.3(3)° respectively].

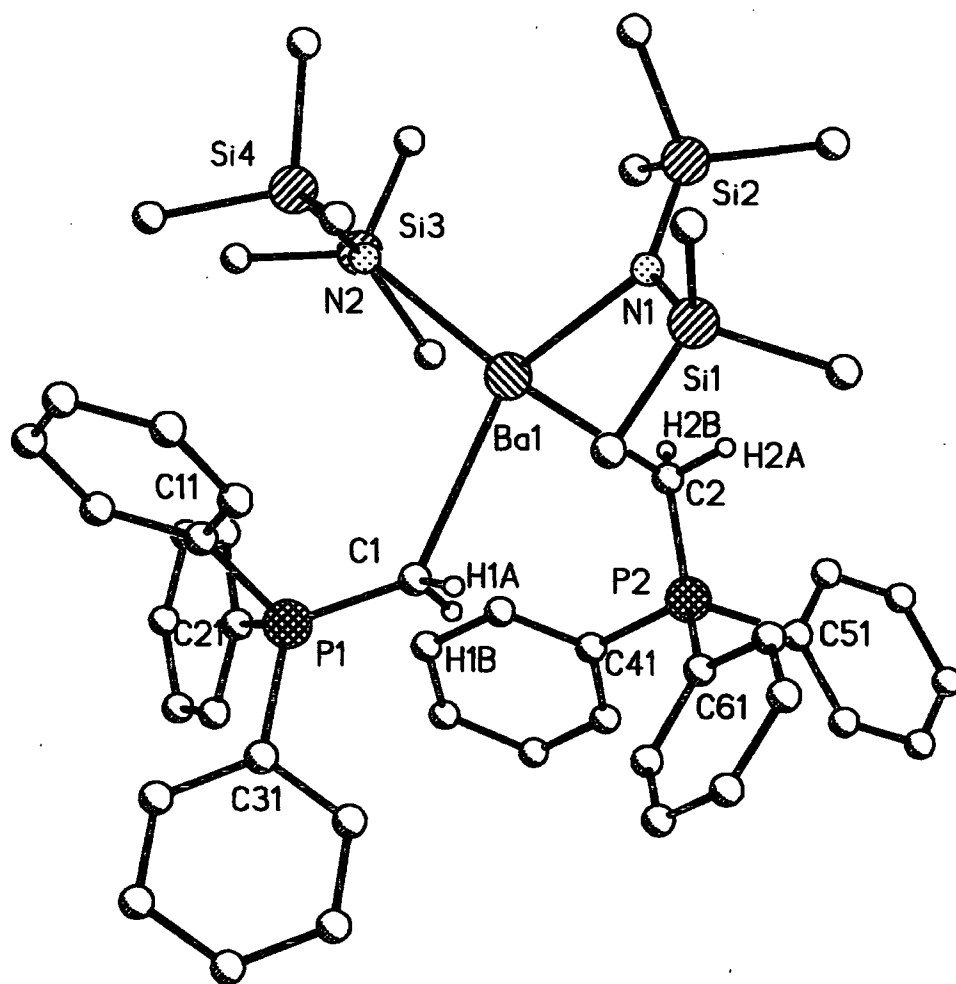


Figure 4.8 Single crystal X-ray structure of $(\text{Ph}_3\text{PCH}_2)_2\text{Ba}[\text{N}(\text{SiMe}_3)_2]_2$. All hydrogen atoms, except those bound to the ylidic carbon atoms, omitted for clarity.

Consideration of the PPh_3 unit in complex **3**, again shows that there is one longer P-C_{ipso} bond of $1.825(7)\text{\AA}$ [P1-C31] compared to 1.833\AA (ave.) in ligand **I**, and two shorter P-C_{ipso} bonds of $1.803(8)$ and $1.800(7)\text{\AA}$ [P1-C11 & P1-C21] compared to the starting ligand [1.818 and 1.821\AA (ave.) respectively]. A consideration of the $\text{C}_{\text{ipso}}\text{-P-C}_{\text{ylidic}}$ angles, again shows that in complex **3** there is one angle noticeably larger than the other two angles, $117.7(4)$, $111.0(4)$ and $111.1(4)^\circ$ [C1-P1-C31, C1-P1-C11 & C1-P1-C21]. It is interesting to note that the two smaller angles in complex **3** are between 4 and 7° smaller than any seen in **1** and **2**, again attributable to the increased size of the barium atom.

A consideration of the bond lengths and angles in the amide groups of **3** shows Ba-N distances of $2.624(2)\text{\AA}$ & $2.640(2)\text{\AA}$ [Ba1-N1 & Ba1-N2] which are close in value to the shorter terminal amide bonds in the original ligand **VIIIc** (2.580\AA for terminal and 2.820\AA for the bridging amides). The N-Si bond lengths in **3** [$1.673(6)\text{\AA}$ & $1.688(6)\text{\AA}$, N1-Si1 & N1-Si2] are again very similar to those in the other complexes (**1** & **2**) and almost identical to those of the starting ligand (1.700 & 1.690\AA). It is interesting to note that there are two unique amide groups hence the two values for Ba-N and also two values for N-Si. Unlike **1** and **2**, **3** does not have a crystallographic centre of symmetry through the metal atom. The reasons for this are unclear but could possibly be accounted for in terms of the greater radius of the barium atom. The Si-N-Si angles at $128.1(4)^\circ$ and $129.9(4)^\circ$ [Si3-N2-Si4 & Si1-N1-Si2] show the smallest decrease from the starting amide (131.7°) relative to **1** and **2**, but are now the largest overall demonstrating the increase in size of the metal going from calcium, through strontium to barium.

Searching the literature reveals that as with **1** and **2**, complex **3** although not unique is one of only a few barium-carbon σ -bonded organometallics that have been reported and is as such very interesting. There are known phosphapropenide,³¹ indenyl³² and bistrimethylsilyl cyclopentadienyl³³ complexes of barium, but of more interest are the crown ether complex²⁴ (Figure 4.9a),

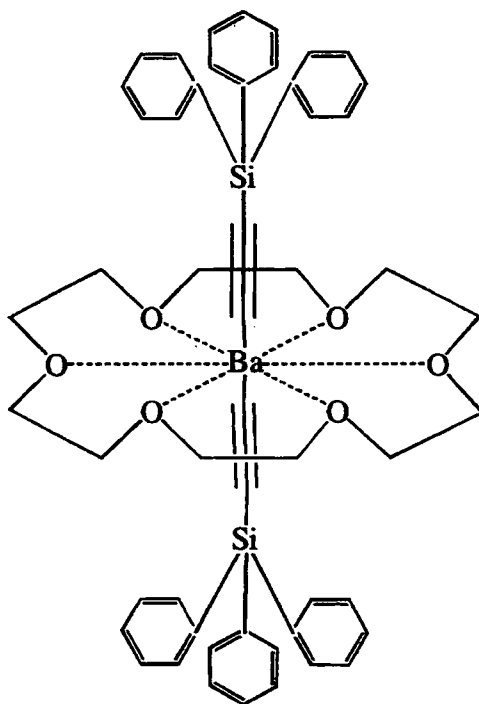


Figure 4.9a

the mono carbene complex reported by Arduengo²⁶ (Figure 4.9b),

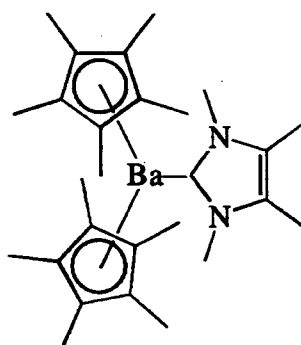


Figure 4.9b

the dimeric barium complex with a 'unique barium-carbon bond' as published by Westerhausen et al³⁴ (Figure 4.9c), and finally a barium phosphonium dibenzylide

³⁴ M. H. Digeser, H. Noth, T. Seifert, A. Pfitzner and M. Westerhausen, *J. Am. Chem. Soc.*, **120**, 6722 (1998).

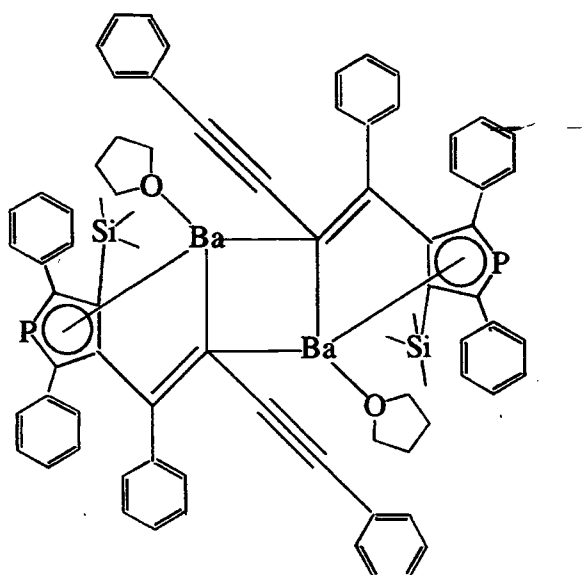


Figure 4.9c.

complex³⁵ (Figure 4.9d) which is of great significance to this work as it contains a phosphonium ylide moiety, albeit a deprotonated anionic one.

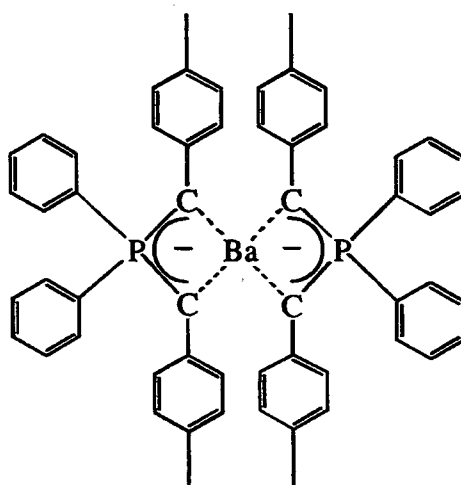


Figure 4.9d.

Comparison of the barium to carbon distance in each of these complexes with respect to complex 3 (Table 4.8) shows that the barium to carbon bond length of our complex is in agreement with those observed bond lengths for the reported complexes.

³⁵ S. Harder and M. Lutz, *Organometallics.*, **16**, 225 (1997).

Complex	[Ba-C]Å
3	3.002(ave.)
a	2.852(3)
b	2.951(2)
c	2.899(2)-3.363(3)
d	2.981(2)-3.479(2)

Table 4.8 Barium-carbon bond lengths.

The barium carbene complex **b** does again contain a neutral carbene ligand and is thus directly comparable with **3**. The Ba-C distance in the carbene complex is shorter than that in **3** as was the case for the analogous calcium complex and **1**.

Considering the structures of complexes **1-3** together it can be seen that the calcium and strontium complexes adopt the same crystal structure whereas the barium exhibits a different orientation of ligands.

There are no accessible classical hydrogen bond donors / acceptors in complexes **1-3** and hence there are very few hydrogen bonds seen. The only visible H-bond is that to the π ring of the solvent which in both complexes is a double set of C-H... π ...H-C bonds (Figure 4.10).

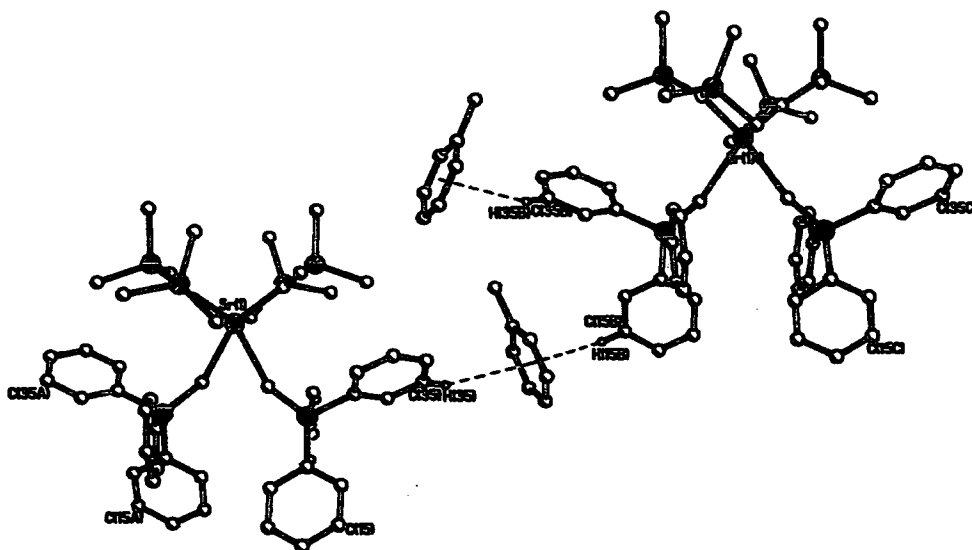


Figure 4.10 Diagram showing non-classical hydrogen bonding present in complexes 1 & 2 (Strontium complex shown). All hydrogen atoms except those involved in hydrogen bonding omitted for clarity.

Considering the two $\pi \dots \text{H} \dots \text{C}$ interactions in 1 and 2 it can be seen that there are $\pi \dots \text{H}$ distances of 2.885(11) to 2.992(11) Å in complex 1 [C15B-H15B and C35B-H35B] and 2.875(12) to 2.973(11) Å in complex 2 [C15B-H15B and C35B-H35B]. There are also $\pi \dots \text{H} \dots \text{C}$ angles [$\pi \dots \text{C15B} \dots \text{H15B}$ and $\pi \dots \text{C35B} \dots \text{H35B}$] of 135.5(2) and 144.1(2)° for complex 1 and 135.3(3) and 145.6(3)° for 2.

The barium complex as already mentioned crystallises in a different space group to the calcium and strontium complexes and thus exhibits different packing and a different molecular structure. There is no solvent present in the crystal structure of complex 3, which considering the syntheses of 1-3 are all the same, means that the lack of solvent must be a feature of the crystal packing. There is no evidence of hydrogen bonding in this complex.

To conclude this discussion of complexes 1-3 there follows a table of data (**Table 4.9**) which includes a comparison of 1-3 with previously characterised analogous lithium and

sodium amide complexes of **1** [where $\text{Li} = \text{Ph}_3\text{PCH}_2\cdot\text{LiN}(\text{SiMe}_3)_2$ and $\text{Na} = \text{Ph}_3\text{PCH}_2\cdot\text{NaN}(\text{SiMe}_3)_2$].³⁶

	1	Li	Na	1	2	3
$\text{R}[\text{P}-\text{C}(\text{ylide})]\text{\AA}$	1.693(ave.)	1.705(ave.)	1.696(ave.)	1.717(3)	1.686(4)	1.704(ave.)
$\Sigma\angle[\text{C}(\text{ylide})]^\circ$	353(ave.)	312(ave.)	337(ave.)	325	329	329(ave.)
$\Sigma\angle[\text{P}]^\circ$	340(ave.)	339(ave.)	342(ave.)	339	338	339(ave.)
$\text{R}[\text{MC}(\text{ylide})]\text{\AA}$	-	2.283(ave.)	2.629(ave.)	2.646(4)	2.742(5)	3.002(ave.)
$[\text{M}-\text{C}(\text{ylide})\text{P}]^\circ$	-	135(ave.)	122(ave.)	134.2(2)	135.3(3)	131(ave.)
$[\text{N}-\text{Si}]\text{\AA}$	-	-	1.698(3)	1.699(3)	1.693(3)	1.681(ave.)
$[\text{Si}-\text{N}-\text{Si}]^\circ$	-	-	123.5(2)	122.4(2)	125.5(2)	129.0(ave.)

Table 4.9 Comparison of 1-3 with some group 1 analogues.

Considering the above table of data it can be seen that the length of the ylidic bond changes little upon complexation with the various metal centres for reasons explained earlier in the discussion of **1-3**. The sum of the angles around the ylidic carbon decreases upon complexation indicating a shift towards a more pyramidalised geometry, whilst the sum of the angles around the phosphorus atom remains similar indicating no change in the geometry of the PPh_3 fragment. Moving down each group of metals it can be seen that the ylidic carbon to metal distance increases as the radius of the metal atom increases which is exactly what is to be expected as the smaller the metal the closer the approach. It can be seen from the table that the metal to ylidic carbon to phosphorus angle does not change much across the series with the exception of the sodium complex which provides an unexplainable anomaly. With the exception of **3** the N-Si distance does not change upon going from group 1 to group 2. The exception of **3** is explained earlier in this chapter and is possibly due to complex **3** having two unique amide groups. The Si-N-Si angle increases with the size of the metal due to steric requirements.

³⁶ R. D. Price, *Ph.D. Thesis*, University of Durham (1999).

4.5 Discussion of complexes 4-8.

Complexes 4 and 5 are analogues of 1-3 except that a different phosphonium ylide, namely $(\text{Me}_2\text{N})_3\text{PCH}_2$ is used. Reaction of the calcium and strontium bis(bistrimethylsilyl)amides VII¹¹ with two equivalents of tris(dimethylamino) methylide II⁹ in toluene solution, followed by cooling at -40°C yielded a crystalline product 4 & 5 in each case. Unfortunately single crystal X-ray diffraction studies were not undertaken for these complexes due to the poor quality of the crystals obtained. However the presence of these two complexes is confirmed by NMR studies, elemental analysis and precise melting points.

A search of the literature reveals that there are only five other examples of complexes containing ligand II. Two of the complexes contain titanium, one of which contains bridging chlorine atoms,³⁷ and the second bridging ylidic carbon atoms³⁸ (Figure 4.11).

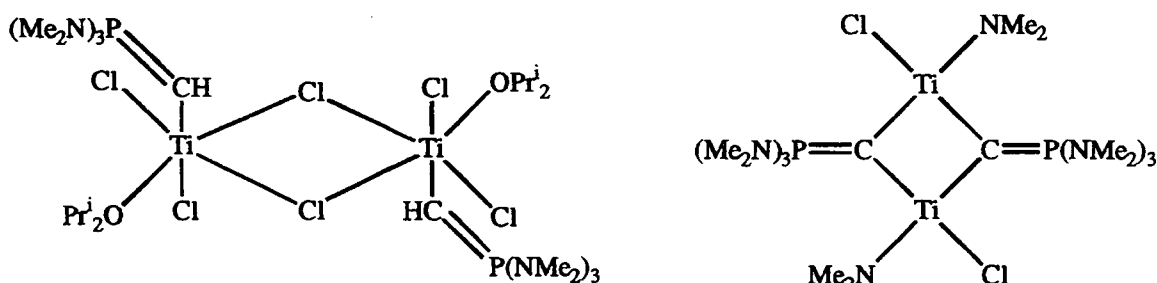


Figure 4.11 Titanium complexes of II.

Grützmacher et al recently published a zinc complex of II (Figure 4.12) as well as the α zincated version.³⁹

³⁷ P. G. Dopico, M. G. Finn, K. A. Hughes and M. Sabat, *Angew. Chem., Int. Ed. Engl.*, **32**, 554 (1993).

³⁸ M. G. Finn and K. A. Reynolds, *J. Org. Chem.*, **62**, 2574 (1997).

³⁹ H. Grützmacher, H. Pritzkow, M. Steiner and L. Zsolnai, *J. Chem. Soc., Chem. Commun.*, 285 (1998).

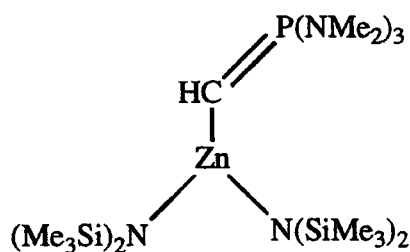


Figure 4.12 Zinc complex of II.

The final two complexes contain lithium and are work done previously in this group (Fig 4.13).³⁶

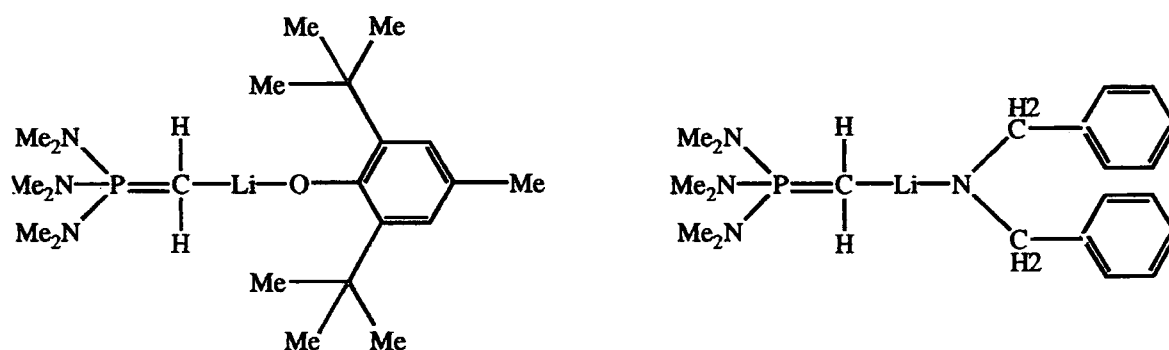


Figure 4.13 Lithium complexes of II.

These two examples, together with the structural data obtained for 1-3 suggest that 4-5 are monomeric with terminal co-ordination of the ligand II to the metal centre (Figure 4.14). The ³¹P NMR data are also consistent with co-ordination of the ligand II.

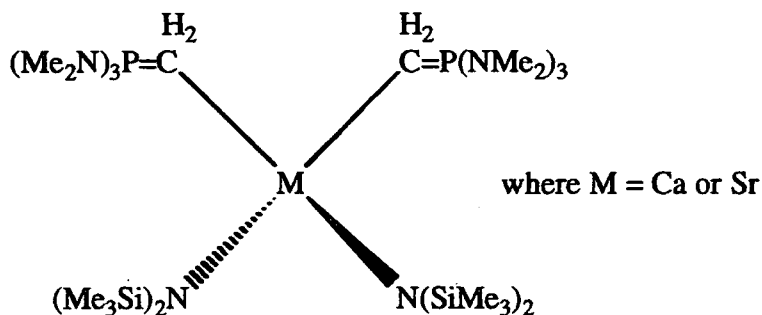


Figure 4.14 Proposed structures of 4 and 5.

Complexes **6** & **7** both contain ligands **I** and **V** and were produced by adding one equivalent of magnesium⁴⁰ or calcium bis(bis(trimethylsilyl)amide **VIIb**¹¹ to two equivalents of triphenylphosphonium methylide **I**⁸ and two equivalents of **V**¹⁰ in toluene solution, followed by cooling at $-40\text{ }^{\circ}\text{C}$ to yield a solid product of **6** and **7** in each case. Unfortunately single crystal X-ray diffraction studies were not undertaken for these complexes due to no single crystal being obtained. However the presence of these two complexes is confirmed by NMR studies, elemental analysis and clean melting points. A proposed structure for **6** and **7** is given in **Figure 4.15**.

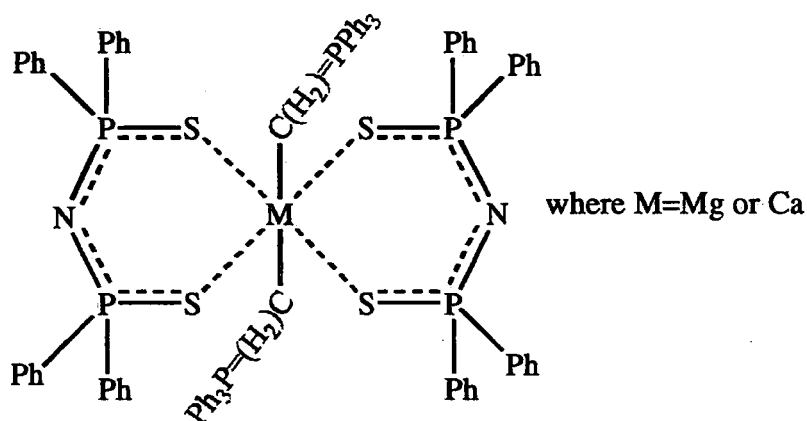


Figure 4.15 Proposed structure of **6** and **7**.

The known co-ordination chemistry of **I** is well documented and has already been discussed elsewhere in this thesis (**Chapter 1**). The transition metal chemistry of **V** has already been mentioned at the start of this chapter,¹⁷ but it is more relevant to this thesis to quote the known s-block chemistry of this particular ligand. There are several reported examples of alkali metal complexes known including lithium,³⁶ sodium⁴¹ and potassium^{42,43} as well as a complex containing barium⁴⁴

Complex **8** was produced by adding one equivalent of the strontium bis(bis(trimethylsilyl)amide **VII**¹¹ to two equivalents of triphenylphosphonium methylide **I**⁸ and two equivalents of 2,6-di-tert-butyl,4-methyl phenol in toluene solution, followed

⁴⁰ J. F. Allan, K. W. Henderson and A. R. Kennedy, *J. Chem. Soc., Chem. Commun.*, 1149 (1997).

⁴¹ J. E. Drake, S. Hernandez-Ortega, R. Rösler, C. Silvestru and J. Yang, *Polyhedron.*, **16**, 4061 (1997).

⁴² A. M. Z. Slawin, J. Ward, D. J. Williams and J. D. Woolins, *J. Chem. Soc., Chem. Commun.*, 421 (1994).

⁴³ R. Cea-Olivares and H. Nöth, *Z. Naturforsch.*, **B42**, 1507 (1987).

⁴⁴ G. Kräuter, S. K. Sunny and W. S. Rees, Jr., *Polyhedron.*, **17**, 391 (1997).

by cooling at $-40\text{ }^{\circ}\text{C}$ to yield a solid product of **8**. The di-basic strontium amide was successful in removing a proton from each phenol to give a strontium bis(ylide) bis(phenol) complex. Unfortunately single crystal X-ray diffraction studies were not undertaken for this complex due to no single crystal being obtained. However the presence of this complex is confirmed by NMR studies, elemental analysis and a clean melting point. Considering the previous complexes and those seen in Chapter 5, it is reasonable to assume that **8** would have the following structure (Figure 4.16).

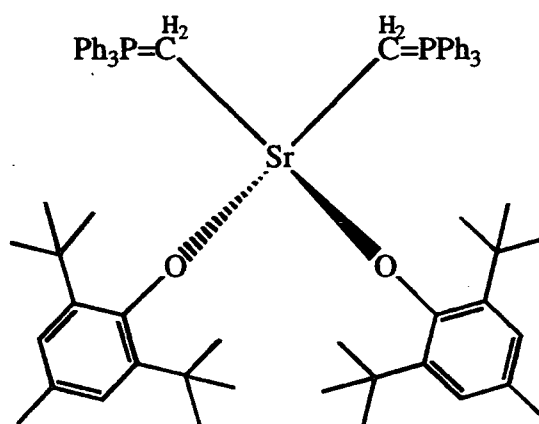


Figure 4.16 Proposed structure of **8**.

I have discussed elsewhere in this thesis (Chapter 1) the known chemistry of ligand **1**. There are strontium aryloxides known and a full description of these can be found in Chapter 5.

4.6 Conclusions.

(1). Complexes **1-3** are the first unambiguous fully characterised examples of neutral phosphonium ylide complexes of calcium, strontium and barium. Unsupported σ -bonding between the ylidic carbon and the metal centre is observed and substantiated by NMR and XRD studies. These complexes have potential uses in synthetic chemistry e.g. the Wittig reaction and are also potential models for heavy alkaline earth metal alkyl systems.

(2). **4** and **5** are further examples of neutral phosphonium ylide complexes of calcium and strontium, whilst **6** and **7** show further neutral ylide co-ordination to a metal centre and also serve to expand the vast area of tetraphenyldithiodiphosphinylimide chemistry. Complex **8** is a novel example of a strontium phosphonium ylide aryloxide complex analogous to the iminophosphorane complexes (**9-11**) seen in Chapter 5.

5. Group 2 Metal Complexes of Iminophosphoranes and Phosphine Oxides.

This chapter deals with the investigation of complexes **9-21**. These complexes were synthesised according to the procedures outlined in **Chapter 3** and are listed in **Table 5.1**.

Complex Number	Chemical Formula
9	$(\text{Ph}_3\text{PNH})_2 \cdot \text{Ca}[\text{OC}_6\text{H}_2(\text{Me})^t\text{Bu}_2]_2$
10	$(\text{Ph}_3\text{PNH})_2 \cdot \text{Sr}[\text{OC}_6\text{H}_2(\text{Me})^t\text{Bu}_2]_2$
11	$(\text{Ph}_3\text{PNH})_2 \cdot \text{Ba}[\text{OC}_6\text{H}_2(\text{Me})^t\text{Bu}_2]_2$
12	$[(\text{Me}_2\text{N})_3\text{PNH}]_2 \cdot \text{Sr}[\text{OC}_6\text{H}_2(\text{Me})^t\text{Bu}_2]_2$
13	$(\text{Ph}_3\text{PNH})_2 \cdot \text{Sr}\{\text{N}[\text{PPh}_2(\text{S})]_2\}_2$
14	$(\text{Ph}_3\text{PNH})_2 \cdot \text{Sr}(\text{OCPh}_3)_2$
15	$(\text{Ph}_2\text{MePNH})_2 \cdot \text{Sr}[\text{OC}_6\text{H}_2(\text{Me})^t\text{Bu}_2]_2$
16	$(\text{Ph}_3\text{PO})_2 \cdot \text{Ca}[\text{N}(\text{SiMe}_3)_2]_2$
17	$(\text{Ph}_3\text{PO})_2 \cdot \text{Sr}[\text{N}(\text{SiMe}_3)_2]_2$
18	$(\text{Ph}_3\text{PO})_2 \cdot \text{Ba}[\text{N}(\text{SiMe}_3)_2]_2$
19	$(\text{Ph}_3\text{PO})_2 \cdot \text{Ca}[\text{OC}_6\text{H}_2(\text{Me})^t\text{Bu}_2]_2$
20	$(\text{Ph}_3\text{PO})_2 \cdot \text{Sr}[\text{OC}_6\text{H}_2(\text{Me})^t\text{Bu}_2]_2$
21	$(\text{Ph}_3\text{PO})_2 \cdot \text{Ba}[\text{OC}_6\text{H}_2(\text{Me})^t\text{Bu}_2]_2$

Table 5.1 Table of complexes discussed in **Chapter 5**.

5.1 Background.

In **Chapter 4** it was demonstrated that phosphonium ylides could behave as neutral Lewis base donors for alkaline earth metals. Previous work from our group has shown that this is also possible using the alkali metals.^{1,2,3} Isoelectronic to phosphonium ylides are the

¹ D. R. Armstrong, M. G. Davidson and D. Moncrieff, *Angew. Chem., Int. Ed. Engl.*, **34**, 478 (1995).

iminophosphoranes and phosphine oxides which have been discussed in detail in Chapter 1.

Iminophosphoranes are an important tool in the field of organic synthesis,^{4,5} in particular C=N double bond formation and nitrogen heterocycle construction via the aza-Wittig reaction.⁶ Recently iminophosphoranes have attracted a lot of interest both as neutral and anionic ligands to the transition metals,⁷ this is not surprising considering that Ligand IV [(Me₂N)₃PNH] is directly analogous to HMPA [(Me₂N)₃PO] which is a widely used but highly toxic Lewis base donor. One recent example of this transition metal chemistry is (t-Bu₃PN)₂TiMe₂ which has been shown to be a highly reactive polyethylene catalyst, one of only a few non-metallocene catalysts that are known.⁸

Until recently, however, their main group chemistry and especially that of the s-block metals has been far less studied.⁹ Previous work done in our group,^{3,10} along with more recently published work^{11,12,13,14,15,16,17,18,19,20} has served to expand this area of chemistry.

² A. S. Batsanov, C. K. Broder, J. A. Cowan, M. G. Davidson, A. E. Goeta, J. A. K. Howard, F. López-Ortiz and R. D. Price, *Chem. Eur. J.*, manuscript in preparation.

³ R. D. Price, *Ph.D. Thesis*, University of Durham (1999) and references cited therein.

⁴ A. W. Johnson with special contributions by W. C. Kaska, K. A. O. Starzewski and D. A. Dixon, *'Ylides and Imines of Phosphorus'*, Wiley, New York (1993), and references cited therein.

⁵ H.-J. Cristau, *Chem. Rev.*, **94**, 1299 (1994).

⁶ (a) S. Eguchi, T. Okano and T. Sasaki, *J. Am. Chem. Soc.*, **105**, 3912 (1983). (b) J. Barluenga, F. López and F. Palacios, *J. Chem. Soc., Chem. Commun.*, 1681 (1985).

⁷ For Review; K. Dehnicke, M. Krieger and W. Massa, *Coord. Chem. Rev.*, **182**, 19 (1999).

⁸ (a) S. J. Brown, X. Gao, F. Guérin, D. G. Harrison, L. Koch, R. E. v. H. Spence, D. W. Stephan, J. W. Swabey, Q. Wang, W. Xu and P. Zoricak, *Organometallics*, **18**, 2046 (1999). (b) F. Guérin and D. W. Stephan, *Angew. Chem., Int. Ed. Engl.*, **39**, 1298 (2000).

⁹ For Review: K. Dehnicke and F. Weller, *Coord. Chem. Rev.*, 103 (1997).

¹⁰ A. S. Batsanov, P. D. Bolton, C. K. Broder, M. G. Davidson, A. E. Goeta, J. A. K. Howard, R. D. Price and D. S. Yufit, manuscript in preparation.

¹¹ A. S. Batsanov, M. G. Davidson, J. A. K. Howard, S. Lamb, C. Lustig and R. D. Price, *J. Chem. Soc., Chem. Commun.*, 1211 (1997).

¹² A. S. Batsanov, P. D. Bolton, R. C. B. Copley, M. G. Davidson, J. A. K. Howard, C. Lustig and R. D. Price, *J. Organomet. Chem.*, **550**, 445 (1998).

¹³ (a) S. Anfang, K. Dehnicke, G. Geisler, K. Harms, G. Seybert and W. Massa, *Z. Anorg. Allg. Chem.*, **624**, 1187 (1998). (b) S. Chitsaz, K. Dehnicke and B. Neumüller, *Z. Anorg. Allg. Chem.*, **625**, 9 (1999).

¹⁴ K. Dehnicke, M. Krieger, J. Magull, A. Müller and B. Neumüller, *Z. Anorg. Allg. Chem.*, **623**, 1081 (1997).

¹⁵ (a) K. Dehnicke, D. Fenske, J. Magull, A. Müller and B. Neumüller, *Z. Anorg. Allg. Chem.*, **623**, 1306 (1997). (b) K. Dehnicke, A. Müller and B. Neumüller, *Angew. Chem., Int. Ed. Engl.*, **36**, 2350 (1997). (c) K. Dehnicke, A. Müller and B. Neumüller, *Chem. Ber.*, 253 (1996).

¹⁶ (a) D. Stalke and A. Steiner, *Angew. Chem., Int. Ed. Engl.*, **34**, 1752 (1995). (b) R. Hasselbring, S. K. Pandey, H. W. Roesky, D. Stalke and A. Steiner, *J. Chem. Soc., Dalton. Trans.*, 3447 (1993). (c) D. Stalke and A. Steiner, *Inorg. Chem.*, **32**, 1977 (1993).

¹⁷ F. López-Ortiz, E. Peláez-Arango, B. Tejerina, E. Pérez-Carreño and S. García-Granda, *J. Am. Chem. Soc.*, **117**, 9972 (1995).

Phosphine oxides, in particular those of alkylidiphenyl phosphines, are used in a variety of organic synthesis reactions such as the Horner reaction,²¹ which is the reaction of a phosphine oxide, in the form of its carbanion, with a carbonyl compound to yield the phosphine oxide and an alkene. Alkylation of phosphine oxides is possible using a base and then addition of an electrophile such as methyl iodide.^{22,23} Acylation is achieved most effectively using a base and then addition of an alkyl carboxylate.^{24,25} Whilst there is a wealth of knowledge concerning organic reactions, the s-block metal chemistry of triphenylphosphine oxide in particular has remained untouched.

In this chapter are presented the first examples of neutral iminophosphorane heavy alkaline earth metal (Ca, Sr and Ba) complexes and also the first series of heavy alkaline earth metal complexes involving neutral co-ordination of triphenylphosphine oxide. In order to avoid N-metallated products, previous knowledge was employed^{1,10} and more acidic phenoxide derivatives were generated *in situ* via a reaction of a phenol with the metal bases (Ligands VIIa-c) to ensure neutral co-ordination products. There follows a summary of the pertinent group 2 metal alkoxide literature.

The interest in the synthesis and subsequent chemistry of main group alkoxides and aryloxides has grown substantially over the past few years. The main reason for this surge in interest in such compounds, many of which were previously poorly characterised,^{26,27,28} is the discovery of superconducting ceramics²⁹ containing alkaline earth metal ions. The classical heat and sinter technique for such superconductors can suffer from poor reproducibility, incorporation of ionic impurities and multi phase products. The excess heat required to ensure suitable reaction rates for the formation of

¹⁸ J. F. Van der Maelen Uria, S. K. Pandey, H. W. Roesky and G. M. Sheldrick, *Acta Cryst. C.*, **50**, 671 (1994).

¹⁹ P. R. Raithby, C. A. Russell, A. Steiner and D. S. Wright, *Angew. Chem., Int. Ed. Engl.*, **36**, 649 (1997).

²⁰ P. B. Hitchcock, M. F. Lappert and Zhong-Xia Wang, *J. Chem. Soc., Chem. Commun.*, 1113 (1997).

²¹ H. Hoffmann, L. Horner and H. G. Wippel, *Chem. Ber.*, **91**, 61 (1958).

²² A. D. Buss and S. Warren, *Tetrahedron. Lett.*, **24**, 111 (1983).

²³ S. Warren and A. T. Zaslona, *Tetrahedron. Lett.*, **23**, 4167 (1982).

²⁴ C. V. Banks and J. J. Richard, *J. Org. Chem.*, **28**, 123 (1963).

²⁵ H. Hoffmann, L. Horner, G. Klahre and H. G. Wippel, *Chem. Ber.*, **92**, 2499 (1959).

²⁶ D. C. Bradley, D. P. Gaur and R. C. Mehrotra, *Metal Alkoxides*, Academic, New York, pp50-51 (1978).

²⁷ (a). L. Lochmann, *J. Organomet. Chem.*, **376**, 1 (1989) and references cited therein. (b). G. J. MacEwen and P. G. Willard, *J. Am. Chem. Soc.*, **111**, 7671 (1989).

²⁸ (a). V. Huch, D. Käfer and M. Veith, *Angew. Chem., Int. Ed. Engl.*, **25**, 375 (1986). (b). J. D. Druliner, P. L. Gai, H. S. Horowitz, S. L. McLain, S. Poon, A. W. Sleight, M. J. Vankarelaar and J. L. Wagner, *Science.*, **243**, 66 (1989).

²⁹ J. G. Bednorz and K. A. Z. Müller, *Phys. B.*, **64**, 89 (1986).

these products is also a disadvantage. The use of hydrocarbon soluble (molecular) alkoxide precursors has been shown to be useful.³⁰ The great advantage of this particular route of synthesis is that the desired stoichiometry may be achieved on the molecular level by selective formation of a binary or tertiary metallic alkoxide e.g. $M_xM'_yM''_z(OR)_n$ and then can be subsequently thermolysed (and/or hydrolysed) to yield the desired ceramic product. Consequently, much recent work in this field has centred on the alkaline earth metal alkoxides (beryllium,^{31,32} magnesium,^{33,34,35,36,37,38} calcium,^{33,39,40,41,42,43,44} strontium^{41,45,46,47} and barium^{41,42,47,48,49,50,51,52}).

³⁰ (a). L. G. Hubert-Pfalzgraf, *New. J. Chem.*, **11**, 663 (1987). (b). K. G. Caulton and J. G. Hubert-Pfalzgraf, *Chem. Rev.*, **90**, 969 (1990).

³¹ R. A. Bartlett, M. M. Olmstead, P. P. Power and K. Rutlandt-Senge, *Inorg. Chem.*, **32**, 1724 (1993).

³² O. Kumberger, J. Riede and H. Schmidbaur, *Chem. Ber.*, **125**, 2701 (1992).

³³ J. M. Harrowfield, R. P. Sharma, B. W. Skelton and A. H. White, *Aust. J. Chem.*, **51**, 761 (1998).

³⁴ J. C. Calabrese, M. A. Cushing Jr and S. D. Ittel, *Inorg. Chem.*, **27**, 867 (1988).

³⁵ F. Bigi, G. Bocelli, A. Cantoni, R. Maggi and G. Sartori, *Chem. Eur. J.*, **3**, 1269 (1997).

³⁶ M. Noltemeyer, R. W. Roesky and M. Scholtz, *Chem. Ber.*, **123**, 2303 (1990).

³⁷ R. E. Cramer, J. W. Gilje and J. A. Meese-Marxtscheffel, *Polyhedron.*, **13**, 1045 (1994).

³⁸ K. W. Henderson, R. E. Mulvey and F. B. M. Reinhard, *J. Am. Chem. Soc.*, **116**, 10777 (1994).

³⁹ J. M. Harrowfield, R. P. Sharma, B. W. Skelton, P. Venugopalam and A. H. White, *Aust. J. Chem.*, **51**, 775 (1998).

⁴⁰ W. J. Evans, W. G. McClelland, M. A. Greci and J. W. Ziller, *Eur. J. Solid State. Inorg. Chem.*, **33**, 145 (1996).

⁴¹ K. G. Caulton, M. H. Chisholm, S. R. Drake, K. Folting, J. C. Huffman and W. E. Streib, *Inorg. Chem.*, **32**, 1970 (1993).

⁴² T. P. Hanusa, C. J. Huffman, J. C. Huffman and K. F. Tesh, *Inorg. Chem.*, **31**, 5572 (1992).

⁴³ G. Hundal, M. S. Hundal, S. Obrai and N. S. Poonia, *Acta Crystallogr. Sect C.*, **55**, 26 (1999).

⁴⁴ V. C. Arunasalem, I. Baxter, M. B. Hursthouse, K. M. A. Malix, D. M. P. Mingos and J. C. Plaxatouras, *Polyhedron.*, **15**, 3971 (1996).

⁴⁵ K. G. Caulton, M. H. Chisholm, S. R. Drake and W. E. Streib, *Inorg. Chem.*, **29**, 2707 (1990).

⁴⁶ S. R. Drake, M. B. Hursthouse, K. M. A. Malix and D. J. Otway, *Polyhedron.*, **11**, 1995 (1992).

⁴⁷ J. M. Harrowfield, B. W. Skelton and A. H. White, *Aust. J. Chem.*, **48**, 1333 (1995).

⁴⁸ T. P. Hanusa and K. F. Tesh, *J. Chem. Soc., Chem. Commun.*, 879 (1991).

⁴⁹ K. G. Caulton, M. H. Chisholm, S. R. Drake, K. Folting and J. C. Huffman, *Inorg. Chem.*, **32**, 816 (1993).

⁵⁰ L. Cot, J-D. Foulon, N. Hovnanian and P. Miele, *Polyhedron.*, **12**, 267 (1993).

⁵¹ J-D. Foulon, N. Hovnanian and P. Miele, *Polyhedron.*, **12**, 209 (1993).

⁵² T. R. Belderrain, J. P. Espinos, A. Fernandez, A. R. Gonzalez-Elipe, D. Leinen, A. Monge, M. Paneque, C. Ruiz and E. Carmona, *J. Chem. Soc., Dalton Trans.*, 1529 (1995).

5.2 Structural investigation of III, IV and VI.

The components used in the synthesis of complexes 9-21 were synthesised according to the procedures outlined in Chapter 3, and are listed in the table below (Table 5.2).

Component Number	Chemical Formula
III	Ph ₃ PNH
IV	(Me ₂ N) ₃ PNH
VI	Ph ₃ PO
45	Ph ₂ MePNH

Table 5.2 Table of components used in complexes 9-21.

Triphenyliminophosphorane **III** has been structurally characterised by both single crystal X-ray diffraction and also neutron diffraction studies.⁵³ The neutron data allowed the position of the hydrogen atom attached to the iminic nitrogen to be determined accurately. The phosphonium centre is, as expected, pyramidalised with C_{ipso}-P-N bond angles in the range 109.1(1) to 115.6(1)° and a P-N_{iminic} bond length of 1.582(2) Å which is in the range of previously studied iminophosphoranes.⁵⁴ Consideration of the P-N_{iminic}-H bond angle shows it be more acute [115.0(2)°] than seen in Ph₃PNPh [130.4(3)°],⁵⁴ which may be due to reduced steric demands, or is indicative of the pyramidalisation of the iminic nitrogen, similar to the phosphonium ylides already discussed (Chapter 1 & 4). Other salient features to note include the existence of N-H...N bridges and also C-H...N contacts which form supramolecular layers of molecules.

Tris(dimethylamino)iminophosphorane **IV** has also been previously studied⁵⁵ and was found to contain a P-N_{iminic} bond length of 1.557(1) Å which again is within the range expected for iminophosphoranes.⁵⁴ There is local C_s symmetry around the phosphorus atom, as was found for the isoelectronic phosphonium ylide [(Me₂N)₃PCH₂], with a sum

⁵³ M. G. Davidson, A. E. Goeta, J. A. K. Howard, C. W. Lehmann, G. M. McIntyre and R. D. Price, *J. Organomet. Chem.*, **550**, 449 (1998).

⁵⁴ (a). M. J. E. Hewlins, *J. Chem. Soc. B.*, 942 (1971). (b). J. Beck, E. Bohm, K. Dehnicke, D. Fenske, W. Hiller, A. Maurer and J. Strahler, *Z. Naturforsch.*, **43B**, 138 (1998).

⁵⁵ C. Lustig and N. W. Mitzel, *J. Chem. Soc., Dalton. Trans.*, 3177 (1999) and references cited therein.

of angles around the pyramidal dimethylamino group = 344° . The phosphonium centre is also pyramidal with a sum of the angles around it of 341° .

Triphenylphosphine oxide VI has three known structurally characterised⁵⁶ polymorphs, that have differing geometric parameters. The average P-O bond length is 1.494Å and other features to note include a unique P-C_{ipso} bond in the orthorhombic polymorph and a pyramidal phosphonium centre.

Compound 45, which in this case has been used as a ligand will be described in further detail in Chapter 7.

5.3 NMR data of complexes 9-21.

All the complexes discussed in this chapter have been analysed by ^{31}P and ^1H NMR spectroscopy (using benzene d^6 as a solvent). All the complexes described herein contain at least one chemically unique phosphorus atom and as such ^{31}P NMR is the most useful technique for analysis. Table 5.3 shows a ^{31}P chemical shift comparison for the un-coordinated components III, IV, VI and 45 and the complexes 9-21.

Complex Number	Component(s) Used.	$\delta^{31}\text{P}$ Complex (ppm)	$\delta^{31}\text{P}$ Component (ppm)
9	III	30.8	17.5
10	III	30.8	17.5
11	III	30.0	17.5
12	IV	45.6	40.0
13	III & V	27.0 & 39.6	17.5 & 57.7
14	III	21.8	17.5
15	45	35.6	14.7
16	VI	33.5	25.9
17	VI	32.8	25.9

⁵⁶ (a). G. Bandoli, G. Bartolozzo, D. A. Clemente, U. Croatto and C. Panattoni, *J. Chem. Soc. A.*, 2778 (1970). (b). G. Ruban and V. Zabel, *Cryst. Struc. Commun.*, 5, 671 (1976). (c). A. L. Spek, *Acta. Cryst.*, C43, 1233 (1987).

18	VI	32.5	25.9
19	VI	33.7	25.9
20	VI	33.7	25.9
21	VI	32.5	25.9

Table 5.3 Table to show the ^{31}P NMR chemical shift comparison between the starting components and complexes.

It can be seen that (with the exception of Ligand V) the ^{31}P shift of the complex shows a shift to lower field (i.e. the ^{31}P frequency and hence the chemical shift is higher) than the starting component. The reason for this was explained in 4.3 of Chapter 4 and is caused by deshielding of the phosphorus atom.

5.4 Structural investigation of complexes 9-11.

Reaction of the metal bis[bis(trimethylsilyl)amides] VIIa-c with two equivalents of triphenyliminophosphorane III and two equivalents of 2,6-di-tert-butyl,4-methyl phenol in toluene followed by cooling at room temperature yielded a crop of colourless crystals of 9-11 in each case. Preliminary characterisation followed by X-ray crystallographic studies revealed 9-11 to be monomeric alkaline earth metal bis(iminophosphorane) bis(phenoxide) complexes.

The solid state structure of 9 (Figure 5.1) contains a central calcium atom surrounded by two 2,6-di-tert-butyl,4-methyl phenoxide groups and two neutral iminophosphorane moieties. Considering the interactions between the calcium atom and the iminic nitrogens it can be seen that there is a Ca-N bond length [2.393Å (ave.)] which is noticeably shorter than the corresponding Ca-C_{ylidic} bond length of 2.646(4)Å seen in compound 1. There is a N1-Ca1-N2 bond of angle of 102.86(11)°, which can be compared to the N-Ca-N angles in the starting amide⁵⁷ [87.60 & 136.83° (exists as dimer)], and is also considerably smaller than the O1-Ca1-O2 angle of 115.14(10)°. This can be attributed to the bulky tertiary butyl groups of the phenoxides pushing themselves away from each other which

⁵⁷ M. Westerhausen, *Coord. Chem. Rev.*, **176**, pp157-210 (1998) and references cited therein.

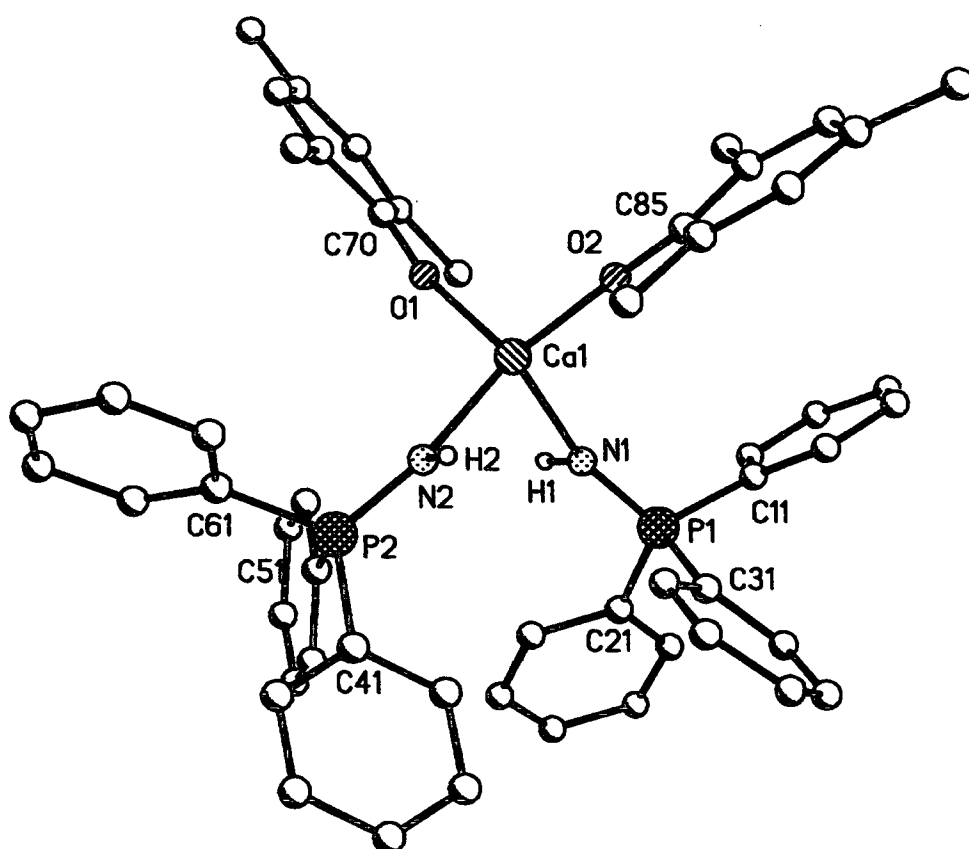


Figure 5.1 Single crystal X-ray structure of $(\text{Ph}_3\text{PNH})_2 \cdot \text{Ca}[\text{OC}_6\text{H}_2(\text{Me})_4\text{Bu}_2]_2$. All hydrogen atoms, except the iminic hydrogens, and all tertiary butyl groups' methyls omitted for clarity.

in turn leaves less room for the iminophosphoranes and hence gives a narrower N1-Ca-N2 angle. There is a Ca1-O1 and Ca1-O2 bond length of 2.148 Å (ave.) which is in the normal range for calcium aryloxides.⁴²

The P-N bond length in the co-ordinated iminophosphoranes is 1.585 Å (ave.) [P1-N1 & P2-N2], which is unchanged from the starting ligand of 1.582(2) Å.⁵³ With the proviso that crystallographically determined freely refined hydrogen atom positions should be treated with caution the P1-N1-H1 and P2-N2-H2 bond angles are 104.38(11) and 108.02(11)° respectively which are both noticeably smaller than the 115.0(2)° of the starting ligand. Looking at the PPh₃ unit of the coordinated ligand in more detail it can be seen that there are two shorter P-C_{ipso} bond lengths of 1.810(3) Å and 1.817(4) Å [P1-C21 & P1-C31] respectively and one longer P-C_{ipso} bond length of 1.823(4) Å [P1-C11]. These values compare favourably with those seen in the starting ligand **III** of 1.810(3), 1.817(3) and 1.818(3) Å respectively. A closer look at the C_{ipso}-P-N angles reveals three distinct values of 109.2(2), 112.9(2) and 115.5(2)° [C31-P1-N1, C21-P1-N1 and C11-P1-N1 respectively] compared to the 109.1(1), 114.6(1) and 115.6(1)° seen in the starting ligand. These data serve to demonstrate that the distorted tetrahedral geometry seen in the free iminophosphorane⁵³ is unchanged upon complexation indicating the ionic nature of the P-N bond and its subsequent interaction with the metal centre.

Searching the literature for examples of alkaline earth metal iminophosphorane complexes reveals that there are only a handful that are known, and more interestingly only a couple that are neutral examples. There are three previously characterised examples of neutral complexation of an iminophosphorane all involving the same iminophosphorane and all published in the same paper by Dehnicke et al¹⁴ [Figures 5.2 (a-c)].

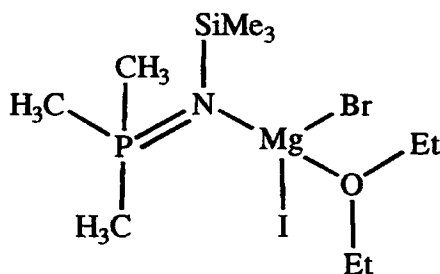


Figure 5.2a

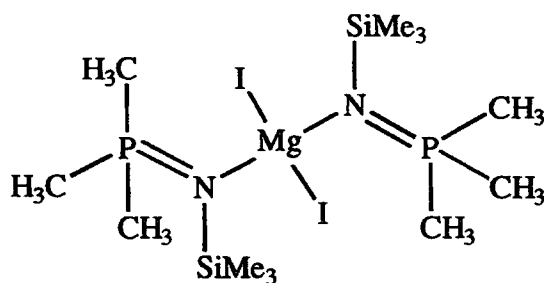


Figure 5.2b

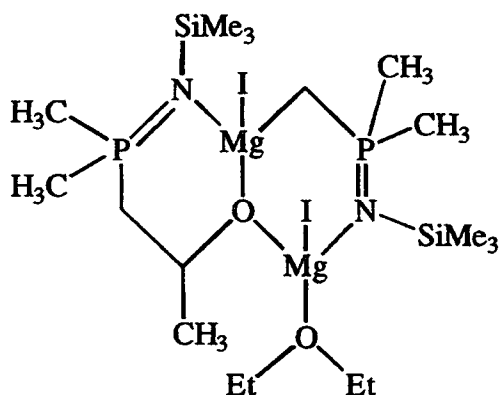


Figure 5.2c

The relevant bond lengths of the previous three compounds are as follows (Table 5.4).

	[P-N]Å	[Mg-N]Å
a	1.583 (ave.)	2.104 (ave.)
b	1.579 (ave.)	2.112 (ave.)
c	1.605 (ave.)	2.062 (ave.)

Table 5.4 Phosphorus-nitrogen and magnesium-nitrogen distances in complexes a-c.

Whilst the metal to nitrogen distances are not directly comparable due to a different metal than in **9**, they are noticeably shorter [Ca-N = 2.393Å(ave.) in **9**]. This is to be expected due to magnesium having a smaller radius which leads to the distance between the metal and the iminic nitrogen being smaller. More interesting are the P-N distances which are all very similar to those seen in complex **1** [1.585(ave.)].

There is only one reported calcium complex in the literature which contains co-ordination to an iminophosphorane type ligand⁵⁸ (Figure 5.3).

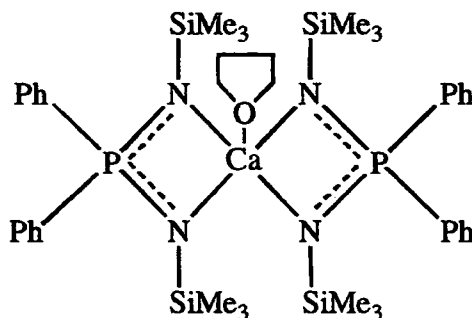


Figure 5.3

The P-N bond length in this bis(trimethylsilyl)amino diphenylphosphinimido calcium complex is 1.618Å(ave.), the range of Ca-N bond lengths is 2.393(2) to 2.546(3)Å and the N-Ca -N bond angle is 119.38(7)° which are all greater than are seen in the neutral complex 9.

Also contained in the same paper are the analogous beryllium and magnesium complexes, which have metal to nitrogen distances of 1.765Å(ave.) and 2.072Å(ave.) respectively. However, this range of complexes is not closely related to 9-11 as they are (a) ionic and (b) chelating phosphorus-nitrogen systems.

There are two other reported magnesium iminophosphorane complexes, neither of which contain a neutral iminophosphorane but should be mentioned for completion. They are a Mg_4N_4 cube complex (Figure 5.4) reported by Dehnicke et al,¹⁴

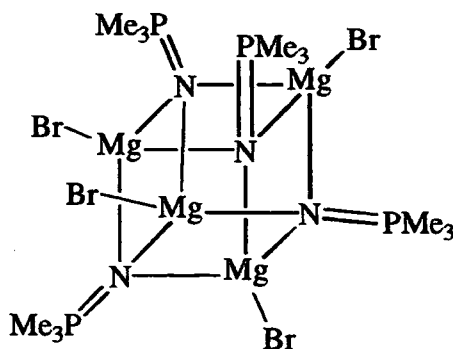


Figure 5.4

⁵⁸ R. Fleischer and D. Stalke, *Inorg. Chem.*, 36, 2413 (1997).

which has a P-N bond length of 1.582Å(ave.) and Mg-N distances in the range 2.081-2.151Å. The other example was reported by our group¹² (Figure 5.5).

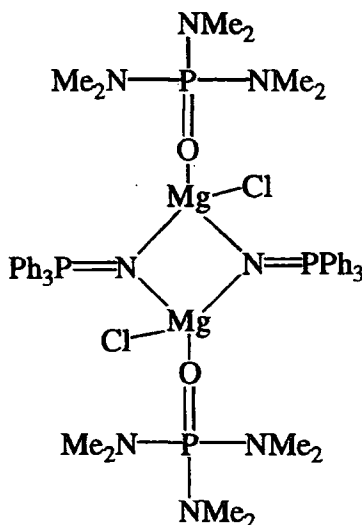


Figure 5.5

which has a P-N bond length of 1.556Å(ave.) and a Mg-N distance of 2.038Å(ave.).

Complex 10 (Figure 5.6), the strontium analogue of 9, crystallises in the space group $Pca2_1$ which is the same as complex 9. Complex 10 is isomorphous with complex 9 and this characteristic means that structural comparisons between the two complexes are very good because the crystal packing forces are the same.

The Sr-N_{iminic} bond length at 2.532Å (ave.) [Sr1-N1 & Sr1 N2] is longer than the Ca-N_{iminic} bond length of 2.393Å (ave.). This lengthening is due to the increased radius of the strontium atom over the calcium atom thus increasing the distance to the iminic nitrogens. The N1-Sr-N2 bond angle of 102.70(12)° is almost identical to that in 9 of 102.86(11)° and again falls between the two values seen in the starting amide [83.60 & 136.83° respectively]. The O1-Sr1-O2 bond angle of 115.4(10)° is identical to the corresponding angle in 9 and again demonstrates that the bulky tertiary butyl groups of the phenoxides force themselves away from each other, thus allowing less room for the iminophosphoranes and hence a smaller N1-Sr1-N2 angle in 9 & 10. There is also a Sr-O bond length of 2.280Å (ave.) [Sr1-O1 & Sr1-O2], which is in the usual range of expected values for strontium aryloxides.⁴⁹

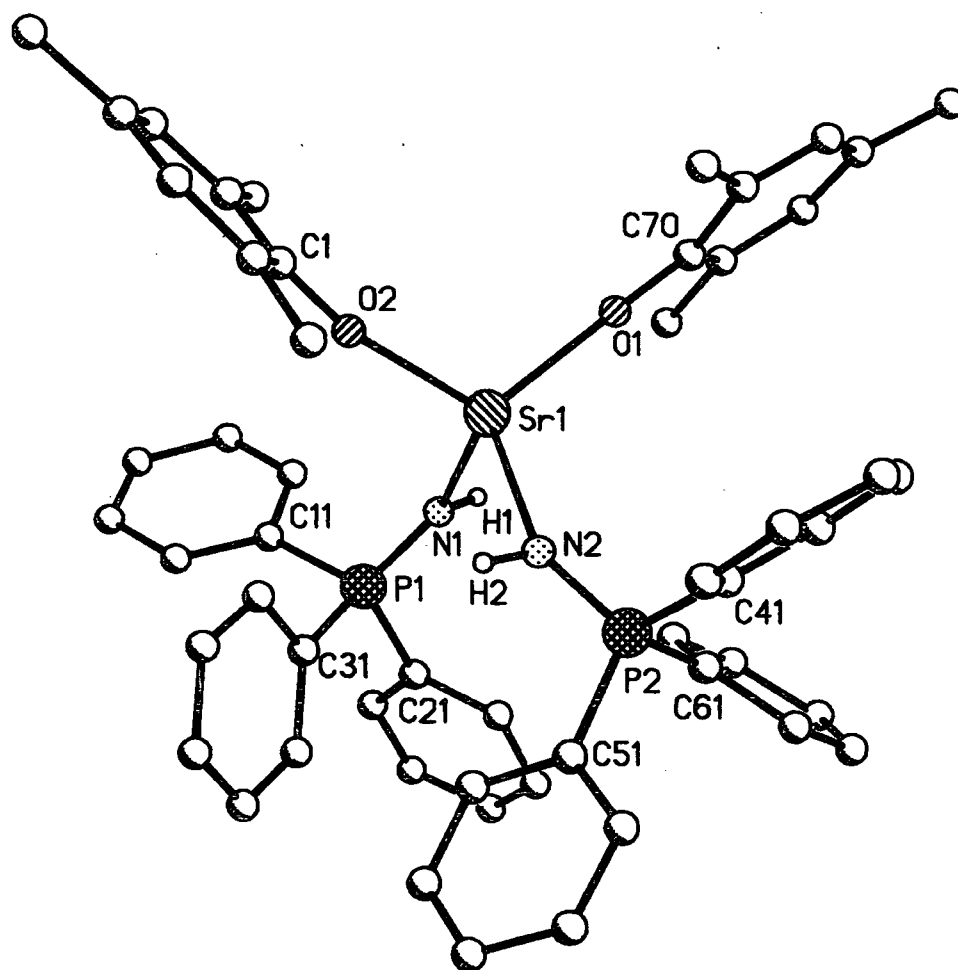


Figure 5.6 Single crystal X-ray structure of $(\text{Ph}_3\text{PNH})_2 \cdot \text{Sr}[\text{OC}_6\text{H}_2(\text{Me})_4\text{Bu}_2]_2$. All hydrogen atoms, except the iminic hydrogens, and all tertiary butyl groups' methyls omitted for clarity.

The P-N bond length in **10** is 1.587 Å (ave.) [P1-N1 & P2-N2], which again is unchanged from the free imine⁵³ [1.582(2) Å] and the P1-N1-H1 and P2-N2-H2 bond angles are 105.29(13) and 108.76(13)° respectively, again noticeably smaller than those in **III** [115.0(2)°]. Consideration of the PPh₃ unit in the coordinated iminophosphorane in **10** shows two shorter C_{ipso}-P bond lengths of 1.803(4) and 1.804(4) Å [C21-P1 & C31-P1] and one longer C_{ipso}-P bond length of 1.815(4) Å [C11-P1], which again are very similar to the starting ligand **III**. The C_{ipso}-P-N angles in **10** are 109.0(2), 114.9(2) and 115.2(2)° [C31-P1-N1, C21-P1-N1 and C11-P1-N1 respectively], again unchanged from the starting iminophosphorane.

Searching the literature for examples of strontium iminophosphorane complexes shows that there is only one complex containing both a strontium atom and an iminophosphorane type ligand. It is a complex published by Stalke et al⁵⁸ (Figure 5.7)

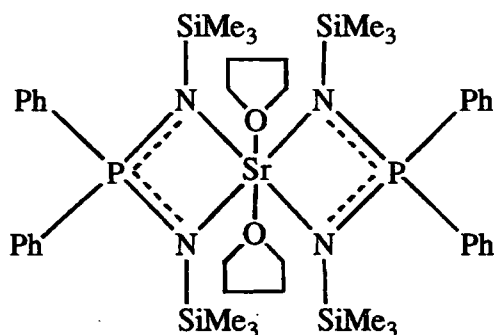


Figure 5.7

and again is neither neutral nor contains a neutral iminophosphorane. The Sr-N bond lengths of 2.610(2), 2.689(3), 2.639(3) and 2.605(2) Å [Sr1-N1, Sr1-N2, Sr1-N3 & Sr1-N4 respectively] are slightly longer than those seen in **10**, whereas the P-N bond lengths of 1.582(4), 1.588(3), 1.584(3) and 1.588(2) Å [P1-N1, P1-N2, P1-N3 & P1-N4 respectively] are almost identical.

Complex **11** (Figure 5.8) crystallises in the space group P-1, which is different to both complex **9** and **10**, thus showing a few structural differences. As with the ylide complexes reported in chapter 4, the barium analogue is not isomorphous with the calcium and strontium examples. The Ba-N bond length of 2.724 Å (ave.) [Ba1-N1 & Ba1-N2] is again greater than that seen in **9** and **10** and is attributable to the increased

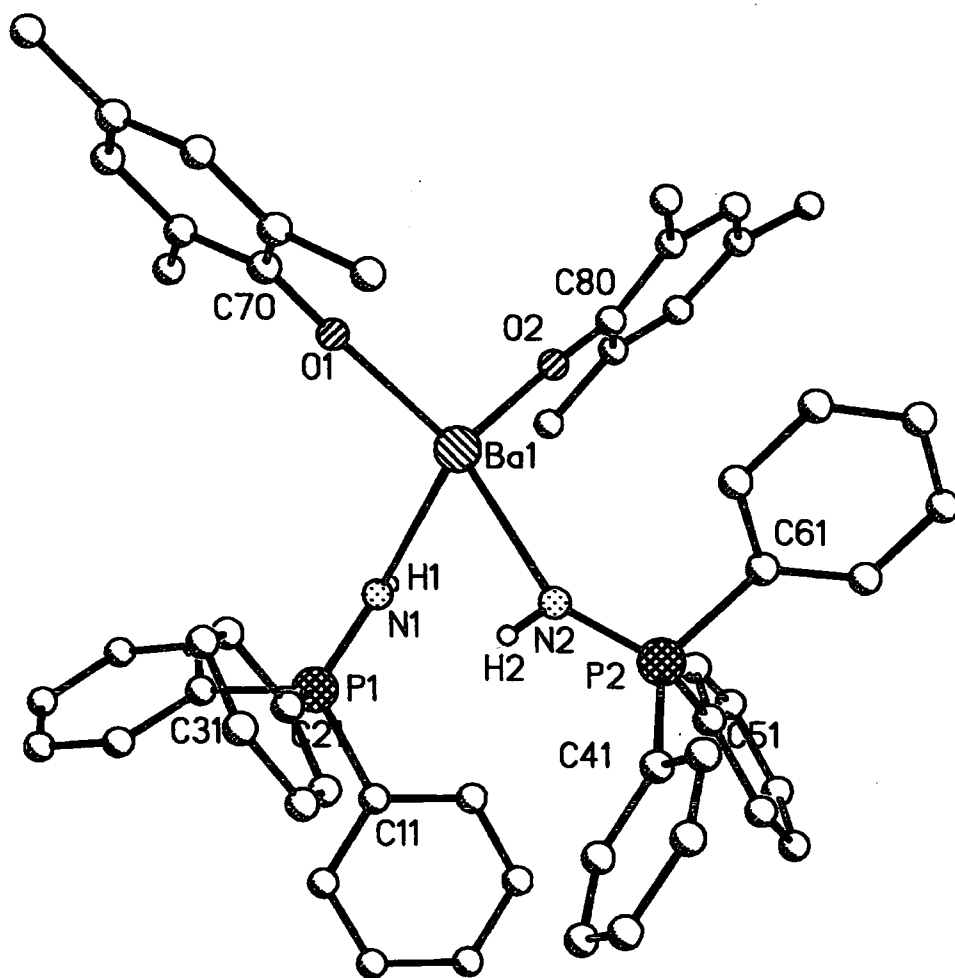


Figure 5.8 Single crystal X-ray structure of $(\text{Ph}_3\text{PNH})_2 \cdot \text{Ba}[\text{OC}_6\text{H}_2(\text{Me})^t\text{Bu}_2]_2$. All hydrogen atoms, except the iminic hydrogens, and all tertiary butyl groups' methyls omitted for clarity.

radius of the barium atom. The N1-Ba-N2 bond angle of $84.95(8)^\circ$ is considerably smaller than that seen in the corresponding angles of **9** and **10** [$102.86(11)^\circ$ and $102.70(12)^\circ$ respectively] and this structural characteristic coupled with the O2-Ba-O1 angle, which at $111.08(6)^\circ$ [$115.14(10)^\circ$ in **9** and **10**] is not dramatically changed gives an overall effect which is the opposite to that seen in compounds **1-3**. In the barium complex **3** the ylides are further apart from one another relative to **1** and **2**, whereas in complex **11** the iminophosphoranes are closer together than in **9** or **10**. As stated above, the actual orientation of the iminophosphoranes in complex **11** is different to that seen in **9** or **10**. This difference is mirrored in complexes **1-3** as the barium-ylide complex **3** has differing ylide orientations compared to **1** and **2**. This trend is expected to repeat itself as the iminophosphorane **III** is isoelectronic with the phosphonium ylide **I**.

The Ba-O bond length at 2.429\AA (ave.) [Ba1-O1 & Ba1-O2] is comparable to other observed Ba-O bond lengths.⁴⁹ The P-N_{imino} bond length is at 1.582\AA (ave.) [P1-N1 & P2-N2] unchanged from the starting free imine and the P1-N1-H1 and P2-N2-H2 angles are $111.80(9)^\circ$ and $106.78(10)^\circ$ respectively. One of these angles is $\sim 6^\circ$ larger than any seen in either **9** or **10**. They are however closer on average to the $115.0(2)^\circ$ seen in the starting ligand **III**.

Consideration of the PPh₃ unit shows there to be two larger C_{ipso}-P-N bond angles of $115.24(13)^\circ$ and $115.28(13)^\circ$ [C31-P1-N1 & C11-P1-N1] and one smaller C_{ipso}-P-N bond angle of $108.47(12)^\circ$ [C21-P1-N1] which while differing slightly from those seen in **9** and **10** are still within the range seen in the starting ligand. Investigating the C_{ipso}-P bond lengths shows two longer [both $1.812(3)\text{\AA}$, C31-P1 & C11-P1 respectively] and one shorter bond [$1.804(3)\text{\AA}$, C21-P1] which overall shows little difference from the free iminophosphorane PPh₃ unit.

There are three previously published complexes of barium and an iminophosphorane type ligand by Stalke et al^{58,59} (Figure 5.9a-c).

⁵⁹ S. K. Pandey, H. W. Roesky, D. Stalke and A. Steiner, *Angew. Chem., Int. Ed. Engl.*, **32**, 596 (1993).

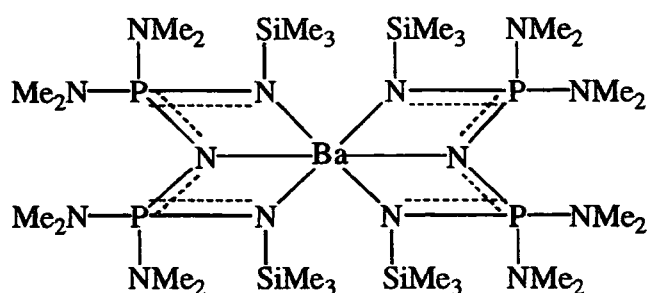


Figure 5.9a

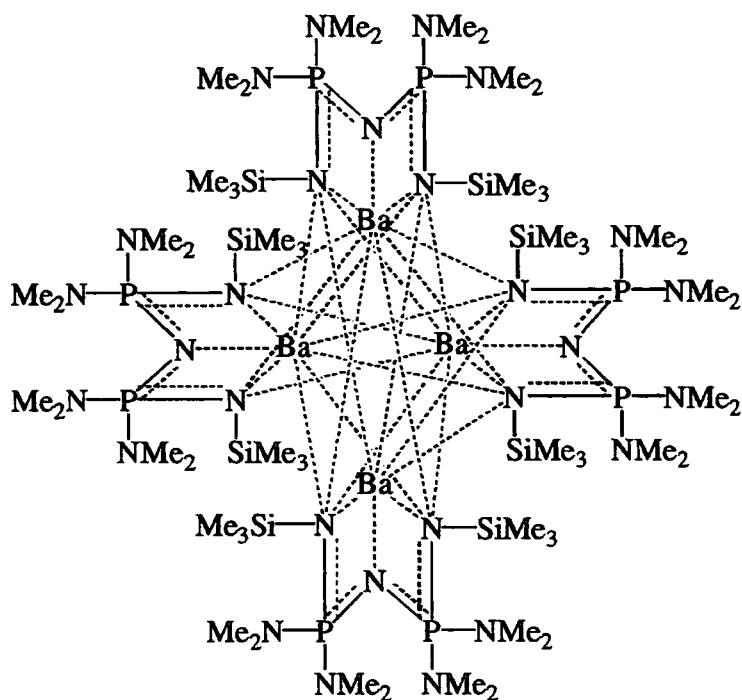


Figure 5.9b

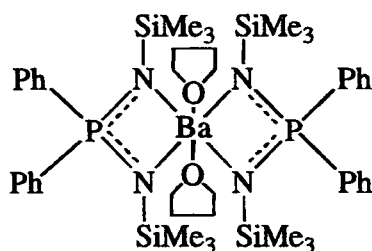


Figure 5.9c

Whilst none of the above contain a neutral iminophosphorane ligand, the P-N and M-N bond lengths are listed in **Table 5.5** below for comparison.

	[P-N]Å	[M-N]Å
a	1.578(ave.)	2.767(ave.)
b	1.556(ave.)	3.335(ave.)
c	1.583(ave.)	2.793(ave.)

Table 5.5 Table showing phosphorus-nitrogen and barium-nitrogen distances for a-c

All of the above values, with the exception of the barium to nitrogen distance in **b** which is an extremely sterically crowded molecule, provide a good correlation with those seen in **9-11** even though as mentioned previously the ligands employed in **a-c** are neither neutral nor contain a true iminophosphorane. The reason for the long bond distance in **b** can be attributed to the very high co-ordination of each barium atom which serves to diminish the bonding capabilities of the barium and hence the bonds are longer and weaker.

A consideration of the crystal packing in complexes **9-11** shows a number of interesting features. Whilst there are no classical hydrogen bonds in these complexes (the only classical donor / acceptor groups in each complex are the O atoms and the N-H groups which are buried near the centre of the molecule) there are a number of non-classical C-H... π bonds* in each case. These particular hydrogen bonds are amongst the weakest known and thus have only a small influence on the overall structure. The H-bonding pattern in the calcium and strontium complexes (**9** & **10**) is rather complicated and includes seven non-classical C-H... π hydrogen bonds with each molecule linked to five other symmetry generated molecules. The two complexes are in nearly identical configurations and given the identical packing it can be assumed that the hydrogen bonding is the same. This is further borne out by considering the bond lengths and angles in **9** and **10** with π ...H interactions of 2.816(18) to 3.102(18)Å for **9** and π ...H

* For examples of 'non-classical hydrogen bonding see M. C. Grossel, A. K. Cheetham, D. A. O. Hope, S. C. Weston. *J. Org. Chem.*, **58**, 6654 (1993) and D. Braga, F. Grepioni, E. Tedesco, *Organometallics.*, **17**, 2669 (1998).

interactions of 2.829(68) to 3.087(19) Å for **10**. The $\pi\cdots\text{H}\cdots\text{C}$ angles range from 125.9(2) to 174.9(5)° for **9** and from 126.3(5) to 174.0(2)° for **10**.

The hydrogen bonding pattern in the barium complex **11** (Figure 5.10) is very simple to visualise. The barium complex forms chains two molecules wide, related by an inversion centre. Again a 'double' non-symmetrical C-H... π ...H-C hydrogen bond is present and originates from one of the 2,6-di-tertbutyl,4-methyl phenoxide groups. Each of these chains is bound to the next one by another set of inversion related hydrogen bonds. The salient H-bond distances and angles are in the range 2.576(9) to 2.827(9) Å for the $\pi\cdots\text{H}$ interactions and in the range 125.9(2) to 149.4(2)° for the $\pi\cdots\text{H}\cdots\text{C}$ interactions.

One final comparison can be made between complexes **9-11** and with the neutral s-block metal complexes of iminophosphoranes recently synthesised by our group.¹⁰ The two reported complexes of most interest are the lithium and sodium analogues of complexes **9-11**, where Li = Ph₃PNH·Li[OC₆H₂(Me)^tBu₂] and Na = Ph₃PNH·Na[OC₆H₂(Me)^tBu₂], see Table 5.6.

	III	Li	Na	9	10	11
R[P-N _(imine)] Å	1.582(2)	1.578(2)	1.581(2)	1.585(ave.)	1.587(ave.)	1.582(ave.)
$\Sigma\angle[\text{N}_{(\text{imine})}]^\circ$	-	359	360	360	360	357
$\Sigma\angle[\text{P}]^\circ$	339	339	338	338	339	357
R[M-N _(imine)] Å	-	1.982(4)	2.307(2)	2.393(ave.)	2.532(ave.)	2.724(ave.)
[M-N _(imine) -P]°	-	146.3(2)	138.0(1)	147.6(ave.)	146.0(ave.)	141.4(ave.)

Table 5.6 Comparison of **9-11** with group 1 analogues.

From the above table it can be seen that for most geometric parameters the values do not change upon complexation. The only parameter which does change is the metal to iminic nitrogen distance which as expected increases as the size of the metal increases.

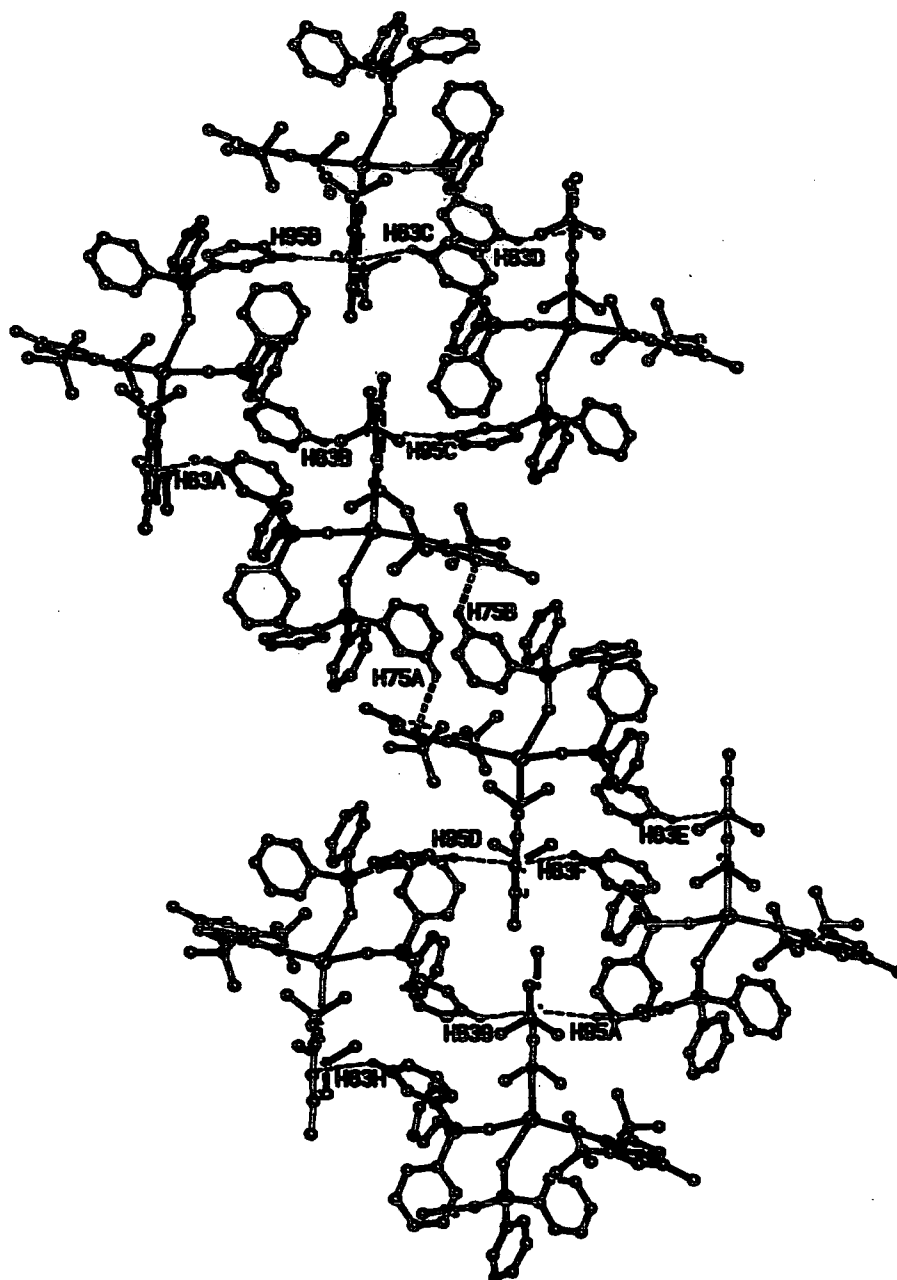


Figure 5.10 Diagram to show hydrogen bonding interactions in complex 11.

5.5 Discussion of complexes 12-15.

Compound 12 was produced by the addition of two equivalents of tris(dimethylamino)iminophosphorane IV and two equivalents of 2,6 di-tert-butyl,4-methyl phenol to one equivalent of strontium bis[bis(trimethylsilyl)amide] VIIIb in a toluene/hexane mixture. The resulting crystalline solid was unfortunately not of a sufficient quality to undergo single crystal X-ray diffraction studies but its composition was confirmed by NMR, elemental analysis and melting point.

Searching the published literature (see section 5.4) reveals no known neutral complexes containing tris(dimethylamino)iminophosphorane and an alkaline earth metal, although the following alkali metal complexes (Figure 5.11a&b) and alkaline earth metal complex (Figure 5.11c) have been synthesised and structurally characterised by our group.³

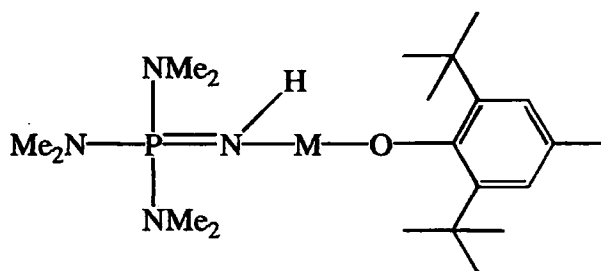


Figure 5.11a where M = Li & Na.

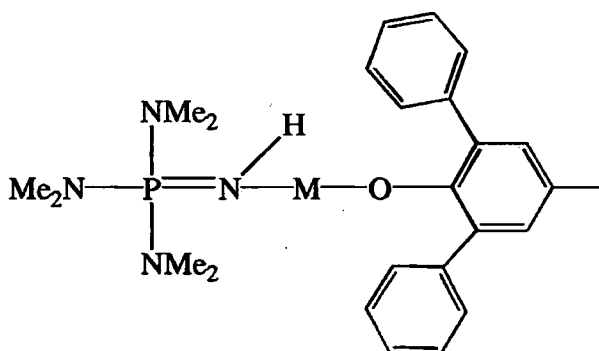


Figure 5.11b where M = Li & Na.

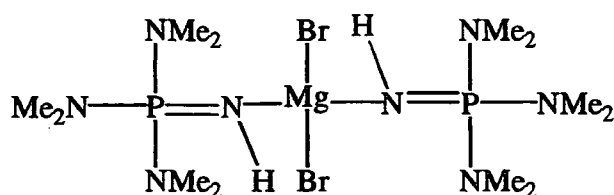
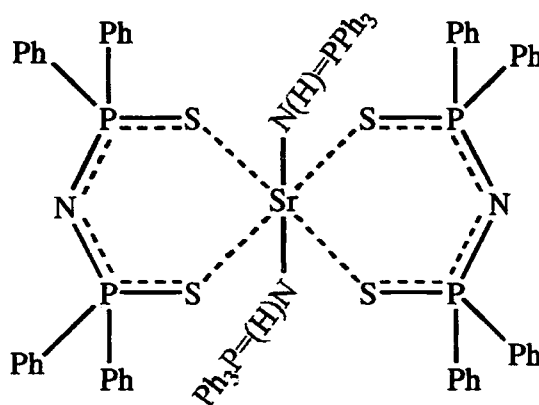


Figure 5.11c

Compound **13** was synthesised by the addition of two equivalents of triphenyliminophosphorane **III** and two equivalents of tetraphenyldithiodiphosphinylimide **V** to one equivalent of strontium bis[bis(trimethylsilyl)amide] **VIIIb** in toluene. As was the case with **12**, the resulting material was not suitable for single crystal X-ray diffraction studies but was analysed by NMR and elemental analysis and also gave a clean melting point. Alkaline earth metal iminophosphorane and tetraphenyldithiodiphosphinylimide complexes have already been discussed elsewhere in this thesis (4.5 and 5.4 respectively) and repetition is not necessary due to no structural data being available for **13**. However a proposed structure for complex **13** (Figure 5.12) could be similar to an analogous alkaline earth metal phosphonium ylide complex **7**.

Figure 5.12 Proposed structure of **13**.

Compound **14**, produced upon the reaction of two equivalents of triphenyliminophosphorane **III** and two equivalents of triphenylmethanol (purchased from Aldrich and used as supplied) with strontium bis[bis(trimethylsilyl)amide] **VIIIb** was again unsuitable for single crystal X-ray diffraction studies. Alkaline earth metal iminophosphorane complexes have already been discussed elsewhere (5.4) and a search

of the literature reveals a barium complex,⁶⁰ two mixed aluminium-sodium complexes⁶¹ and a mixed aluminium-lithium complex containing Ph_3CO^- .⁶¹ A proposed structure (Figure 5.13) is shown and it is thought that complex 14 would be similar to analogous iminophosphorane-aryloxide complexes (9-11) in which each aryloxide is replaced with a triphenylmethoxide.

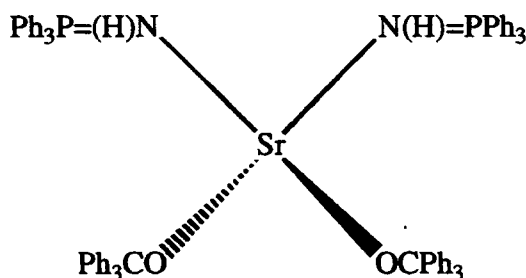


Figure 5.13 Proposed structure of 14.

Compound 15 was synthesised via addition of two equivalents of methyldiphenyliminophosphorane 45 and two equivalents of 2,6-di-tert-butyl, 4-methyl phenol to strontium bis[bis(trimethylsilyl)amide] VIIIb in toluene. A crystalline material was obtained but failed to diffract when subjected to X-ray analysis. Its composition was determined however by NMR, elemental analysis and by virtue of having a clean melting point. Strontium aryloxides have already been discussed prior to this point, and as no structural data for 15 are available further discussion would not be pertinent. A search of the database (CSD) does however reveal that there are no known structures containing Ph_2MePNH 45, nor in fact has its structure been previously determined (see Chapters 6 & 7 of this thesis).

⁶⁰ K. G. Caulton, M. H. Chisholm, S. R. Drake, K. Folting and W. E. Streib, *Inorg. Chem.*, **31**, 3205 (1992).

⁶¹ J. Knizek, I. Krossing, H. Noth, W. Ponikvar and T. Seifert, *Chem. Eur. J.*, **4**, 2191 (1998).

5.6 Discussion of complexes 16-18 and structural investigation of complexes 19-21.

Reaction of the metal bis[bis(trimethylsilyl)amides] **VIIa-c** with two equivalents of triphenylphosphine oxide **VI** in hot toluene followed by cooling at room temperature yielded a crop of colourless crystals of **16-18** in each case. Preliminary characterisation revealed **16-18** to be monomeric alkaline earth metal bis[bis(trimethylsilyl)amido] bis(triphenylphosphine oxide) complexes. Elemental analysis and a clean melting point uncharacteristic of either starting material further substantiated the above structural conclusion. Unfortunately, crystals suitable for X-ray analysis could not be obtained and complexes **16-18** are thus assumed to be of a similar structure to the isoelectronic phosphonium ylide complexes **1-3** (Figure 5.14).

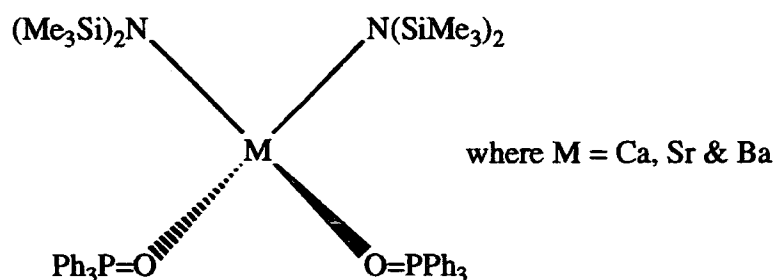


Figure 5.14 Proposed structure of complexes 16-18.

Reaction of the metal bis[bis(trimethylsilyl)amides] **VIIa-c** with two equivalents of triphenylphosphine oxide **VI** and two equivalents of 2,6-di-tert-butyl,4-methyl phenol in toluene followed by cooling at room temperature yielded a crop of colourless crystals of **19-21** in each case. Preliminary characterisation followed by X-ray crystallographic studies revealed **19-21** to be monomeric alkaline earth metal bis(triphenylphosphine oxide) bis(phenoxide) complexes.

The solid state structure of **19** (Figure 5.15) consists of a central calcium atom surrounded by two 2,6-di-tert-butyl,4-methyl phenoxide groups and two neutral triphenylphosphine oxide ligands. A closer inspection of the calcium-oxygen interactions reveals a Ca-O_{ox} bond length of 2.268 Å (ave.) [Ca1-O1 & Ca1-O2] which is shorter than is seen for the analogous Ca-C_{ylidic} bond length of 2.646(4) Å seen in **1**, and the Ca-N_{iminic}

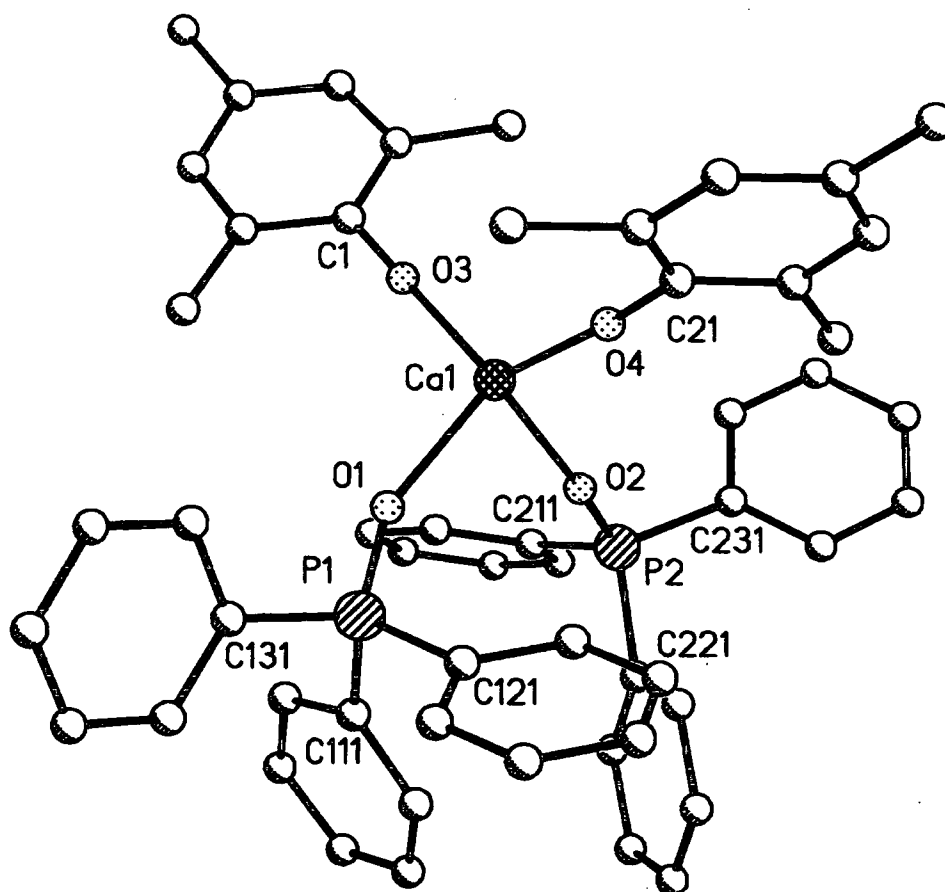


Figure 5.15 Single crystal X-ray structure of $(\text{Ph}_3\text{PO})_2 \cdot \text{Ca}[\text{OC}_6\text{H}_2(\text{Me})^t\text{Bu}_2]_2$. All hydrogen atoms and all tertiary butyl groups' methyls omitted for clarity.

bond length of 2.393 Å(ave.) seen in **9**. These bond lengths decrease as the electronegativity of the isoelectronic moieties they are bound to increases e.g bond length [M-CH₂ > M-NH > M-O] and electronegativity [M-O > M-NH > M-CH₂]. The bond length also decreases as the size of the moiety it is bonding to decreases [PCH₂ > PNH > PO].

The O_{ox}-Ca-O_{ox} bond angle of 94.75(4)° [O1-Ca1-O2] seems to fall in the middle of the previously mentioned C-Ca-C angle of 82.5(1)° in **1** and the 102.86(11)° seen for the N-Ca-N angle in **9**. Considering the phenoxides it can be seen that there is a O_{ph}-Ca-O_{ph} angle of 123.07(4)° [O3-Ca1-O4] which is close to 8° wider than the analogous angle of 115.14(10) in **9**. The bulky tertiary butyl groups of the phenol used force themselves away from each other and for this particular molecule the phosphine oxides can get closer together as there is no substituent on the oxide oxygen, whereas in **9** the iminic nitrogen is protonated thus having greater steric requirements. There is also a Ca-O_{ph} bond length of 2.152 Å(ave.) [Ca1-O3 & Ca1-O4] which is in the expected range of values for calcium aryloxides.⁴²

The P=O bond length for the co-ordinated phosphine oxide in **19** is 1.499 Å(ave.) [P1-O1 & P2-O2] which is unchanged with respect to the free phosphine oxide [1.494(ave.)].⁵⁶

The free orthorhombic form of triphenylphosphine oxide⁶² is compared to the two coordinated triphenylphosphine oxide units in **Table 5.7**.

	[C _{ipso} -P-O]°			[C _{ipso} -P] Å		
Free Ph ₃ PO	111.57(5)	111.95(5)	113.63(6)	1.803(4)	1.808(3)	1.799(3)
Ph ₃ PO 1	112.44(7)	111.34(8)	113.04(7)	1.7993(17)	1.7965(18)	1.7917(17)
Ph ₃ PO 2	111.62(7)	111.55(7)	111.62(7)	1.7929(18)	1.7964(17)	1.8046(18)

Table 5.7 Selected angles and bond lengths for free triphenylphosphine oxide and the two coordinated ligands found in **19**.

It can be seen from the above table that there are two distinct Ph₃PO units co-ordinated to the metal centre, both of which are similar in geometry to the free phosphine oxide.

⁶² C. P. Brock, J. D. Dunitz and W. B. Schweizer, *J. Am. Chem. Soc.*, **107**, 6964 (1985).

Searching the literature for previously published calcium-phosphine oxide complexes reveals seven examples, and in each of these complexes HMPA is used as the phosphine oxide. Four of these complexes contain mixed metals e.g calcium-titanium,⁶³ calcium-platinum,⁶⁴ calcium-mercury⁶⁵ and calcium-cobalt.⁶⁶ The other three complexes contain calcium as the sole metal and are as follows ;

a bis-benzophenone ketyl radical anion complex by Hou et al⁶⁷ (Figure 5.16a),

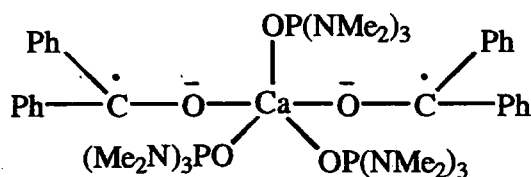


Figure 5.16a

a bis benzoxazolyl-2-thionato complex by Snaith et al⁶⁸ (Figure 5.16b)

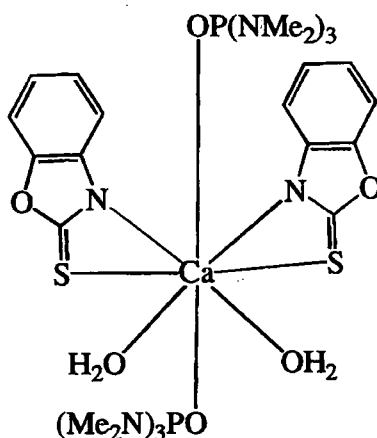


Figure 5.16b (bond lengths in diagram not representative of true values).

⁶³ M. Bjorgvinsson, A. Demsar, L. Golic, S. Patricek, A. Petric, A. Pevec and H. W. Roesky, *J. Chem. Soc., Dalton. Trans.*, 4043 (1998).

⁶⁴ M. G. Davidson, P. R. Raithby, R. Snaith, D. Stalke and D. S. Wright, *Angew. Chem., Int. Ed. Engl.*, **30**, 1648 (1991).

⁶⁵ M. G. Davidson, S. C. Llewellyn, M.-I. L. Solera, P. R. Raithby, R. Snaith and D. S. Wright, *J. Chem. Soc., Chem. Commun.*, 573 (1992).

⁶⁶ M. G. Davidson, M. Gerloch, S. C. Llewellyn, P. R. Raithby and R. Snaith, *J. Chem. Soc., Chem. Commun.*, 1363 (1993).

⁶⁷ M. Hoshino, Z. Hou, X. Jia and Y. Wakatsuki, *Angew. Chem., Int. Ed. Engl.*, **36**, 1292 (1997).

⁶⁸ P. Mikulcik, P. R. Raithby, R. Snaith and D. S. Wright, *Angew. Chem., Int. Ed. Engl.*, **30**, 428 (1991).

and of most interest a calcium oxide-phenoxide complex⁴¹ (Figure 5.16c).

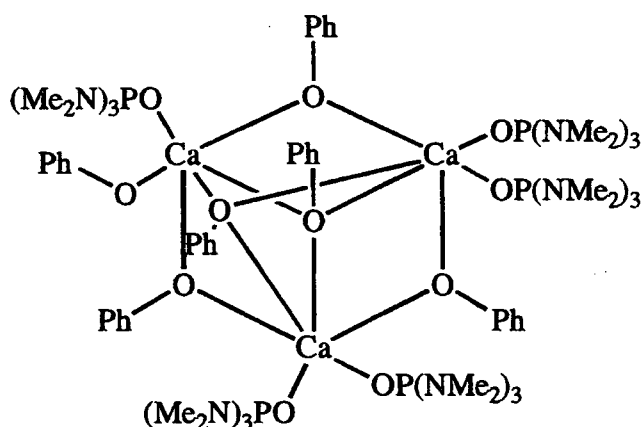


Figure 5.16c

The P-O and Ca-O (oxide and phenol) bond lengths for the above three complexes (Figure 5.16a-c) are presented in Table 5.8 below along with those for complex 19.

	[P-O]Å	[Ca-O _{ox}]Å	[Ca-O _{ph}]Å
19	1.499(ave.)	2.268(ave.)	2.152(ave.)
a	1.461(ave.)	2.301(ave.)	-
b	1.485(ave.)	2.267(ave.)	-
c	1.478(ave.)	2.310(ave.)	terminal 2.350(ave.)

Table 5.8 Selected P-O and Ca-O bond lengths for complexes a-c and 19.

The interesting point to note from the above table is that for c the terminal Ca-O_{ph} distance is greater than the Ca-O_{ox} distance which is surprising given that the phenoxide oxygen is deprotonated and hence negatively charged, whereas the phosphine oxide is neutral.

The solid state structure of 20 (Figure 5.17), the strontium analogue of 19, contains a central strontium atom surrounded by two 2,6-di-tert-butyl,4-methyl phenoxide groups and two neutral triphenylphosphine oxide ligands. Considering the interactions between the strontium atom and the oxygen of the phosphorus species it can be seen that there is a

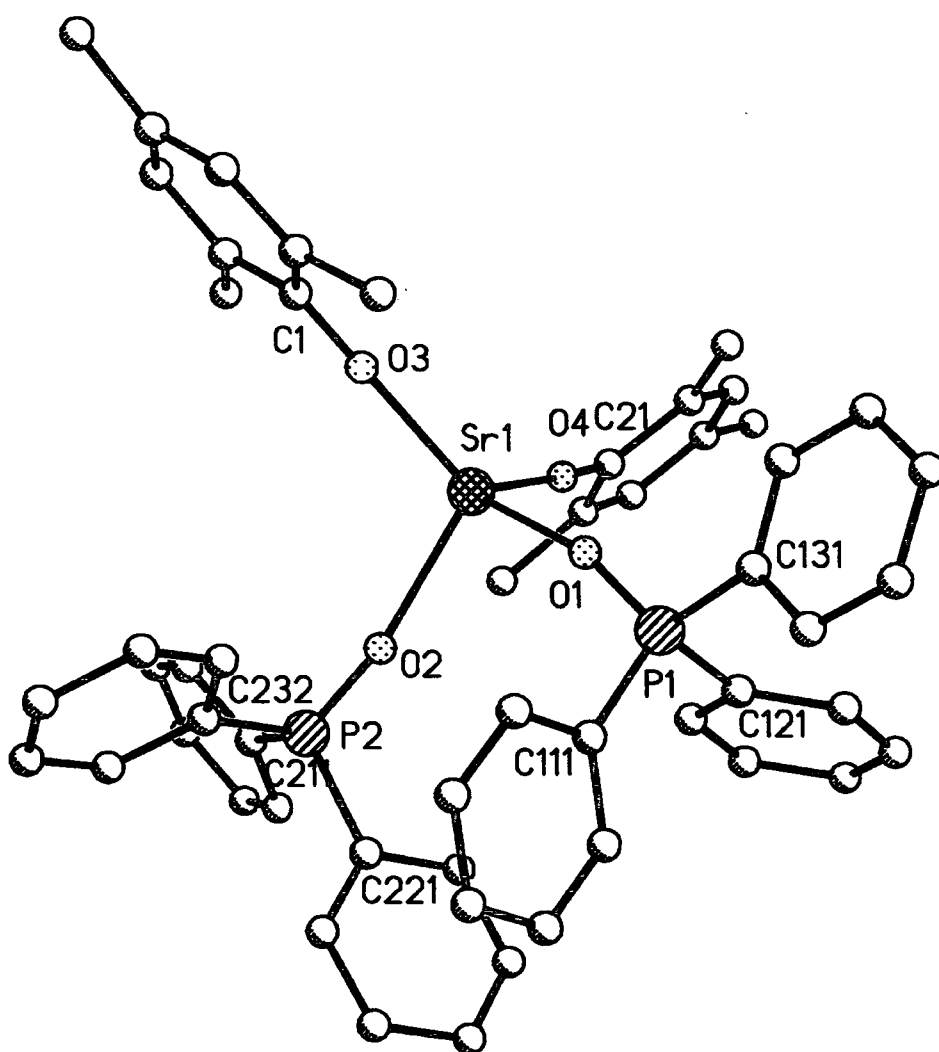


Figure 5.17 Single crystal X-ray structure of $(\text{Ph}_3\text{PO})_2 \cdot \text{Sr}[\text{OC}_6\text{H}_2(\text{Me})^t\text{Bu}_2]_2$. All hydrogen atoms and all tertiary butyl groups' methyls omitted for clarity.

Sr-O_{ox} bond length [2.413Å(ave.), Sr1-O1 & Sr1-O2] which is again shorter than both the corresponding Sr-C_{ylidic} bond length of 2.742(5)Å seen in **2** and also the Sr-N_{iminic} bond length of 2.532Å(ave.) seen in **10**, again due to the increasing electronegativity and decreasing size of the moiety it is binding to [PO vs. PNH vs. PCH₂]

The O(1)-Sr1-O(2) bond angle of 93.00(14)° which relates to the angle between the two phosphine oxides molecules, falls between the angles previously seen in **2** [C-Sr-C = 81.6(2)°] and **10** [N-Sr-N = 102.70(12)°]. Considering the above angle along with the O(3)-Sr1-O(4) bond angle of 124.01(11)° which is noticeably wider than that seen in **10** of 115.4(10)°, it can be seen that again the bulky tertiary butyl groups on the phenoxides force themselves away from each other. In this case the phosphine oxides can get closer together as there is no substituent on the oxide oxygen unlike in **10** where the iminic nitrogen is protonated thus having greater steric requirements. There is also a Sr-O_{ph} bond length of 2.284Å(ave.) [Sr1-O1 & Sr1-O2] which is in the expected range of values for strontium aryloxides.⁴⁹

The P=O bond length for the co-ordinated phosphine oxide in **20** is 1.491Å(ave.) [P1-O1 & P2-O2] which is unchanged with respect to the free phosphine oxide [1.494Å(ave.)].⁵⁶ Close inspection of their PPh₃ units shows there to be two distinct phosphine oxides. Both of these are compared with the orthorhombic form of the free phosphine oxide⁶² in Table 5.9.

	[C _{ipso} -P-O]°			[C _{ipso} -P]Å		
Free Ph ₃ PO	111.57(5)	111.95(5)	113.63(6)	1.803(4)	1.808(3)	1.799(3)
Ph ₃ PO 1	112.1(2)	111.7(2)	111.9(2)	1.793(5)	1.796(5)	1.798(5)
Ph ₃ PO 2	111.4(2)	111.4(2)	111.2(2)	1.794(5)	1.799(5)	1.810(5)

Table 5.9 Selected angles and bond lengths for triphenylphosphine oxide.

It can be seen from the above table that some structural features of the phosphine oxide change upon complexation e.g. there is an angle in the free oxide which is larger than the others and is not seen in the co-ordinated oxides.

A search of the literature reveals five complexes containing a strontium atom interacting with a phosphine oxide, and they all contain HMPA as the phosphine oxide. There is a crown ether thiophenoxide complex prepared by Chadwick et al,⁶⁹ and the others which are reported as follows, a mixed strontium-barium HMPA phenoxide complex prepared by Chisholm et al,⁴⁹ and of more direct relevance to this work, a strontium HMPA phenoxide complex again by Chisholm et al⁴¹ (Figure 5.18a).

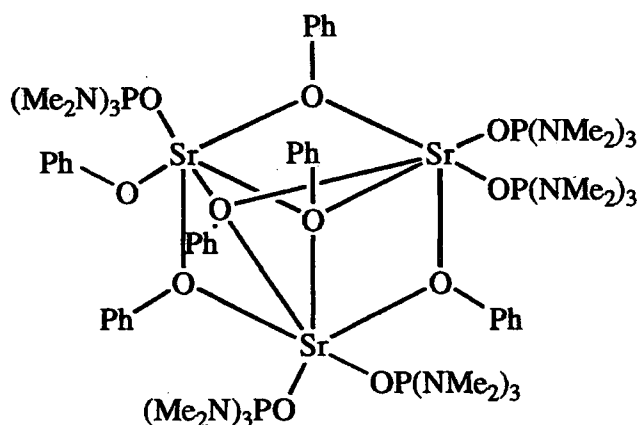


Figure 5.18a

There is also a pair of complexes by Snaith et al⁷⁰ (Figure 5.18b & c).

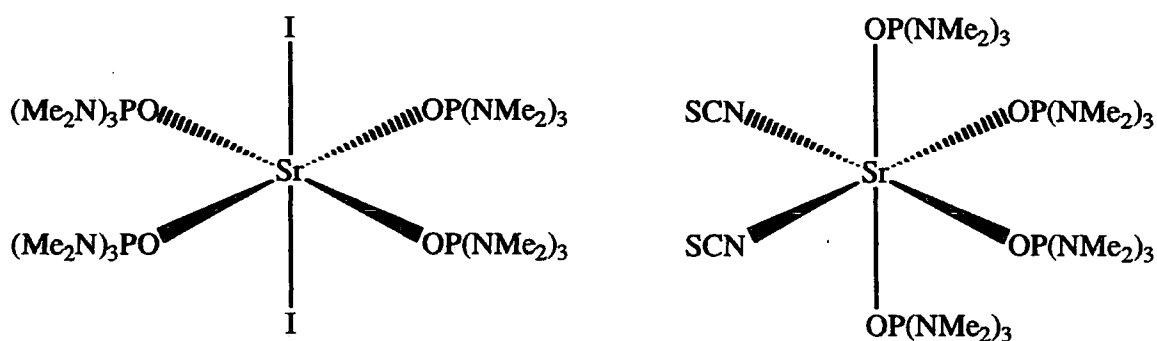


Figure 5.18b & c

The P-O distances and Sr-O (oxide and phenol) distances of the above three complexes are presented in Table 5.10 below along with those for compound 20.

⁶⁹ S. Chadwick, U. English and K. Rutlandt-Senge, *J. Chem. Soc., Chem. Commun.*, 2149 (1998).

⁷⁰ D. Barr, A. T. Brooker, M. J. Doyle, S. R. Drake, P. R. Raithby, R. Snaith and D. S. Wright, *J. Chem. Soc., Chem. Commun.*, 893 (1989).

	[P-O]Å	[Sr-O _{ox}]Å	[Sr-O _{ph}]Å
20	1.491(ave.)	2.413(ave.)	2.284(ave.)
a	1.485(ave.)	2.409(ave.)	Terminal 2.369(ave.)
b	1.444(ave.)	2.440(ave.)	-
c	1.455(ave.)	2.444(ave.)	-

Table 5.10 Selected P-O and Sr-O bond lengths for complexes a-c and 20

As can be seen from the above table there is little difference between the structural features of the compounds **a-c** and **20**, except for the appearance of a slightly shorter Sr-O_{ph} bond length in **20** when compared to **a**.

Complex **21** (Figure 5.19) crystallises in the space group P2₁/c and in continuing with this series of complexes (**19-21**), **21** contains a central barium atom surrounded by two neutral triphenylphosphine oxide ligands and two 2,6 di-tert-butyl,4-methyl phenoxide groups. The Ba-O bond length in this complex at 2.573Å(ave.) [Ba1-O1 & Ba1-O2], is again noticeably shorter than the corresponding Ba-C_{ylide} bond length [3.003Å(ave.)] in **3** and Ba-N_{iminic} bond length 2.724Å(ave.) in **11**, again due to the increased electronegativity of oxygen and the less sterically crowded PO unit compared to CH₂ and NH.

The O1-Ba1-O2 bond angle of 91.61(5)° is similar to that seen in both **19** and **20** and is a similar size to those seen in **3** [C-Ba-C = 92.5(2)°] and **11** [N-Ba-N = 84.95(8)°]. The O3-Ba1-O4 bond angle of 125.32(5)° is similar to those in **19** and **20** [123.07(4) & 124.01(11)° respectively] and again the bulky tertiary butyl groups dictate the geometry. The Ba-O_{ph} bond length of 2.424Å(ave.) [Ba1-O3 & Ba1-O4] is within the expected range for barium aryloxides⁴⁹ and compares well with that seen in **11** [2.429Å(ave.)].

Consideration of the P=O bond in **21** along with the PPh₃ units of the co-ordinating phosphine oxides, shows there to be an average P=O bond length of 1.496Å [P1-O1 & P2-O2], again little changed from the free oxide 1.494Å(ave.).⁵⁶ Table 5.11 compares the C_{ipso}-P-O angle and the C_{ipso}-P bond lengths in the free orthorhombic Ph₃P=O⁶² with those of the co-ordinating Ph₃P=O units.

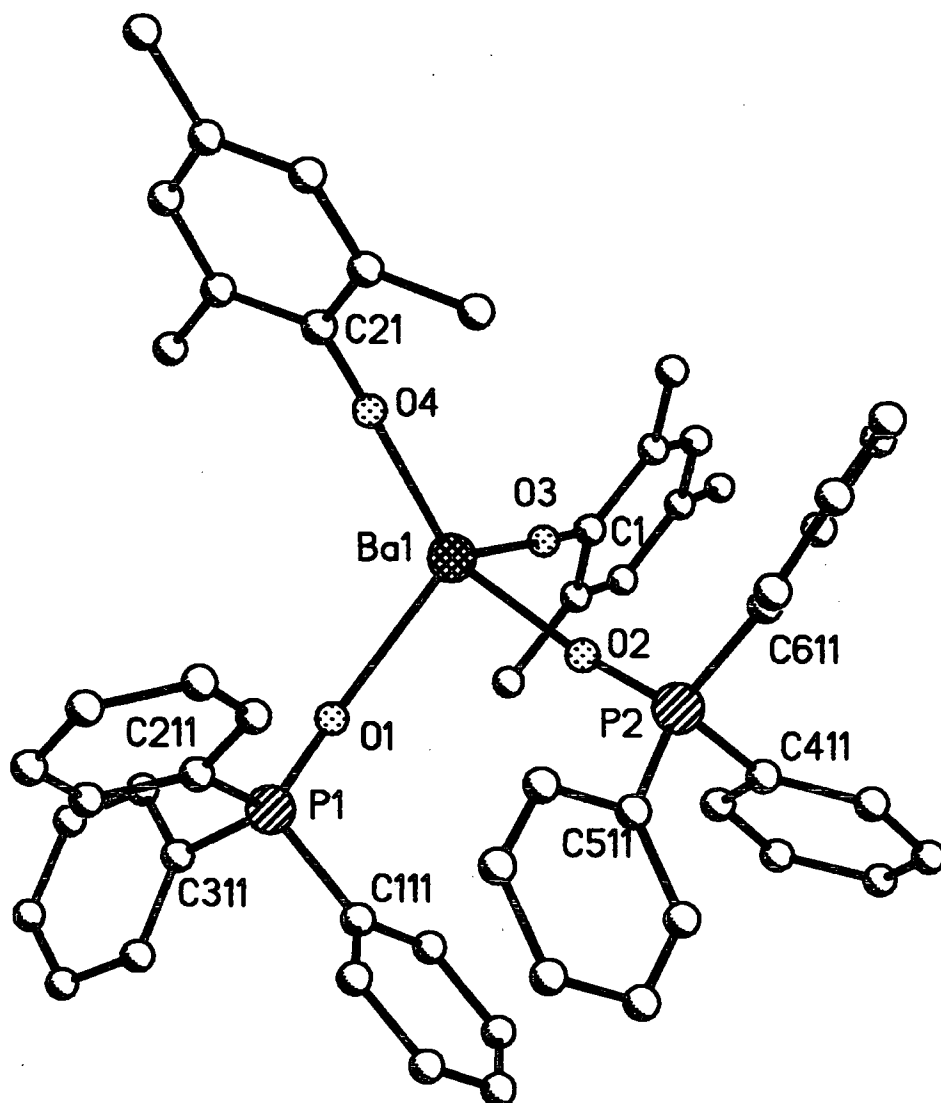
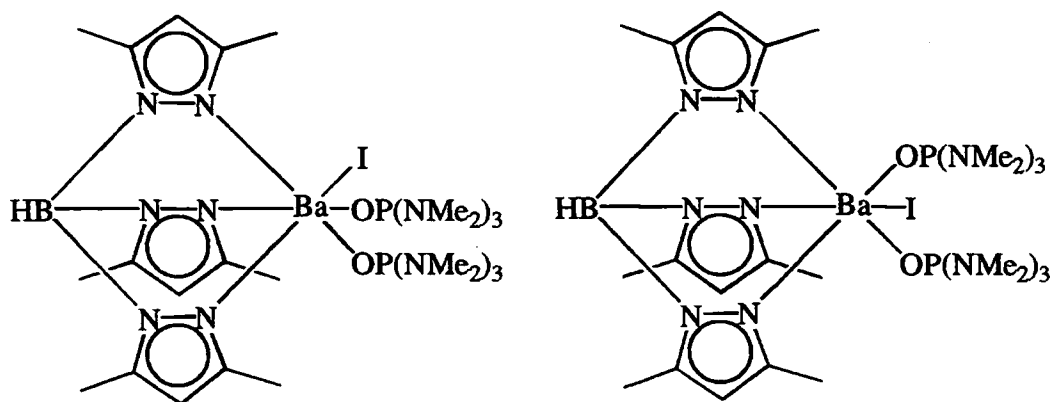


Figure 5.19 Single crystal X-ray structure of $(\text{Ph}_3\text{PO})_2\text{-Ba}[\text{OC}_6\text{H}_2(\text{Me})^t\text{Bu}_2]_2$. All hydrogen atoms and all tertiary butyl groups' methyls omitted for clarity.

	[C _{ipso} -P-O] ^o			[C _{ipso} -P]Å		
Free Ph ₃ PO	111.57(5)	111.95(5)	113.63(6)	1.803(4)	1.808(3)	1.799(3)
Ph ₃ PO 1	111.87(10)	111.84(10)	111.41(11)	1.787(2)	1.798(2)	1.801(3)
Ph ₃ PO 2	111.44(10)	111.19(9)	110.93(10)	1.796(2)	1.797(2)	1.803(2)

Table 5.11 Selected angles and bond lengths for triphenylphosphine oxide.

Of the ten reported barium-phosphine oxide complexes in the literature two are non-neutral complexes,^{67,71} and two are mixed metal complexes (strontium-barium⁴⁹ and copper-barium⁷²). The remaining six are detailed below and consist of the following two near identical complexes by Belderrain et al⁷³ (Figure 5.20a & b),

**Figure 5.20a & b**

a benzoxazolyl-2-thionato complex by Snaith et al⁶⁸ (Figure 5.20c),

⁷¹ F. A. Banbury, M. G. Davidson, A. Martin, P. R. Raithby, R. Snaith, K. L. Verhorevoort and D. S. Wright, *J. Chem. Soc., Chem. Commun.*, 1152 (1992).

⁷² B. Borup, J. C. Huffman and K. G. Caulton, *J. Organomet. Chem.*, 536, 109 (1997).

⁷³ T. R. Belderrain, L. Contreras, M. Paneque, E. Carmona, A. Monge and C. Ruiz, *J. Organomet. Chem.*, 474, C5 (1994); *Polyhedron*, 15, 3453 (1996).

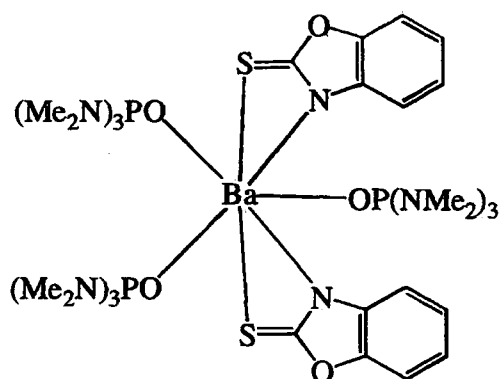


Figure 5.20c

a siloxane complex⁷⁴ (Figure 5.20d) and two complexes which contain phosphine oxides and phenoxides. The first is a hexakis phenoxide hexakis HMPA octa barium toluene solvate⁴⁹ **e**, and the second complex shown in Figure 5.20f which is of particular relevance to this work as it is analogous to complex **21** but uses a different phosphine oxide.⁵²

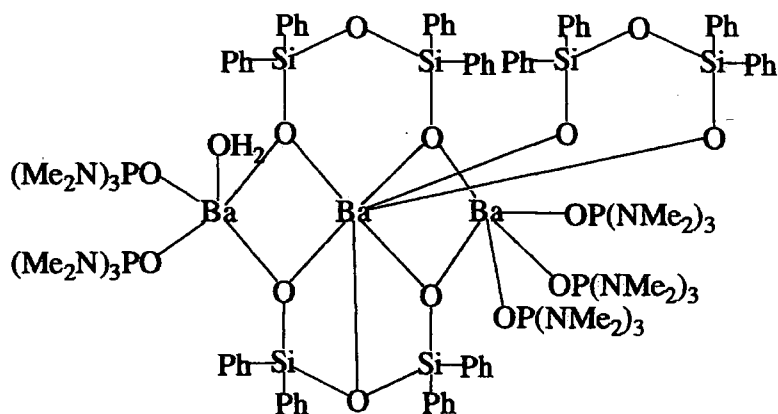


Figure 5.20d

⁷⁴ J. A. Barr, S. R. Drake, D. J. Williams and A. M. Z. Slawin, *J. Chem. Soc., Chem. Commun.*, 866 (1993).

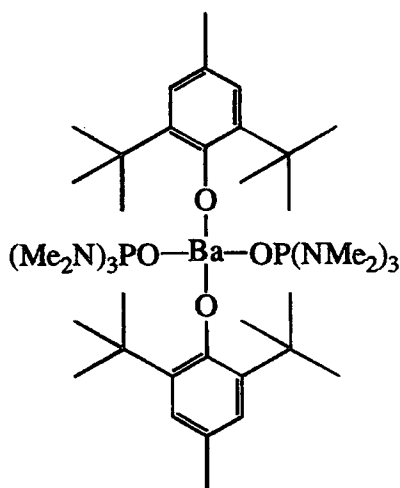


Figure 5.20f

The following table (Table 5.12) compares the various Ba-O bond lengths and angles seen in the above compounds and 21.

	[P=O]Å	[Ba-O _{ox}]Å	[Ba-O _{ph}]Å	[O _{ox} -Ba-O _{ox}] ^o	[O _{ph} -Ba-O _{ph}] ^o
a	1.438(ave.)	2.60(3)(ave.)	-	-	-
b	1.438(ave.)	2.60(3)(ave.)	-	-	-
c	1.455(ave.)	2.60(3)(ave.)	-	-	-
d	1.476(ave.)	2.711(ave.)	-	-	-
e	1.479(ave.)	2.591(ave.)	terminal 2.691(ave.)	-	-
f	1.479(9)	2.578(8)	2.414(8)	98.8(3)	117.3(3)
21	1.496(ave.)	2.573(ave.)	2.424(ave.)	91.61(5)	125.34(5)

Table 5.12 Selected bond lengths and angles for a-f and 21.

It is clear from the above table that the Ba-O_{ox} distance remains largely unchanged throughout the range of complexes regardless of the co-ordination number of barium (e.g. 7 in **c** and **d**, 4 in **21** and **f**) or the phosphine oxide used (HMPA in **a-f** and Ph₃PO in **21**). One point to note is that the phosphine oxides are much closer (~7°) in **21** compared to **f** with a concomitant spreading out of the phenoxides (~8°) explained by the increasing steric hindrance of the NMe₂ groups over the phenyl rings [(Me₂N)₃PO vs Ph₃PO].

5.7 Conclusions.

(1). Complexes **9-11** and **19-21**, along with **1-3** (from Chapter 4) form an interesting series of nine complexes of the type $\text{Ph}_3\text{P}=\text{X}\cdot\text{MY}_2$ where $\text{X} = \text{CH}_2$ (**1-3**), NH (**9-11**) and O (**19-21**), $\text{Y} = \text{N}(\text{SiMe}_3)_2$ (**1-3**) and $\text{OC}_6\text{H}_2(\text{Me})^t\text{Bu}_2$ (**9-11** & **19-21**) and $\text{M} = \text{Ca}$ (**1**, **9** & **19**), Sr (**2**, **10** & **20**) & Ba (**3**, **11** & **21**). A summary of the salient bond lengths and angles is shown below in Table 5.13.

Comp. No.	M	X	[P-X]Å	[X-M]Å	[P-X-M]°	[X-M-X]°	[Y-M-Y]°
1	Ca	CH ₂	1.717(ave.)	2.646(ave.)	134.2(ave.)	82.5(2)	121.05(14)
9	Ca	NH	1.585(ave.)	2.393(ave.)	147.6(ave.)	102.86(11)	115.14(10)
19	Ca	O	1.499(ave.)	2.268(ave.)	161.9(ave.)	94.75(4)	123.07(4)
2	Sr	CH ₂	1.686(ave.)	2.742(ave.)	135.3(ave.)	81.6(2)	120.18(14)
10	Sr	NH	1.587(ave.)	2.532(ave.)	146.0(ave.)	102.7(12)	114.66(10)
20	Sr	O	1.491(ave.)	2.413(ave.)	161.6(ave.)	93.00(1)	124.01(11)
3	Ba	CH ₂	1.704(ave.)	3.002(ave.)	133.0(ave.)	92.5(2)	111.8(2)
11	Ba	NH	1.582(ave.)	2.724(ave.)	141.4(ave.)	84.95(8)	111.08(6)
21	Ba	O	1.496(ave.)	2.573(ave.)	160.7(ave.)	91.61(5)	125.37(5)

Table 5.13 Comparison of salient bond lengths and angles for complexes of the type $\text{Ph}_3\text{P}=\text{X}\cdot\text{MY}_2$.

Considering the above table it can be seen that:

- The bond length [P-X] and angle [P-X-M] for complexes with the same X group do not change upon changing the metal.
- Upon going from $\text{X} = \text{CH}_2$ to $\text{X} = \text{NH}$ to $\text{X} = \text{O}$ for any one particular metal the bond lengths [P-X and X-M] decrease and the bond angle [P-X-M] increases. This is due

to an increase in electronegativity in going from $X = CH_2$ to $X = O$ and also a decrease in steric size e.g. two protons on CH_2 , one on NH and none on O .

(c). Comparison of the $X-M$ bond length for the same X group but differing M shows an increase in moving from $M = Ca$ to $M = Sr$ to $M = Ba$. This is due to the increase in size of the metal in going down group 2 from Ca to Ba .

(d). Comparison of the $X-M-X$ angle shows that when $X = CH_2$ the angle is smaller. This is due to Y in this case being more bulky $\{N(SiMe_3)_2$ vs $[OC_6H_2(Me)^tBu_2]\}$.

(e). Comparison of the $Y-M-Y$ angle shows that when $X = NH$ and $Y = [OC_6H_2(Me)^tBu_2]$ it is at a minimum.

(2). Complexes **9-11** are the first structurally characterised neutral iminophosphorane complexes of calcium, strontium and barium. Complexes **19-21** are the first structurally characterised triphenylphosphine oxide complexes of calcium, strontium and barium. The complexes **9-11** and **19-21** as well as being structurally interesting in their own right may well have further synthetic uses e.g. aza-Wittig reaction (**9-11**) and Horner reaction (**19-21**).

(3). Complexes **16-18** are directly analogous to complexes **1-3** and are expected to adopt the same structure in the crystal form. Single crystal X-ray diffraction studies are required on these complexes for confirmation of their exact structure.

6. Structural Diversity in Lithium Iminophosphorane Complexes and Related Systems.

This chapter deals with the investigation of complexes **22-27**. These complexes were synthesised according to the procedures outlined in **Chapter 3** and are listed in **Table 6.1**.

Complex Number	Chemical Formula
22	$\text{Ph}_3\text{PNH}\cdot\text{LiN}[\text{PPh}_2(\text{S})]_2$
23	$(\text{Ph}_2\text{MePN})_2\text{Li}_3[\text{OC}_6\text{H}_2(\text{Me})^t\text{Bu}_2]$
24	$\text{Ph}_2\text{MePNH}\cdot\text{LiOS}(\text{O})(\text{CF}_3)\text{NSO}_2\text{CF}_3$
25	$\text{Ph}_3\text{PNH}\cdot\text{LiOS}(\text{O})(\text{CF}_3)\text{NSO}_2\text{CF}_3$
26	$\text{TMEDA}\cdot\text{LiOS}(\text{O})(\text{CF}_3)\text{NSO}_2\text{CF}_3$
27	$\text{Ph}_2[\text{C}(\text{H})(\text{Ph})\text{CO}_2\text{Me}]\text{PNCO}_2\text{Me}$

Table 6.1 Table of complexes and compounds discussed in Chapter 6.

6.1 Introduction.

The production of, and subsequent use of s-block metallated iminophosphoranes has previously been discussed in **Chapter 1 (3.5)**. Their potential use in organic synthesis has been documented^{1,2} and further studies are well under way. Having produced novel s-block iminophosphorane complexes with simple ligands (see **Chapter 5**), attempts were made to produce complexes with more structural diversity. The mode of co-ordination of the iminophosphorane in the alkaline earth metal iminophosphorane complexes (**Chapter 5**) is the same in each case i.e. neutral Lewis base donation of the lone pair on the iminic nitrogen to the metal centre. In order to vary this mode of co-ordination, chelating ligands were used (complex **22**), excess $^t\text{BuLi}$ was added in order to facilitate the deprotonation of the iminophosphorane (complex **23**) and also the use of weakly coordinating anions was employed (complexes **24-26**). Compound **27**, the product of a doubly deprotonated benzyl iminophosphorane will be discussed separately in section 6.5.

¹ J. Ackrell, F. Galeazzi, J. M. Muchowski and L. Tokes, *Can. J. Chem.*, **57**, 2696 (1979).

² L. Chiche, H.-J. Cristau, J. Kadoura and E. Toreilles, *Bull. Soc. Chim. Fr.*, **4**, 515 (1989).

6.2 NMR Data of Complexes 22-26.

All the complexes discussed in this chapter have been analysed, where possible by ^{31}P and ^1H NMR spectroscopy (using d^6 -benzene as a solvent). All the complexes described herein (excluding **26**) contain at least one chemically unique phosphorus atom and as such ^{31}P NMR is the most useful technique for analysis. **Table 6.2** shows a ^{31}P chemical shift comparison for the un-coordinated ligands **III**, **V** and **45** and the complexes **22-26**.

Complex Number	Ligand(s) Used.	$\delta^{31}\text{P}$ Complex (ppm)	$\delta^{31}\text{P}$ Ligand.(ppm)
22	III & V	31.5 & 39.1	17.5 & 57.7
23	45	-1.8	14.7
24	45	33.7	14.7
25	III	33.0	17.5
26	-	-	-

Table 6.2 Table to show the ^{31}P NMR chemical shift comparison between the starting ligands and complexes.

It can be seen from the above table that the ^{31}P chemical shift for ligand **III** shows a shift to lower field (i.e. the chemical shift is higher) indicating that the ligand has co-ordinated to the metal without any structural change to itself. In the case of **V** and **45** (in complex **23**) there is a shift to higher field (i.e. the chemical shift is lower) indicating that the ligand had been deprotonated. Finally in complex **24**, the ^{31}P chemical shift for ligand **45** shows a shift to higher frequency indicating that the ligand is coordinating without any structural change to itself (i.e. neutrally).

6.3 Discussion of complexes 22 and 23.

Addition of one equivalent of *n*-butyl lithium to a reaction mixture of one equivalent of triphenyliminophosphorane **III** and one equivalent of tetraphenyldithiodiphosphinylamide **V** in toluene resulted in the formation of a white precipitate. Upon heating to aid dissolution and then subsequent cooling a crystalline material was obtained. Compound

22 was analysed fully by NMR, elemental analysis and melting point analysis.

Unfortunately single crystal X-ray diffraction studies could not be carried out, but a dimeric structure such as that shown in **Figure 6.1** could be expected.

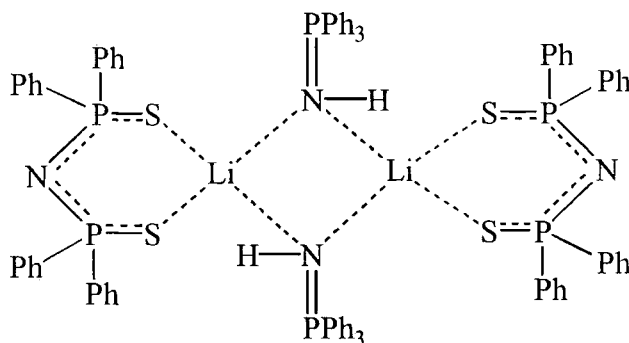


Figure 6.1 Proposed structure for complex **22**.

Compound **23** was obtained by the addition of 2 equivalents of n-butyl lithium to one equivalent of methyldiphenyliminophosphorane **42** and one equivalent of 2,6-di-tert-butyl,4-methyl phenol in toluene at -78°C. After subsequent warming to aid dissolution and further cooling to room temperature a crop of colourless crystals was obtained. The product was analysed by NMR, elemental analysis and melting point analysis. The complex was found to contain two deprotonated iminophosphoranes, 3 lithiums and one phenoxide per molecule. Single crystal X-ray diffraction studies would serve to determine the exact geometry of this molecule, thought to be of a 'ladder type'^{3,4} structure (**Figure 6.2 and 6.3**)

³ D. R. Armstrong, D. Barr, W. Clegg, R. E. Mulvey, D. Reed, R. Snaith and K. Wade, *J. Chem. Soc., Dalton Trans.*, 1071 (1987).

⁴ D. R. Armstrong, D. Barr, W. Clegg, R. E. Mulvey, D. Reed, R. Snaith and K. Wade, *J. Chem. Soc., Chem. Commun.*, 869 (1986).

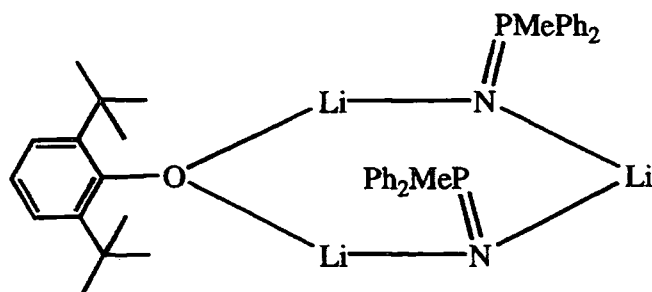


Figure 6.2 Proposed structure of 23.

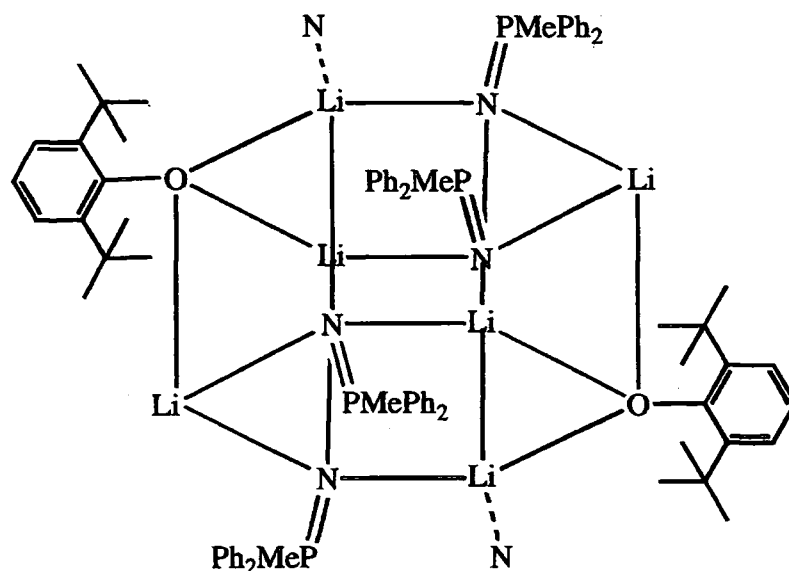


Figure 6.3 Proposed structure of 23 showing possible ring stacking.

6.4 Discussion of complexes 24-26.

6.4.1 Background.

In a recent study of gas-phase acidities,⁵ the nitrogen acid $(\text{CF}_3\text{SO}_2)_2\text{NH}^6$ was found to be amongst the strongest neutral Bronsted acids and the term 'gas phase superacid' has been suggested.³ The remarkably high acidity of $(\text{CF}_3\text{SO}_2)\text{NH}$ in the gas phase has been

⁵ F. Anvia, D. D. DesMarteau, L.-Q. Hu, N. V. Ignat'ev, N. V. Kondratenko, I. A. Koppel, P.-C. Maria, M. Notario, K.-S. Sung, R. W. Taft, M. V. Vlasov, A. Y. Volkonskii, L. M. Yagupolskii, Y. L. Yagupolskii and S.-Z. Zhu, *J. Am. Chem. Soc.*, **116**, 3047 (1994).

⁶ (a). D. D. DesMarteau and J. Foropoulos, *Inorg. Chem.*, **23**, 3720 (1984).

attributed to a pronounced electron delocalisation over the approximately tetrahedral $\text{O}_2\text{SCF}_3\text{N}$ skeletal groups both in the protonated amide and more so in the conjugate anion $[(\text{CF}_3\text{SO}_2)_2\text{N}]^-$. A recent publication contains single crystal X-ray diffraction studies undertaken on $(\text{CF}_3\text{SO}_2)_2\text{NH}$ and $[\text{Mg}(\text{H}_2\text{O})_6][(\text{CF}_3\text{SO}_2)_2\text{N}]_2 \cdot 2\text{H}_2\text{O}$, and their determined molecular structures.⁷

More recently a 1,2,3-trisubstituted imidazolium salt of the bis(trifluoromethanesulphonyl)amide ion was reported.⁸ Molten organic salts such as this have use in a variety of electrochemical devices, such as photo-electrochemical cells.⁹ The bis(trifluoromethanesulphonyl)amido ligand has also been reported to show good catalytic activity in the Diels Alder reaction when complexed to ytterbium(III) or yttrium(III).¹⁰

With the above complexes showing such a diverse range of physical properties and activities, attempts to complex N-lithio bis(trifluoromethanesulphonyl)amide with nitrogen donors (e.g. iminophosphoranes) were made and the resulting complexes are detailed in this section.

6.4.2 Structural investigation of complex 24 and discussion of complexes 25-26.

Reaction of one equivalent of N-lithio bis(trifluoromethanesulphonyl)amide with one equivalent of methyldiphenyliminophosphorane **45** in hot toluene, followed by cooling at room temperature yielded a crop of colourless crystals. Preliminary characterisation followed by X-ray crystallographic studies revealed **24** (Figure 6.4) to be a dimeric complex containing two lithio amide and two neutral iminophosphorane groups.

⁷ F. Aubke, P. Betz, J. Bruckmann, A. Haas, Ch. Klare, C. Krüger and Y.-H. Tsay, *Inorg. Chem.*, **35**, 1918 (1996).

⁸ M. Forsyth, J. J. Golding, D. R. Macfarlane, B. W. Skelton, L. Spiccia and A. H. White, *J. Chem. Soc., Chem. Commun.*, 1593 (1998).

⁹ P. Bonhote, A. Dias, M. Gratzel, K. Kalyanasundaram and N. Papageorgiou, *Inorg. Chem.*, **35**, 1168 (1996).

¹⁰ O. Kotera, K. Mikami, Y. Motoyama and M. Tanaka, *Inorg. Chem. Commun.*, **1**, 10 (1998).

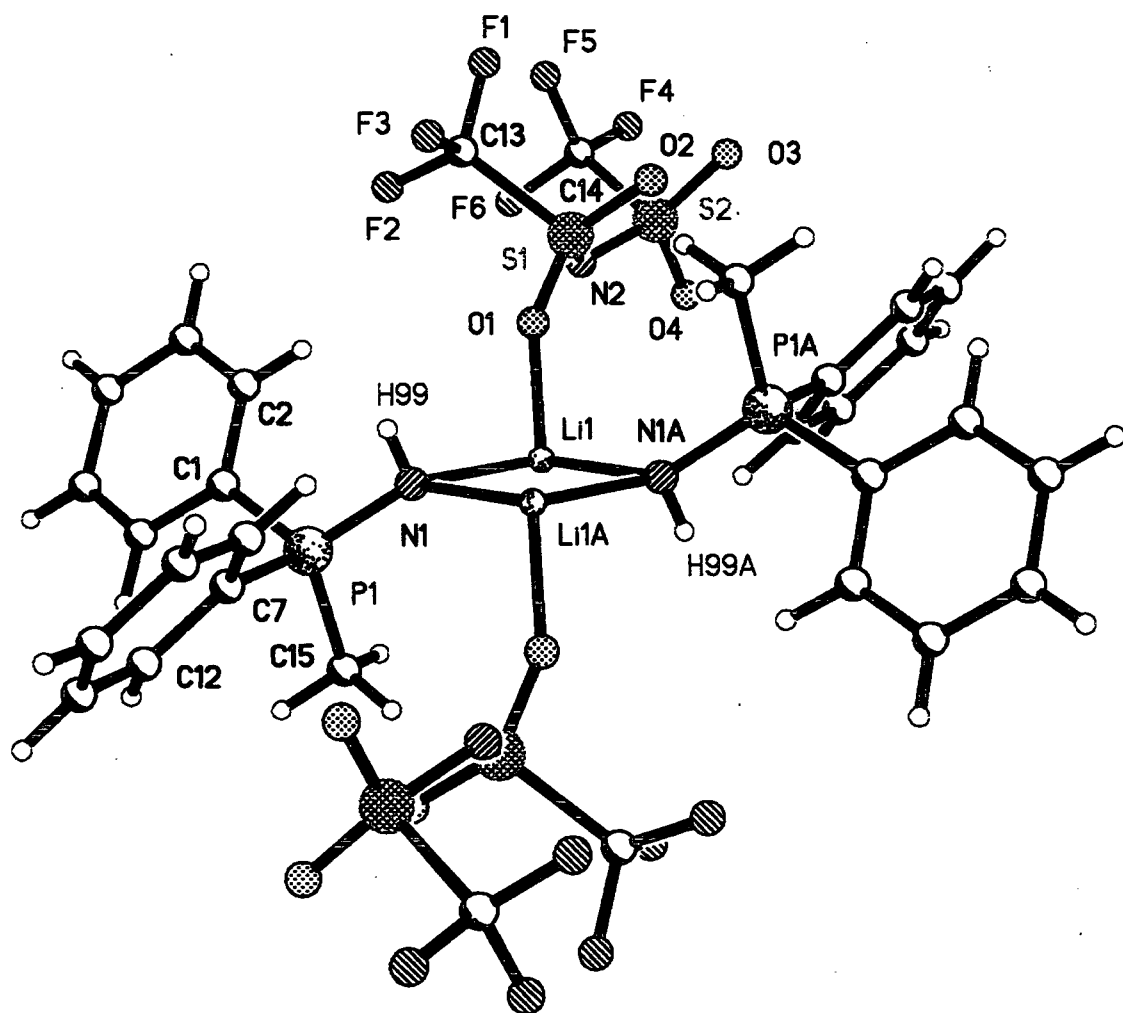


Figure 6.4 Single crystal X-ray structure of $\text{Ph}_2\text{MePNH} \cdot \text{LiOS}(\text{O})(\text{CF}_3)\text{NSO}_2\text{CF}_3$.

Structural features of this complex to note include a S-N bond length of 1.560Å(ave.) [S1-N2 & S2-N2], a S-O bond length of 1.420Å(ave.) [S1-O1, S1-O2, S2-O3 & S2-O4], a S-C bond length of 1.801Å(ave.) [S1-C13 & S2-C14] and a S-N-S bond angle of 126.8°(ave.) [S1-N2-S2 & S3-N1-S4]. These structural parameters will be compared with other known structures of this type in due course. One particularly striking aspect of this structure involves consideration of two adjacent dimers. It can be seen that lithium-oxygen interactions cause the formation of a 12-membered ring (Figure 6.5a&b).

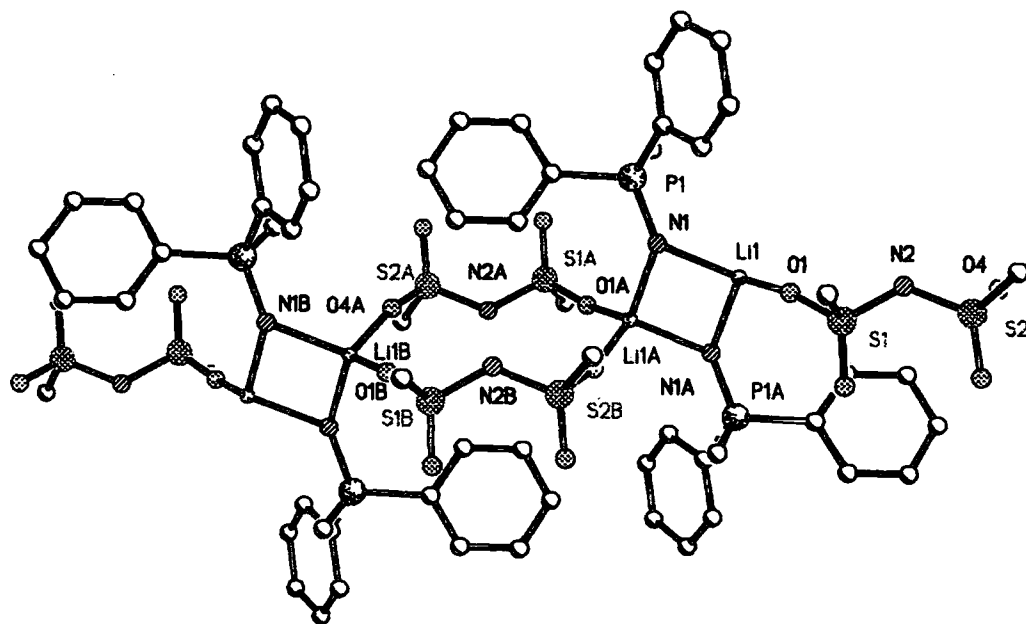


Figure 6.5a The polymeric structure of complex 24 showing the twelve membered ring. All hydrogen and fluorine atoms omitted for clarity.

A search of the CSD reveals this ring to be unique in its $-(\text{LiOSNSO})_2-$ formation. The nitrogen atoms in the ring are 'up' and 'down' respectively (Figure 6.5b) due to their associated amido ligands being inverted with respect to each other.

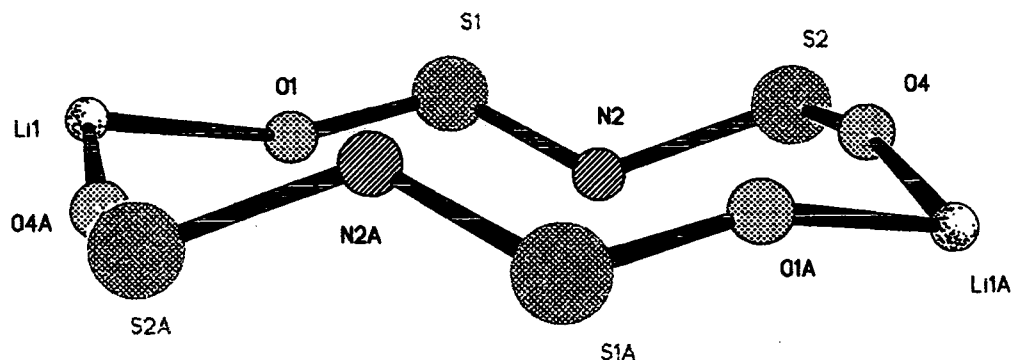
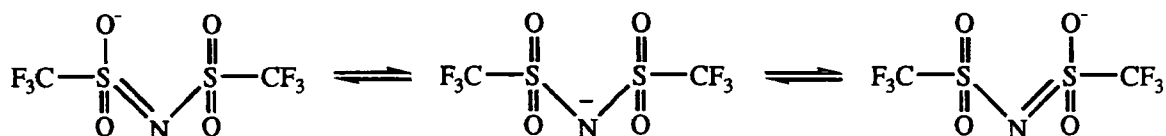


Figure 6.5b Diagram to show conformation of the twelve membered ring.

The shortest Li-O distance is 1.926(15)Å [Li1-O1] which is of the order expected for a typical Li-O interaction,¹¹ and suggests that the negative charge is on the oxygen and not on the nitrogen. This is explained by considering the following resonance canonical forms of the amido ligand (Scheme 6.1).



Scheme 6.1 Resonance canonical forms of the amide.

Consideration of the central Li_2N_2 core reveals the following structure (Figure 6.6).

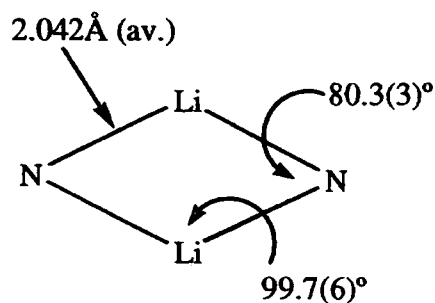


Figure 6.6 Diagram to show Li_2N_2 core in complex 24

¹¹ J. C. Huffman, R. L. Geerts and K. G. Caulton, *J. Crystallogr. Spectro. Res.*, **14**, 541 (1984).

Considering the following molecules which also contain Li_2N_2 cores (Figure 6.7a-c) and their respective bond lengths and bond angles (Table 6.3),

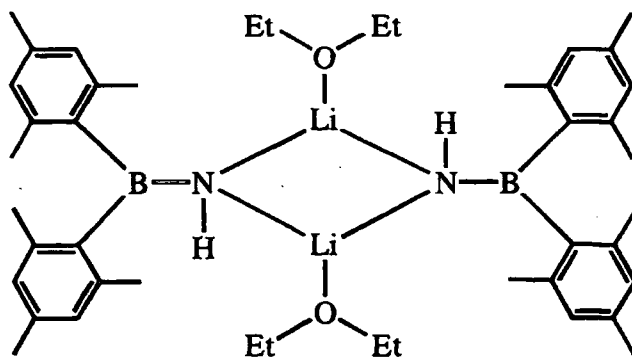


Figure 6.7a¹²

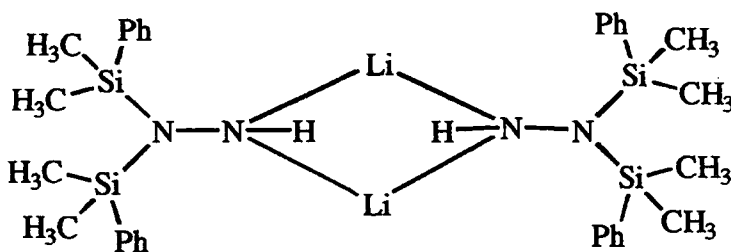


Figure 6.7b¹³

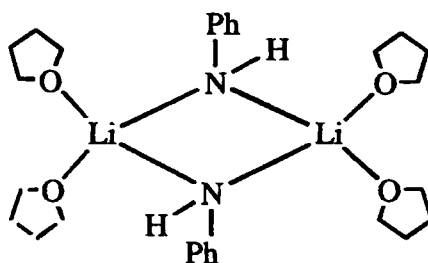


Figure 6.7c¹⁴

¹² R. A. Bartlett, H. Chen, H. V. R. Dias, M. M. Olmstead and P. P. Power, *J. Am. Chem. Soc.*, **110**, 446 (1988).

¹³ U. Klingebiel, M. Schafer and H. Witte-Abel, *Z. Anorg. Allg. Chem.*, **624**, 271 (1998).

¹⁴ R. von Bulow, H. Gornitzka, T. Kottke and D. Stalke, *J. Chem. Soc., Chem. Commun.*, 1639 (1996).

Complex	[Li-N]Å	[N-Li-N]°	[Li-N-Li]°
24	2.042(ave.)	99.7(6)	80.3(3)
a	2.010(ave.)	105.07(3)	74.9(2)
b	1.974(ave.)	103.0(3)	77.0(2)
c	2.038(ave.)	103.2(4)	76.8(4)

Table 6.3 Bond lengths and angles for Li₂N₂ cores in complexes a-c and 24

it can be seen that the N-Li-N angle is narrower and the Li-N-Li angle wider than the other examples possibly due to the steric requirements around the ring in **24**.

Consideration of the co-ordinated iminophosphorane **45** with respect to the free iminophosphorane (Table 6.4), shows that the P-N bond appears to be

	Iminophosphorane in 24	Free iminophosphorane 45 ¹⁵
[P-N] Å	1.585(7) [P1-N1]	1.563(4)
[C _{ipso} -P] Å	1.787(8) [C1-P1]	1.808(6)
	1.789(9) [C7-P1]	1.810(5)
	1.774(9) [C15-P1]	1.800(5)
[C _{ipso} -P-N _{imine}] °	114.2(4) [C1-P1-N1]	116.5(3)
	112.4(4) [C7-P1-N1]	113.5(2)
	110.0(4) [C15-P1-N1]	108.9(2)

Table 6.4 Selected bond lengths and angles for the co-ordinated and free iminophosphoranes

elongated in the complex with respect to the free iminophosphorane, due no doubt to electron donation of the nitrogen lone pair to the two attached lithium atoms which negates any back bonding effect that the lone pair may have. This in turn weakens and thus lengthens the P-N_{imine} bond in the complex **24**. The shortest C_{ipso}-P interaction and smallest C_{ipso}-P-N_{imine} bond angle reported in each case relates to the methyl group of the methyldiphenyliminophosphorane.

¹⁵ See Chapter 7 of this thesis for the structure of methyldiphenyliminophosphorane.

A search of the CSD reveals that the bis(trifluoromethanesulphonyl)amido ligand has been little studied with only a handful of reported structures being available. These consist of the determined molecular structures of the following (Figure 6.8a-e).

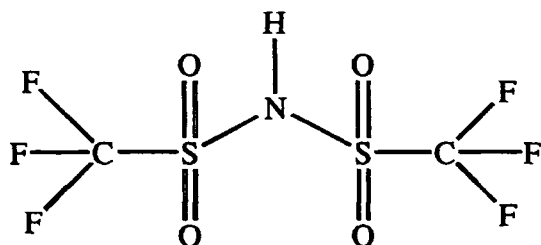


Figure 6.8a Bis(trifluoromethanesulphonyl)amide⁷

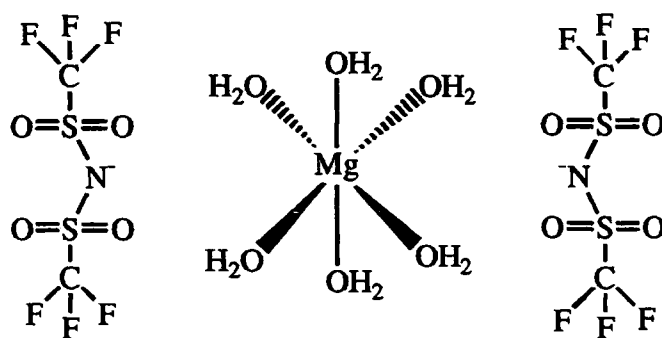


Figure 6.8b A magnesium bis[bis(trifluoromethanesulphonyl)amide] complex⁷

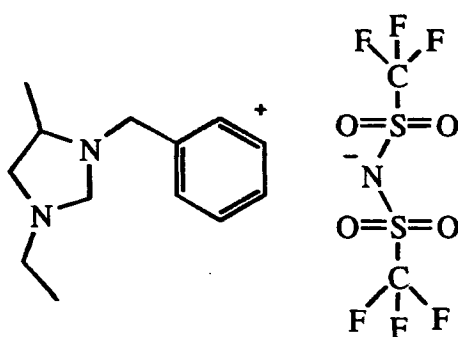


Figure 6.8c A 1,2,3-trisubstituted imidazolium salt of the bis(trifluoromethanesulphonyl)amide ion⁸

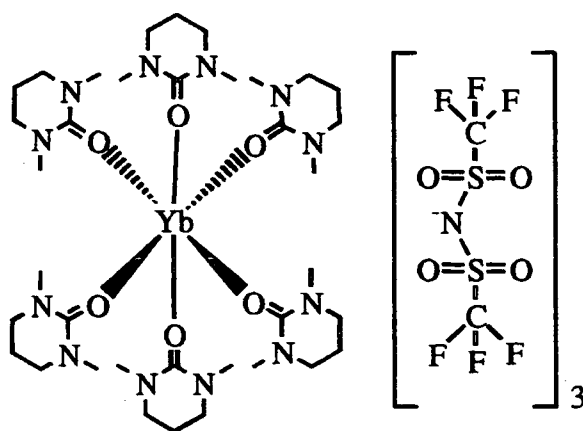


Figure 6.8d Ytterbium (III) complex of the bis(trifluoromethanesulphonyl)amide ion¹⁰

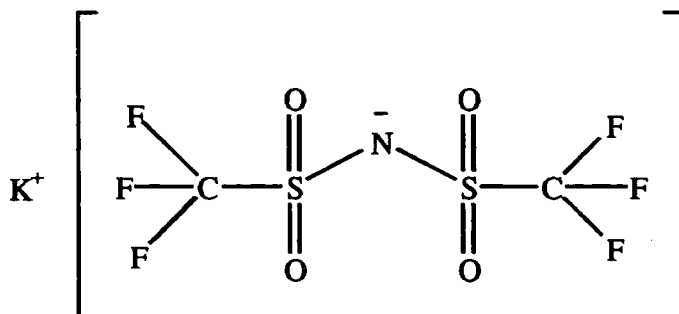


Figure 6.8e A potassium bis(trifluoromethanesulfonyl)amide¹⁶

Consideration of the important structural features of **a-e** and **24** is given in the following table of bond lengths and angles (Table 6.5).

¹⁶ R. Ruzicka and Z. Zak, *Z. Kristallogr.*, **213**, 217 (1998).

	Amide	[S-N]Å	[S-N-S]°	[S-O]Å	[S-C]Å	[N-H]Å
24	lithiated	1.560 (ave.)	126.8(5)	1.420(ave.)	1.801(ave.)	-
a ⁷	ligand	1.644(1)	128.4(2)	1.409(2)	1.840(3)	0.99(4)
a ¹⁶	ligand	1.647(ave.)	127.6(2)	1.417(ave.)	1.840(3)	0.88(4)
b ⁷	free anion	1.577(3)	125.0(2)	1.418(3)	1.812(5)	-
c ⁸	free anion	1.569(ave.)	125.0(2)	1.421(ave.)	1.818(ave.)	-
d ¹⁰	free anion	-	No structural data available for d .			-
e ¹⁶	free anion	1.568 (ave.)	126.7(3)	1.431 (ave.)	1.825 (ave.)	-

Table 6.5 Selected bond lengths and angles for a-e and 24

It can be seen from the above table that upon deprotonation of the amide the S-N bond length gets smaller due to electron delocalisation across the S-N-S bond. The S-N-S bond angle decreases by only a couple of degrees upon deprotonation thus giving a narrower angle along with shortened bond lengths. There is little pattern in the S=O bond lengths when comparing the above complexes, but there is however, a shortening of the S-C bond upon deprotonation again due to increased electron delocalisation across the whole molecule. The discrepancies in the N-H bond lengths shown above are difficult to discuss as it is extremely hard to determine the position of freely refined hydrogens atoms using data acquired by X-ray diffraction studies. Based on the data above complex **24** does not show any particularly striking features except for shorter S-C interactions.

Complex **25**, an analogous compound to **24** but containing triphenyliminophosphorane **III** instead of methyldiphenyliminophosphorane **45**, was prepared by adding one equivalent of N-lithiotrifluoromethanesulphonamide to one equivalent of triphenyliminophosphorane **III** in toluene. The reaction was heated to aid dissolution and left to cool at room temperature whereupon a crystalline material was obtained. Preliminary analysis by NMR, elemental analysis and melting point analysis showed this complex to be of the same stoichiometry as **24**. Single crystal X-ray diffraction studies were not undertaken on **25**, but the structure can be assumed to be very similar to that seen in **24**.

In an attempt to obtain the isolated twelve membered ring containing lithium, complex **26** was produced by adding one equivalent of N-lithiotrifluoromethanesulphonamide to one equivalent of N,N,N',N'-tetramethylethylenediamine in toluene. After stirring for one hour the mixture was heated to aid dissolution and left to cool at room temperature, whereupon a crystalline material was obtained. Preliminary analysis by NMR and melting point analysis revealed the stoichiometry to be 1:1 which was further confirmed by elemental analysis. Single crystal X-ray diffraction studies were not undertaken on this complex due to the poor quality of the crystals obtained. A possible structure for complex **26** is as follows (Figure 6.9).

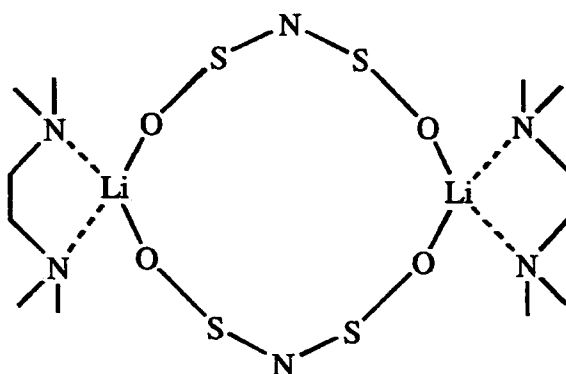


Figure 6.9 Proposed structure for **26**, CF₃ groups and non-interacting oxygen groups omitted for clarity.

6.5 Compound **27** : The search for a di-anion.

6.5.1 Background.

The structural determination of reaction intermediates in organophosphonate anion chemistry has been driven by the extraordinary synthetic utility of these reagents.¹⁷ Many solution and solid state structures of phosphorus stabilised anions have been reported over the past few years including lithiated phosphonates,¹⁸

¹⁷ (a). H. Hoffmann, L. Horner and H. G. Wippel, *Chem. Ber.*, **91**, 61 (1958); (b). W. D. Emmons and W. S. J. Wadsworth, *J. Am. Chem. Soc.*, **83**, 1733 (1961); (c). B. E. Maryanoff and A. B. Reitz, *Chem. Rev.*, **89**, 863 (1989); (d). J. Clayden and S. Warren., *Angew. Chem., Int. Ed. Engl.*, **35**, 241 (1996).

phosphinoides,¹⁹ phosphonamides and thiophosphonamides.²⁰ A problem that sometimes occurs when the above mono-lithiated reagents are used synthetically along with electrophiles is that more acidic products are formed which, in turn leads to unwanted side-products. To overcome this limitation a process that takes advantage of a di-anionic intermediate has been developed.²¹ Di-carbanions have already been used in several reactions as supernucleophiles and even in asymmetric synthesis.²² Despite the synthetic value of these reagents there is still a demand for more information about their structure and recently the solid state structure of a di-lithiated phosphonate (**Figure 6.10**) was determined.²³ However, until now the synthetic utility of di-anions containing the $P(C^-)=N^-$ unit has not been explored.

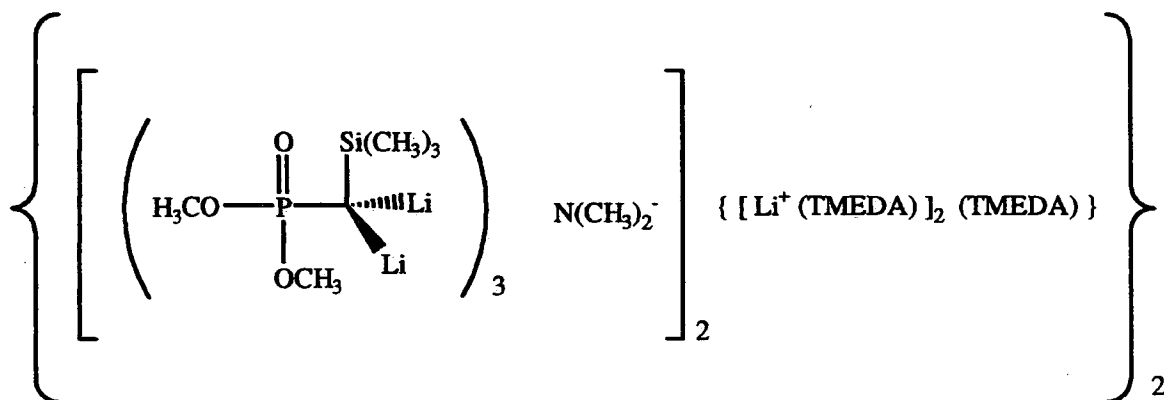
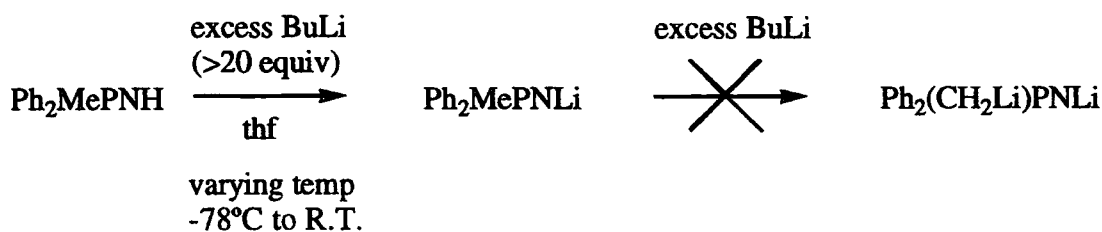


Figure 6.10 A di-lithiated phosphonate complex.

- ¹⁸ (a). G. Boche, G. Frenking, F. Haller, K. Harms, M. Marsch and W. Zarges., *Chem. Ber.*, **124**, 861 (1991). (b). S. E. Denmark, P. C. Miller, K. A. Swiss and S. R. Wilson, *Heteroatom. Chem.*, **9**, 209 (1998).
- ¹⁹ (a). S. E. Denmark, K. A. Swiss and S. R. Wilson, *Angew. Chem., Int. Ed. Engl.*, **35**, 2515 (1996). (b). J. E. Davies, R. P. Davies, L. Dunbar, P. R. Raithby, M. G. Russell, R. Snaith, S. Warren and A. E. H. Wheatley, *Angew. Chem., Int. Ed. Engl.*, **36**, 2334 (1997).
- ²⁰ (a). S. E. Denmark and R. L. Dorow., *J. Am. Chem. Soc.*, **112**, 864 (1990). (b). S. E. Denmark, P. C. Miller and S. R. Wilson, *J. Am. Chem. Soc.*, **113**, 1468 (1991). (c). S. E. Denmark, K. A. Swiss and S. R. Wilson., *J. Am. Chem. Soc.*, **115**, 3826 (1993). (d). S. E. Denmark, M. Kranz, K. A. Swiss and S. R. Wilson., *J. Org. Chem.*, **61**, 8551 (1996).
- ²¹ (a). F. Eymery, B. Iorea and P. Savignac, *Tetrahedron. Lett.*, **39**, 3693 (1998). (b). C. M. Thompson, 'Dianion Chemistry in Organic Synthesis', CRC Press, Boca Raton, FL, pp. 1-250 (1994).
- ²² See for example ; (a). P. Bonete and C. Nájera, *Tetrahedron. Lett.*, **52**, 4111 (1996). (b). F. Caturia and C. Nájera, *Tetrahedron. Lett.*, **52**, 4111 (1996). (c). I. Marek and J.-F. Normant, *Chem. Rev.*, **96**, 3241 (1996). (d). J. F. K. Müller, M. Neuburger and M. Zehnder, *Helv. Chim. Acta.*, **80**, 2182 (1997).
- ²³ J. F. K. Müller, M. Neuburger and B. Spingler, *Angew. Chem., Int. Ed. Engl.*, **38**, 92 (1999).

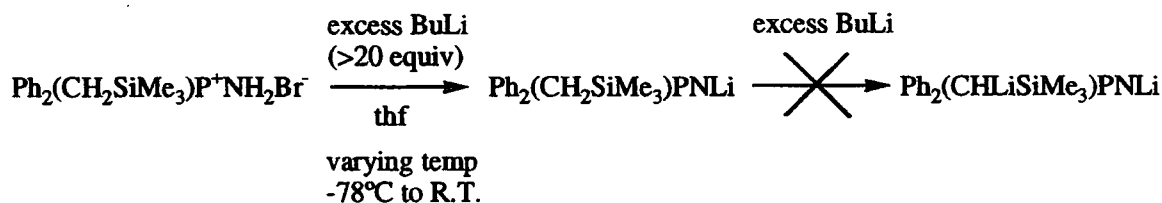
6.5.2 Initial attempts to produce a di-anion.

Initial attempts at producing a di-anion centred around compound **45** Ph_2MePNH (methyldiphenyliminophosphorane). It was believed that with an excess of butyl lithium in thf it would be possible to produce the di-lithated iminophosphorane which could then be used in further reactions. However even with an excess of butyl lithium (n , s & t -BuLi were all tried as well as adding HMPA to the mixture to form a super base) only mono-lithiation at the iminic nitrogen occurred (**Scheme 6.2**).



Scheme 6.2 Attempts to produce di-anion using compound **45**.

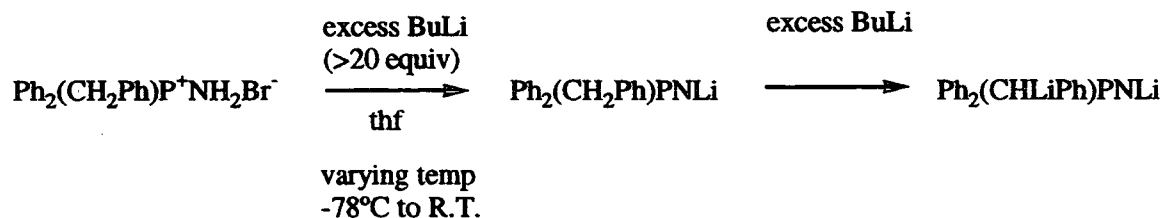
The next approach used was to attach a functional group which would serve to stabilise any anion formed. The compound chosen was $\text{Ph}_2(\text{CH}_2\text{SiMe}_3)\text{P}^+\text{NH}_2\text{Br}^-$. Addition of three equivalents of BuLi should have formed the iminophosphorane (1 equivalent) and then di-lithiated (2 equivalents). However as before the final product was the mono-lithiated iminophosphorane (**Scheme 6.3**). Another problem with this particular attempt was that the initial phosphine $\text{Ph}_2(\text{CH}_2\text{SiMe}_3)\text{P}$ was very difficult to produce in large quantities using a standard Grignard procedure.



Scheme 6.3 Attempts to produce di-anion using trimethylsilylmethyl group.

The next attempt at producing a di-anion proved much more fruitful. Compound **44** $\text{Ph}_2(\text{CH}_2\text{Ph})\text{P}^+\text{NH}_2\text{Br}^-$, benzyldiphenylphosphonio ammonium bromide was used in the

same way as before and a very distinct colour change (to bright orange) was noted upon addition of butyl lithium (Scheme 6.4).



Scheme 6.4 Production of a di-lithiated iminophosphorane from 44.

Upon ascertaining that the di-lithiated iminophosphorane could be produced by this route, attempts to isolate it were made. The reaction was repeated at -78°C in thf but upon warming to room temperature the intense colour was lost which raised questions over the di-lithiated iminophosphorane's stability. The reaction was repeated and the solution stored at -80°C in the freezer but no solid product could be obtained. It was then decided to quench the di-anion by reacting it with an electrophile.

6.5.3 Synthesis of 44, the subsequent di-anion and compound 27.

Compound 44, benzyldiphenylphosphonio ammonium bromide was produced by a three step process (Scheme 6.5) using methods adapted from known iminophosphorane syntheses (e.g triphenyliminophosphorane III). This novel iminophosphorane salt was produced by first synthesising benzyldiphenylphosphine using chlorodiphenylphosphine and benzylmagnesium chloride in toluene. The next step involved bromination of the phosphine by refluxing with bromine. After isolation of the benzyldiphenylphosphorus dibromide, gaseous ammonia was passed through a solution of the dibromide. The salt was isolated by dissolving in chloroform, filtration to remove ammonium bromide and then full precipitation using diethyl ether. After drying *in vacuo* the salt was fully analysed using multi-nuclear NMR, elemental analysis and melting point analysis.

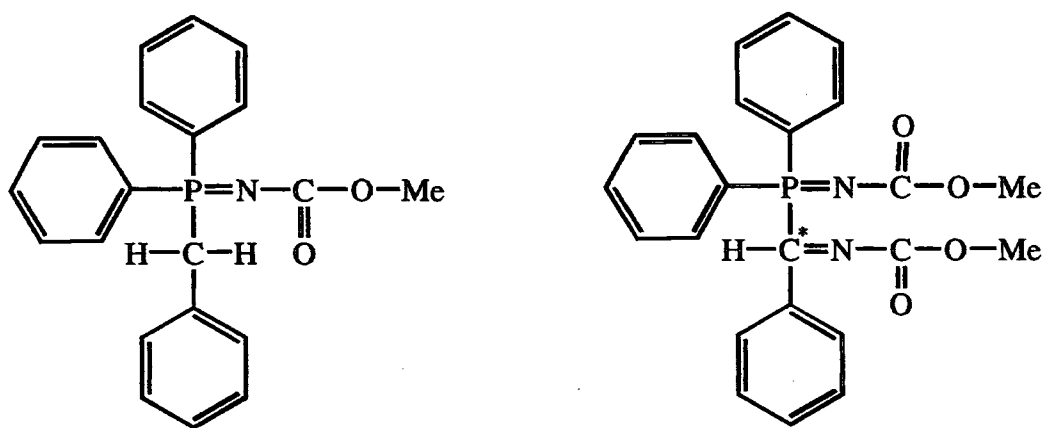


Figure 6.11a and 6.11b Mono and Di-addition products.

There are also two doublets, one of which relates to the di-addition product (4.1ppm) and the second which relates to the mono-addition product (5.8ppm), with coupling constants ($^2J_{\text{PH}}$) of 13.2 and 12.8Hz respectively. These were confirmed by considering a ^{31}P decoupled ^1H spectrum in which the two doublets became singlets. More importantly the decoupled spectra showed a doublet at 7.65ppm ($^3J_{\text{HH}} = 8.0\text{Hz}$) which relates to the four ortho protons on the phenyl rings attached to the phosphorus atom in the mono-addition product, and a doublet of doublets at 7.72ppm ($^3J_{\text{HH}} = 8.0$ and 15.2Hz) which again relates to the same ortho protons but these are in the di-addition product. The doublet of doublets is due to the formation of a chiral centre in the di-addition product (**Figure 6.11b**) which is attached to the phosphorus atom and hence the ortho protons are diastereospecific.

The di-lithiation of the iminophosphorane salt **44** promises to have a great impact in the area of synthetic organic chemistry. In order to obtain the maximum yield of the di-addition product further adjustments to the reaction conditions must be undertaken e.g. longer reaction times and temperature variations. Further studies are underway to improve this yield and attempts are being made to isolate and structurally characterise the di-lithiated compound.

6.6 Conclusions.

- (1). Evidence for the first reported iminophosphorane lithium tetraphenyldithiodiphosphinylamide complex **22**. This complex is only the second reported example of a lithiated tetraphenyldithiodiphosphinylamido complex, the first being $(\text{Ph}_2\text{PS})_2\text{NLi}\cdot\text{OPPh}_2\text{Me}$.²⁴
- (2). Evidence for the mono-deprotonated iminophosphorane $(\text{Ph}_2\text{MePN}^-)$ seen by ³¹P NMR. Attempts to doubly deprotonate this iminophosphorane have failed, compound **45** proving to be more fruitful (see compound **27**).
- (3). **24** is the first structurally characterised complex to contain methyldiphenyliminophosphorane, thus giving useful structural information with regards to its co-ordination mode (for first structural analysis of the free iminophosphorane see compound **45**, Chapter 7).

24 is the first structurally characterised complex to contain the lithiated amide $\text{LiN}(\text{SO}_2\text{CF}_3)_2$.

Complex **24** also contains the first structurally characterised 12-membered ring of the type $(\text{LiOSNSO})_2$. Further complexes of the type seen in **24** can be reproduced with other iminophosphoranes and nitrogen donors (complexes **25** and **26**).

- (4). Compound **27** shows evidence that a di-anion produced from compound **44** $[\text{Ph}_2(\text{CHPh})\text{PN}^-]$ exists and can be used in further reactions. Preliminary studies have shown that compound **27** can be produced in a 70% yield. Further work is underway to analyse the product using advanced NMR techniques. Attempts to improve the yield by using a combination of longer reaction times and temperature variations are ongoing, as is the use of other electrophiles to give a range of reaction products. It is hoped that in the future this reagent may have a significant impact in synthetic organic chemistry.

²⁴ R. D. Price, *Ph.D. Thesis*, University of Durham (1999).

7. Group 15 Salts and Ylides.

This chapter deals with the investigation of complexes **28-50**. These complexes were synthesised according to the procedures outlined in **Chapter 3** and are listed in **Table 7.1**.

Complex Number	Chemical Formula
28	$\text{Ph}_2(\text{o-C}_6\text{H}_4\text{OMe})\text{P}^+\text{CH}_3\text{Br}^-$
29	$\text{Ph}_2(\text{o-C}_6\text{H}_4\text{OMe})\text{P}^+\text{CH}_2\text{PhBr}^-$
30	$\text{Ph}_2(\text{o-C}_5\text{H}_5\text{N})\text{P}^+\text{CH}_2\text{PhBr}^-$
31	$\text{Ph}_2(\text{o-C}_6\text{H}_4\text{CH}_2\text{NMe}_2)\text{P}^+\text{CH}_2\text{PhBr}^-$
32	$[\text{C}_6\text{H}_4(\text{o-CH}_2\text{P}^+\text{Ph}_3\text{Br}^-)]_2$
33	$\text{Ph}_2\text{P}^+(\text{CH}_3\text{Br}^-)\text{C}_4\text{H}_8\text{P}^+(\text{CH}_3\text{Br}^-)\text{Ph}_2$
34	$\text{Ph}_2(\text{o-C}_6\text{H}_4\text{OMe})\text{PCH}_2$
35	$\text{Ph}_2(\text{o-C}_6\text{H}_4\text{OMe})\text{PCHPh}$
36	$\text{Ph}_2(\text{o-C}_5\text{H}_5\text{N})\text{PCHPh}$
37	$\text{Ph}_2(\text{o-C}_6\text{H}_4\text{CH}_2\text{NMe}_2)\text{PCHPh}$
38	$\text{Ph}_2\text{MePCHPh}$
39	Ph_3AsCHPh
40	$\{\text{C}_6\text{H}_4[\text{o-C(H)PPh}_3]\}_2$
41	$\text{C}_6\text{H}_4[\text{C(H)PPh}_3]_2$
42	$\text{Ph}_2\text{P}(\text{CH}_2)\text{C}_4\text{H}_8\text{P}(\text{CH}_2)\text{Ph}_2$
43	$\text{Ph}_3\text{P(H)CC}_3\text{H}_6\text{C(H)PPh}_3$
44	$\text{Ph}_2\text{P}^+(\text{CH}_2\text{Ph})\text{NH}_2\text{Br}^-$
45	Ph_2MePNH
46	Ph_2EtPNH
47	$\text{Ph}_3\text{PNH}_2^+ \cdot \text{N}[\text{PPh}_2(\text{S})]_2$
48	$\text{Ph}_3\text{PCH}_2 \cdot \text{HOCPh}_3$
49	$\text{Ph}_3\text{PNH} \cdot \text{HOCPh}_3$
50	$\text{Ph}_3\text{PO} \cdot \text{HOCPh}_3$

Table 7.1 Compounds and Complexes discussed in Chapter 7.

7.1 Background.

The preparation and subsequent reactions of phosphonium ylides and the isoelectronic iminophosphoranes were discussed in detail in **Chapter 1**. The single crystal X-ray structures of group 15 ylides are by themselves very interesting, as many of them exhibit structural phenomena, such as hydrogen bonding in the solid state. The greater the number of structures which can be collected will enable a better understanding of the P-C or P-N bond contained in these compounds.

In **Chapters 4, 5 and 6**, it was demonstrated that ylides and iminophosphoranes can be co-ordinated to s-block metals. This co-ordination chemistry may be increased in its versatility by adding more donor atoms to the ylide or iminophosphorane e.g. consider the phosphonium ylide example shown in **Figure 7.1**

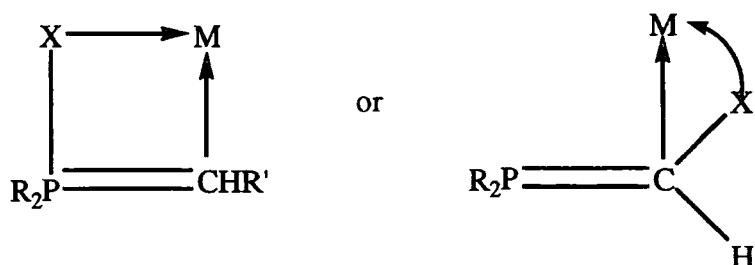


Figure 7.1 Phosphonium ylide with additional donor groups added.

A consideration of ylides containing additional donor groups may have great significance synthetically e.g. the Wittig reaction (1.2.6). Intramolecular co-ordination would allow lithium complexed ylides for example, to react with the carbonyl group without the addition of a third component, thus giving control of stereochemistry e.g. **Figure 7.2**.

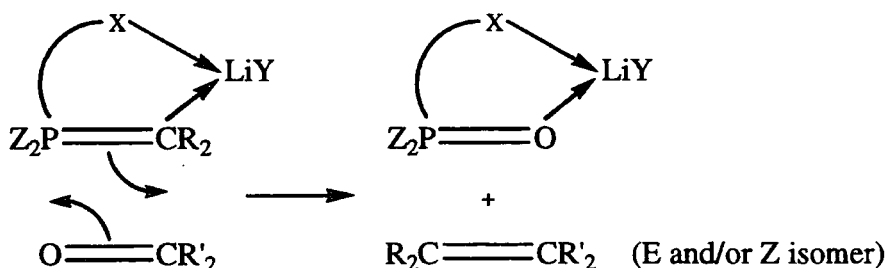


Figure 7.2 The effect of additional donor groups on the Wittig reaction.

This additional co-ordination chemistry may be expanded further if phosphonium bis-ylides are considered (**Figure 7.3**).

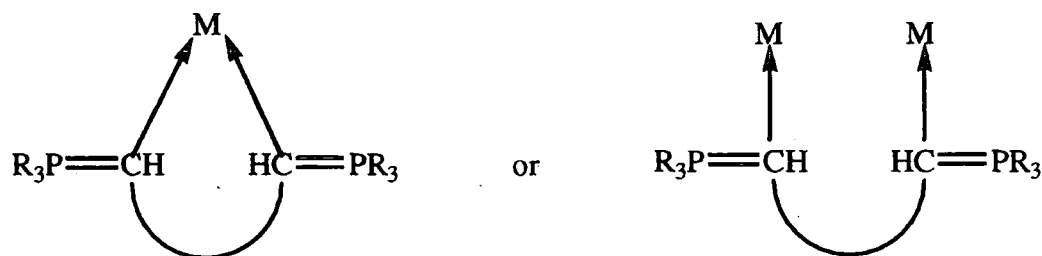


Figure 7.3 Co-ordination of a phosphonium bis-ylide to a metal.

The synthesis and subsequent co-ordination chemistry of phosphonium bis-ylides is limited, due perhaps, to their inherent instability (see 1.2.4).

This chapter contains the synthesis and structural characterisation of a number of group 15 salts and ylides containing additional oxygen and nitrogen donor atoms. Also contained in this chapter are a number of syntheses of salts with organic anions.

7.2 Discussion of compounds 28-33.

Compound **28** was prepared by the addition of methyl bromide to o-anisylidiphenyl phosphine in toluene. The solution was stirred for 4 hours and the resulting precipitate was filtered and dried *in vacuo*. Preliminary investigations by NMR and elementary analysis confirmed the presence of the required salt. A small sample of o-anisylidiphenylphosphonium methyl bromide was recrystallised in acetonitrile to yield a crop of crystals suitable for X-ray analysis. Considering the solid state structure of **28** (**Figure 7.4**) it can be seen that there is a P1-C2 bond length of 1.7882(17) Å which is in the range usually seen for phosphonium salts.¹ A consideration of the o-anisylidiphenylphosphine unit in **28** reveals P-C_{ipso} bond lengths of 1.7912(18), 1.7934(18) and 1.7958(16) Å [P1-C11, P1-C21 and P1-C31 respectively],

¹ A. W. Johnson with special contributions by W. C. Kaska, K. A. O. Starzewski and D. A. Dixon, 'Ylides and Imines of Phosphorus', John Wiley & Sons Inc., New York, (1993).

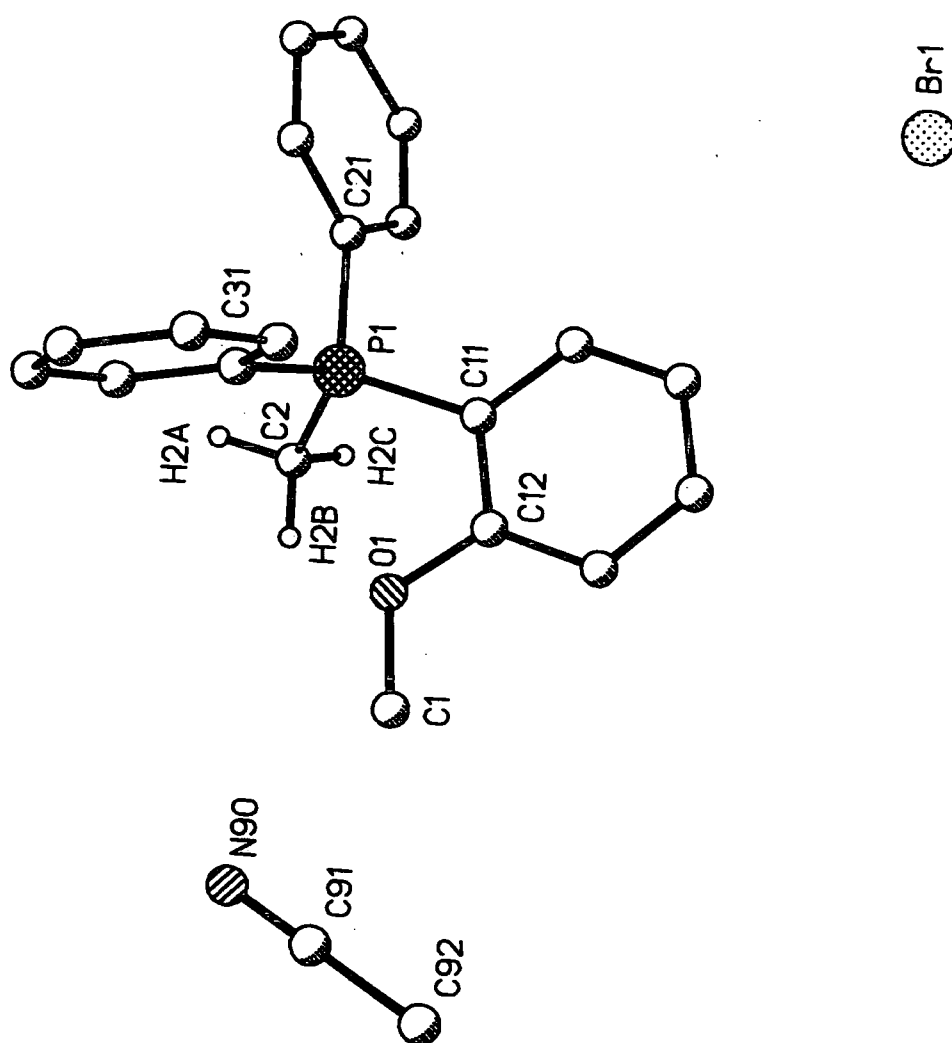


Figure 7.4 Single crystal X-ray structure of $\text{Ph}_2(o\text{-C}_6\text{H}_4\text{OMe})\text{P}^+\text{CH}_3\text{Br}^-\cdot\text{MeCN}$. All hydrogens, except those on C2, omitted for clarity.

as well as $C_{\text{ipso}}\text{-P-C}$ bond angles of $107.66(8)$, $110.54(8)$ and $111.90(8)^\circ$ [$C21\text{-P1-C2}$, $C11\text{-P1-C2}$ & $C31\text{-P1-C2}$ respectively], which are typical of the “2 longer and wider, 1 shorter and narrower” phenomena exhibited by $C_{\text{ipso}}\text{-P}$ interactions within the PPh_3 unit in phosphonium salts and ylides (see **Chapter 1**). There is also an $\text{O-C}_{\text{methyl}}$ bond length of $1.428(2)\text{\AA}$ [O1-C1] and $\text{C-O-C}_{\text{methyl}}$ bond angle of $118.47(16)^\circ$ [C12-O1-C1] which can be compared to other structures where the anisyl group is present (compounds **29** and **35**). It can also be seen from **Figure 7.4** that there is acetonitrile in the crystal lattice due to recrystallisation in that particular solvent.

By considering the packing diagram of **28** (**Figure 7.5**) it was found that each bromine atom has eight close contacts with alkyl and aryl C-H groups from the cation, and the CH_3 group of the acetonitrile solvent molecule. With normalised C-H distances of 1.08\AA , and if $D = \text{C-H}\dots\text{Br}$ distance, $d = \text{H}\dots\text{Br}$ distance & $\theta = \text{C-H}\dots\text{Br}$ angle, then for the shortest heavy atom interaction, D is 3.699\AA ($\text{C22-H22}\dots\text{Br1}$), $d = 2.674\text{\AA}$ ($\text{H22}\dots\text{Br1}$) and $\theta = 158.2^\circ$ ($\text{C22-H22}\dots\text{Br1}$). The longest heavy atom interaction has the following values, D is 3.835\AA ($\text{C2-H2}\dots\text{Br1}$), $d = 2.756\text{\AA}$ ($\text{H2}\dots\text{Br1}$) and $\theta = 177.2^\circ$ ($\text{C2-H2}\dots\text{Br1}$).

Compound **29** was prepared by the addition of benzyl bromide to *o*-anisyl diphenylphosphine in toluene. The reaction mixture was stirred for 24 hours upon which time there was a white precipitate. A small amount of this solid was recrystallised in hot acetonitrile to yield a sample of crystals suitable for X-ray analysis. Single crystal X-ray diffraction studies revealed the structure of **29** (**Figure 7.6**) to be typical of a phosphonium benzylylide salt,² as typified by a P-C8 bond length of $1.8198(15)\text{\AA}$ and *o*-anisyl diphenylphosphine unit characteristics including $C_{\text{ipso}}\text{-P}$ bond lengths of $1.7994(14)$, $1.8018(14)$ and $1.8039(15)\text{\AA}$ [P-C1 , P-C11 & P-C21 respectively] and $C_{\text{ipso}}\text{-P-C}$ bond angles of $106.99(7)$, $109.50(7)$ and $110.85(7)^\circ$ [C1-P-C8 , C11-P-C8 & C21-P-C8 respectively].

Other structural features to note include P-C-H bond angles of $105.0(11)$ and $106.9(10)^\circ$ [P-C8-H81 & P-C8-H82] and a P-C8-C31 bond angle of $115.94(10)^\circ$. Considering the anisyl methyl group it can be seen that there is an $\text{O-C}_{\text{methyl}}$ bond length of $1.4421(18)\text{\AA}$

² See for example A. C. Skapski and F. A. Stephens, *J. Cryst. Mol. Struct.*, **4**, 77 (1974) or J. Hubner, M. Meisel, H. Vogt and D. Wulff-Molder, *Z. Naturforsch., Teil. B.*, **52**, 1321 (1997).

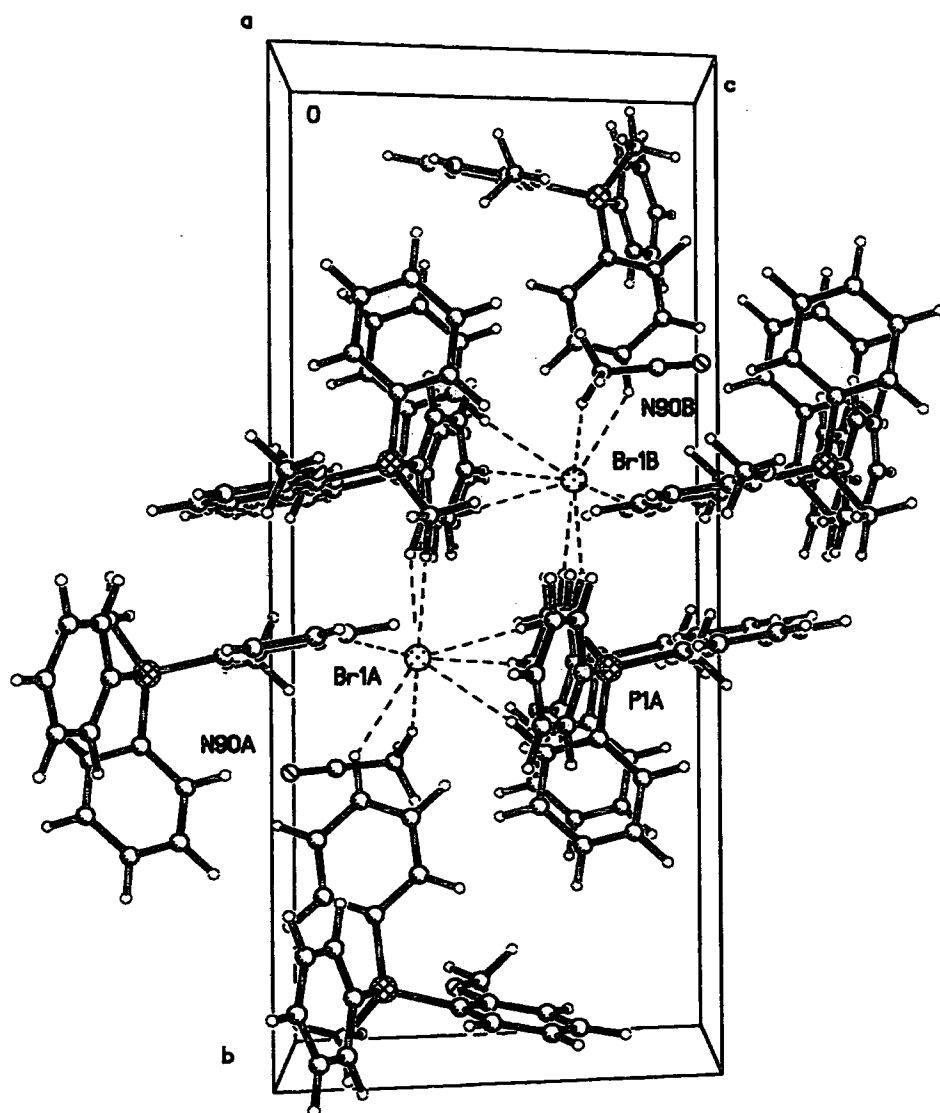


Figure 7.5 Packing diagram showing H...Br interactions in 28.

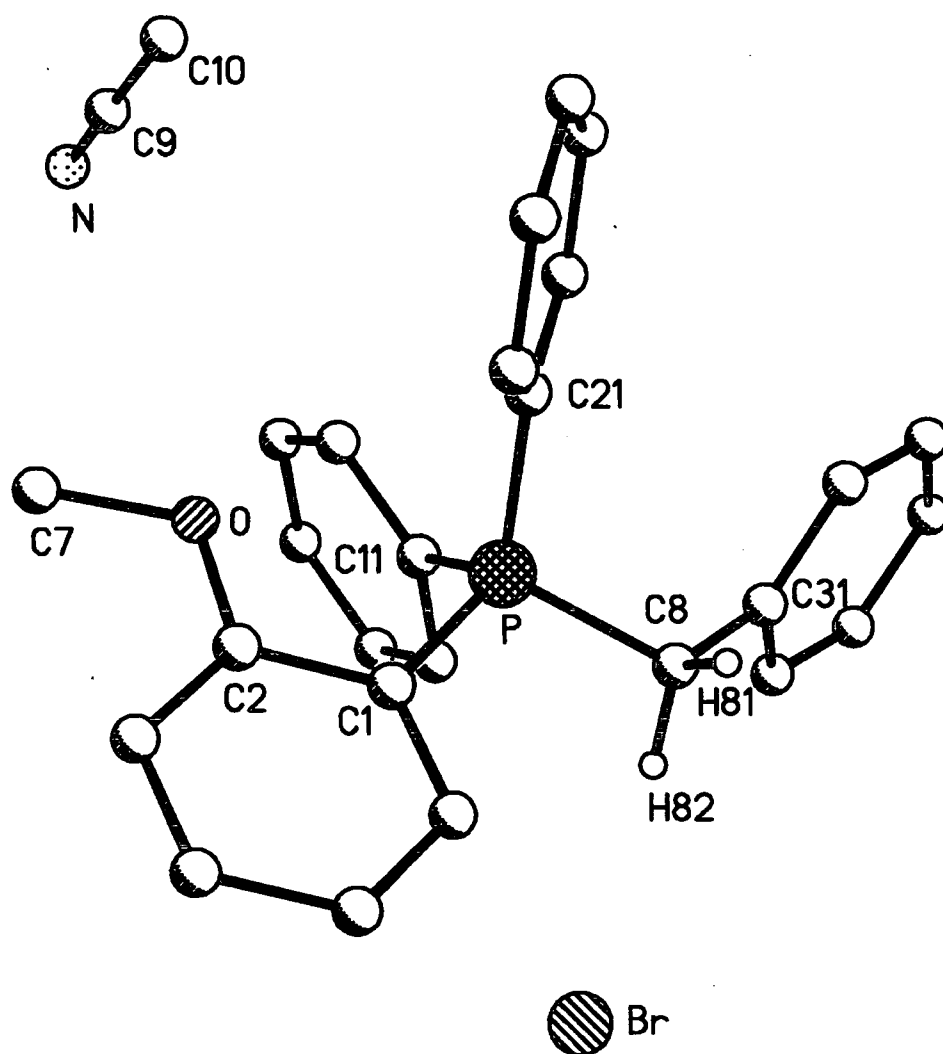


Figure 7.6 Single crystal X-ray structure of $\text{Ph}_2(\text{o-C}_6\text{H}_4\text{OMe})\text{P}^+\text{CH}_2\text{PhBr}^-\cdot\text{MeCN}$.

All hydrogen atoms, except those bonded to C8, omitted for clarity.

[O-C7] and a C-O-C bond angle of $117.84(12)^\circ$ [C2-O-C7], which compares well with **28** [$1.428(2)\text{\AA}$ and $118.47(16)^\circ$ respectively]. The structure of **29** has previously been published,³ Their determined structure (Table 7.2) has different cell parameters to **29** and does not include any solvent molecules, hence there are a number of subtle changes in the structural geometry.

	29	M ^c Ewen et al ³
[a] \AA	12.382(4)	15.528(4)
[b] \AA	10.677(3)	16.692(4)
[c] \AA	18.905(5)	17.921(5)
[α] $^\circ$	90	90
[β] $^\circ$	102.22(1)	90
[γ] $^\circ$	90	90
[P-C]	1.8198(15)	1.815(10)
[C _{ipso} -P]	1.7994(14)	1.799(11)
	1.8010(14)	1.823(11)
	1.8039(15)	1.840(12)
[C _{ipso} -P-C _{ytide}]	106.99(7)	107.89(8)
	109.50(7)	108.35(9)
	110.85(7)	109.01(4)
[P-C-H]	105.0(11) & 106.9(10)	-
[P-C-C]	115.94(10)	114.69(6)
[O-C _{methyl}]	1.4421(18)	1.400(6)
[C-O-C]	117.84(12)	114.04(2)

Table 7.2 Comparison of 29 with previously published structure.

As the table shows the main differences are in the P-C-C bond angle [$115.94(10)$ vs $114.69(6)^\circ$] and the C-O-C_{methyl} angle of $117.84(12)$ vs $114.04(2)^\circ$.

³ W. E. M^cEwen, R. J. Wikholm and J. S. Wood., *Phosphorus and Sulfur*, **3**, 163 (1977).

By considering the packing diagram of **29** (Figure 7.7) it was found that each bromine atom has close contacts with alkyl and aryl C-H groups from the cation, and in this particular structure the acetonitrile molecule acts as an acceptor rather than a donor with $D = 3.507\text{\AA}$ (C-H...N), $d = 2.448\text{\AA}$ (H...N) and $\theta = 166.5^\circ$ (C-H...N). With normalised C-H distances of 1.08\AA , then for the shortest heavy atom interaction, D is 3.701\AA (C24-H24...BrA), $d = 2.841\text{\AA}$ (H24...BrA) and $\theta = 136.6^\circ$ (C24-H24...BrA). The longest heavy atom interaction has the following values, D is 3.931\AA (C16-H16...BrA), $d = 2.880\text{\AA}$ (H16...BrA) and $\theta = 177.2^\circ$ (C16-H16...BrA).

Compound **30** was produced by the reaction of 2-pyridyldiphenylphosphine with benzyl bromide in toluene. The reaction was stirred for 24 hours, after which time a white precipitate was filtered off and dried *in vacuo*. A small portion of the solid was recrystallised in hot acetonitrile to yield a sample of crystals suitable for X-ray analysis (hence the acetonitrile in the lattice), which when undertaken revealed the structure of **30** (Figure 7.8) to again be typical of a phosphonium benzylide salt^{2,3} with a P1-C1 bond length of $1.812(2)\text{\AA}$ and a 2-pyridyldiphenylphosphine unit with the following unremarkable structural features; C_{ipso} -P bond lengths of $1.803(2)$, $1.805(2)$ and $1.809(2)\text{\AA}$ [P1-C21, P1-C31 & P1-C41 respectively] and C_{ipso} -P-C bond angles of $108.18(10)$, $109.40(10)$ and $112.24(10)^\circ$ [C21-P1-C1, C41-P1-C1 & C31-P1-C1 respectively]. There is also a P1-C1-C11 bond angle of $114.61(14)^\circ$ and two P-C-H bond angles of 108.6° [P1-C1-H1A & P1-C1-H1B], although great care should be taken with these last two values as the exact positions of freely refined hydrogen atoms cannot be determined accurately by X-ray diffraction techniques. This salt is the first structurally characterised phosphonium benzylide salt containing a pyridine ring in the molecular structure.

By considering the packing diagram of **30** (Figure 7.9) it was found that each bromine atom has seven close contacts with alkyl and aryl C-H groups from the cation, and in this structure the acetonitrile molecule again acts as an acceptor rather than a donor with $D = 3.549\text{\AA}$ (C21-H21...N26), $d = 2.560\text{\AA}$ (H21...N26) and $\theta = 151.9^\circ$ (C21-H21...N26). With normalised C-H distances of 1.08\AA , then for the shortest heavy atom interaction, D is 3.732\AA (C32-H32...Br1), $d = 2.705\text{\AA}$ (H32...Br1) and $\theta = 158.7^\circ$ (C32-H32...Br1).

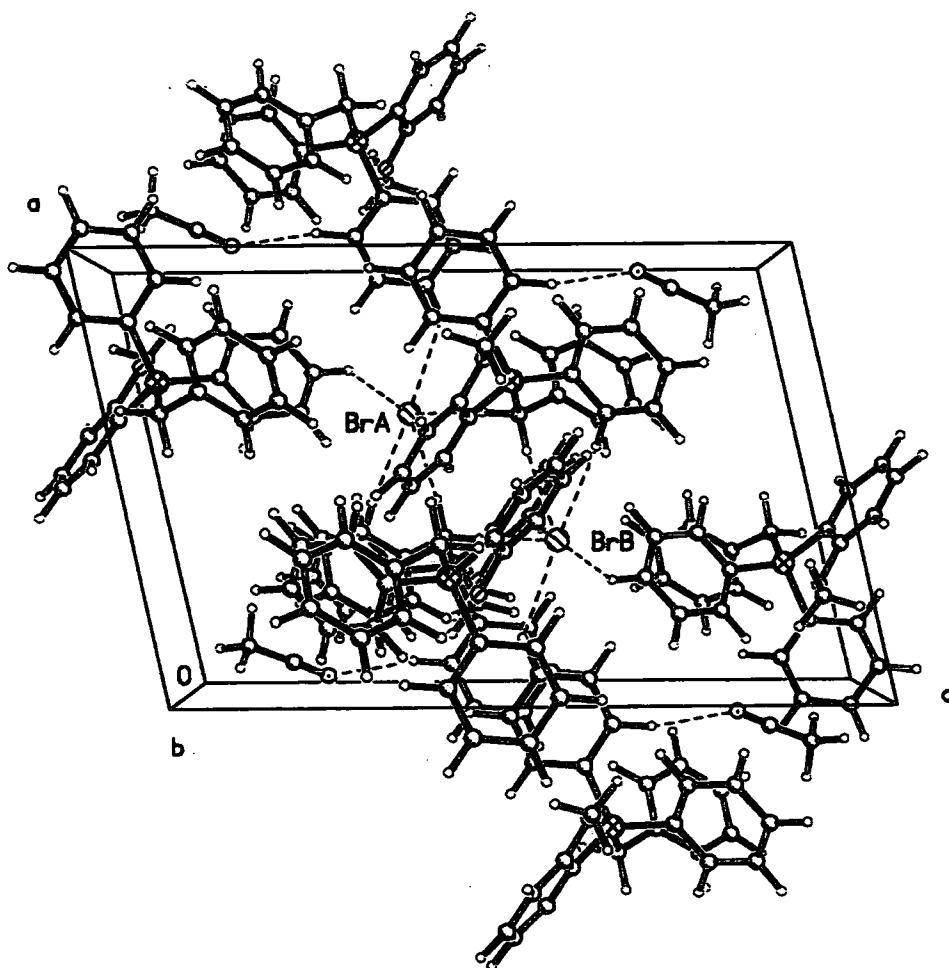


Figure 7.7 Packing diagram showing the C-H...Br and C-H...N interactions in compound 29.

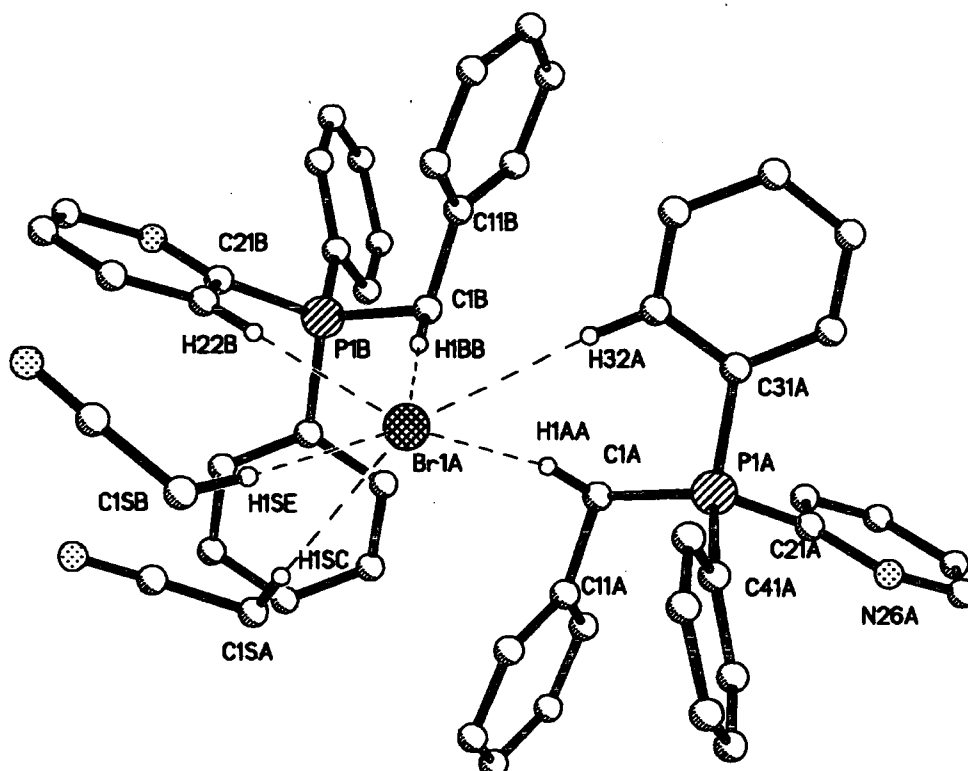


Figure 7.8 Single crystal X-ray structure of $\text{Ph}_2(\text{o-C}_5\text{H}_5\text{N})\text{P}^+\text{CH}_2\text{PhBr}^-\cdot\text{MeCN}$. All hydrogen atoms, except those involved in interaction with the bromine atom, omitted for clarity.

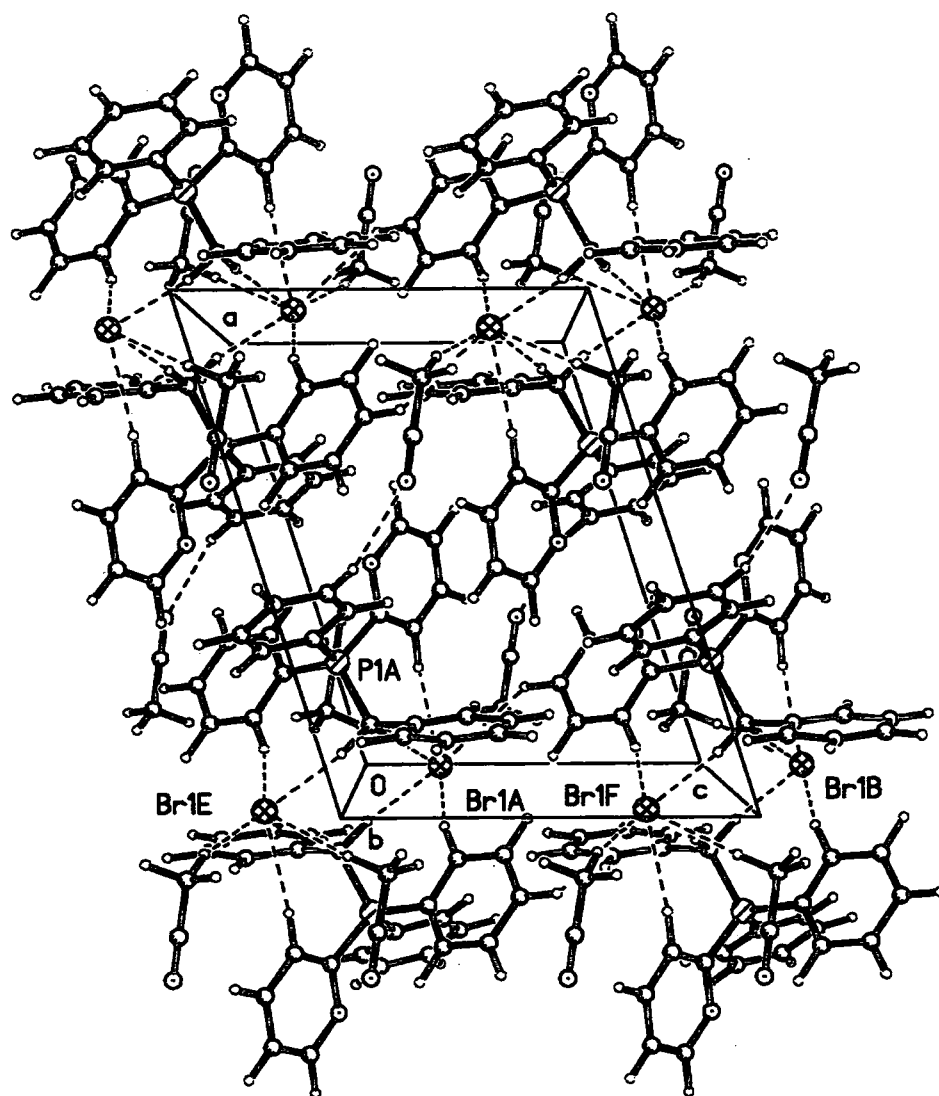


Figure 7.9 Packing diagram showing the C-H...Br and C-H...N interactions in compound 30.

The longest heavy atom interaction has the following values, D is 3.852 Å (C34-H34...Br1), d = 3.058 Å (H34...Br1) and θ = 130.8° (C34-H34...Br1).

Compound **31** was produced by the addition of benzyl bromide to σ -diphenylphosphino-*N,N'*-dimethylbenzylamine in toluene. After stirring overnight the salt was fully precipitated using diethyl ether, isolated and dried *in vacuo*. Crystals of this compound could not be obtained and hence no X-ray structural analysis was undertaken. The compound was however, fully analysed by NMR, elemental analysis and melting point analysis.

Compound **32** was prepared by the addition of 2 equivalents of triphenyl phosphine to 2,2'-bis(bromomethyl)-1,1'-biphenyl in acetonitrile. After heating the reaction mixture at 35°C for 24 hours the resulting salt was filtered off and dried *in vacuo*. A small amount of this solid was recrystallised in hot acetonitrile to yield a crop of crystals suitable for X-ray diffraction. Whilst this molecule has been synthesised before⁴ it has never been structurally characterised. Considering the solid state structure of **32** (Figure 7.10) it is apparent that there are two separate $\text{CH}_2\text{P}^+\text{Ph}_3\text{Br}^-$ groups to examine.

The first has a P1-C2 bond length of 1.820(3) Å and a PPh_3 unit with the following structural parameters; $\text{C}_{\text{ipso}}\text{-P}$ bond lengths of 1.794(4), 1.794(4) and 1.802(4) Å [P1-C61, P1-C71 & P1-C81 respectively] and $\text{C}_{\text{ipso}}\text{-P-C}$ bond angles of 108.90(17), 110.23(16) and 111.11(17)° [C61-P1-C2, C71-P1-C2 & C81-P1-C2 respectively]. The other chemically identical $\text{CH}_2\text{P}^+\text{Ph}_3\text{Br}^-$ unit contains a P2-C1 bond length of 1.807(4) Å, $\text{C}_{\text{ipso}}\text{-P}$ bond lengths of 1.797(5), 1.802(4) and 1.803(4) Å [C31-P2, C51-P2 & C41-P2 respectively] and $\text{C}_{\text{ipso}}\text{-P-C}$ bond angles of 107.8(2), 109.2(2) and 112.7(2)° [C41-P2-C1, C31-P2-C1 & C51-P2-C1 respectively].

Other features of this salt to note are that it is a cisoid molecule and also that there is a twist angle of 60.4° through which the two joining phenyls are displaced. This is undoubtedly due to the large steric bulk of the salt groups.

⁴ H. J. Bestmann, H. Burzlaff, R. Ruppert and W. Schafer, *Chem. Ber.*, **99**, 2848 (1966).

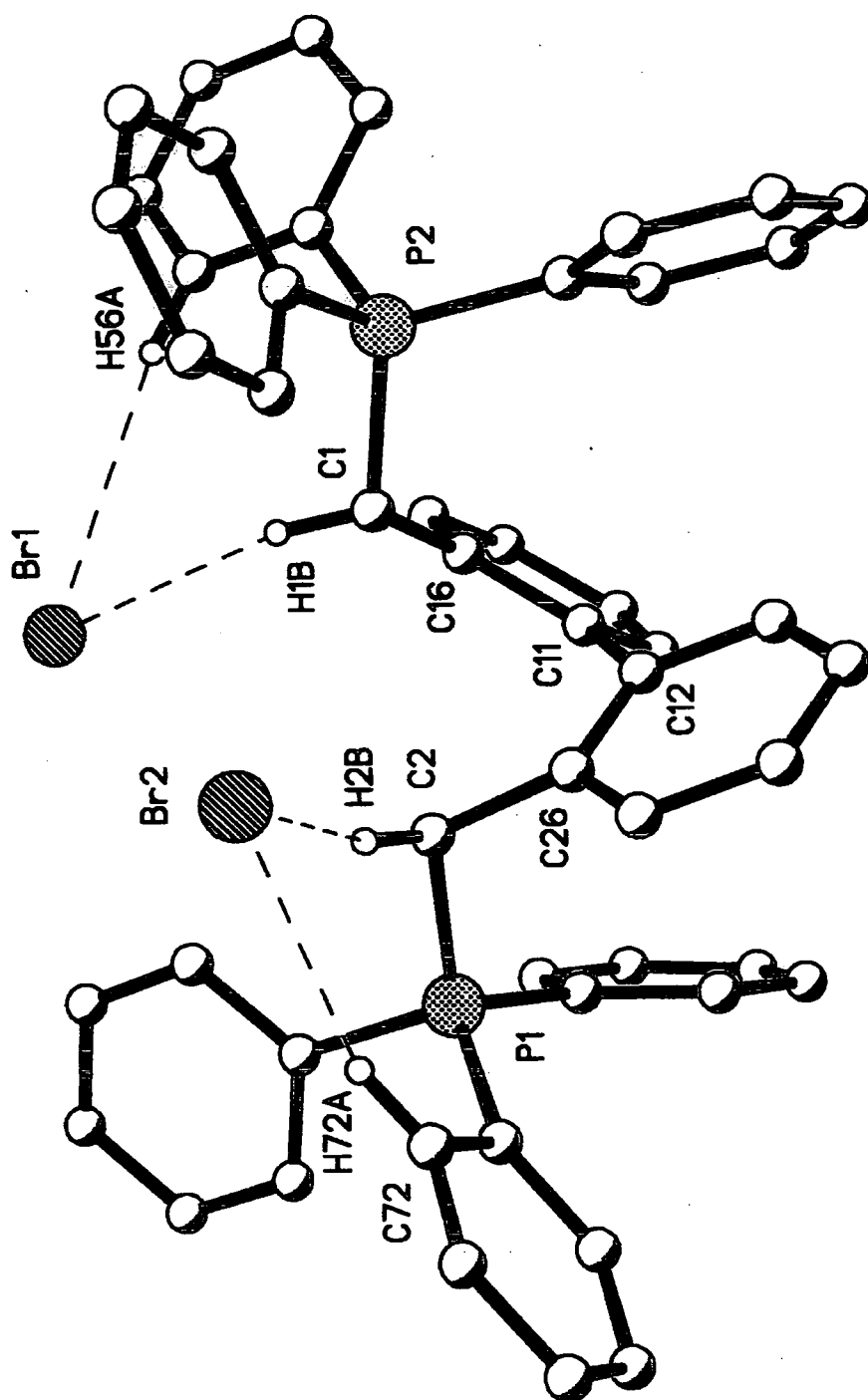


Figure 7.10 Single crystal X-ray structure of $[C_6H_4(o-CH_2P^+Ph_3Br^-)]_2 \cdot 2MeCN$. All hydrogen atoms, except H1A, H1B, H56A and H72A, and solvent omitted for clarity.

Upon obtaining the NMR data it was difficult to ascertain the assignments of each peak, and it was necessary to consider a ^{31}P decoupled ^1H spectrum. This enabled the determination of the $^2J_{\text{HH}}$ splitting constants, and from these data that the protons on the CH_2 groups adjacent to the phosphorus atoms are non-equivalent, a fact observed by Herrmann et al⁵ in their study of $(\text{C}_6\text{H}_4\text{CH}_2\text{PPh}_2)_2$. These diastereotopic protons giving two doublets nearly 2ppm apart indicate that the molecule is indeed pro-chiral.

In order to assign the other peaks a ^1H - ^1H COSY NMR spectrum was required. One interesting feature of this molecule is that the proton ortho to the salt group on each phenyl ring has a chemical shift at 5.6ppm, which is lower than is usually seen for an aromatic proton ($>6.5\text{ppm}$). This observed phenomenon is due to the fact that these particular protons are not in the plane of the ring as is normal, and thus they are influenced by the diamagnetic current running through the centre of the ring. This influences the magnetic environment of these ortho protons and hence a different chemical shift than expected is observed.

As can be seen from the packing diagram (Figure 7.11) there is significant hydrogen bonding in the structure. The ranges of values seen for hydrogen bonding interactions in 32 are $\text{H}\dots\text{Br}$ distances of 2.58-3.01Å and $\text{C-H}\dots\text{Br}$ angles of 154.5-169.9°.

Other than the ones shown above there are many more intermolecular donor-acceptor interactions which make the whole system polymeric (Figure 7.11) i.e. nitrogen atoms on the acetonitrile solvent molecules hydrogen bonding to hydrogen atoms on the biphenyl molecule. Molecules in which the anion is chelated by alkyl and aryl C-H groups have been seen before.⁶ These interactions are a common structural feature in hydrogen bonded systems.

⁵ E. Herdtweck, W. A. Herrmann, P. Kiprof and C. W. Kohlpaintner, *Inorg. Chem.*, **30**, 4271 (1991).

⁶ M. G. Davidson, *J. Chem. Soc., Chem. Commun.*, 919 (1995).

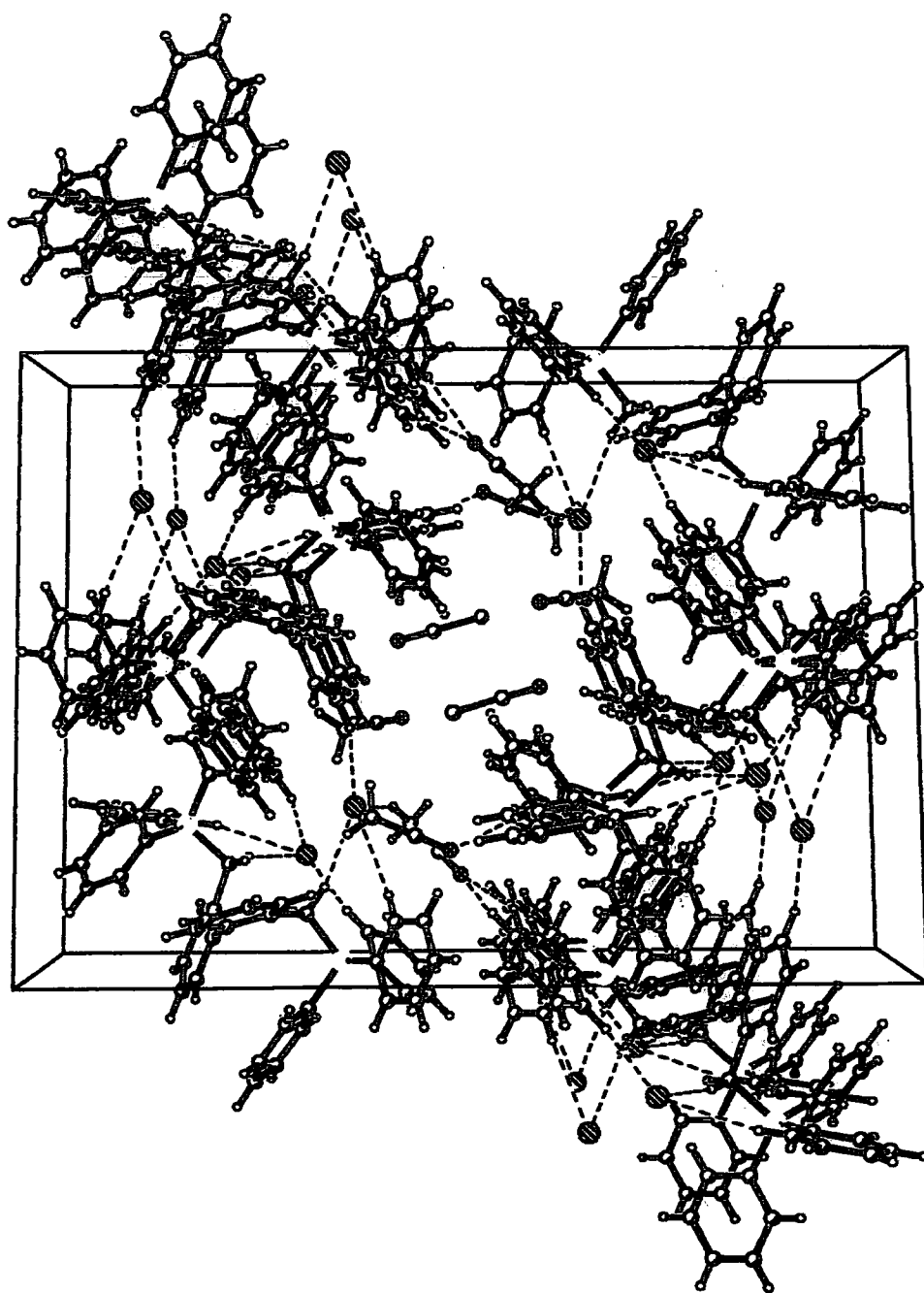


Figure 7.11 Packing diagram showing H...Br interactions in 32.

Compound **33**, a bis-ylide salt was prepared by the addition of methyl bromide to 1,4 bis(diphenylphosphino)butane in acetonitrile. The reaction was stirred for 24 hours upon which time the salt was precipitated fully using dry diethyl ether. The salt was then isolated and dried *in vacuo*. The salt was characterised by multi-nuclear NMR, elemental analysis and melting point analysis. Single crystal X-ray diffraction studies were not undertaken for this molecule as no suitable single crystals could be grown.

7.3 Discussion of compounds 34-39.

Compound **34**, a phosphonium ylide was produced by the deprotonation of compound **28** using sodium amide in thf. After stirring overnight, the suspension was filtered to remove sodium bromide and any unreacted sodium amide. The thf was reduced in volume to a minimal amount and the ylide was redissolved with heating. Upon cooling in a freezer it yielded a bright yellow solid, which was fully characterised using NMR, elemental analysis and melting point analysis. Crystals of **34** proved unobtainable and thus single crystal X-ray diffraction studies were not undertaken. The structure of **34** would be very similar to triphenylphosphonium methyllide.⁷

Compound **35**, a phosphonium benzylide was produced by the deprotonation of its corresponding salt **29** in thf over a period of 24 hours. After this time the sodium bromide and any unreacted sodium amide were filtered off and then the thf was reduced *in vacuo* to leave a slurry. Toluene was added and the mixture was heated to aid dissolution. The solution was then left at room temperature whereupon crystals suitable for X-ray diffraction were obtained. The solid state structure of **35** (Figure 7.12), a phosphonium benzylide, is typical of such a compound⁸ with a shortened P1-C1 bond length of 1.6930(14)Å when compared with the starting salt **29** [1.8198(15)Å]. The C_{ipso}-P bond lengths, 1.8019(14), 1.8159(14) and 1.8220(14)Å [C11-P1, C31-P1 & C41-P1 respectively] and C_{ipso}-P-C_{ylide} bond angles of 107.77(7), 113.995(7) and 115.11(7)° [C11-

⁷ W. Graf, J. Jeong, G. Muller, A. Schier, H. Schmidbaur and D. L. Wilkinson, *New. J. Chem.*, **13**, 341 (1989).

⁸ A. S. Batsanov, M. G. Davidson, J. A. K. Howard, S. Lamb and C. Lustig, *J. Chem. Soc., Chem. Commun.*, 1791 (1996). M. G. Davidson, J. A. K. Howard and D. S. Yufit, *J. Chem. Soc., Perkin Trans 2.*, 249 (2000).

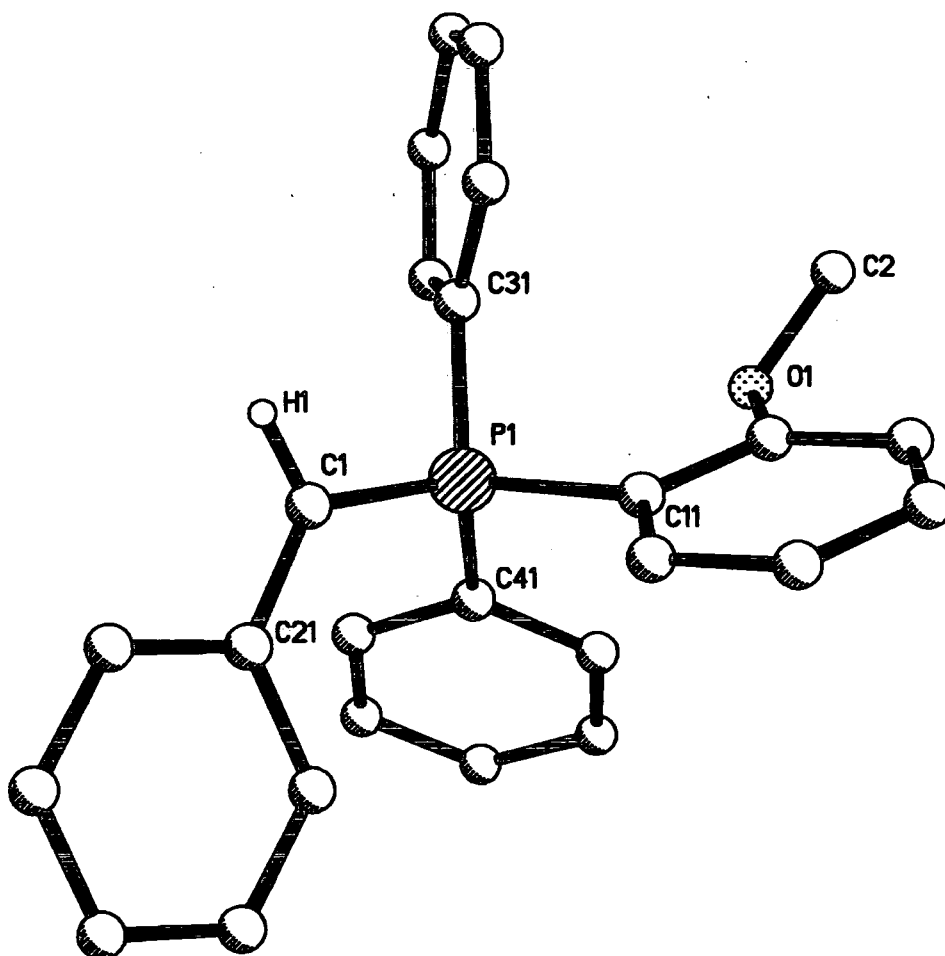


Figure 7.12 Single crystal X-ray structure of $\text{Ph}_2(o\text{-C}_6\text{H}_4\text{OMe})\text{PCHPh}$. All hydrogen atoms, except the ylidic proton, omitted for clarity.

P1-C1, C31-P1-C1 & C41-P1-C1], whilst noticeably different from the starting salt **29** [1.7994(14)°, 1.8010(14)°, 1.8039(15)°, 106.99(7)Å, 109.50(7)Å and 110.85(7)Å respectively] still exhibit one shorter and two longer C_{ipso}-P bond lengths and one narrower and two wider C_{ipso}-P-C_{ylide} bond angles in accordance with the existence of the unique phosphorus substituent (**Chapter 1**). Other features to note of interest in this ylide are a P1-C1-H1 bond angle of 112.2(11)°, a P1-C1-C21 bond angle of 128.33(11)°, an O-C_{methyl} bond length of 1.420(3)Å [O1-C2] and a C12-O1-C2 bond angle of 117.22(14)° which are relatively unchanged from **29**. This is the first reported full structural characterisation of an anisyl phosphonium benzylide, although the structure of the bromide salt is already known.³

Compound **36**, another novel phosphonium benzylide was synthesised by the deprotonation of **30** in thf over 24 hours. After filtration and subsequent reduction of thf, toluene was added and the mixture heated to aid dissolution. After standing at room temperature overnight, crystals suitable for X-ray diffraction were obtained. The solid state structure of **36** (**Figure 7.13**), a 2-pyridyl diphenyl phosphonium benzylide exhibits a P1-C1 bond length of 1.693(2)Å which is shorter than that seen in the starting salt **30** [1.812(2)Å].

The geometry about the phosphorus in the 2-pyridyldiphenylphosphine unit consists of C_{ipso}-P bond lengths of 1.813(2), 1.832(2) and 1.836(2)Å [C11-P1, C31-P1 & C41-P1 respectively] and C_{ipso}-P-C_{ylide} bond angles of 108.43(7), 113.28(8) and 116.69(8)° [C11-P1-C1, C31-P1-C1 & C41-P1-C1 respectively], again little changed from the starting salt **30**, although the C_{ipso}-P bond lengths are slightly longer and the C_{ipso}-P-C_{ylide} bond angles are slightly wider in the ylide. This difference could be due to the increased electron density in the P-C bond which serves to negate any potential back bonding from the ylidic carbon atom into the σ* orbitals on the phosphorus, making the bonds both longer and hence weaker. There are also P1-C1-H1A and P1-C1-C21 bond angles of 116.42(6)° and 127.17(12)° respectively which are considerably wider than those seen in **30**, explained by the loss of one of the protons and hence the geometry moving from sp³ type to sp² type [tetrahedral (109.5°) to trigonal (120°)].

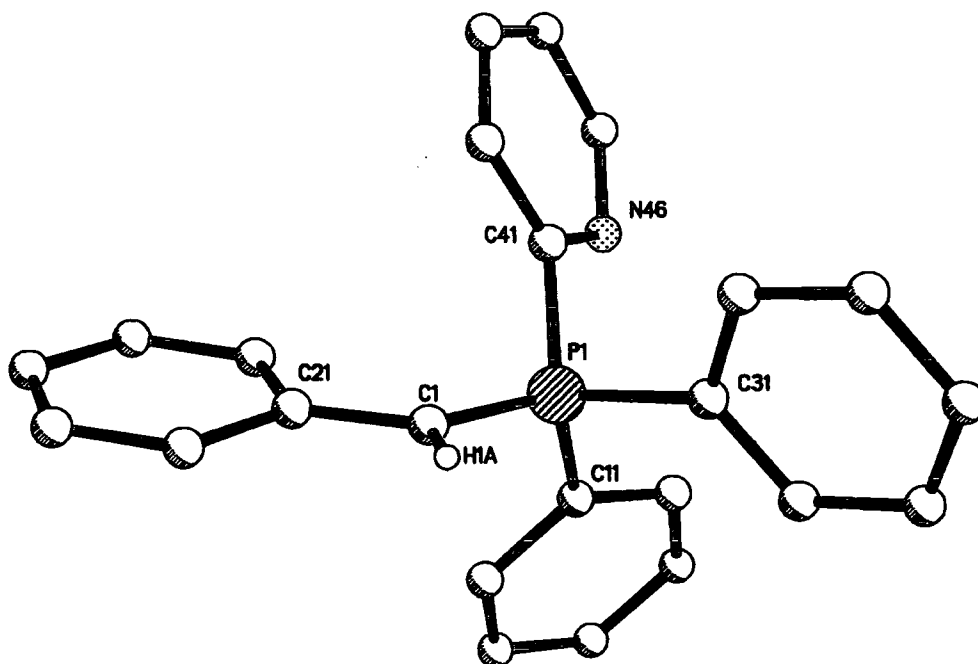


Figure 7.13 Single crystal X-ray structure of $\text{Ph}_2(\text{o-C}_5\text{H}_5\text{N})\text{PCHPh}$. All hydrogens, except the ylidic proton, omitted for clarity.

Compound **37**, o-diphenylphosphino-N,N'-dimethylbenzylamine phosphonium benzylide, was produced by the deprotonation of the corresponding benzyl salt **31**. Sodium amide was used as the base for deprotonation and the reaction was carried out in thf overnight. After stirring for 24 hours the reaction mixture was filtered and the thf reduced *in vacuo*. After addition of toluene the reaction mixture was heated to aid dissolution and left to stand at -30° whereupon a red solid was obtained. Unfortunately no single crystals of this ylide were obtained, but the ylide was fully characterised by NMR, elemental analysis and melting point analysis.

Compound **38**, methyldiphenyl phosphonium benzylide was produced by deprotonation of the corresponding bromide salt to yield a bright orange crystalline material. Whilst crystals of this compound were obtained and subjected to single crystal X-ray diffraction studies, a structure could not be determined, as the crystals would not diffract. It is thought that the structure of this ylide would be similar to the structures of triphenylphosphonium benzylide and triphenylarsonium benzylide **39** (Figure 7.14).

Compound **39**, triphenylarsonium benzylide (Figure 7.14) was produced by deprotonation of triphenylarsonium benzyl bromide⁹ using sodium amide in thf. The reaction mixture was stirred at room temperature for 72 hours resulting in a bright orange solution. After filtration the thf was reduced *in vacuo*, toluene added and the mixture heated to aid dissolution. Refrigeration of the solution at -20°C yielded a solid which upon recrystallisation in toluene yielded crystals suitable for X-ray analysis.

The solid state structure of **39** (Figure 7.14), triphenylarsonium benzylide reveals the following interesting features; an As(1)-C(7) bond length of 1.823(4)Å along with C_{ipso}-As bond lengths of 1.928(4), 1.937(4) and 1.941(4)Å [C11-As1, C21-As1 & C31-As1 respectively] and C_{ipso}-As-C_{ylide} angles of 107.30(19), 114.02(19) and 115.5(2)° [C11-As1-C7, C21-As1-C7 & C31-As1-C7 respectively]. Another structural feature to note is the As1-C7-C1 bond angle of 125.3(3)°. The structure of triphenylphosphonium benzylide was first determined in our group⁹ and further studies have been carried out on it since.⁹ The most important point to note is that the structures are isomorphous, which

⁹ S. Lamb, *Ph.D. Thesis.*, University of Durham (1998) and references cited therein.

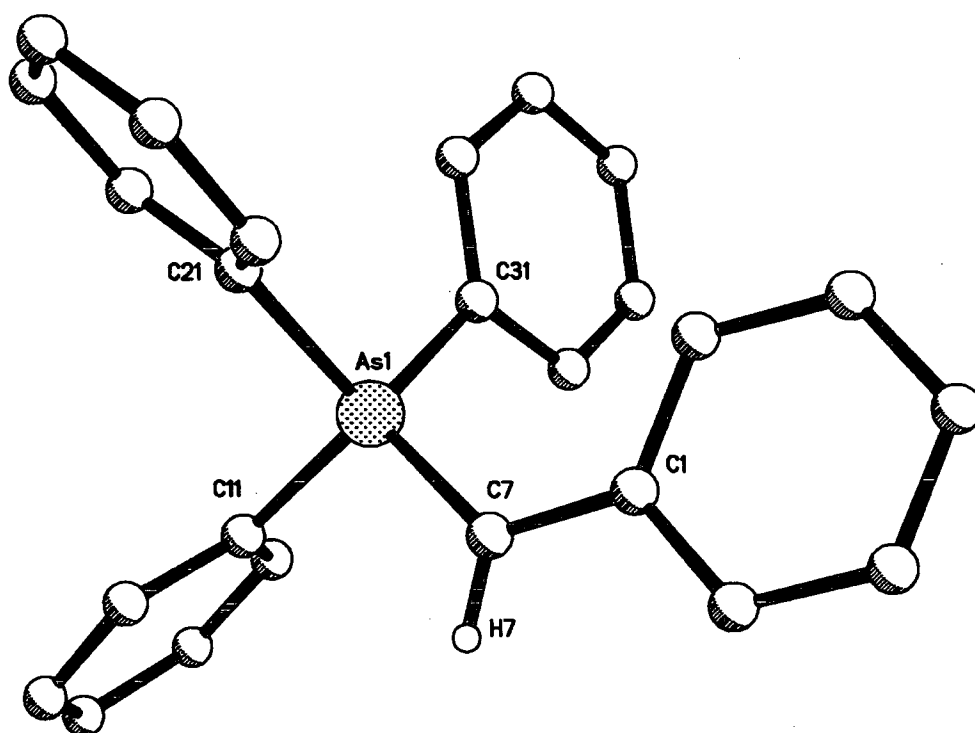


Figure 7.14 Single crystal X-ray structure of Ph_3AsCHPh . All hydrogen atoms, except the ylidic proton, have been removed for clarity.

means that any packing forces are the same and allows a direct comparison of the structural parameters (Table 7.5).

Ph ₃ AsCHPh 39		Ph ₃ PCHPh	
[As-C]Å	1.823(4)	[P-C]Å	1.6993(5)
[C _{ipso} -As]Å	1.928(4)	[C _{ipso} -P]Å	1.8056(6)
	1.937(4)		1.8173(4)
	1.941(4)		1.8216(4)
[C _{ipso} -As-C _{ylide}]°	107.30(19)	[C _{ipso} -P-C _{ylide}]°	107.1(1)
	114.02(19)		113.2(1)
	115.5(2)		116.7(1)
[As-C _{ylidic} -C]°	125.3(3)	[P-C _{ylidic} -C]°	127.0(1)

Table 7.5 Comparison of 39 with Ph₃CHPh

From the above table it can be seen that in terms of the four quoted analogous bond lengths the phosphonium ylide has shorter bonds by approximately 0.1Å in each case. In terms of the C_{ipso}-As-C_{ylide} angle, both ylides are very similar in that they both contain one narrower angle and two wider angles making the case for the existence of a “unique arsenic substituent” as in the analogous phosphonium ylide (Chapter 1). The As-C_{ylidic}-C angle is almost 2° less than the corresponding angle in the phosphonium ylide. An explanation for this could be that as the arsenic atom is larger than the phosphorus atom the substituents are further away from the atom centre and so they are more free to move apart, whereas in the phosphonium case the steric hindrance forces the substituents into a fixed geometry thus giving the greater angle. However, the key point to note here is that if the difference in size between the arsenic and the phosphorus atoms is calculated from the bond lengths i.e. [(C_{ipso}-As)-(C_{ipso}-P)] = 1.941-1.822 = 0.119Å, this difference is very close to the difference between the As-C_{ylidic} and P-C_{ylidic} bond lengths (1.823-1.699 = 0.124Å). This means that the actual physical distances between the phosphorus and ylidic carbon and the arsenic and ylidic carbon are actually very similar in size. This goes against all perceived wisdom which states that P=CHR is more ‘double bonded’ than As=CHR, which means we would expect the distance between the phosphorus and the ylidic carbon to be noticeably smaller than the equivalent distance in the arsenic benzylylide.

Searching the literature reveals no known structures of non-stabilised arsonium benzylides although the stabilised ylides are well documented¹⁰. There are structures of three non-stabilised salts already determined; triphenylarsonium benzyl bromide,¹⁰ and the bromide and hexafluorophosphate salts of R-benzyl(methyl)(4-methylphenyl)(naphthalen-1-yl)arsonium¹¹ (Figure 7.15).

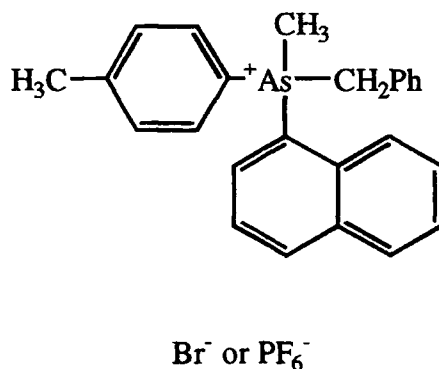


Figure 7.15 A benzyl arsonium salt

7.4 Discussion of compounds 40-43.

Compound **40**, 2,2'-bis[methylide(triphenylphosphonium)]-1,1'-biphenyl was produced by the addition of sodium hydride to the bis-bromide salt **32**, in thf. After stirring overnight the dark red suspension was filtered and the thf reduced *in vacuo* to a minimal level. After heating to aid dissolution the solution was left to stand whereupon a bright solid formed. Preliminary characterisation by NMR, elemental analysis and melting point analysis revealed the compound to be the expected bis-ylide. Unfortunately it was not possible to obtain a crystalline sample of the ylide and thus single crystal X-ray diffraction studies could not be undertaken. Many solvent variations were tried in an attempt to obtain crystals but to no avail.

¹⁰ I. Gosney, D. Lloyd and R. A. Ormiston, *Chem. Soc. Rev.*, **16**, 45 (1987).

¹¹ D. G. Allen, C. L. Raston, B. W. Skelton, A. H. White and S. B. Wild, *Aust. J. Chem.*, **6**, 1171 (1984).

Compound **41**, α,α' bis(triphenylphosphonium methylide)-o-xylene was synthesised by addition of potassium hydride to the bromide salt as supplied by Aldrich, in thf. The resulting solution was filtered and then the thf was removed *in vacuo*. The product was dissolved in a 3:2 mixture of toluene:hexane. The solution was stored in a freezer at -30°C to yield a very small amount of solid ylide. Characterisation of the bis-ylide was achieved through a combination of NMR, elemental analysis and melting point analysis. This bis-ylide has been prepared previously¹² but never isolated as a solid product. Unfortunately crystals of this bis-ylide could not be obtained and thus no structural data could be collected.

Compound **42**, 1,4 bis(diphenylphosphonium methylide) butane was prepared by the addition of sodium amide to the bis-bromide salt **31**, in thf. The mixture was stirred under argon for 24 hours upon which time it was filtered to remove sodium bromide and any unreacted sodium amide and the thf was reduced to a minimal amount *in vacuo*. The resulting suspension was dissolved in toluene with heating and left to cool at room temperature whereupon a yellow crystalline solid was obtained. The quality of the crystals was insufficient to enable single crystal X-ray diffraction studies to be undertaken but the existence of the bis-ylide was confirmed by various analytical tools such as multi-nuclear NMR, elemental analysis and melting point analysis.

Compound **43**, was synthesised by the stirring of sodium amide and 1,5 bis(triphenylphosphino) pentane dibromide in a 1:1 mixture of toluene:thf overnight. The resulting red suspension was filtered to remove any unreacted sodium amide and sodium bromide and then reduced *in vacuo* to leave a slurry. The resulting suspension was dissolved with heating and left to crystallise at room temperature. The resulting red crystals were subjected to single crystal X-ray diffraction but were found not to diffract. Subsequent batches of crystals were also tried and failed. Other characterisation tools used were multi-nuclear NMR, elemental analysis and melting point analysis.

The selection of complexes **40-43** serves to demonstrate the inherent difficulty in obtaining solid bis-ylides. Whilst no actual crystal structures could be determined, it is heartening to note that chemically pure solid samples of phosphonium bis-ylides have

¹² B. E. Douglas, C. E. Griffin and K. R. Martin, *J. Org. Chem.*, **27**, 1627 (1962).

been produced. Whether solvent choice could allow crystallisation or whether it is the instability of phosphonium bis-ylides in general remains to be seen.

As well as not being able to produce single crystals of the phosphonium bis-ylides none of the ylides could be co-ordinated to a metal centre in the desired way described at the start of this chapter. This may have been caused by the fact that most of the ylides synthesised, and used in subsequent reactions were the more unreactive benzylides.

7.5 Discussion of compounds 44-46 (see also 6.5).

Compound **44**, benzyldiphenylphosphonio ammonium bromide was produced by a three step process using methods adapted from previously reported iminophosphorane syntheses.¹³ This novel iminophosphorane salt was produced by first synthesising benzyldiphenylphosphine using chlorodiphenylphosphine and benzylmagnesium chloride in toluene. The next step involved bromination of the phosphine by refluxing with bromine. After isolation of the benzyldiphenylphosphorus dibromide, gaseous ammonia was passed through a solution of the dibromide. The salt was isolated by dissolving in chloroform, filtration to remove ammonium bromide and then full precipitation using diethyl ether. After drying *in vacuo* the salt was fully analysed using multi-nuclear NMR, elemental analysis and melting point analysis. The purpose of producing this salt was for use in the synthesis of dianions which can then be used in synthetic organic chemistry (see 6.5).

Compound **45**, methyldiphenyliminophosphorane was produced using methods adapted from previously reported iminophosphorane synthesis.^{13,14} Whilst this iminophosphorane has been previously reported and characterised,¹³ it has been produced here in a much improved yield and has been structurally characterised by single crystal X-ray diffraction studies for the first time. The first synthesis step involves refluxing the methyldiphenylphosphine with hexachloroethane to form the dichlorophosphine. The next step involves preparation of the amino salt, which is achieved by bubbling gaseous

¹³ R. Appel and H. Scholer, *Chem. Ber.*, **110**, 2382 (1977).

¹⁴ M. G. Davidson, A. E. Goeta, J. A. K. Howard, C. W. Lehmann, G. M. McIntyre and R. D. Price, *J. Organomet. Chem.*, **550**, 449 (1998).

ammonia through a solution of the dichlorophosphine. The final step involves deprotonation of the salt to give the iminophosphorane. All of the three steps proceed in a yield of around 80%, giving an overall yield of over 50% which is high for the production of a non-stabilised iminophosphorane.

Consideration of the molecular structure of the iminophosphorane **45** (Figure 7.16) gives the following structural information. The phosphonium centre is as expected pyramidalised [sum of angles = 339°] with $C_{\text{ipso}}\text{-P-N}$ bond angles of $108.2(2)$, $113.9(2)$ and $117.1(2)^\circ$ [$C1\text{-P1-N1}$, $C11\text{-P1-N1}$ & $C21\text{-P1-N1}$] respectively and $C_{\text{ipso}}\text{-P}$ bond lengths of $1.799(5)$, $1.811(5)$ and $1.801(4)\text{\AA}$ [$C1\text{-P1}$, $C11\text{-P1}$ & $C21\text{-P1}$ respectively] which along with a $\text{P-N}_{\text{iminic}}$ bond length of $1.561(4)\text{\AA}$ [P1-N1] compares well with previously studied iminophosphoranes,¹⁵ and also compares well with triphenyliminophosphorane.¹⁴ Allowing for the limitations of hydrogen atom positions determined by X-ray diffraction there is a P1-N1-H1 bond angle of $110.0(2)^\circ$ which is more acute than that seen in triphenyliminophosphorane [$115.0(2)^\circ$]¹⁴ and Ph_3PNPh [$130.4(3)^\circ$].¹⁵ This structural feature is most probably due to steric demands or may be indicative of the pyramidalisation of the iminic nitrogen similar to the phosphonium ylides already discussed.

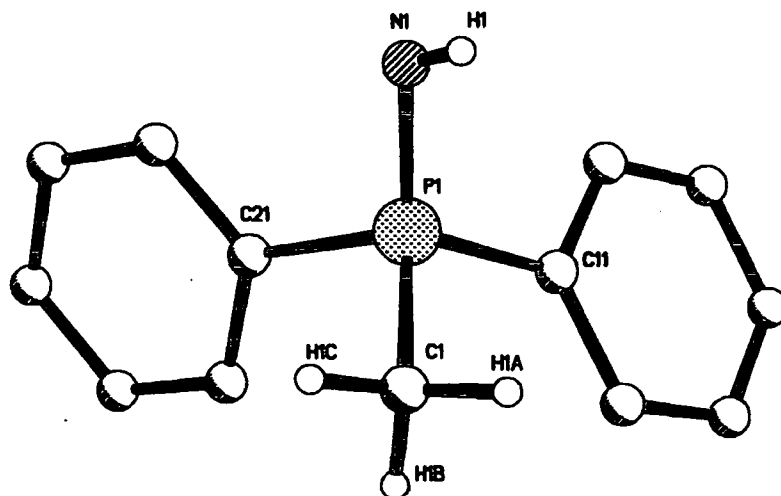


Figure 7.16 Single crystal X-ray structure of Ph_2MePNH . All hydrogen atoms, except the iminic hydrogen atom, omitted for clarity.

¹⁵ M. J. E. Hewlins, *J. Chem. Soc., B.*, 942 (1971); J. Beck, E. Bohm, K. Dehnicke, D. Fenske, W. Hiller, A. Maurier and J. Strahler, *Z. Naturforsch.*, **43B**, 138 (1998).

Compound **46**, ethyldiphenyl iminophosphorane was again produced by adapting methods previously reported^{13,16} to give an improved yield. Reaction of ethyldiphenyl phosphine with hexachloroethane was followed by reaction with hexamethyldisilylazane to give the salt and a silyl iminophosphorane, which were separated and the salt subsequently deprotonated to give the required iminophosphorane. Preliminary characterisation by NMR, elemental analysis and melting point analysis revealed that **46** was indeed the required iminophosphorane. Unfortunately no single crystals of **46** could be obtained and thus no XRD studies could be undertaken.

7.6 Discussion of complexes 47-50.

Complex **47** was produced by the reaction of triphenyliminophosphorane **III** with tetraphenyldithiodiphosphinylimide in toluene. The mixture was stirred at room temperature for 2 hours whereupon a white precipitate had formed. The mixture was heated to aid dissolution and then left to cool at room temperature whereupon crystals were obtained. Preliminary characterisation followed by single crystal X-ray diffraction studies revealed the structure of **47** (**Figure 7.17**) to be a complex of triphenyliminophosphorane and tetraphenyldithiodiphosphinylimide, in which the triphenyliminophosphorane is reprotonated to give a P(V) salt and thus the NPS ligand is deprotonated to give (NPS)⁻.

Considering first the reprotonated iminophosphorane there is a P1-N1 bond length of 1.636(3)Å which is noticeably longer than that in the starting iminophosphorane¹⁴ of 1.582(2)Å. This is consistent with the gain of a proton to give a formal single bond between the phosphorus and nitrogen atoms, and is thus longer than seen in the iminic 'double bond'. A look at the PPh₃ unit in the protonated iminophosphorane reveals C_{ipso}-P bond lengths of 1.790(3), 1.791(3) and 1.797(3)Å [C11-P1, C21-P1 & C31-P1 respectively] and also C_{ipso}-P-N_{iminic} bond angles of 106.47(15), 108.65(14) and 114.78(14)° [C11-P1-N1, C21-P1-N1 & C31-P1-N1 respectively]. These compare favourably with starting ligand ; C_{ipso}-P bond lengths of 1.810(3), 1.817(3) and 1.818(3)Å and C_{ipso}-P-N_{iminic} bond angles of 109.1(1), 114.6(1) and 115.6(1).¹⁴

¹⁶ R. Appel, *Chem. Ber.*, **98**, 1355 (1965).

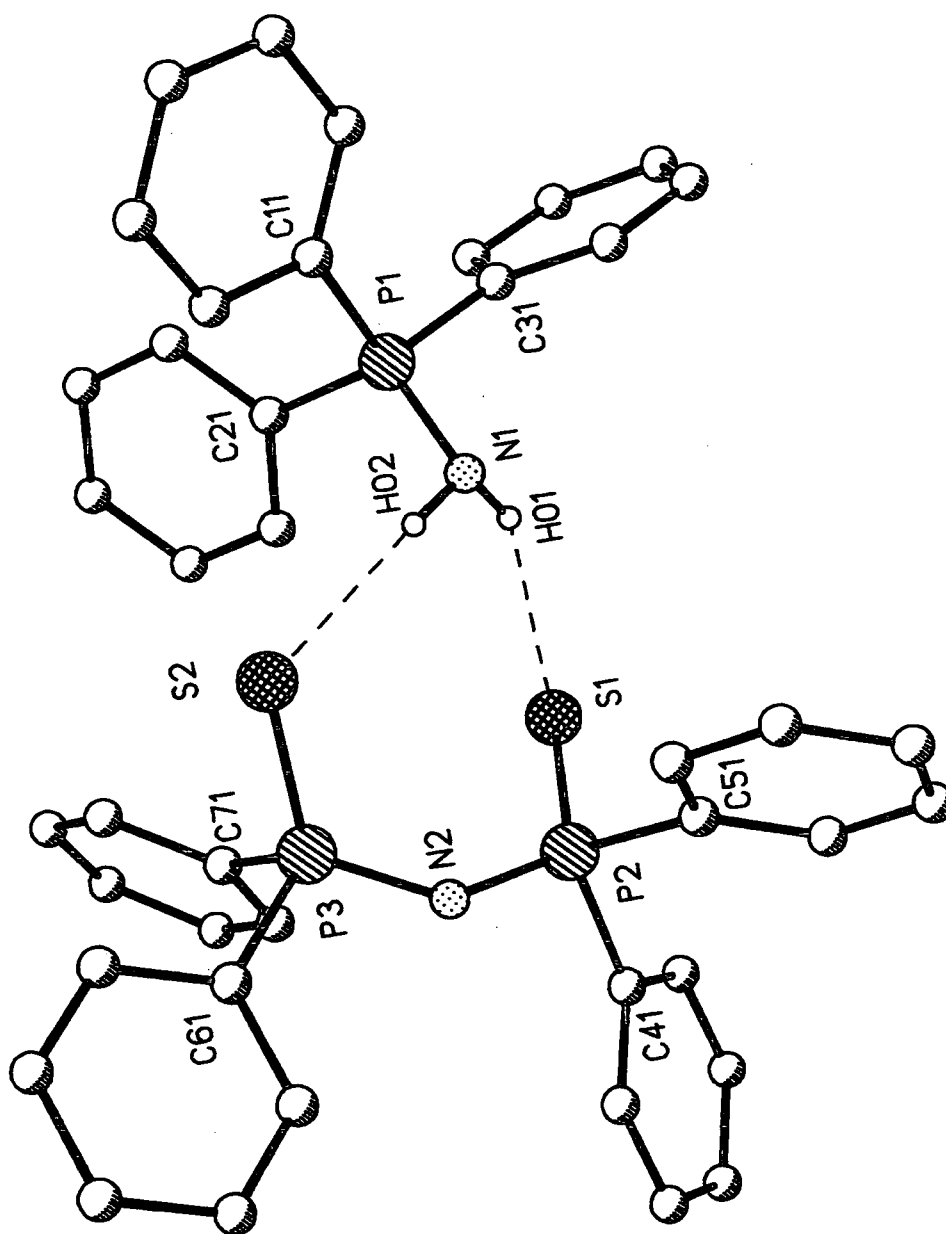


Figure 7.17 Single crystal X-ray structure of $\text{Ph}_3\text{PNH}_2^+ \cdot \text{N}[\text{PPh}_2(\text{S})]_2^-$. All hydrogen atoms, except H01 and H02, omitted for clarity.

Looking at the deprotonated tetraphenyldithiodiphosphinylimide ligand it can be seen that there is a P-S bond length of 1.9954 Å(ave.) [P2-S1 & P3-S2], a N-P bond length of 1.595 Å(ave.) [P2-N2 & P3-N2], a C_{ipso}-P bond length of 1.821 Å(ave.) and also P2-N2-P3 and N-P-S bond angles of 138.39(16)° and 120.99°(ave.) [N2-P2-S1 & N2-P3-S2] respectively.

Considering the interactions between the cation and the anion it can be seen that each N-H group acts as a H-bond donor to one P-S group. The N...S distances (N1-S1 and N1-S2) are 3.39(3) and 3.28(3) Å respectively, the H...S distances (H01-S1 & H02-S2) are 2.6(3) and 2.4(3) Å and the N-H-S angles are 152(3) and 172(3)° [N1-H01-S1 & N1-H02-S2 respectively].

Whilst there are many transition metal complexes of tetraphenyldithiodiphosphinylimide known,¹⁷ there are only a couple of structures published in the literature which do not contain transition metals. They are a bismuth complex,¹⁸ a selenium complex,¹⁹ a potassium complex,²⁰ an antimony complex,²¹ a barium complex²² and a thallium complex.²³ The most relevant however, is one example containing the deprotonated NPS ligand with an organic cation (Figure 7.18).²⁴

¹⁷ See for example ; (a). P. Bhattacharyya, A. M. Z. Slawin and M. B. Smith, *J. Chem. Soc., Dalton Trans.*, 2467 (1998). (b). I. Haiduc, M. Noltemeyer, H. W. Roesky, C. Silvestru and H.-G. Schmidt, *Polyhedron.*, **12**, 69 (1993). (c). S. Abram, U. Abram, J. R. Dilworth, A. Kirmse, E. S. Lang, J. Weemann and J. D. Woolins, *J. Chem. Soc., Dalton Trans.*, 623 (1997).

¹⁸ K. M. Barkigia, C. O. Quicksall and D. J. Williams, *Inorg. Chem.*, **21**, 2097 (1982).

¹⁹ S. Huseby and K. Maartmann-Moe, *Acta. Chem. Scand. Ser. A.*, **37**, 219 (1983).

²⁰ R. Cea-Olivares and H. Noth, *Z. Naturforsch., Teil B.*, **42**, 1507 (1987).

²¹ G. L. Abbati, M. Arca, A. Cornia, F. A. Devillanova, A. Garau, F. Isais, V. Lippolis and G. Verani, *Z. Anorg. Allg. Chem.*, **625**, 517 (1999).

²² G. Krauter, W. S. Rees Junior and S. K. Sunny, *Polyhedron.*, **17**, 391 (1998).

²³ J. S. Casas, A. Castineiras, I. Haiduc, A. Sanchez, J. Soroo and E. M. Vazquez-Lopez, *Polyhedron.*, **14**, 805 (1995).

²⁴ R. Cea-Olivares, I. Haiduc, S. Hernandez-Ortega and C. Silvestru, *Polyhedron.*, **14**, 2041 (1995).

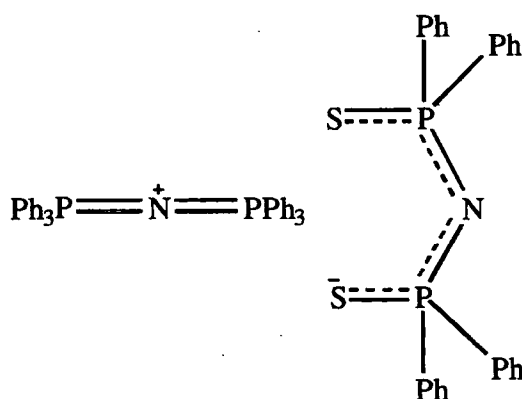


Figure 7.18 A bis(triphenyl)phosphine iminium tetraphenyldithiodiphosphinylimido complex

Whilst $\text{Ph}_3\text{P}=\text{N}=\text{PPh}_3$ is very similar to Ph_3PNH , the anions adopt remarkably differing geometries in the two structures. A comparison of the pertinent bond lengths and angles in **47** and the published salt (**Table 7.7**) reveals there to be a linear P-N-P backbone in the co-ordinated NPS ligand. Of the 100+ structures published containing this anion this is one of only a handful in which a linear backbone is seen.²⁵ Compound **47** does not show this linear backbone and its P-N-P angle of $138.39(16)^\circ$ falls into the range of values usually seen ($134\text{--}142^\circ$). Whilst 'crystal packing forces' of a vague nature could be invoked, it is plausible to attribute the differing conformations to the N-H...S bonding found in **47**. The PNP cation has no strong H-bond donor groups, therefore cation-anion H-bonds cannot influence the structure.

²⁵ (a). H. Homburg, H. Kuppers and W. Kalz, *Acta. Cryst.*, **C41**, 1420 (1985). (b). R. Bau and R. D. Wilson., *J. Am. Chem. Soc.*, **96**, 7601 (1994), (c). F. Calderazzo, G. Pampaloni and G. Pelizzi, *J. Organomet. Chem.*, **C41**, 233 (1982). (d). A. Laguna, M. Laguna, P. G. Jones, G. M. Sheldrick and R. Uson, *J. Chem. Soc., Dalton Trans.*, 366 (1981). (e). G. Longoni, M. Manassero and M. Samsoni, *J. Organomet. Chem.*, **C41**, 174 (1979).

	47	$\text{Ph}_3\text{P}=\text{N}=\text{PPh}_3^+ \text{SPh}_2\text{PNPPh}_2\text{S}^-$
P-S	1.9954Å(ave.)	1.975Å(ave.)
N-P	1.595Å(ave.)	— 1.554Å(ave.)
C _{ipso} -P	1.821Å(ave.)	1.820Å(ave.)
P-N-P	138.39(16)°	180°
N-P-S	120.99°(ave.)	117.4°(ave.)

Table 7.7 Comparison of bond lengths and angles in 47 and the salt.

A further search of the literature reveals a number of triarylaminophosphonium salts, for example, $[\text{Ph}_3\text{PNH}_2]^+[\text{Ph}_2\text{C}_6\text{H}_2\text{O}]^-$,²⁷ $[\text{Ph}_3\text{PNH}_2]_2^+[\text{CH}_2(2,6\text{-}^t\text{Bu}_2\text{-C}_6\text{H}_2\text{O})]^-$ ⁹ and triphenylphosphoranylidene ammonium azide $[\text{Ph}_3\text{PNH}_2]^+[\text{N}_3]^-$.²⁶ The structural parameters in the above examples are very similar to those found in 47.

Complex 48 was produced by the addition of triphenylphosphonium methyllide I with triphenylmethanol in toluene. The reaction mixture was heated to aid dissolution and upon standing for 24 hours at -30°C a crystalline material was obtained. Characterisation by NMR, elemental analysis and melting point analysis showed that complex 48 was a salt in which the proton from the methanol had transferred to the ylide to produce the phosphonium salt and a triphenylmethoxide anion. Unfortunately the crystalline material was unsuitable for X-ray analysis. However the structure of this complex is thought to be similar to that seen in analogous complexes such as $[\text{Ph}_3\text{PCH}_3^+\text{OC}_6\text{H}_5]^-$.⁹

Complex 49 was produced by the interaction of triphenyliminophosphorane III with triphenylmethanol in toluene. The reaction mixture was stirred for 1 hour and then heated to aid dissolution. After standing for 1 hour at room temperature needle-like crystals suitable for X-ray diffraction were obtained. The crystals were subjected to single crystal X-ray diffraction studies but failed to diffract. No structural information could thus be obtained but characterisation by multinuclear NMR, elemental analysis and melting point analysis showed that in an analogous fashion to 47 the phosphonium moiety had been reprotonated to give the salt along with the complementary methoxide anion. It can be

²⁶ (a). C. Bleasdale and W. Clegg, *Acta. Cryst., Sect. C (Cr. Str. Comm.)*, **C50**, 740 (1994). (b). T. T. Borek, E. N. Duesler, M. A. Hiskey, W. Koestle, R. T. Paine, E. A. Pruss and G. L. Wood, *Inorg. Chem.*, **38**, 3738 (1999).

assumed that the molecular structure of this complex is very similar to **49** and also that of analogous iminophosphorane complexes such as $[\text{Ph}_3\text{PNH}_2^+\text{Ph}_2\text{C}_6\text{H}_3\text{O}^-]$.²⁷

Complex **50** was produced by the addition of triphenylphosphine oxide **VI** to triphenylmethanol in toluene. After stirring for 2 hours a white precipitate had formed which was subsequently dissolved with heating to yield a crop of crystals suitable for X-ray analysis. Preliminary investigations followed by single crystal X-ray diffraction studies revealed the structure of **50** (Figure 7.19) to be the expected 1:1 dimer of triphenylphosphine oxide and triphenylmethanol. The structure is disordered with half a dimer per asymmetric crystal unit i.e. with only one molecular site which is half occupied by both triphenylmethanol and triphenylphosphine oxide. The two molecules interact via a O-H...O hydrogen bond of length 2.12(3) Å and with a O-H...O angle of 148.5(3)°. The closest approach of the two oxygen atoms is 2.86(5) Å.

Considering the phosphine oxide part of the complex, there is a P1A-O1A bond length of 1.370(4) Å, C_{ipso}-P bond lengths of 1.685(3), 1.703(3) and 1.749(3) Å [C11A-P1A, C21A-P1A & C31A-P1A] and C_{ipso}-P-O angles of 111.53(17), 113.12(18) and 116.38(18)° [C11A-P1A-O1A, C21A-P1A-O1A & C31A-P1A-O1A] respectively. The free phosphine oxide²⁸ has a P-O bond length of 1.494 Å (ave.), C_{ipso}-P bond lengths of 1.799(4), 1.803(3) and 1.808(3) Å and C_{ipso}-P-O angles of 111.57(5), 111.95(5) and 113.63(6)° respectively.

Looking more closely at the triphenylmethanol fragment of the complex it can be seen that there is a C1-O1 bond length of 1.624(5) Å, C_{ipso}-C bond lengths of 1.612(5), 1.628(15) and 1.641(16) Å [C11-C1, C21-C1 & C31-C1] as well as C_{ipso}-C-O bond angles of 104.3(9), 105.5(9) and 106.6(9)° [C11-C1-O1, C21-C1-O1 & C31-C1-O1 respectively]. A comparison of these with the structure of the major tetramer of free triphenylmethanol^{29,*} can be found in Table 7.8.

²⁷ R. D. Price, *Ph.D. Thesis*, University of Durham (1999) and references cited therein.

²⁸ C. P. Brock, J. D. Dunitz and W. B. Schweizer, *J. Am. Chem. Soc.*, **107**, 6964 (1985).

²⁹ G. Ferguson, J. F. Gallacher, C. Glidewell, J. N. Low and S. N. Scrimgeour, *Acta. Cryst., Sect C (Cr. Str. Comm.)*, **C48**, 1272 (1992).

* Molecule exists as H-bonded tetramers which are disordered over two orientations with occupancies of 0.71 and 0.29 respectively. The data for the major tetramer is given but because of the disorder and the relatively low percentage of observed data (24.1%) the accuracy of this structure is not high.

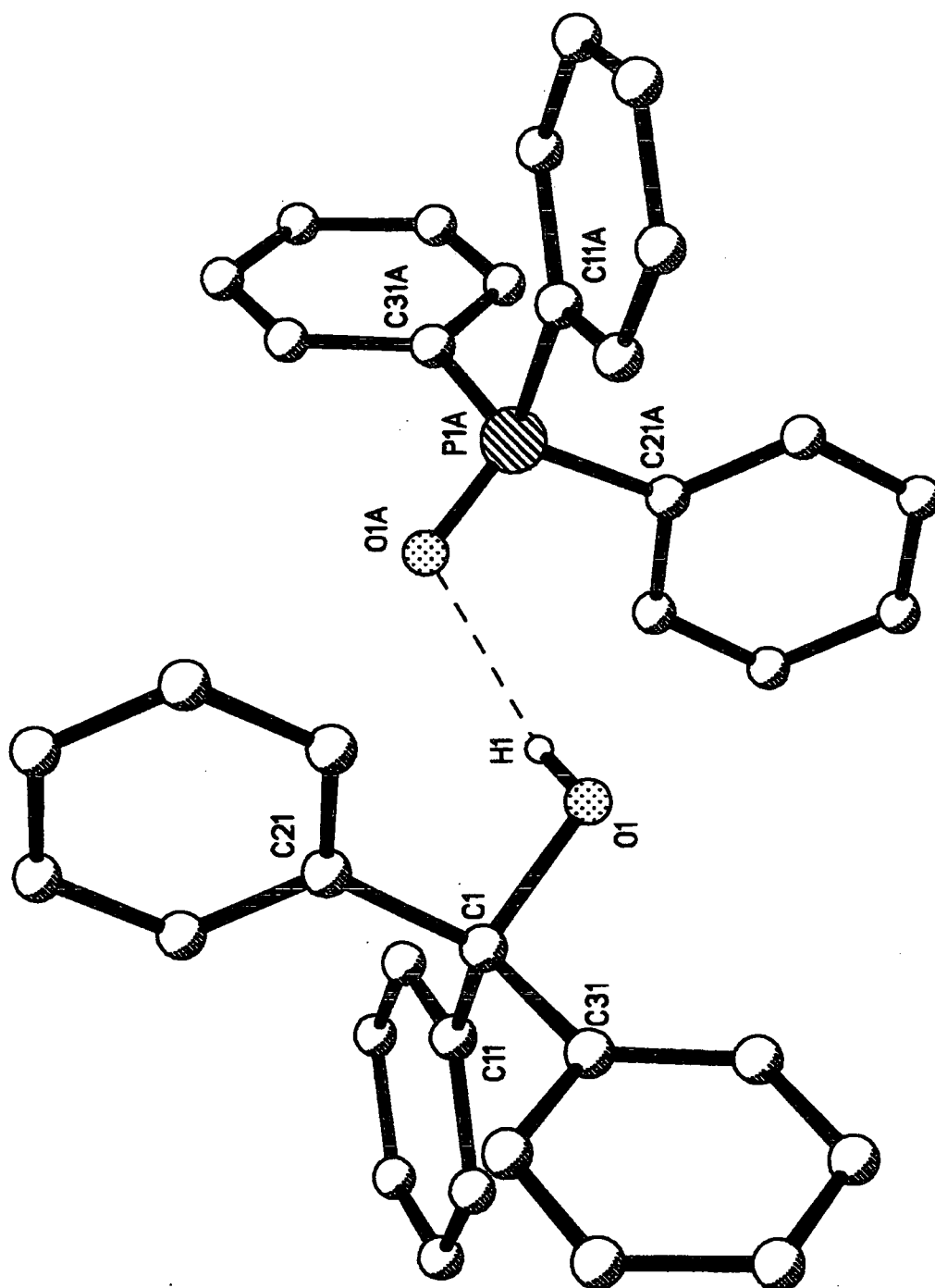


Figure 7.19 Single crystal X-ray structure of $\text{Ph}_3\text{CO} \cdot \text{HOPPh}_3$. All hydrogen atoms, except H1, omitted for clarity.

[C-O]Å	[C _{ipso} -C]Å	[C _{ipso} -C-O]Å
1.448(19) 1	1.514(7) 1	107.9(6) 1
1.434(11) 2	1.510(12) 2	109.1(8) 2
1.44(5) 3	1.509(14) 2	108.6(7) 2
1.49(3) 4	1.522(10) 2	107.3(7) 2
	1.40(2) 3	105.0(2) 3
	1.54(3) 4	108.0(2) 4
	1.53(4) 4	108.0(2) 4
	1.58(3) 4	106.0(2) 4

Table 7.8 Bond lengths and angles for free triphenylmethanol.²⁹ Numbers in bold indicate which particular molecule of the major tetramer that the data refers to.

Consideration of the above data shows that the bond lengths in the triphenylmethanol part of **50** are noticeably elongated upon co-ordination to the triphenylphosphine oxide.

The structure of this molecule has been published subsequent to our determination³⁰ and a comparison of the observed bond lengths and angles in the two structures shows there to be agreement within the geometry of the triphenylphosphine oxide and triphenylmethanol moieties, but there are discrepancies in the quoted hydrogen bond geometry (see **Table 7.9**)

	50	Steiner
O-H...O	148.5(3)°	161.0(6)°
H...O	2.12(3)Å	2.04(6)Å
O...O	2.86(5)Å	2.824(5)Å

Table 7.9 Comparison of hydrogen bonding in **50 and Steiner's complex.³⁰**

As can be seen from the table above the O-H...O angle is 12.5° narrower in **50** than it is in Steiner's complex.

³⁰ T. Steiner, *Acta. Cryst., Sect C(Cr. Str. Comm.)*, **C56**, 1033 (2000).

Considering the two unit cells it can be seen that Steiner's is notably different **Table 7.10**.

	Steiners complex ³⁰	50
[a]Å	10.3590(10)	8.5213(17)
[b]Å	12.693(2)	15.866(3)
[c]Å	10.102(7)	10.972(2)
[α]°	97.49(3)	90
[β]°	91.42(2)	101.91(4)
[γ]°	94.960(10)	90

Table 7.10 Comparison of cell parameters between Steiner's complex and 50.

This difference for the same chemical entity implies that they are two different polymorphs.

Searching the literature reveals other structurally characterised adducts in which triphenylphosphine oxide interacts with an alcohol group e.g. 4-(triphenylmethyl)phenol triphenylphosphine oxide,³¹ triphenylphosphine oxide pentafluorophenol³² and triphenylphosphine oxide 4-nitrophenol.³³

³¹ R. Boese, G. R. Desiraju, R. K. R. Jetti, A. Nangia, V. R. Thalladi and H.-C. Weiss, *Acta. Cryst., Sect C(Cr. Str. Comm.)*, **C55**, 1530 (1999).

³² T. Gramstad, S. Husebye and K. Maartmann-Moe, *Acta. Chem. Scand., Ser. B.*, **40**, 26 (1986).

³³ R. M. Fuguen and J. R. Lechat, *Acta. Cryst., Sect C(Cr. Str. Comm.)*, **C48**, 1690 (1992).

7.7 Conclusions.

- (1). Compounds **28-31** are examples of phosphonium methyllide and benzylide salts. **28, 30** and **31** are novel and have never before been published, whilst the single crystal X-ray diffraction study of **29** has been previously undertaken.³ Attempts to successfully deprotonate these compounds to give the corresponding phosphonium ylides resulted in the formation of compounds **34-37**.
- (2). Compounds **32** and **33** are examples of novel phosphonium bis-ylides salts. The solid state structure of **32** has been determined and shows some interesting features. The solid state structure of **33** was not determined as no crystals of the salt could be obtained. Attempts to deprotonate these compounds to give the corresponding phosphonium bis-ylides **40** and **42** were successful.
- (3). Compound **34** produced by the deprotonation of compound **28** is a novel phosphonium methyllide. Many attempts were made to try and crystallise this compound but to no avail, and thus no structural data could be obtained.
- (4). Compounds **35-39** are examples of novel benzylides, **35-38** being phosphonium benzylides and **39** being an arsonium benzylide. Compounds **35** and **36** are novel benzylides and have been structurally characterised using X-ray diffraction techniques. Compound **37** is a novel benzylide but unfortunately no crystals of this compound could be obtained. Compound **38** has been produced before and again crystallisation proved difficult. Compound **39** is the first structurally characterised arsonium benzylide and its similarities and differences with triphenylphosphonium benzylide are discussed in this chapter.
- (5). Compounds **40-43** are all examples of phosphonium bis-ylides. Compound **41** has been produced before in the solution state¹² but never before characterised in the solid state. Whilst none of these four compounds gave crystals suitable for X-ray diffraction it is heartening to be able to show that bis-ylides can be produced in the solid state with a view to using them as solid synthetic reagents.

- (6). Compound **44** is a novel iminophosphorane salt which has been used to produce di-anions (see **Chapter 6**), and has shown great potential as a useful reagent for organic chemistry.
- (7). Compounds **45** and **46** are iminophosphoranes which have been synthesised before. However, modifications to the synthesis have produced greater yields and the structure of methyldiphenyliminophosphorane **45** has been reported for the first time.
- (8). **47** is a novel and structurally interesting complex formed by the reaction of triphenyliminophosphorane and tetraphenyldithiodiphosphinylimide. It highlights the basicity of the iminic nitrogen (lone pair) in accepting a proton and also the acidity of the imidic hydrogen in relinquishing itself.
- (9). Complexes **48-50** were formed by reaction of triphenylmethanol with the isoelectronic series of compounds : triphenylphosphonium methylide, triphenyliminophosphorane and triphenylphosphine oxide. Crystals of **48** and **49** proved unsuitable for X-ray analysis, although the structure of **50** was obtained. It has recently been published³⁰ and shows some differences in comparison with our structural data.

Appendix A**Supplementary Crystallographic Data**

No used in text	Table number
1	A.1a/b
2	A.2a/b
3	A.3a/b
9	A.4a/b
10	A.5a/b
11	A.6a/b
19	A.7a/b
20	A.8a/b
21	A.9a/b
24	A.10a/b
28	A.11a/b
29	A.12a/b
30	A.13a/b
32	A.14a/b
35	A.15a/b
36	A.16a/b
39	A.17a/b
45	A.18a/b
47	A.19a/b
50	A.20a/b

Full electronic versions of cif files (labelled as in the above table) in ASCII format, are available on the CD accompanying this thesis.

Appendix A – Crystallographic Data

Table A.1a Crystal data and structure refinement for 1.

Identification code	1	
Empirical formula	C ₆₄ H ₈₆ Ca N ₂ P ₂ Si ₄	
Formula weight	1097.73	
Temperature	150(2) K	
Wavelength	0.71073 Å	
Crystal system	Monoclinic	
Space group	C2/c	
Unit cell dimensions	a = 30.598(6) Å	α = 90°.
	b = 12.393(3) Å	β = 129.03(3)°.
	c = 22.023(4) Å	γ = 90°.
Volume	6487.5(23) Å ³	
Z	4	
Density (calculated)	1.124 Mg/m ³	
Absorption coefficient	0.258 mm ⁻¹	
F(000)	2360	
Crystal size	0.5 x 0.1 x 0.1 mm ³	
Theta range for data collection	1.71 to 27.49°.	
Index ranges	-39 ≤ h ≤ 28, -16 ≤ k ≤ 15, -23 ≤ l ≤ 28	
Reflections collected	24039	
Independent reflections	7208 [R(int) = 0.0627]	
Refinement method	Full-matrix least-squares on F ²	
Data / restraints / parameters	7145 / 0 / 345	
Goodness-of-fit on F ²	1.198	
Final R indices [I > 2σ(I)]	R1 = 0.0610, wR2 = 0.0983	
R indices (all data)	R1 = 0.1154, wR2 = 0.1347	
Largest diff. peak and hole	0.333 and -0.330 e.Å ⁻³	

Appendix A – Crystallographic Data

Table A.1b Atomic coordinates ($\times 10^4$) and equivalent isotropic displacement parameters ($\text{\AA}^2 \times 10^3$) for 1. $U(\text{eq})$ is defined as one third of the trace of the orthogonalized U_{ij} tensor.

	x	y	z	U(eq)
Ca(1)	0	7908(1)	7500	20(1)
P(1)	-923(1)	10371(1)	6026(1)	21(1)
Si(1)	-683(1)	6853(1)	8269(1)	24(1)
N(1)	-99(1)	6971(2)	8340(2)	24(1)
C(1)	-729(1)	9513(3)	6771(2)	25(1)
Si(2)	511(1)	6319(1)	9038(1)	25(1)
C(11)	-1214(1)	11671(3)	5998(2)	24(1)
C(12)	-1674(1)	12143(3)	5316(2)	34(1)
C(13)	-1873(2)	13141(3)	5341(2)	43(1)
C(14)	-1612(2)	13672(3)	6036(3)	41(1)
C(16)	-951(2)	12211(3)	6700(2)	39(1)
C(21)	-1457(1)	9756(3)	5085(2)	25(1)
C(22)	-1883(2)	9152(3)	4981(2)	42(1)
C(23)	-2309(2)	8717(4)	4254(3)	57(1)
C(24)	-2313(2)	8875(4)	3634(3)	55(1)
C(25)	-1897(2)	9483(4)	3727(2)	47(1)
C(26)	-1466(2)	9925(3)	4452(2)	36(1)
C(31)	-331(1)	10716(3)	6063(2)	21(1)
C(32)	-172(1)	11784(3)	6104(2)	26(1)
C(33)	293(1)	12016(3)	6149(2)	31(1)
C(34)	591(1)	11194(3)	6139(2)	31(1)
C(35)	434(1)	10133(3)	6090(2)	33(1)
C(35)	-1147(2)	13211(3)	6713(3)	46(1)
C(36)	-23(1)	9881(3)	6057(2)	26(1)
C(41)	-1247(1)	7834(3)	7542(2)	29(1)
C(42)	-549(2)	7097(3)	9220(2)	38(1)
C(43)	-1043(2)	5497(3)	7926(2)	39(1)
C(44)	1030(1)	6524(3)	8855(2)	33(1)
C(45)	883(2)	6837(3)	10060(2)	40(1)
C(46)	445(2)	4816(3)	9071(3)	45(1)
C(51)	2685(2)	3014(4)	11948(2)	45(1)
C(52)	2145(2)	3346(4)	11613(2)	48(1)
C(53)	1959(2)	4360(4)	11295(3)	61(1)

Appendix A – Crystallographic Data

C(54)	2305(2)	5063(4)	11292(3)	61(1)
C(55)	2836(2)	4751(4)	11612(3)	55(1)
C(56)	3026(2)	3726(4)	11938(2)	47(1)
C(57)	2893(2)	1918(4)	12321(3)	84(2)

Appendix A – Crystallographic Data

Table A.2a Crystal data and structure refinement for **2**.

Identification code	2	
Empirical formula	C ₆₄ H ₈₆ N ₂ P ₂ Si ₄ Sr	
Formula weight	572.63	
Temperature	153(2) K	
Wavelength	0.71073 Å	
Crystal system	Monoclinic	
Space group	C2/c	
Unit cell dimensions	a = 30.612(5) Å	α = 90°.
	b = 12.435(2) Å	β = 129.028(6)°.
	c = 22.039(3) Å	γ = 90°.
Volume	6517.2(17) Å ³	
Z	8	
Density (calculated)	1.167 Mg/m ³	
Absorption coefficient	0.987 mm ⁻¹	
F(000)	2432	
Crystal size	0.3 x 0.3 x 0.3 mm ³	
Theta range for data collection	1.71 to 27.45°.	
Index ranges	-39 ≤ h ≤ 26, -15 ≤ k ≤ 16, -27 ≤ l ≤ 23	
Reflections collected	17240	
Independent reflections	7139 [R(int) = 0.0980]	
Refinement method	Full-matrix least-squares on F ²	
Data / restraints / parameters	7125 / 0 / 345	
Goodness-of-fit on F ²	0.984	
Final R indices [I > 2σ(I)]	R1 = 0.0549, wR2 = 0.1113	
R indices (all data)	R1 = 0.1251, wR2 = 0.1874	
Largest diff. peak and hole	0.678 and -0.728 e.Å ⁻³	

Appendix A – Crystallographic Data

Table A.2b Atomic coordinates ($\times 10^4$) and equivalent isotropic displacement parameters ($\text{\AA}^2 \times 10^3$) for 2. $U(\text{eq})$ is defined as one third of the trace of the orthogonalized U^{ij} tensor.

	x	y	z	U(eq)
Sr(1)	0	7922(1)	7500	24(1)
P(1)	939(1)	10430(1)	8996(1)	26(1)
Si(1)	-685(1)	6828(1)	8299(1)	27(1)
N(1)	-99(1)	6919(2)	8392(2)	25(1)
C(1)	455(2)	4787(3)	9101(3)	48(1)
Si(2)	517(1)	6289(1)	9080(1)	30(1)
C(2)	880(2)	6791(4)	10103(3)	48(1)
C(3)	1032(2)	6535(3)	8892(2)	32(1)
C(4)	-1045(2)	5482(3)	7955(3)	43(1)
C(5)	-1233(2)	7810(3)	7552(2)	32(1)
C(6)	-569(2)	7100(4)	9230(2)	42(1)
C(7)	746(2)	9591(4)	8264(3)	31(1)
C(8)	42(2)	9907(3)	8964(2)	33(1)
C(9)	-420(2)	10126(4)	8919(2)	36(1)
C(10)	-591(2)	11174(4)	8852(2)	37(1)
C(11)	-308(2)	12004(4)	8829(2)	36(1)
C(12)	165(2)	11792(3)	8894(2)	31(1)
C(13)	342(2)	10747(3)	8951(2)	23(1)
C(14)	1224(2)	11728(3)	9028(2)	31(1)
C(15)	1683(2)	12190(4)	9709(3)	36(1)
C(16)	1890(2)	13178(4)	9689(3)	51(1)
C(17)	1631(3)	13711(4)	8999(3)	57(2)
C(18)	1162(2)	13268(4)	8321(3)	53(1)
C(19)	965(2)	12284(4)	8329(3)	43(1)
C(20)	1469(2)	9807(3)	9928(2)	32(1)
C(21)	1880(2)	9182(4)	10023(3)	47(1)
C(22)	2308(2)	8729(5)	10743(3)	59(2)
C(23)	2313(2)	8888(4)	11364(3)	61(2)
C(24)	1911(2)	9506(4)	11284(3)	55(2)
C(25)	1486(2)	9965(4)	10565(2)	38(1)
C(26)	2090(3)	6941(5)	12687(4)	87(2)
C(27)	2292(2)	8030(4)	13040(3)	50(1)
C(28)	2834(2)	8360(4)	13373(3)	51(1)

Appendix A – Crystallographic Data

C(29)	3021(2)	9365(5)	13680(3)	61(2)
C(30)	2677(3)	10077(5)	13678(3)	63(2)
C(31)	2154(2)	9767(5)	13372(3)	56(2)
C(32)	1955(2)	8756(5)	13051(3)	50(1)

Appendix A – Crystallographic Data

Table A.3a Crystal data and structure refinement for **3**.

Identification code	3	
Empirical formula	C50 H70 N2 P2 Si4 Ba	—
Formula weight	1010.75	
Temperature	150(2) K	
Wavelength	0.71073 Å	
Crystal system	Monoclinic	
Space group	P2(1)/n	
Unit cell dimensions	a = 9.884(2) Å	$\alpha = 90^\circ$.
	b = 23.521(5) Å	$\beta = 98.91(3)^\circ$.
	c = 24.193(5) Å	$\gamma = 90^\circ$.
Volume	5556.3(19) Å ³	
Z	4	
Density (calculated)	1.206 Mg/m ³	
Absorption coefficient	0.890 mm ⁻¹	
F(000)	2096	
Crystal size	0.25 x 0.10 x 0.10 mm ³	
Theta range for data collection	1.21 to 27.49°.	
Index ranges	-12 ≤ h ≤ 12, -30 ≤ k ≤ 30, -31 ≤ l ≤ 31	
Reflections collected	60610	
Independent reflections	12724 [R(int) = 0.1973]	
Refinement method	Full-matrix least-squares on F ²	
Data / restraints / parameters	12685 / 0 / 560	
Goodness-of-fit on F ²	1.115	
Final R indices [I > 2σ(I)]	R1 = 0.0698, wR2 = 0.1222	
R indices (all data)	R1 = 0.1831, wR2 = 0.1860	
Largest diff. peak and hole	0.899 and -1.118 e.Å ⁻³	

Appendix A – Crystallographic Data

Table A.3b Atomic coordinates ($\times 10^4$) and equivalent isotropic displacement parameters ($\text{\AA}^2 \times 10^3$) for 3. $U(\text{eq})$ is defined as one third of the trace of the orthogonalized U^{ij} tensor.

	x	y	z	U(eq)
Ba(1)	-2622(1)	7367(1)	7630(1)	31(1)
P(1)	-2981(2)	6266(1)	9034(1)	34(1)
Si(1)	-5600(2)	8337(1)	7390(1)	48(1)
N(1)	-4329(6)	8093(2)	7072(2)	36(2)
C(1)	-2938(10)	6933(3)	8762(4)	42(2)
P(2)	-97(2)	8455(1)	8793(1)	33(1)
Si(2)	-3878(2)	8278(1)	6451(1)	42(1)
N(2)	-2041(6)	6519(2)	6992(2)	39(2)
C(2)	-680(9)	8296(4)	8111(3)	40(2)
Si(3)	-405(3)	6436(1)	6893(1)	49(1)
Si(4)	-3429(3)	6151(1)	6695(1)	49(1)
C(11)	-4231(7)	5830(3)	8608(3)	33(2)
C(12)	-3997(9)	5258(4)	8481(3)	48(2)
C(13)	-5008(10)	4946(4)	8158(3)	56(2)
C(14)	-6258(9)	5181(5)	7965(3)	60(3)
C(15)	-6494(9)	5744(5)	8087(4)	63(3)
C(16)	-5513(8)	6058(4)	8413(3)	49(2)
C(21)	-1351(7)	5917(3)	9063(3)	31(2)
C(22)	-538(7)	5784(3)	9576(3)	39(2)
C(23)	709(8)	5506(3)	9581(4)	47(2)
C(24)	1140(8)	5360(3)	9085(4)	49(2)
C(25)	349(8)	5500(3)	8577(4)	45(2)
C(26)	-873(7)	5783(3)	8562(3)	36(2)
C(31)	-3468(7)	6196(3)	9728(3)	36(2)
C(32)	-3655(7)	6688(3)	10025(3)	38(2)
C(33)	-4099(8)	6654(4)	10538(3)	48(2)
C(34)	-4399(8)	6139(4)	10756(3)	47(2)
C(35)	-4205(8)	5638(4)	10468(3)	52(2)
C(36)	-3733(8)	5670(3)	9958(3)	44(2)
C(41)	1044(7)	7908(3)	9107(3)	32(2)
C(42)	851(7)	7355(3)	8925(3)	43(2)
C(43)	1698(8)	6919(3)	9158(4)	50(2)
C(44)	2760(8)	7032(4)	9578(3)	51(2)

Appendix A – Crystallographic Data

C(45)	2971(10)	7591(4)	9778(4)	78(3)
C(46)	2114(10)	8016(4)	9535(4)	67(3)
C(51)	851(7)	9116(3)	8965(3)	32(2)
C(52)	832(8)	9412(3)	9458(3)	45(2)
C(53)	1646(9)	9891(4)	9578(4)	54(2)
C(54)	2459(10)	10082(4)	9210(4)	66(3)
C(55)	2485(11)	9784(4)	8722(4)	80(3)
C(56)	1686(9)	9305(4)	8599(4)	61(3)
C(61)	-1535(7)	8517(3)	9173(3)	35(2)
C(62)	-1536(9)	8244(3)	9684(3)	50(2)
C(63)	-2646(11)	8309(4)	9964(4)	68(3)
C(64)	-3714(10)	8646(5)	9756(4)	68(3)
C(65)	-3729(9)	8923(5)	9256(4)	75(3)
C(66)	-2638(9)	8861(4)	8969(4)	61(3)
C(71)	-7345(9)	8267(5)	6978(4)	93(4)
C(72)	-5413(12)	9117(4)	7596(4)	85(3)
C(73)	-5635(9)	7935(4)	8061(3)	62(3)
C(74)	-3832(13)	9067(4)	6315(5)	97(4)
C(75)	-4981(9)	7960(5)	5834(3)	71(3)
C(76)	-2113(8)	8015(4)	6414(3)	56(2)
C(81)	-16(10)	6670(5)	6188(4)	84(3)
C(82)	758(9)	6852(4)	7432(4)	67(3)
C(83)	239(11)	5679(4)	6934(4)	79(3)
C(84)	-3411(12)	5373(4)	6887(4)	86(3)
C(85)	-5023(9)	6460(4)	6918(4)	61(3)
C(86)	-3736(10)	6164(4)	5899(3)	71(3)

Appendix A – Crystallographic Data

Table A.4a Crystal data and structure refinement for **9**.

Identification code	9	
Empirical formula	C ₆₆ H ₇₈ Ca N ₂ O ₂ P ₂	
Formula weight	1033.32	
Temperature	150(2) K	
Wavelength	0.71073 Å	
Crystal system	Orthorhombic	
Space group	Pca2(1)	
Unit cell dimensions	a = 25.644(5) Å	α = 90°.
	b = 11.540(2) Å	β = 90°.
	c = 19.818(4) Å	γ = 90°.
Volume	5864.9(20) Å ³	
Z	4	
Density (calculated)	1.170 Mg/m ³	
Absorption coefficient	0.206 mm ⁻¹	
F(000)	2216	
Crystal size	0.30 x 0.15 x 0.10 mm ³	
Theta range for data collection	1.59 to 27.49°.	
Index ranges	-33 ≤ h ≤ 33, -14 ≤ k ≤ 14, -25 ≤ l ≤ 25	
Reflections collected	66148	
Independent reflections	13450 [R(int) = 0.1182]	
Refinement method	Full-matrix least-squares on F ²	
Data / restraints / parameters	13428 / 1 / 672	
Goodness-of-fit on F ²	1.161	
Final R indices [I > 2σ(I)]	R1 = 0.0579, wR2 = 0.0955	
R indices (all data)	R1 = 0.1086, wR2 = 0.1186	
Absolute structure parameter	0.00(4)	
Largest diff. peak and hole	0.286 and -0.338 e.Å ⁻³	

Appendix A – Crystallographic Data

Table A.4b Atomic coordinates ($\times 10^4$) and equivalent isotropic displacement parameters ($\text{\AA}^2 \times 10^3$) for **9**. $U(\text{eq})$ is defined as one third of the trace of the orthogonalized U^{ij} tensor.

	x	y	z	U(eq)
Ca(1)	3844(1)	9210(1)	505(1)	19(1)
P(1)	3698(1)	10984(1)	2135(1)	23(1)
O(1)	3147(1)	8375(2)	140(1)	23(1)
N(1)	3576(1)	10328(3)	1453(2)	27(1)
P(2)	3990(1)	11737(1)	-713(1)	22(1)
O(2)	4480(1)	8070(2)	721(1)	24(1)
N(2)	4158(1)	10657(3)	-266(1)	27(1)
C(11)	3699(2)	10084(3)	2891(2)	30(1)
C(12)	4162(2)	9542(3)	3085(2)	36(1)
C(13)	4169(2)	8789(4)	3634(2)	46(1)
C(14)	3714(2)	8575(4)	3987(2)	56(1)
C(15)	3251(2)	9081(4)	3787(2)	55(1)
C(16)	3239(2)	9828(4)	3234(2)	41(1)
C(21)	3258(1)	12190(3)	2291(2)	26(1)
C(22)	3134(1)	12601(4)	2934(2)	34(1)
C(23)	2802(2)	13541(4)	3001(2)	42(1)
C(24)	2599(2)	14088(4)	2435(2)	40(1)
C(25)	2728(2)	13703(4)	1799(2)	39(1)
C(26)	3050(2)	12751(4)	1723(2)	33(1)
C(31)	4349(1)	11588(3)	2094(2)	22(1)
C(32)	4568(1)	12101(3)	2662(2)	29(1)
C(33)	5068(1)	12542(3)	2644(2)	33(1)
C(34)	5351(1)	12498(3)	2053(2)	32(1)
C(35)	5129(2)	12032(4)	1476(2)	38(1)
C(36)	4629(1)	11576(3)	1493(2)	31(1)
C(41)	4441(1)	12947(3)	-702(2)	27(1)
C(42)	4652(2)	13269(4)	-89(2)	48(1)
C(43)	4983(2)	14241(5)	-47(3)	62(2)
C(44)	5097(2)	14847(4)	-617(3)	53(1)
C(45)	4893(2)	14532(4)	-1226(3)	63(2)
C(46)	4561(2)	13588(4)	-1274(2)	42(1)
C(51)	3375(1)	12290(3)	-405(2)	23(1)
C(52)	2956(1)	11528(4)	-339(2)	34(1)

Appendix A – Crystallographic Data

C(53)	2472(2)	11939(4)	-143(2)	41(1)
C(54)	2404(2)	13110(4)	0(2)	38(1)
C(55)	2818(2)	13870(4)	-53(2)	36(1)
C(56)	3304(1)	13454(3)	-258(2)	28(1)
C(61)	3889(1)	11434(3)	-1599(2)	24(1)
C(62)	3458(2)	11806(4)	-1952(2)	41(1)
C(63)	3406(2)	11594(4)	-2642(2)	51(1)
C(64)	3795(2)	11016(4)	-2978(2)	48(1)
C(65)	4225(2)	10611(5)	-2628(2)	53(1)
C(66)	4271(2)	10819(4)	-1945(2)	44(1)
C(70)	2771(1)	7656(3)	-55(2)	21(1)
C(71)	2318(1)	7488(3)	362(2)	23(1)
C(72)	1931(1)	6724(3)	140(2)	27(1)
C(73)	1948(1)	6159(3)	-479(2)	28(1)
C(74)	2386(1)	6352(3)	-879(2)	26(1)
C(75)	2802(1)	7063(3)	-690(2)	22(1)
C(76)	1503(1)	5409(3)	-713(3)	42(1)
C(77)	2252(1)	8142(3)	1034(2)	26(1)
C(78)	3274(1)	7210(3)	-1159(2)	24(1)
C(80)	4869(1)	7370(3)	889(2)	22(1)
C(81)	4792(1)	6431(3)	1358(2)	26(1)
C(82)	5227(1)	5809(3)	1577(2)	32(1)
C(83)	5729(1)	6019(3)	1342(2)	31(1)
C(84)	5787(1)	6853(3)	851(2)	30(1)
C(85)	5376(1)	7525(3)	603(2)	23(1)
C(86)	6193(2)	5367(4)	1626(3)	51(1)
C(87)	4242(1)	6126(3)	1624(2)	29(1)
C(88)	5477(1)	8453(3)	59(2)	25(1)
C(771)	2682(2)	7789(4)	1536(2)	35(1)
C(772)	1726(2)	7894(4)	1381(2)	37(1)
C(773)	2259(1)	9461(3)	900(2)	31(1)
C(781)	3228(2)	6482(4)	-1802(2)	37(1)
C(782)	3322(2)	8487(3)	-1391(2)	35(1)
C(783)	3776(1)	6809(3)	-808(2)	32(1)
C(871)	4238(2)	4997(4)	2048(2)	45(1)
C(872)	4046(2)	7103(4)	2085(2)	40(1)
C(873)	3862(1)	5910(3)	1038(2)	34(1)
C(881)	5401(1)	9676(3)	361(2)	30(1)

Appendix A – Crystallographic Data

C(882)	5106(1)	8278(3)	-546(2)	30(1)
C(883)	6035(1)	8401(4)	-227(2)	39(1)

Appendix A – Crystallographic Data

Table A.5a Crystal data and structure refinement for 10.

Identification code	10	
Empirical formula	C66 H78 N2 O2 P2 S ₁₂	
Formula weight	1080.86	
Temperature	150(2) K	
Wavelength	0.71073 Å	
Crystal system	Orthorhombic	
Space group	Pca2(1)	
Unit cell dimensions	a = 25.692(5) Å	α = 90°.
	b = 11.696(2) Å	β = 90°.
	c = 19.927(4) Å	γ = 90°.
Volume	5987.9(21) Å ³	
Z	4	
Density (calculated)	1.199 Mg/m ³	
Absorption coefficient	0.997 mm ⁻¹	
F(000)	2288	
Crystal size	0.35 x 0.25 x 0.20 mm ³	
Theta range for data collection	1.59 to 27.49°.	
Index ranges	-33 ≤ h ≤ 33, -15 ≤ k ≤ 15, -25 ≤ l ≤ 25	
Reflections collected	66948	
Independent reflections	13720 [R(int) = 0.0955]	
Refinement method	Full-matrix least-squares on F ²	
Data / restraints / parameters	13659 / 1 / 672	
Goodness-of-fit on F ²	1.180	
Final R indices [I > 2σ(I)]	R1 = 0.0535, wR2 = 0.0869	
R indices (all data)	R1 = 0.0865, wR2 = 0.1052	
Absolute structure parameter	-0.012(5)	
Largest diff. peak and hole	0.331 and -0.312 e.Å ⁻³	

Appendix A – Crystallographic Data

Table A.5b Atomic coordinates ($\times 10^4$) and equivalent isotropic displacement parameters ($\text{\AA}^2 \times 10^3$) for **10**. $U(\text{eq})$ is defined as one third of the trace of the orthogonalized U^{ij} tensor.

	x	y	z	U(eq)
Sr(1)	-1143(1)	-5752(1)	6853(1)	23(1)
P(1)	-986(1)	-3159(1)	8089(1)	25(1)
C(1)	-2703(1)	-7517(3)	7004(2)	26(1)
N(1)	-807(1)	-4231(3)	7660(2)	33(1)
O(1)	-480(1)	-6969(2)	6607(1)	28(1)
P(2)	-1311(1)	-3942(1)	5185(1)	30(1)
O(2)	-1882(1)	-6618(2)	7240(1)	26(1)
N(2)	-1443(1)	-4587(3)	5864(2)	35(1)
C(11)	-1098(2)	-3441(4)	8973(2)	32(1)
C(12)	-1538(2)	-3102(5)	9303(2)	49(1)
C(13)	-1605(2)	-3343(5)	9986(3)	60(2)
C(14)	-1230(2)	-3903(5)	10329(2)	55(1)
C(15)	-793(3)	-4287(7)	9997(3)	88(2)
C(16)	-730(2)	-4058(6)	9319(3)	70(2)
C(21)	-545(2)	-1960(3)	8070(2)	32(1)
C(22)	-434(2)	-1275(4)	8617(3)	51(1)
C(23)	-109(2)	-348(5)	8567(4)	75(2)
C(24)	104(2)	-82(5)	7954(4)	71(2)
C(25)	-1(2)	-714(6)	7400(4)	76(2)
C(26)	-323(2)	-1669(5)	7455(3)	60(2)
C(31)	-1598(2)	-2642(3)	7763(2)	26(1)
C(32)	-1680(2)	-1499(4)	7613(2)	32(1)
C(33)	-2165(2)	-1106(4)	7402(2)	39(1)
C(34)	-2566(2)	-1876(4)	7327(2)	43(1)
C(35)	-2492(2)	-3024(4)	7465(2)	43(1)
C(36)	-2008(2)	-3409(4)	7679(2)	33(1)
C(41)	-1313(2)	-4845(4)	4436(2)	40(1)
C(42)	-859(2)	-5407(4)	4253(2)	47(1)
C(43)	-862(3)	-6173(5)	3713(3)	64(2)
C(44)	-1318(3)	-6368(5)	3366(3)	81(2)
C(45)	-1771(3)	-5840(6)	3559(3)	79(2)
C(46)	-1774(2)	-5066(5)	4100(2)	58(2)
C(51)	-1740(2)	-2744(4)	5031(2)	33(1)

Appendix A – Crystallographic Data

C(52)	-1868(2)	-2328(4)	4393(2)	41(1)
C(53)	-2198(2)	-1401(5)	4328(3)	51(1)
C(54)	-2389(2)	-854(5)	4896(3)	52(1)
C(55)	-2253(2)	-1235(4)	5523(3)	49(1)
C(56)	-1933(2)	-2175(4)	5596(2)	40(1)
C(61)	-655(2)	-3383(3)	5232(2)	26(1)
C(62)	-384(2)	-3389(4)	5835(2)	38(1)
C(63)	122(2)	-2974(4)	5857(3)	46(1)
C(64)	357(2)	-2538(4)	5284(2)	38(1)
C(65)	79(2)	-2496(4)	4688(2)	38(1)
C(66)	-424(2)	-2903(4)	4667(2)	34(1)
C(70)	-94(2)	-7667(3)	6445(2)	25(1)
C(71)	412(2)	-7504(3)	6729(2)	26(1)
C(72)	822(2)	-8183(4)	6499(2)	34(1)
C(73)	760(2)	-9009(4)	6010(2)	35(1)
C(74)	260(2)	-9209(4)	5766(2)	33(1)
C(75)	-173(2)	-8587(3)	5973(2)	29(1)
C(76)	1229(2)	-9666(4)	5741(3)	55(2)
C(77)	-719(2)	-8876(4)	5711(2)	34(1)
C(78)	506(2)	-6577(3)	7269(2)	29(1)
C(80)	-2254(2)	-7334(3)	7423(2)	24(1)
C(81)	-2225(1)	-7933(3)	8051(2)	24(1)
C(82)	-2633(2)	-8649(3)	8232(2)	28(1)
C(83)	-3068(2)	-8841(3)	7827(2)	32(1)
C(84)	-3086(2)	-8280(3)	7219(2)	29(1)
C(86)	-3508(2)	-9608(4)	8054(3)	47(1)
C(87)	-1748(2)	-7772(3)	8521(2)	28(1)
C(88)	-2762(2)	-6864(4)	6335(2)	29(1)
C(771)	-730(2)	-9976(4)	5281(3)	55(1)
C(772)	-917(2)	-7894(5)	5262(2)	50(1)
C(773)	-1098(2)	-9090(4)	6296(2)	42(1)
C(781)	131(2)	-6742(4)	7865(2)	35(1)
C(782)	1063(2)	-6603(4)	7547(3)	44(1)
C(783)	425(2)	-5374(3)	6963(2)	33(1)
C(871)	-1704(2)	-6514(4)	8751(2)	40(1)
C(872)	-1790(2)	-8506(4)	9160(2)	41(1)
C(873)	-1252(2)	-8149(4)	8163(2)	35(1)
C(881)	-3283(2)	-7119(4)	5986(2)	41(1)

Appendix A – Crystallographic Data

C(882)	-2756(2)	-5559(3)	6472(2)	34(1)
C(883)	-2327(2)	-7211(4)	5845(2)	39(1)

Appendix A – Crystallographic Data

Table A.6a Crystal data and structure refinement for **11**.

Identification code	11	
Empirical formula	C ₆₆ H ₇₈ Ba N ₂ O ₂ P ₂	
Formula weight	1130.58	
Temperature	150(2) K	
Wavelength	0.71073 Å	
Crystal system	Triclinic	
Space group	P-1	
Unit cell dimensions	a = 12.600(3) Å	α = 80.26(3)°.
	b = 14.888(3) Å	β = 71.04(3)°.
	c = 18.656(4) Å	γ = 69.53(3)°.
Volume	3094.8(11) Å ³	
Z	2	
Density (calculated)	1.213 Mg/m ³	
Absorption coefficient	0.736 mm ⁻¹	
F(000)	1180	
Crystal size	0.50 x 0.30 x 0.10 mm ³	
Theta range for data collection	1.16 to 27.48°.	
Index ranges	-12 ≤ h ≤ 16, -18 ≤ k ≤ 19, -23 ≤ l ≤ 24	
Reflections collected	22792	
Independent reflections	14074 [R(int) = 0.0310]	
Refinement method	Full-matrix least-squares on F ²	
Data / restraints / parameters	14039 / 0 / 672	
Goodness-of-fit on F ²	1.060	
Final R indices [I > 2σ(I)]	R1 = 0.0353, wR2 = 0.0715	
R indices (all data)	R1 = 0.0494, wR2 = 0.0823	
Largest diff. peak and hole	0.535 and -0.381 e.Å ⁻³	

Appendix A – Crystallographic Data

Table A.6b Atomic coordinates ($\times 10^4$) and equivalent isotropic displacement parameters ($\text{\AA}^2 \times 10^3$) for 11. U(eq) is defined as one third of the trace of the orthogonalized U^{ij} tensor.

	x	y	z	U(eq)
Ba(1)	6686(1)	2436(1)	2575(1)	25(1)
P(1)	7869(1)	2368(1)	4344(1)	29(1)
O(1)	4828(1)	3750(1)	2722(1)	28(1)
N(1)	7402(2)	1909(2)	3853(1)	39(1)
P(2)	10114(1)	2330(1)	1342(1)	33(1)
O(2)	6493(2)	972(1)	2312(1)	29(1)
N(2)	8835(2)	2708(2)	1918(1)	45(1)
C(11)	9358(2)	1720(2)	4396(2)	34(1)
C(12)	10092(3)	1048(3)	3873(2)	71(1)
C(13)	11257(4)	565(4)	3885(3)	103(2)
C(14)	11678(3)	757(3)	4405(3)	83(1)
C(15)	10958(3)	1412(3)	4933(2)	64(1)
C(16)	9794(3)	1893(2)	4936(2)	49(1)
C(21)	7886(2)	3553(2)	3922(2)	33(1)
C(22)	6822(3)	4250(2)	3890(2)	49(1)
C(23)	6809(4)	5164(2)	3557(2)	64(1)
C(24)	7849(4)	5379(2)	3260(2)	61(1)
C(25)	8907(3)	4699(2)	3294(2)	60(1)
C(26)	8927(3)	3788(2)	3622(2)	45(1)
C(31)	6992(2)	2513(2)	5323(1)	30(1)
C(32)	6907(2)	3248(2)	5734(2)	39(1)
C(33)	6309(3)	3278(2)	6502(2)	45(1)
C(34)	5800(3)	2574(2)	6866(2)	45(1)
C(35)	5868(3)	1845(2)	6462(2)	43(1)
C(36)	6449(2)	1825(2)	5692(2)	37(1)
C(41)	10964(2)	3143(2)	1185(2)	37(1)
C(42)	11106(3)	3743(2)	531(2)	46(1)
C(43)	11648(3)	4443(2)	462(2)	60(1)
C(44)	12041(3)	4528(2)	1050(2)	60(1)
C(45)	11912(3)	3936(2)	1698(2)	56(1)
C(46)	11378(3)	3239(2)	1770(2)	48(1)
C(51)	11026(2)	1154(2)	1609(2)	35(1)
C(52)	12240(3)	906(2)	1481(2)	44(1)

Appendix A – Crystallographic Data

C(53)	12893(3)	-10(2)	1684(2)	54(1)
C(54)	12339(3)	-689(3)	2015(2)	60(1)
C(55)	11131(3)	-460(3)	2137(2)	68(1)
C(56)	10477(3)	462(2)	1940(2)	54(1)
C(61)	9962(2)	2178(2)	447(2)	33(1)
C(62)	9010(3)	2825(2)	209(2)	49(1)
C(63)	8888(3)	2732(3)	-486(2)	65(1)
C(64)	9699(3)	2001(3)	-939(2)	63(1)
C(65)	10639(3)	1366(3)	-712(2)	55(1)
C(66)	10766(3)	1459(2)	-24(2)	43(1)
C(70)	3827(2)	4463(2)	2768(1)	24(1)
C(71)	2808(2)	4493(2)	3409(1)	26(1)
C(72)	1767(2)	5253(2)	3434(2)	33(1)
C(73)	1670(2)	5987(2)	2864(2)	35(1)
C(74)	2664(2)	5956(2)	2250(1)	29(1)
C(75)	3744(2)	5226(2)	2182(1)	24(1)
C(76)	511(3)	6800(2)	2931(2)	58(1)
C(77)	2859(2)	3698(2)	4062(2)	33(1)
C(78)	4844(2)	5249(2)	1509(1)	26(1)
C(80)	6454(2)	189(2)	2084(1)	25(1)
C(81)	6686(2)	-704(2)	2530(1)	26(1)
C(82)	6745(2)	-1529(2)	2234(2)	33(1)
C(83)	6549(2)	-1518(2)	1544(2)	35(1)
C(84)	6251(2)	-637(2)	1140(2)	33(1)
C(85)	6186(2)	218(2)	1392(1)	28(1)
C(86)	6688(3)	-2434(2)	1218(2)	56(1)
C(87)	6896(2)	-748(2)	3305(2)	32(1)
C(88)	5840(3)	1180(2)	926(2)	36(1)
C(771)	3809(3)	3654(2)	4426(2)	43(1)
C(772)	3126(3)	2717(2)	3756(2)	43(1)
C(773)	1675(3)	3882(2)	4697(2)	50(1)
C(781)	5862(2)	5251(2)	1800(2)	30(1)
C(782)	4598(2)	6157(2)	971(2)	36(1)
C(783)	5263(2)	4374(2)	1034(2)	34(1)
C(871)	7061(3)	-1755(2)	3720(2)	47(1)
C(872)	5830(3)	-42(2)	3834(2)	43(1)
C(873)	8034(3)	-501(2)	3188(2)	43(1)
C(881)	5496(3)	1072(2)	229(2)	57(1)

Appendix A – Crystallographic Data

C(882)	6892(3)	1576(2)	616(2)	43(1)
C(883)	4755(3)	1913(2)	1415(2)	42(1)

Appendix A – Crystallographic Data

Table A.7a Crystal data and structure refinement for 19.

Identification code	19	
Empirical formula	C ₆₆ H ₇₆ Ca O ₄ P ₂	
Formula weight	1035.29	
Temperature	170(2) K	
Wavelength	0.71073 Å	
Crystal system	Monoclinic	
Space group	P2(1)/c	
Unit cell dimensions	a = 18.6994(4) Å	α = 90°.
	b = 15.7878(3) Å	β = 106.6970(10)°.
	c = 21.0082(3) Å	γ = 90°.
Volume	5940.59(19) Å ³	
Z	4	
Density (calculated)	1.158 Mg/m ³	
Absorption coefficient	0.205 mm ⁻¹	
F(000)	2216	
Crystal size	0.50 x 0.25 x 0.20 mm ³	
Theta range for data collection	3.51 to 27.49°.	
Index ranges	-24 ≤ h ≤ 24, -20 ≤ k ≤ 20, -26 ≤ l ≤ 26	
Reflections collected	55228	
Independent reflections	13548 [R(int) = 0.0516]	
Completeness to theta = 27.49°	99.4 %	
Max. and min. transmission	0.9601 and 0.9044	
Refinement method	Full-matrix least-squares on F ²	
Data / restraints / parameters	13548 / 0 / 673	
Goodness-of-fit on F ²	1.028	
Final R indices [I > 2σ(I)]	R1 = 0.0439, wR2 = 0.1047	
R indices (all data)	R1 = 0.0598, wR2 = 0.1135	
Extinction coefficient	0.0000(3)	
Largest diff. peak and hole	0.412 and -0.359 e.Å ⁻³	

Appendix A – Crystallographic Data

Table A.7b Atomic coordinates ($\times 10^4$) and equivalent isotropic displacement parameters ($\text{\AA}^2 \times 10^3$) for 19. U(eq) is defined as one third of the trace of the orthogonalized U^{ij} tensor.

	x	y	z	U(eq)
Ca(1)	2626(1)	6237(1)	3030(1)	22(1)
P(1)	4127(1)	5603(1)	2311(1)	28(1)
O(1)	3619(1)	5715(1)	2742(1)	33(1)
C(1)	2256(1)	4938(1)	4235(1)	26(1)
P(2)	1198(1)	5602(1)	1451(1)	28(1)
O(2)	1789(1)	5954(1)	2035(1)	33(1)
C(2)	2727(1)	4231(1)	4501(1)	27(1)
O(3)	2402(1)	5433(1)	3777(1)	28(1)
C(3)	2548(1)	3724(1)	4977(1)	33(1)
O(4)	2740(1)	7591(1)	3135(1)	28(1)
C(4)	1947(1)	3877(1)	5220(1)	39(1)
C(5)	1498(1)	4565(1)	4961(1)	38(1)
C(6)	1630(1)	5097(1)	4476(1)	30(1)
C(7)	1808(1)	3342(2)	5771(1)	58(1)
C(8)	3422(1)	4044(1)	4277(1)	37(1)
C(9)	3867(1)	3280(2)	4641(1)	54(1)
C(10)	3958(1)	4804(2)	4415(1)	50(1)
C(11)	3186(2)	3829(2)	3531(1)	63(1)
C(12)	1123(1)	5865(1)	4226(1)	35(1)
C(13)	473(1)	5916(2)	4538(1)	54(1)
C(14)	1584(1)	6677(1)	4418(1)	42(1)
C(15)	770(1)	5813(1)	3472(1)	42(1)
C(21)	2804(1)	8416(1)	3244(1)	24(1)
C(22)	2238(1)	8988(1)	2882(1)	26(1)
C(23)	2327(1)	9851(1)	3014(1)	32(1)
C(24)	2945(1)	10193(1)	3477(1)	35(1)
C(25)	3492(1)	9635(1)	3821(1)	32(1)
C(26)	3447(1)	8762(1)	3721(1)	27(1)
C(27)	3024(1)	11138(1)	3596(1)	54(1)
C(28)	1548(1)	8660(1)	2345(1)	33(1)
C(29)	1797(1)	8233(1)	1785(1)	39(1)
C(30)	1105(1)	8037(1)	2647(1)	46(1)
C(31)	1009(1)	9374(1)	2021(1)	57(1)

Appendix A – Crystallographic Data

C(32)	4090(1)	8183(1)	4106(1)	33(1)
C(33)	4725(1)	8685(1)	4592(1)	50(1)
C(34)	4437(1)	7732(1)	3617(1)	40(1)
C(35)	3814(1)	7535(1)	4527(1)	45(1)
C(111)	3777(1)	4837(1)	1662(1)	35(1)
C(112)	3643(1)	5030(1)	996(1)	42(1)
C(113)	3367(1)	4421(1)	512(1)	50(1)
C(114)	3223(1)	3631(2)	691(1)	62(1)
C(115)	3382(2)	3412(2)	1348(1)	90(1)
C(116)	3654(2)	4024(2)	1836(1)	76(1)
C(121)	4246(1)	6580(1)	1915(1)	33(1)
C(122)	4927(1)	6829(2)	1844(1)	62(1)
C(123)	4986(2)	7585(2)	1528(1)	76(1)
C(124)	4375(2)	8087(1)	1285(1)	61(1)
C(125)	3699(2)	7849(1)	1356(1)	60(1)
C(126)	3638(1)	7098(1)	1674(1)	49(1)
C(131)	5049(1)	5277(1)	2767(1)	31(1)
C(132)	5510(1)	4856(1)	2454(1)	38(1)
C(133)	6254(1)	4721(1)	2786(1)	43(1)
C(134)	6543(1)	5008(1)	3428(1)	44(1)
C(135)	6083(1)	5403(1)	3748(1)	44(1)
C(136)	5339(1)	5543(1)	3422(1)	36(1)
C(211)	990(1)	4519(1)	1582(1)	35(1)
C(212)	327(1)	4134(1)	1233(1)	47(1)
C(213)	216(1)	3280(1)	1316(1)	55(1)
C(214)	750(2)	2812(2)	1740(1)	69(1)
C(215)	1408(2)	3181(2)	2088(2)	111(1)
C(216)	1527(2)	4038(2)	2008(1)	83(1)
C(221)	1490(1)	5623(1)	708(1)	32(1)
C(222)	1888(1)	6323(1)	595(1)	43(1)
C(223)	2119(1)	6371(1)	24(1)	53(1)
C(224)	1951(1)	5734(2)	-437(1)	54(1)
C(225)	1559(1)	5035(2)	-332(1)	55(1)
C(226)	1329(1)	4971(1)	242(1)	44(1)
C(231)	341(1)	6200(1)	1285(1)	36(1)
C(232)	-95(1)	6126(1)	1722(1)	45(1)
C(233)	-713(1)	6643(2)	1644(1)	59(1)
C(234)	-900(1)	7237(2)	1142(1)	67(1)

Appendix A – Crystallographic Data

C(235)	-475(1)	7308(2)	713(1)	69(1)
C(236)	140(1)	6790(1)	775(1)	51(1)

Appendix A – Crystallographic Data

Table A.8a Crystal data and structure refinement for **20**.

Identification code	20	
Empirical formula	C ₆₆ H ₇₆ O ₄ P ₂ Sr	
Formula weight	1082.83	
Temperature	170(2) K	
Wavelength	0.71073 Å	
Crystal system	Monoclinic	
Space group	P2(1)/c	
Unit cell dimensions	a = 18.825(4) Å	α = 90°.
	b = 15.905(3) Å	β = 107.30(3)°.
	c = 21.124(4) Å	γ = 90°.
Volume	6039(2) Å ³	
Z	4	
Density (calculated)	1.191 Mg/m ³	
Absorption coefficient	0.991 mm ⁻¹	
F(000)	2288	
Crystal size	0.5 x 0.5 x 0.4 mm ³	
Theta range for data collection	3.61 to 25.05°.	
Index ranges	-22 ≤ h ≤ 22, -16 ≤ k ≤ 18, -25 ≤ l ≤ 25	
Reflections collected	28907	
Independent reflections	10580 [R(int) = 0.1021]	
Completeness to theta = 25.05°	98.9 %	
Refinement method	Full-matrix least-squares on F ²	
Data / restraints / parameters	10580 / 0 / 673	
Goodness-of-fit on F ²	1.055	
Final R indices [I > 2σ(I)]	R1 = 0.0715, wR2 = 0.1486	
R indices (all data)	R1 = 0.1171, wR2 = 0.1688	
Extinction coefficient	0.0000(4)	
Largest diff. peak and hole	1.010 and -0.980 e.Å ⁻³	

Appendix A – Crystallographic Data

Table A.8b Atomic coordinates ($\times 10^4$) and equivalent isotropic displacement parameters ($\text{\AA}^2 \times 10^3$) for **20**. $U(\text{eq})$ is defined as one third of the trace of the orthogonalized U^{ij} tensor.

	x	y	z	U(eq)
Sr(1)	2645(1)	6245(1)	3068(1)	34(1)
P(1)	4180(1)	5630(1)	2318(1)	43(1)
O(1)	3696(2)	5716(2)	2757(2)	48(1)
C(1)	2249(2)	4886(3)	4290(2)	40(1)
P(2)	1184(1)	5581(1)	1419(1)	40(1)
O(2)	1779(2)	5917(2)	2003(2)	48(1)
C(2)	2704(2)	4170(3)	4539(2)	40(1)
O(3)	2400(2)	5384(2)	3841(2)	44(1)
C(3)	2528(3)	3666(3)	5006(2)	47(1)
O(4)	2741(2)	7674(2)	3166(2)	40(1)
C(4)	1939(3)	3830(3)	5256(3)	51(1)
C(5)	1504(3)	4521(3)	5011(3)	50(1)
C(6)	1635(3)	5053(3)	4528(2)	44(1)
C(7)	1805(3)	3293(4)	5801(3)	75(2)
C(8)	3378(3)	3978(3)	4294(2)	50(1)
C(9)	3815(3)	3196(4)	4642(3)	72(2)
C(10)	3929(3)	4715(4)	4433(3)	65(2)
C(11)	3111(4)	3771(4)	3556(3)	71(2)
C(12)	1139(3)	5824(3)	4285(3)	50(1)
C(13)	491(3)	5885(4)	4591(3)	72(2)
C(14)	1615(3)	6629(3)	4481(3)	58(1)
C(15)	786(3)	5787(3)	3530(3)	59(1)
C(21)	2799(2)	8493(3)	3258(2)	35(1)
C(22)	2229(2)	9053(3)	2890(2)	39(1)
C(23)	2306(3)	9906(3)	3009(2)	46(1)
C(24)	2921(3)	10257(3)	3473(3)	48(1)
C(25)	3478(3)	9717(3)	3818(2)	45(1)
C(26)	3442(2)	8851(3)	3732(2)	38(1)
C(27)	2992(4)	11202(3)	3570(4)	75(2)
C(28)	1544(3)	8699(3)	2364(2)	47(1)
C(29)	1790(3)	8262(3)	1811(2)	54(1)
C(30)	1112(3)	8090(4)	2674(3)	65(2)
C(31)	999(3)	9392(3)	2019(3)	73(2)

Appendix A – Crystallographic Data

C(32)	4086(3)	8284(3)	4124(2)	45(1)
C(33)	4718(3)	8789(3)	4598(3)	62(1)
C(34)	4421(3)	7815(3)	3646(3)	53(1)
C(35)	3808(3)	7651(3)	4555(3)	56(1)
C(111)	3825(3)	4864(3)	1676(2)	45(1)
C(112)	3672(3)	5048(3)	1007(3)	54(1)
C(113)	3383(3)	4437(4)	534(3)	61(1)
C(114)	3238(4)	3668(4)	717(3)	73(2)
C(115)	3400(5)	3460(5)	1375(4)	106(3)
C(116)	3684(4)	4070(4)	1855(3)	93(2)
C(121)	4259(3)	6605(3)	1915(2)	47(1)
C(122)	4919(4)	6905(4)	1852(3)	79(2)
C(123)	4944(4)	7652(5)	1541(4)	93(2)
C(124)	4327(5)	8122(4)	1293(3)	81(2)
C(125)	3662(4)	7840(4)	1348(3)	78(2)
C(126)	3632(3)	7091(3)	1660(3)	67(2)
C(131)	5109(2)	5320(3)	2767(2)	43(1)
C(132)	5566(3)	4910(3)	2458(3)	52(1)
C(133)	6299(3)	4764(3)	2791(3)	58(1)
C(134)	6589(3)	5025(3)	3434(3)	61(1)
C(135)	6133(3)	5413(4)	3754(3)	66(2)
C(136)	5393(3)	5557(3)	3421(3)	54(1)
C(211)	970(3)	4503(3)	1544(2)	45(1)
C(212)	297(3)	4135(3)	1199(3)	57(1)
C(213)	170(3)	3296(4)	1283(3)	67(2)
C(214)	694(4)	2822(4)	1702(3)	76(2)
C(215)	1375(5)	3176(4)	2049(4)	108(3)
C(216)	1498(4)	4021(4)	1970(3)	83(2)
C(221)	1469(2)	5607(3)	681(2)	43(1)
C(222)	1844(3)	6306(3)	565(3)	57(1)
C(223)	2075(3)	6346(4)	-4(3)	68(2)
C(224)	1949(3)	5706(4)	-442(3)	67(2)
C(225)	1571(3)	5001(4)	-330(3)	66(2)
C(226)	1337(3)	4950(3)	227(2)	53(1)
C(231)	336(3)	6188(3)	1262(2)	48(1)
C(232)	-68(3)	6132(3)	1720(3)	59(1)
C(233)	-672(3)	6653(4)	1659(3)	72(2)
C(234)	-874(4)	7228(4)	1153(4)	83(2)

Appendix A – Crystallographic Data

C(235)	-483(4)	7280(4)	709(4)	82(2)
C(236)	113(3)	6764(3)	754(3)	62(2)

Appendix A – Crystallographic Data

Table A.9a Crystal data and structure refinement for 21.

Identification code	21	
Empirical formula	C66 H76 Ba O4 P2	
Formula weight	1132.55	
Temperature	170(2) K	
Wavelength	0.71070 Å	
Crystal system	Monoclinic	
Space group	P2(1)/c	
Unit cell dimensions	a = 18.6970(2) Å	$\alpha = 90^\circ$.
	b = 16.2840(2) Å	$\beta = 109.0010(6)^\circ$.
	c = 21.3500(3) Å	$\gamma = 90^\circ$.
Volume	6146.08(13) Å ³	
Z	4	
Density (calculated)	1.224 Mg/m ³	
Absorption coefficient	0.742 mm ⁻¹	
F(000)	2360	
Crystal size	0.50 x 0.50 x 0.40 mm ³	
Theta range for data collection	3.52 to 25.00°.	
Index ranges	-20 ≤ h ≤ 22, -19 ≤ k ≤ 19, -23 ≤ l ≤ 25	
Reflections collected	67302	
Independent reflections	10796 [R(int) = 0.0432]	
Completeness to theta = 25.00°	99.6 %	
Max. and min. transmission	0.7556 and 0.7078	
Refinement method	Full-matrix least-squares on F ²	
Data / restraints / parameters	10796 / 0 / 673	
Goodness-of-fit on F ²	1.071	
Final R indices [I > 2sigma(I)]	R1 = 0.0259, wR2 = 0.0617	
R indices (all data)	R1 = 0.0308, wR2 = 0.0655	
Extinction coefficient	0.00000(12)	
Largest diff. peak and hole	0.418 and -0.394 e.Å ⁻³	

Appendix A – Crystallographic Data

Table A.9b. Atomic coordinates ($\times 10^4$) and equivalent isotropic displacement parameters ($\text{\AA}^2 \times 10^3$) for **21**. $U(\text{eq})$ is defined as one third of the trace of the orthogonalized U^{ij} tensor.

	x	y	z	U(eq)
Ba(1)	2273(1)	1205(1)	6834(1)	29(1)
P(1)	689(1)	573(1)	7597(1)	42(1)
O(1)	1134(1)	653(1)	7132(1)	53(1)
C(1)	2736(1)	-206(1)	5639(1)	35(1)
P(2)	3806(1)	512(1)	8581(1)	36(1)
O(2)	3191(1)	814(1)	7982(1)	46(1)
C(2)	2313(1)	-939(1)	5412(1)	37(1)
O(3)	2568(1)	279(1)	6067(1)	42(1)
C(3)	2504(1)	-1427(1)	4956(1)	46(1)
O(4)	2261(1)	2694(1)	6762(1)	37(1)
C(4)	3074(1)	-1228(2)	4699(1)	53(1)
C(5)	3482(1)	-519(2)	4930(1)	49(1)
C(6)	3335(1)	-4(1)	5392(1)	39(1)
C(7)	1660(1)	-1175(1)	5664(1)	46(1)
C(8)	1051(1)	-503(2)	5509(1)	59(1)
C(9)	1261(2)	-1968(2)	5343(1)	68(1)
C(10)	1979(2)	-1331(2)	6414(1)	70(1)
C(11)	3220(2)	-1737(2)	4160(2)	82(1)
C(12)	3797(1)	785(1)	5625(1)	47(1)
C(13)	4436(2)	884(2)	5323(2)	74(1)
C(14)	3278(2)	1540(2)	5414(1)	58(1)
C(15)	4176(1)	774(2)	6383(1)	56(1)
C(21)	2225(1)	3495(1)	6689(1)	30(1)
C(22)	1576(1)	3871(1)	6227(1)	33(1)
C(23)	1560(1)	4723(1)	6165(1)	39(1)
C(24)	2146(1)	5222(1)	6526(1)	46(1)
C(25)	2773(1)	4848(1)	6978(1)	42(1)
C(26)	2830(1)	4004(1)	7072(1)	34(1)
C(27)	900(1)	3345(1)	5819(1)	40(1)
C(28)	1153(1)	2740(2)	5377(1)	53(1)
C(29)	563(1)	2879(1)	6285(1)	47(1)
C(30)	259(1)	3864(2)	5353(1)	56(1)
C(31)	2101(2)	6150(1)	6447(2)	73(1)

Appendix A – Crystallographic Data

C(32)	3524(1)	3622(1)	7597(1)	44(1)
C(33)	4107(2)	4272(2)	7959(2)	74(1)
C(34)	3924(1)	3023(2)	7264(1)	62(1)
C(35)	3278(1)	3175(2)	8127(1)	50(1)
C(111)	1118(1)	-140(1)	8255(1)	43(1)
C(112)	1335(2)	-888(2)	8087(2)	95(1)
C(113)	1674(3)	-1462(2)	8582(2)	118(2)
C(114)	1799(2)	-1270(2)	9229(2)	74(1)
C(115)	1578(1)	-546(2)	9398(1)	58(1)
C(116)	1239(1)	28(2)	8914(1)	50(1)
C(211)	625(1)	1539(2)	7987(1)	50(1)
C(212)	-38(2)	1841(2)	8030(2)	87(1)
C(213)	-30(3)	2602(3)	8346(2)	110(1)
C(214)	620(3)	3028(2)	8598(2)	98(1)
C(215)	1277(2)	2727(2)	8557(2)	89(1)
C(216)	1286(2)	1986(2)	8254(2)	71(1)
C(311)	-255(1)	230(1)	7183(1)	44(1)
C(312)	-684(1)	-141(2)	7522(1)	50(1)
C(313)	-1430(1)	-341(2)	7199(1)	57(1)
C(314)	-1751(1)	-174(2)	6538(1)	65(1)
C(315)	-1325(2)	169(2)	6192(1)	75(1)
C(316)	-579(1)	379(2)	6510(1)	60(1)
C(411)	4040(1)	-541(1)	8487(1)	38(1)
C(412)	4719(1)	-890(2)	8866(1)	47(1)
C(413)	4862(1)	-1712(2)	8793(1)	52(1)
C(414)	4345(2)	-2184(2)	8345(1)	61(1)
C(415)	3666(2)	-1853(2)	7969(2)	84(1)
C(416)	3515(2)	-1029(2)	8040(1)	67(1)
C(511)	3526(1)	572(1)	9309(1)	37(1)
C(512)	3644(1)	-60(2)	9768(1)	45(1)
C(513)	3407(1)	22(2)	10316(1)	56(1)
C(514)	3045(1)	730(2)	10403(1)	60(1)
C(515)	2918(2)	1354(2)	9948(2)	61(1)
C(516)	3156(1)	1278(1)	9406(1)	47(1)
C(611)	4657(1)	1107(1)	8723(1)	40(1)
C(612)	5032(1)	1058(2)	8257(1)	55(1)
C(613)	5641(2)	1565(2)	8307(2)	71(1)
C(614)	5878(2)	2127(2)	8814(2)	78(1)

Appendix A – Crystallographic Data

C(615)	5519(2)	2174(2)	9280(2)	76(1)
C(616)	4911(1)	1665(2)	9238(1)	56(1)

Appendix A – Crystallographic Data

Table A.10a Crystal data and structure refinement for **24**.

Identification code	24	
Empirical formula	C ₁₅ H ₁₄ F ₆ Li N ₂ O ₄ P S ₂	
Formula weight	502.31	
Temperature	170(2) K	
Wavelength	0.71069 Å	
Crystal system	Triclinic	
Space group	P-1	
Unit cell dimensions	a = 8.988(4) Å	α = 67.90(3)°.
	b = 11.094(4) Å	β = 77.14(2)°.
	c = 11.858(5) Å	γ = 69.02(2)°.
Volume	1017.6(7) Å ³	
Z	2	
Density (calculated)	1.639 Mg/m ³	
Absorption coefficient	0.420 mm ⁻¹	
F(000)	508	
Crystal size	0.20 x 0.10 x 0.10 mm ³	
Theta range for data collection	3.63 to 24.28°.	
Index ranges	-9 ≤ h ≤ 10, -12 ≤ k ≤ 9, -13 ≤ l ≤ 13	
Reflections collected	4006	
Independent reflections	2865 [R(int) = 0.0448]	
Completeness to theta = 24.28°	86.8 %	
Max. and min. transmission	0.9592 and 0.9208	
Refinement method	Full-matrix least-squares on F ²	
Data / restraints / parameters	2865 / 0 / 281	
Goodness-of-fit on F ²	1.136	
Final R indices [I > 2σ(I)]	R1 = 0.0862, wR2 = 0.1906	
R indices (all data)	R1 = 0.1135, wR2 = 0.2070	
Extinction coefficient	0.016(3)	
Largest diff. peak and hole	0.416 and -0.496 e.Å ⁻³	

Appendix A – Crystallographic Data

Table A.10b Atomic coordinates ($\times 10^4$) and equivalent isotropic displacement parameters ($\text{\AA}^2 \times 10^3$) for **24**. $U(\text{eq})$ is defined as one third of the trace of the orthogonalized U^{ij} tensor.

	x	y	z	U(eq)
S(1)	2641(2)	3787(2)	8129(2)	46(1)
S(2)	-371(2)	3387(2)	8493(2)	48(1)
P(1)	-5166(2)	7932(2)	8497(2)	42(1)
N(1)	-4869(8)	6330(6)	8943(6)	45(2)
O(3)	348(6)	1963(5)	8698(5)	59(1)
O(2)	3408(6)	2361(5)	8525(5)	56(1)
O(1)	3129(6)	4626(5)	8543(4)	56(1)
O(4)	-1719(6)	3813(5)	9312(4)	53(1)
F(1)	2990(6)	3632(5)	5938(4)	81(2)
F(2)	2425(7)	5643(5)	5970(4)	86(2)
F(3)	4747(7)	4261(7)	6296(5)	105(2)
F(4)	-2394(7)	3540(6)	7167(5)	99(2)
F(5)	-180(6)	3747(6)	6163(5)	94(2)
F(6)	-1865(6)	5395(5)	6689(4)	76(1)
C(15)	-6469(9)	8623(7)	9620(6)	48(2)
Li(1)	3545(14)	5226(11)	9748(10)	48(3)
C(1)	-6108(8)	8814(6)	7092(6)	40(2)
C(2)	-6333(9)	8093(7)	6451(6)	54(2)
C(3)	-7071(11)	8737(8)	5401(7)	63(2)
C(4)	-7675(10)	10142(7)	4981(7)	55(2)
C(5)	-7462(10)	10885(7)	5603(7)	61(2)
C(6)	-6693(9)	10237(7)	6652(7)	56(2)
C(7)	-3363(8)	8390(6)	8282(6)	40(2)
C(8)	-1896(9)	7424(7)	8268(6)	47(2)
C(9)	-475(9)	7738(8)	8094(7)	54(2)
C(10)	-536(9)	9038(8)	7954(7)	53(2)
C(11)	-1990(10)	10006(7)	7996(7)	56(2)
C(12)	-3398(9)	9694(7)	8149(6)	51(2)
C(13)	3224(9)	4370(9)	6498(7)	56(2)
C(14)	-1246(9)	4060(8)	7051(7)	56(2)
N(2)	769(7)	4274(5)	8245(5)	43(1)

Appendix A – Crystallographic Data

Table A.11a Crystal data and structure refinement for **28**.

Identification code	28	
Empirical formula	C22 H23 Br N O P	
Formula weight	428.29	
Temperature	170(2) K	
Wavelength	0.71070 Å	
Crystal system	Monoclinic	
Space group	P2(1)/c	
Unit cell dimensions	a = 8.6550(2) Å	$\alpha = 90^\circ$.
	b = 24.2090(3) Å	$\beta = 104.4490(10)^\circ$.
	c = 10.7610(2) Å	$\gamma = 90^\circ$.
Volume	2183.42(7) Å ³	
Z	4	
Density (calculated)	1.303 Mg/m ³	
Absorption coefficient	1.966 mm ⁻¹	
F(000)	880	
Crystal size	0.28 x 0.27 x 0.25 mm ³	
Theta range for data collection	4.26 to 27.50°.	
Index ranges	-11<=h<=11, -31<=k<=31, -13<=l<=13	
Reflections collected	22875	
Independent reflections	4967 [R(int) = 0.0407]	
Completeness to theta = 27.50°	99.0 %	
Refinement method	Full-matrix least-squares on F ²	
Data / restraints / parameters	4967 / 0 / 239	
Goodness-of-fit on F ²	1.029	
Final R indices [I>2sigma(I)]	R1 = 0.0290, wR2 = 0.0680	
R indices (all data)	R1 = 0.0351, wR2 = 0.0715	
Extinction coefficient	0.0067(6)	
Largest diff. peak and hole	0.422 and -0.414 e.Å ⁻³	

Appendix A – Crystallographic Data

Table A.11b Atomic coordinates ($\times 10^4$) and equivalent isotropic displacement parameters ($\text{\AA}^2 \times 10^3$) for **28**. U(eq) is defined as one third of the trace of the orthogonalized U^{ij} tensor.

	x	y	z	U(eq)
Br(1)	17949(1)	5899(1)	3146(1)	29(1)
P(1)	11177(1)	5994(1)	-2574(1)	23(1)
O(1)	8952(2)	5896(1)	-1040(1)	35(1)
C(1)	7627(3)	5899(1)	-471(2)	45(1)
C(2)	9851(2)	5490(1)	-3478(2)	28(1)
C(11)	11676(2)	5825(1)	-901(2)	26(1)
C(12)	10432(2)	5802(1)	-274(2)	28(1)
C(13)	10762(2)	5700(1)	1035(2)	36(1)
C(14)	12334(3)	5621(1)	1707(2)	43(1)
C(15)	13579(3)	5637(1)	1108(2)	42(1)
C(16)	13243(2)	5741(1)	-197(2)	33(1)
C(21)	12942(2)	6003(1)	-3161(2)	26(1)
C(22)	13699(2)	5503(1)	-3284(2)	37(1)
C(23)	15001(3)	5500(1)	-3806(2)	42(1)
C(24)	15553(3)	5986(1)	-4227(2)	46(1)
C(25)	14826(3)	6474(1)	-4079(3)	59(1)
C(26)	13527(3)	6488(1)	-3543(3)	47(1)
C(31)	10327(2)	6675(1)	-2779(2)	25(1)
C(32)	10783(3)	7060(1)	-1792(2)	38(1)
C(33)	10185(3)	7594(1)	-1974(2)	46(1)
C(34)	9145(3)	7742(1)	-3114(2)	45(1)
C(35)	8698(3)	7361(1)	-4093(2)	42(1)
C(36)	9292(2)	6825(1)	-3933(2)	32(1)
N(90)	4746(3)	7076(1)	141(3)	76(1)
C(91)	4736(3)	7034(1)	1186(3)	60(1)
C(92)	4733(5)	6977(1)	2529(3)	82(1)

Appendix A – Crystallographic Data

Table A.12a. Crystal data and structure refinement for **29**.

Identification code	29	
Empirical formula	C ₂₈ H ₂₇ Br N O P	
Formula weight	504.39	
Temperature	120(2) K	
Wavelength	0.71073 Å	
Crystal system	Monoclinic	
Space group	P2(1)/c	
Unit cell dimensions	a = 12.382(4) Å	α = 90°.
	b = 10.677(3) Å	β = 102.22(1)°.
	c = 18.905(5) Å	γ = 90°.
Volume	2442.7(12) Å ³	
Z	4	
Density (calculated)	1.372 Mg/m ³	
Absorption coefficient	1.769 mm ⁻¹	
F(000)	1040	
Crystal size	0.44 x 0.40 x 0.10 mm ³	
Theta range for data collection	1.68 to 29.11°.	
Index ranges	-16 ≤ h ≤ 16, -14 ≤ k ≤ 14, -25 ≤ l ≤ 25	
Reflections collected	30120	
Independent reflections	6536 [R(int) = 0.0347]	
Completeness to theta = 29.11°	99.7 %	
Absorption correction	Integration	
Max. and min. transmission	0.8452 and 0.4626	
Refinement method	Full-matrix least-squares on F ²	
Data / restraints / parameters	6536 / 0 / 387	
Goodness-of-fit on F ²	1.029	
Final R indices [I > 2σ(I)]	R1 = 0.0259, wR2 = 0.0603	
R indices (all data)	R1 = 0.0345, wR2 = 0.0641	
Largest diff. peak and hole	0.413 and -0.302 e.Å ⁻³	

Appendix A – Crystallographic Data

Table A.12b Atomic coordinates ($\times 10^4$) and equivalent isotropic displacement parameters ($\text{\AA}^2 \times 10^3$) for **29**. $U(\text{eq})$ is defined as one third of the trace of the orthogonalized U^{ij} tensor.

	x	y	z	U(eq)
Br	6458(1)	3573(1)	4132(1)	20(1)
P	2886(1)	2910(1)	4270(1)	14(1)
O	2463(1)	340(1)	4599(1)	22(1)
C(1)	3695(1)	1990(1)	4989(1)	16(1)
C(2)	3397(1)	728(1)	5068(1)	17(1)
C(3)	4022(1)	-21(1)	5608(1)	21(1)
C(4)	4921(1)	509(2)	6081(1)	23(1)
C(5)	5209(1)	1758(2)	6022(1)	22(1)
C(6)	4604(1)	2499(1)	5473(1)	19(1)
C(7)	2239(1)	-987(2)	4546(1)	26(1)
C(8)	3598(1)	4399(1)	4259(1)	16(1)
C(11)	2756(1)	2150(1)	3405(1)	17(1)
C(12)	1835(1)	1417(2)	3111(1)	23(1)
C(13)	1774(2)	814(2)	2450(1)	28(1)
C(14)	2631(2)	946(2)	2082(1)	27(1)
C(15)	3545(1)	1678(2)	2372(1)	25(1)
C(16)	3623(1)	2276(1)	3037(1)	20(1)
C(21)	1541(1)	3138(1)	4473(1)	15(1)
C(22)	619(1)	3463(1)	3932(1)	19(1)
C(23)	-400(1)	3630(1)	4117(1)	21(1)
C(24)	-515(1)	3485(1)	4828(1)	21(1)
C(25)	401(1)	3192(2)	5368(1)	22(1)
C(26)	1429(1)	3018(1)	5192(1)	18(1)
C(31)	3152(1)	5252(1)	3623(1)	17(1)
C(32)	2193(1)	5958(1)	3594(1)	22(1)
C(33)	1828(2)	6797(2)	3026(1)	28(1)
C(34)	2426(2)	6941(2)	2489(1)	30(1)
C(35)	3376(2)	6242(2)	2508(1)	27(1)
C(36)	3741(1)	5399(1)	3072(1)	21(1)
N	-381(1)	-995(2)	2924(1)	40(1)
C(9)	-730(2)	-532(2)	3366(1)	32(1)
C(10)	-1140(2)	78(2)	3949(1)	57(1)

Appendix A – Crystallographic Data

Table A.13a. Crystal data and structure refinement for **30**.

Identification code	30	
Empirical formula	C ₂₆ H ₂₄ Br N ₂ P	
Formula weight	475.35	
Temperature	150(2) K	
Wavelength	0.71073 Å	
Crystal system	Monoclinic	
Space group	P2(1)/c	
Unit cell dimensions	a = 12.647(3) Å	α = 90°.
	b = 20.007(4) Å	β = 107.55(3)°.
	c = 9.4980(19) Å	γ = 90°.
Volume	2291.4(8) Å ³	
Z	4	
Density (calculated)	1.378 Mg/m ³	
Absorption coefficient	1.879 mm ⁻¹	
F(000)	976	
Crystal size	0.55 x 0.4 x 0.2 mm ³	
Theta range for data collection	1.69 to 27.50°.	
Index ranges	-16 ≤ h ≤ 15, -25 ≤ k ≤ 25, -12 ≤ l ≤ 12	
Reflections collected	25945	
Independent reflections	5267 [R(int) = 0.0354]	
Completeness to theta = 27.50°	99.9 %	
Absorption correction	Semi-empirical from equivalents	
Max. and min. transmission	0.529407 and 0.384758	
Refinement method	Full-matrix least-squares on F ²	
Data / restraints / parameters	5267 / 0 / 283	
Goodness-of-fit on F ²	1.069	
Final R indices [I > 2σ(I)]	R1 = 0.0330, wR2 = 0.0778	
R indices (all data)	R1 = 0.0433, wR2 = 0.0834	
Largest diff. peak and hole	1.087 and -0.410 e.Å ⁻³	

Appendix A – Crystallographic Data

Table A.13b. Atomic coordinates ($\times 10^4$) and equivalent isotropic displacement parameters ($\text{\AA}^2 \times 10^3$) for **30**. $U(\text{eq})$ is defined as one third of the trace of the orthogonalized U^{ij} tensor.

	x	y	z	U(eq)
Br(1)	331(1)	3755(1)	2426(1)	26(1)
P(1)	2693(1)	5183(1)	643(1)	19(1)
C(1)	1382(2)	5309(1)	1011(2)	22(1)
C(11)	1419(2)	5813(1)	2217(2)	22(1)
C(12)	1232(2)	6489(1)	1871(3)	31(1)
C(13)	1181(2)	6949(1)	2954(3)	39(1)
C(14)	1313(2)	6733(1)	4375(3)	40(1)
C(15)	1507(2)	6062(1)	4738(3)	38(1)
C(16)	1567(2)	5605(1)	3667(2)	29(1)
C(21)	3702(2)	4775(1)	2155(2)	23(1)
C(22)	3381(2)	4267(1)	2943(3)	28(1)
C(23)	4203(2)	3930(1)	4021(3)	37(1)
C(24)	5300(2)	4103(1)	4290(3)	38(1)
C(25)	5586(2)	4609(1)	3482(3)	40(1)
N(26)	4792(2)	4948(1)	2399(3)	41(1)
C(31)	2445(2)	4666(1)	-982(2)	22(1)
C(32)	1481(2)	4749(1)	-2162(2)	28(1)
C(33)	1343(2)	4377(1)	-3446(2)	30(1)
C(34)	2149(2)	3927(1)	-3529(3)	30(1)
C(35)	3089(2)	3840(1)	-2327(3)	37(1)
C(36)	3244(2)	4211(1)	-1061(3)	30(1)
C(41)	3233(2)	5981(1)	288(2)	21(1)
C(42)	2994(3)	6194(1)	-1149(3)	44(1)
C(43)	3362(3)	6815(2)	-1439(3)	60(1)
C(44)	3981(2)	7206(1)	-298(3)	42(1)
C(45)	4198(2)	6987(1)	1131(3)	37(1)
C(46)	3819(2)	6377(1)	1442(2)	29(1)
C(1S)	1490(3)	2857(2)	-360(4)	43(1)
C(2S)	2652(2)	2702(1)	349(3)	38(1)
N(3S)	3556(2)	2570(1)	888(3)	55(1)

Appendix A – Crystallographic Data

Table A.14a. Crystal data and structure refinement for **32**.

Identification code	32	
Empirical formula	C ₅₄ H ₄₈ Br ₂ N ₂ P ₂	
Formula weight	946.747	
Temperature	150(2) K	
Wavelength	0.71073 Å	
Crystal system	Monoclinic	
Space group	P2(1)/n	
Unit cell dimensions	a = 11.296(2) Å	α = 90°.
	b = 25.987(5) Å	β = 98.31(3)°.
	c = 18.690(4) Å	γ = 90°.
Volume	5428.8(19) Å ³	
Z	4	
Density (calculated)	1.436 Mg/m ³	
Absorption coefficient	2.360 mm ⁻¹	
F(000)	2400	
Crystal size	0.3 x 0.3 x 0.2 mm ³	
Theta range for data collection	3.54 to 25.00°.	
Index ranges	-13 ≤ h ≤ 12, -28 ≤ k ≤ 30, -22 ≤ l ≤ 22	
Reflections collected	31940	
Independent reflections	9539 [R(int) = 0.1013]	
Completeness to theta = 25.00°	99.7 %	
Refinement method	Full-matrix least-squares on F ²	
Data / restraints / parameters	9539 / 0 / 607	
Goodness-of-fit on F ²	1.200	
Final R indices [I > 2σ(I)]	R1 = 0.0614, wR2 = 0.1113	
R indices (all data)	R1 = 0.1037, wR2 = 0.1299	
Largest diff. peak and hole	0.691 and -0.923 e.Å ⁻³	

Appendix A – Crystallographic Data

Table A.14b. Atomic coordinates ($\times 10^4$) and equivalent isotropic displacement parameters ($\text{\AA}^2 \times 10^3$) for **32**. $U(\text{eq})$ is defined as one third of the trace of the orthogonalized U^{ij} tensor.

	x	y	z	U(eq)
Br(1)	4614(1)	2016(1)	6659(1)	41(1)
P(1)	8083(1)	1527(1)	5015(1)	21(1)
C(1)	7021(4)	2889(2)	6607(2)	23(1)
Br(2)	9372(1)	1349(1)	7617(1)	51(1)
P(2)	7193(1)	3399(1)	7272(1)	23(1)
C(2)	8191(2)	1938(1)	5809(1)	25(1)
C(11)	7726(2)	3062(1)	5387(1)	24(1)
C(12)	7492(2)	3267(1)	4688(1)	32(1)
C(13)	6401(5)	3485(2)	4426(2)	36(1)
C(14)	5493(4)	3497(2)	4862(2)	35(1)
C(15)	5698(4)	3297(2)	5550(2)	30(1)
C(16)	6807(4)	3081(2)	5827(2)	23(1)
C(21)	8953(4)	2853(2)	5637(2)	25(1)
C(22)	9928(4)	3188(2)	5651(2)	33(1)
C(23)	11095(4)	3025(2)	5855(3)	37(1)
C(24)	11327(5)	2518(2)	6068(3)	39(1)
C(25)	10369(4)	2179(2)	6061(2)	32(1)
C(26)	9185(4)	2337(2)	5840(2)	24(1)
C(31)	8310(4)	3843(2)	7061(2)	27(1)
C(32)	9416(4)	3872(2)	7495(3)	38(1)
C(33)	10281(5)	4210(2)	7325(3)	51(2)
C(34)	10044(5)	4517(2)	6722(3)	54(2)
C(35)	8957(6)	4497(2)	6290(3)	49(2)
C(36)	8081(5)	4158(2)	6452(3)	38(1)
C(41)	7661(4)	3109(2)	8144(2)	26(1)
C(42)	8371(5)	2667(2)	8215(3)	43(1)
C(43)	8778(6)	2475(2)	8897(3)	54(2)
C(44)	8462(5)	2706(2)	9506(3)	48(2)
C(45)	7737(5)	3132(2)	9438(3)	48(2)
C(46)	7342(5)	3335(2)	8764(3)	42(1)
C(51)	5823(4)	3747(2)	7307(2)	25(1)
C(52)	5859(5)	4275(2)	7433(3)	37(1)
C(53)	4810(5)	4535(2)	7511(3)	46(1)

Appendix A – Crystallographic Data

C(54)	3738(5)	4272(2)	7458(3)	44(1)
C(55)	3694(4)	3745(2)	7335(3)	38(1)
C(56)	4744(4)	3476(2)	7262(2)	32(1)
C(61)	6736(4)	1151(2)	4933(2)	22(1)
C(62)	5844(4)	1246(2)	5365(3)	33(1)
C(63)	4792(5)	965(2)	5250(3)	41(1)
C(64)	4594(5)	603(2)	4705(3)	37(1)
C(65)	5483(4)	508(2)	4278(3)	35(1)
C(66)	6545(4)	777(2)	4393(2)	30(1)
C(71)	9335(4)	1096(2)	5070(2)	23(1)
C(72)	9752(4)	866(2)	5734(2)	28(1)
C(73)	10696(4)	521(2)	5791(3)	35(1)
C(74)	11233(4)	401(2)	5186(3)	37(1)
C(75)	10806(4)	617(2)	4527(3)	35(1)
C(76)	9865(4)	970(2)	4459(2)	30(1)
C(81)	7996(4)	1925(2)	4220(2)	26(1)
C(82)	9030(4)	2156(2)	4029(2)	29(1)
C(83)	8933(5)	2465(2)	3416(2)	36(1)
C(84)	7834(5)	2550(2)	3008(3)	39(1)
C(85)	6802(5)	2336(2)	3202(3)	39(1)
C(86)	6885(4)	2020(2)	3810(2)	31(1)
N(1)	3160(5)	213(2)	7019(3)	58(1)
C(91)	2724(6)	1100(2)	7545(4)	61(2)
C(92)	2975(5)	600(2)	7258(3)	44(1)
N(2)	7371(5)	105(2)	6409(3)	66(2)
C(93)	6372(5)	707(2)	7244(3)	55(2)
C(94)	6932(5)	366(2)	6777(3)	41(1)
N(4)	4962(8)	821(3)	9045(5)	110(3)
C(97)	6527(9)	1512(4)	8866(6)	118(4)
C(98)	5676(9)	1128(4)	8976(5)	90(3)
N(110)	7118(10)	5812(6)	4587(6)	145(7)
C(110)	7114(13)	5397(7)	4440(8)	81(7)
C(111)	7280(30)	4862(8)	4256(12)	126(13)
N(300)	3680(20)	4627(9)	3764(13)	124(12)
C(310)	4180(60)	4941(19)	4280(30)	110(30)
C(320)	4980(70)	4860(20)	4110(30)	110(30)
N(410)	6510(70)	4809(14)	4090(20)	240(30)
N(310)	4840(80)	5130(30)	4680(40)	90(40)

Appendix A – Crystallographic Data

Table A.15a. Crystal data and structure refinement for **35**.

Identification code	35	
Empirical formula	C ₂₆ H ₂₃ O P	
Formula weight	382.41	
Temperature	120(2) K	
Wavelength	0.71073 Å	
Crystal system	Monoclinic	
Space group	P2(1)/n	
Unit cell dimensions	a = 9.1236(4) Å	α = 90°.
	b = 18.8155(7) Å	β = 99.8970(10)°.
	c = 12.1068(6) Å	γ = 90°.
Volume	2047.4(2) Å ³	
Z	4	
Density (calculated)	1.241 Mg/m ³	
Absorption coefficient	0.148 mm ⁻¹	
F(000)	808	
Crystal size	0.40 x 0.40 x 0.38 mm ³	
Theta range for data collection	2.02 to 27.48°.	
Index ranges	-11 ≤ h ≤ 11, -24 ≤ k ≤ 24, -15 ≤ l ≤ 15	
Reflections collected	22809	
Independent reflections	4687 [R(int) = 0.0270]	
Absorption correction	Multiscan	
Max. and min. transmission	0.956245 and 0.861543	
Refinement method	Full-matrix least-squares on F ²	
Data / restraints / parameters	4686 / 0 / 345	
Goodness-of-fit on F ²	1.074	
Final R indices [I > 2σ(I)]	R1 = 0.0364, wR2 = 0.0822	
R indices (all data)	R1 = 0.0473, wR2 = 0.0916	
Largest diff. peak and hole	0.347 and -0.335 e.Å ⁻³	

Appendix A – Crystallographic Data

Table A.15b. Atomic coordinates ($\times 10^4$) and equivalent isotropic displacement parameters ($\text{\AA}^2 \times 10^3$) for 35. U(eq) is defined as one third of the trace of the orthogonalized U^{ij} tensor.

	x	y	z	U(eq)
P(1)	9505(1)	1506(1)	4768(1)	19(1)
C(22)	7202(2)	1401(1)	6582(1)	28(1)
C(31)	11313(2)	1521(1)	4360(1)	21(1)
O(1)	9240(1)	1708(1)	2266(1)	32(1)
C(26)	8949(2)	666(1)	7779(1)	28(1)
C(41)	8775(2)	2405(1)	4737(1)	21(1)
C(11)	8323(2)	1036(1)	3635(1)	22(1)
C(34)	14093(2)	1485(1)	3724(1)	33(1)
C(36)	11895(2)	879(1)	4055(1)	26(1)
C(16)	7430(2)	486(1)	3920(1)	27(1)
C(21)	8609(2)	1064(1)	6776(1)	23(1)
C(1)	9687(2)	1111(1)	6040(1)	23(1)
C(23)	6249(2)	1366(1)	7361(2)	35(1)
C(25)	7981(2)	632(1)	8541(1)	35(1)
C(32)	12115(2)	2145(1)	4323(2)	32(1)
C(12)	8368(2)	1159(1)	2500(1)	26(1)
C(42)	7780(2)	2667(1)	3823(1)	27(1)
C(35)	13292(2)	861(1)	3749(1)	32(1)
C(45)	8660(2)	3529(1)	5677(2)	35(1)
C(44)	7677(2)	3781(1)	4766(2)	35(1)
C(15)	6589(2)	70(1)	3100(2)	35(1)
C(24)	6631(2)	987(1)	8351(2)	39(1)
C(46)	9207(2)	2837(1)	5670(1)	29(1)
C(43)	7234(2)	3357(1)	3839(2)	34(1)
C(33)	13503(2)	2125(1)	3993(2)	37(1)
C(14)	6635(2)	207(1)	1988(2)	41(1)
C(13)	7518(2)	743(1)	1677(2)	38(1)
C(2)	9981(3)	1626(1)	1333(2)	52(1)

Appendix A – Crystallographic Data

Table A.16a. Crystal data and structure refinement for **36**.

Identification code	36	
Empirical formula	C ₂₄ H ₂₀ N P	
Formula weight	353.36	
Temperature	150(2) K	
Wavelength	0.71073 Å	
Crystal system	Triclinic	
Space group	P-1	
Unit cell dimensions	a = 9.221(1) Å	α = 78.807(4)°.
	b = 9.708(1) Å	β = 89.170(4)°.
	c = 10.599(1) Å	γ = 83.566°.
Volume	924.9(2) Å ³	
Z	2	
Density (calculated)	1.269 Mg/m ³	
Absorption coefficient	0.155 mm ⁻¹	
F(000)	372	
Crystal size	0.50 x 0.35 x 0.16 mm ³	
Theta range for data collection	1.96 to 27.48°.	
Index ranges	-11 ≤ h ≤ 11, -12 ≤ k ≤ 12, -13 ≤ l ≤ 13	
Reflections collected	10060	
Independent reflections	4217 [R(int) = 0.0233]	
Completeness to theta = 27.50°	99.9 %	
Absorption correction	Semi-empirical from equivalents	
Max. and min. transmission	0.956 and 0.847	
Refinement method	Full-matrix least-squares on F ²	
Data / restraints / parameters	4207 / 0 / 235	
Goodness-of-fit on F ²	1.083	
Final R indices [I > 2σ(I)]	R1 = 0.0406, wR2 = 0.0865	
R indices (all data)	R1 = 0.0538, wR2 = 0.0974	
Largest diff. peak and hole	0.310 and -0.303 e.Å ⁻³	

Appendix A – Crystallographic Data

Table A.16b. Atomic coordinates ($\times 10^4$) and equivalent isotropic displacement parameters ($\text{\AA}^2 \times 10^3$) for **36**. $U(\text{eq})$ is defined as one third of the trace of the orthogonalized U^{ij} tensor.

	x	y	z	U(eq)
P(1)	440(1)	1449(1)	2661(1)	19(1)
C(1)	642(2)	-316(2)	2711(2)	24(1)
C(11)	1421(2)	2079(2)	3890(2)	21(1)
C(12)	1196(2)	3461(2)	4065(2)	24(1)
C(13)	1982(2)	3864(2)	5006(2)	33(1)
C(14)	2996(2)	2905(2)	5764(2)	34(1)
C(15)	3219(2)	1518(2)	5597(2)	32(1)
C(16)	2420(2)	1101(2)	4657(2)	26(1)
C(21)	1936(2)	-1169(2)	2397(2)	23(1)
C(22)	1944(2)	-2654(2)	2567(2)	27(1)
C(23)	3124(2)	-3509(2)	2216(2)	33(1)
C(24)	4355(2)	-2939(2)	1685(2)	36(1)
C(25)	4406(2)	-1492(2)	1540(2)	34(1)
C(26)	3232(2)	-623(2)	1901(2)	28(1)
C(31)	-1483(2)	2020(2)	2820(2)	21(1)
C(32)	-2434(2)	1998(2)	1808(2)	28(1)
C(33)	-3920(2)	2393(2)	1916(2)	33(1)
C(34)	-4466(2)	2813(2)	3027(2)	32(1)
C(35)	-3532(2)	2827(2)	4037(2)	30(1)
C(36)	-2041(2)	2432(2)	3937(2)	25(1)
C(41)	1035(2)	2473(2)	1137(2)	21(1)
C(42)	994(2)	1926(2)	21(2)	27(1)
C(43)	1408(2)	2729(2)	-1134(2)	30(1)
C(44)	1834(2)	4054(2)	-1143(2)	30(1)
C(45)	1863(2)	4530(2)	4(2)	34(1)
N(46)	1477(2)	3756(2)	1143(1)	32(1)

Appendix A – Crystallographic Data

Table A.17a. Crystal data and structure refinement for **39**.

Identification code	39	
Empirical formula	C25 H21 As	
Formula weight	396.34	
Temperature	150(2) K	
Wavelength	0.71073 Å	
Crystal system	Monoclinic	
Space group	P2(1)/c	
Unit cell dimensions	a = 9.51290(10) Å	$\alpha = 90^\circ$.
	b = 11.109 Å	$\beta = 92.00^\circ$.
	c = 18.5358(2) Å	$\gamma = 90^\circ$.
Volume	1957.66(3) Å ³	
Z	4	
Density (calculated)	1.345 Mg/m ³	
Absorption coefficient	1.741 mm ⁻¹	
F(000)	816	
Crystal size	0.3 x 0.3 x 0.3 mm ³	
Theta range for data collection	3.53 to 25.00°.	
Index ranges	-11 ≤ h ≤ 10, -13 ≤ k ≤ 13, -22 ≤ l ≤ 20	
Reflections collected	11492	
Independent reflections	3438 [R(int) = 0.0874]	
Completeness to theta = 25.00°	99.7 %	
Refinement method	Full-matrix least-squares on F ²	
Data / restraints / parameters	3438 / 0 / 240	
Goodness-of-fit on F ²	0.960	
Final R indices [I > 2σ(I)]	R1 = 0.0525, wR2 = 0.1277	
R indices (all data)	R1 = 0.0680, wR2 = 0.1324	
Extinction coefficient	0.0000(8)	
Largest diff. peak and hole	1.827 and -1.487 e.Å ⁻³	

Appendix A – Crystallographic Data

Table A.17b. Atomic coordinates ($\times 10^4$) and equivalent isotropic displacement parameters ($\text{\AA}^2 \times 10^3$) for **39**. $U(\text{eq})$ is defined as one third of the trace of the orthogonalized U^{ij} tensor.

	x	y	z	U(eq)
As(1)	5443(1)	7710(1)	592(1)	20(1)
C(7)	5662(5)	9097(4)	1110(3)	23(1)
C(1)	6920(4)	9457(4)	1505(2)	23(1)
C(2)	6960(5)	10555(4)	1898(2)	25(1)
C(3)	8137(5)	10907(4)	2304(3)	30(1)
C(4)	9346(5)	10206(4)	2346(3)	32(1)
C(5)	9360(5)	9151(4)	1943(3)	33(1)
C(6)	8192(4)	8777(4)	1528(3)	26(1)
C(11)	3456(5)	7498(4)	394(2)	22(1)
C(12)	2668(5)	6667(4)	771(3)	29(1)
C(13)	1222(5)	6628(5)	641(3)	37(1)
C(14)	563(5)	7388(4)	148(3)	33(1)
C(15)	1364(5)	8204(4)	-232(3)	32(1)
C(16)	2812(5)	8250(4)	-117(3)	26(1)
C(21)	6321(4)	7693(4)	-335(2)	20(1)
C(22)	7237(4)	8649(4)	-487(2)	23(1)
C(23)	7897(5)	8678(4)	-1134(3)	30(1)
C(24)	7677(5)	7771(5)	-1634(3)	32(1)
C(25)	6753(5)	6844(5)	-1500(3)	35(1)
C(26)	6082(5)	6807(4)	-854(3)	31(1)
C(31)	6172(4)	6289(4)	1086(2)	22(1)
C(32)	7115(5)	5513(4)	761(3)	27(1)
C(33)	7629(5)	4518(4)	1150(3)	36(1)
C(34)	7185(5)	4297(4)	1837(3)	36(1)
C(35)	6233(5)	5064(4)	2161(3)	36(1)
C(36)	5749(5)	6074(4)	1783(3)	28(1)

Appendix A – Crystallographic Data

Table A.18a. Crystal data and structure refinement for 45.

Identification code	45	
Empirical formula	C13 H14 P N	
Formula weight	215.22	
Temperature	293(2) K	
Wavelength	0.71070 Å	
Crystal system	Triclinic	
Space group	P-1	
Unit cell dimensions	a = 6.0780(8) Å	$\alpha = 94.330(7)^\circ$.
	b = 8.3900(13) Å	$\beta = 102.776(8)^\circ$.
	c = 12.1580(18) Å	$\gamma = 106.238(9)^\circ$.
Volume	574.24(14) Å ³	
Z	2	
Density (calculated)	1.320 Mg/m ³	
Absorption coefficient	0.214 mm ⁻¹	
F(000)	245	
Crystal size	0.3 x 0.125 x 0.05 mm ³	
Theta range for data collection	1.74 to 24.95°.	
Index ranges	-7<=h<=7, -9<=k<=9, -13<=l<=14	
Reflections collected	4788	
Independent reflections	1983 [R(int) = 0.0861]	
Completeness to theta = 24.95°	99.1 %	
Refinement method	Full-matrix least-squares on F ²	
Data / restraints / parameters	1983 / 0 / 184	
Goodness-of-fit on F ²	1.713	
Final R indices [I>2sigma(I)]	R1 = 0.0926, wR2 = 0.2360	
R indices (all data)	R1 = 0.1203, wR2 = 0.2654	
Largest diff. peak and hole	1.196 and -0.840 e.Å ⁻³	

Appendix A – Crystallographic Data

Table A.18b. Atomic coordinates ($\times 10^4$) and equivalent isotropic displacement parameters ($\text{\AA}^2 \times 10^3$) for 45. U(eq) is defined as one third of the trace of the orthogonalized U^{ij} tensor.

	x	y	z	U(eq)
C(1)	3327(10)	2294(8)	4239(5)	37(1)
C(11)	2802(8)	-995(6)	3139(4)	27(1)
C(12)	3733(9)	-2178(7)	2701(4)	32(1)
C(13)	2676(9)	-3851(8)	2637(5)	37(1)
C(14)	632(9)	-4424(7)	3031(5)	37(1)
C(15)	-316(10)	-3292(7)	3459(5)	37(1)
C(16)	703(9)	-1606(7)	3505(5)	32(1)
C(21)	3274(8)	1776(6)	1860(4)	27(1)
C(22)	858(9)	1566(7)	1420(4)	34(1)
C(23)	69(10)	2064(7)	382(4)	36(1)
C(24)	1652(9)	2716(7)	-264(5)	35(1)
C(25)	4061(10)	2911(7)	168(5)	37(1)
C(26)	4848(9)	2447(7)	1210(4)	33(1)
N(1)	7121(7)	1585(5)	3455(4)	32(1)
P(1)	4378(2)	1206(2)	3225(1)	29(1)

Appendix A – Crystallographic Data

Table A.19a. Crystal data and structure refinement for **47**.

Identification code	47	
Empirical formula	C42 H37 N2 P3 S2	
Formula weight	726.77	
Temperature	120(2) K	
Wavelength	0.71073 Å	
Crystal system	Monoclinic	
Space group	P2(1)/n	
Unit cell dimensions	a = 11.278(3) Å	α = 90°.
	b = 16.057(5) Å	β = 95.53(2)°.
	c = 20.570(5) Å	γ = 90°.
Volume	3707.7(18) Å ³	
Z	4	
Density (calculated)	1.302 Mg/m ³	
Absorption coefficient	0.306 mm ⁻¹	
F(000)	1520	
Crystal size	0.26 x 0.10 x 0.09 mm ³	
Theta range for data collection	1.61 to 25.00°.	
Index ranges	-13<=h<=13, -15<=k<=19, -22<=l<=24	
Reflections collected	21964	
Independent reflections	6526 [R(int) = 0.0867]	
Completeness to theta = 25.00°	100.0 %	
Absorption correction	None	
Max. and min. transmission	0.9778 and 0.9425	
Refinement method	Full-matrix least-squares on F ²	
Data / restraints / parameters	6526 / 0 / 484	
Goodness-of-fit on F ²	1.004	
Final R indices [I>2sigma(I)]	R1 = 0.0448, wR2 = 0.0791	
R indices (all data)	R1 = 0.0927, wR2 = 0.0926	
Largest diff. peak and hole	0.301 and -0.314 e.Å ⁻³	

Appendix A – Crystallographic Data

Table A.19b. Atomic coordinates ($\times 10^4$) and equivalent isotropic displacement parameters ($\text{\AA}^2 \times 10^3$) for 47. U(eq) is defined as one third of the trace of the orthogonalized U^{ij} tensor.

	x	y	z	U(eq)
P(1)	7296(1)	3371(1)	4197(1)	20(1)
P(2)	4001(1)	4178(1)	2054(1)	18(1)
P(3)	6048(1)	3274(1)	1567(1)	18(1)
S(1)	3902(1)	3627(1)	2916(1)	24(1)
S(2)	7495(1)	3467(1)	2187(1)	23(1)
N(1)	6695(3)	3989(2)	3624(1)	23(1)
N(2)	4933(2)	3882(1)	1564(1)	20(1)
C(11)	8873(3)	3560(2)	4300(1)	20(1)
C(12)	9549(3)	3350(2)	3789(2)	25(1)
C(13)	10770(3)	3439(2)	3867(2)	29(1)
C(14)	11334(3)	3736(2)	4448(2)	30(1)
C(15)	10671(3)	3943(2)	4957(2)	34(1)
C(16)	9434(3)	3857(2)	4883(2)	30(1)
C(21)	7123(3)	2283(2)	4024(1)	20(1)
C(22)	7973(3)	1714(2)	4287(2)	24(1)
C(23)	7869(3)	879(2)	4129(2)	28(1)
C(24)	6910(3)	602(2)	3714(2)	30(1)
C(25)	6052(3)	1161(2)	3462(2)	34(1)
C(26)	6156(3)	2003(2)	3605(2)	29(1)
C(31)	6620(2)	3626(2)	4924(1)	22(1)
C(32)	6197(3)	3009(2)	5318(2)	27(1)
C(33)	5662(3)	3229(2)	5874(2)	31(1)
C(34)	5578(3)	4062(2)	6048(2)	29(1)
C(35)	6015(3)	4673(2)	5664(2)	28(1)
C(36)	6531(3)	4464(2)	5101(2)	25(1)
C(41)	2543(2)	4140(2)	1588(1)	18(1)
C(42)	1505(3)	3998(2)	1887(2)	26(1)
C(43)	398(3)	4028(2)	1530(2)	31(1)
C(44)	315(3)	4202(2)	869(2)	29(1)
C(45)	1337(3)	4338(2)	564(2)	29(1)
C(46)	2442(3)	4308(2)	921(2)	26(1)
C(51)	4249(2)	5288(2)	2177(1)	19(1)
C(52)	5402(3)	5606(2)	2190(1)	22(1)

Appendix A – Crystallographic Data

C(53)	5619(3)	6447(2)	2307(1)	25(1)
C(54)	4694(3)	6973(2)	2415(1)	24(1)
C(55)	3535(3)	6669(2)	2397(1)	25(1)
C(56)	3312(3)	5834(2)	2279(1)	22(1)
C(61)	6514(2)	3342(2)	745(1)	19(1)
C(62)	5811(3)	3743(2)	243(2)	27(1)
C(63)	6182(3)	3786(2)	-380(2)	31(1)
C(64)	7245(3)	3430(2)	-516(2)	33(1)
C(65)	7941(3)	3025(2)	-25(2)	31(1)
C(66)	7587(3)	2980(2)	598(2)	26(1)
C(71)	5563(3)	2198(2)	1635(1)	22(1)
C(72)	4354(3)	1997(2)	1565(2)	28(1)
C(73)	3980(3)	1175(2)	1610(2)	37(1)
C(74)	4808(4)	551(2)	1716(2)	43(1)
C(75)	6018(4)	733(2)	1776(2)	44(1)
C(76)	6389(3)	1549(2)	1735(2)	31(1)

Appendix A – Crystallographic Data

Table A.20a. Crystal data and structure refinement for **50**.

Identification code	50	
Empirical formula	C ₃₇ H ₃₁ O ₂ P	— —
Formula weight	538.588	
Temperature	150(2) K	
Wavelength	0.71073 Å	
Crystal system	Monoclinic	
Space group	P2(1)/c	
Unit cell dimensions	a = 8.5213(17) Å	α = 90°.
	b = 15.866(3) Å	β = 101.91(3)°.
	c = 10.972(2) Å	γ = 90°.
Volume	1451.4(5) Å ³	
Z	4	
Density (calculated)	1.232 Mg/m ³	
Absorption coefficient	0.127 mm ⁻¹	
F(000)	568	
Crystal size	0.55 x 0.40 x 0.25 mm ³	
Theta range for data collection	3.54 to 25.00°.	
Index ranges	-10 ≤ h ≤ 10, -18 ≤ k ≤ 18, -13 ≤ l ≤ 13	
Reflections collected	13222	
Independent reflections	2533 [R(int) = 0.0255]	
Completeness to theta = 25.00°	99.5 %	
Refinement method	Full-matrix least-squares on F ²	
Data / restraints / parameters	2533 / 0 / 193	
Goodness-of-fit on F ²	1.280	
Final R indices [I > 2σ(I)]	R1 = 0.0547, wR2 = 0.1102	
R indices (all data)	R1 = 0.0604, wR2 = 0.1124	
Extinction coefficient	0.0097(11)	
Largest diff. peak and hole	0.305 and -0.258 e.Å ⁻³	

Appendix A – Crystallographic Data

Table A.20b. Atomic coordinates ($\times 10^4$) and equivalent isotropic displacement parameters ($\text{\AA}^2 \times 10^3$) for **50**. $U(\text{eq})$ is defined as one third of the trace of the orthogonalized U^{ij} tensor.

	x	y	z	U(eq)
P(1)	4310(2)	367(1)	7886(3)	20(1)
C(1)	4360(18)	373(10)	7662(14)	83(6)
O(1)	4015(2)	496(1)	9053(2)	65(1)
C(11)	3316(3)	-450(2)	7059(2)	35(1)
C(12)	3402(3)	-1214(2)	7701(2)	48(1)
C(13)	2590(4)	-1922(2)	7155(3)	57(1)
C(14)	1661(3)	-1871(2)	5957(3)	53(1)
C(15)	1562(3)	-1122(2)	5309(2)	47(1)
C(16)	2387(3)	-413(2)	5854(2)	37(1)
C(21)	6274(3)	244(2)	7884(2)	37(1)
C(22)	7325(3)	773(2)	8677(2)	49(1)
C(23)	8968(4)	687(2)	8803(3)	61(1)
C(24)	9581(4)	77(2)	8127(3)	63(1)
C(25)	8551(4)	-443(2)	7320(3)	55(1)
C(26)	6889(3)	-361(2)	7201(2)	43(1)
C(31)	3750(3)	1240(1)	6922(2)	30(1)
C(32)	2491(3)	1729(2)	7158(2)	39(1)
C(33)	2025(3)	2459(2)	6486(2)	48(1)
C(34)	2797(3)	2707(2)	5554(2)	48(1)
C(35)	4028(3)	2216(2)	5286(2)	45(1)
C(36)	4509(3)	1489(2)	5968(2)	37(1)

Appendix B

Research Colloquia, Lectures and Conferences Attended

Appendix B – Colloquia, Lectures and Conferences attended.

Only those attended by the author are shown.

University of Durham (1997 – 1999).

1997

- October 15 Dr R M Ormerod, Department of Chemistry, Keele University,
Studying catalysts in action.
- October 21 Professor A F Johnson, IRC, Leeds,
Reactive processing of polymers: science and technology.
- October 22 Professor R J Puddephatt (RSC Endowed Lecture), University of Western
Ontario,
Organoplatinum chemistry and catalysis.
- October 23 Professor M R Bryce, University of Durham, Inaugural Lecture,
New tetrathiafulvalene derivatives in molecular, supramolecular and
macromolecular chemistry: controlling the electronic properties of organic
solids.
- October 27 Professor W Roper FRS, University of Auckland, New Zealand,
Organometallic chemistry.
- October 28 Professor A P de Silva, The Queen's University, Belfast,
Luminescent signalling systems.
- November 5 Dr M Hii, Oxford University,
Studies of the Heck reaction.
- November 11 Professor V Gibson, Imperial College, London,
Metallocene polymerisation.

Appendix B – Colloquia, Lectures and Conferences attended.

- November 20 Dr L Spiccia, Monash University, Melbourne, Australia,
Polynuclear metal complexes.
- November 25 Dr R Withnall, University of Greenwich,
Illuminated molecules and manuscripts.
- November 26 Professor R W Richards, University of Durham, Inaugural Lecture,
A random walk in polymer science.
- December 2 Dr C J Ludman, University of Durham,
Explosions.
- December 10 Sir G Higginson, former Professor of Engineering in Durham and retired
Vice-Chancellor of Southampton Univ,
1981 and all that.

1998

- January 20 Professor J Brooke, University of Lancaster,
What's in a formula? Some chemical controversies of the 19th century.
- January 21 Professor D Cardin, University of Reading,
Organometallic chemistry.
- January 27 Professor R Jordan, Dept. of Chemistry, Univ. of Iowa, USA,
Cationic transition metal and main group metal alkyl complexes in olefin
polymerisation.
- February 3 Dr J Beacham, ICI Technology,
The chemical industry in the 21st century.
- February 4 Professor P Fowler, Department of Chemistry, Exeter University,
Classical and non-classical fullerenes.

Appendix B – Colloquia, Lectures and Conferences attended.

- February 17 Dr S Topham, ICI Chemicals and Polymers,
Perception of environmental risk; The River Tees, two different rivers.
- February 18 Professor G Hancock, Oxford University,
Surprises in the photochemistry of tropospheric ozone.
- February 25 Dr C Jones, Swansea University,
Low coordination arsenic and antimony chemistry.
- March 11 Professor M J Cook, Dept of Chemistry, UEA,
How to make phthalocyanine films and what to do with them.
- March 18 Dr J Evans, Oxford University,
Materials which contract on heating (from shrinking ceramics to bullet
proof vests.
- October 7 Dr S Rimmer, Ctr Polymer, University of Lancaster,
New polymer colloids.
- October 9 Professor M F Hawthorne, Department Chemistry & Biochemistry,
UCLA, USA,
RSC endowed lecture.
- October 23 Professor J C Scaiano, Department of Chemistry, University of Ottawa,
Canada,
In search of hypervalent free radicals, RSC endowed lecture.
- October 26 Dr W Peirs, University of Calgary, Alberta, Canada,
Reactions of the highly electrophilic boranes $\text{HB}(\text{C}_6\text{F}_5)_2$ and $\text{B}(\text{C}_6\text{F}_5)_3$ with
zirconium and tantalum based metallocenes.
- October 27 Professor A Unsworth, University of Durham,
What's a joint like this doing in a nice girl like you?
In association with The North East Polymer Association.

Appendix B – Colloquia, Lectures and Conferences attended.

- October 28 Professor J P S Badyal, Department of Chemistry, University of Durham,
Tailoring solid surfaces, Inaugural lecture.
- November 4 Dr N Kaltsoyannis, Department of Chemistry, UCL, London,
Computational adventures in d & f element chemistry.
- November 3 Dr C J Ludman, Chemistry Department, University of Durham,
Bonfire night lecture.
- November 12 Professor S Loeb, University of Windsor, Ontario, Canada,
From macrocycles to metallo-supramolecular chemistry.
- November 17 Dr J McFarlane,
Nothing but sex and sudden death!
- December 1 Professor N Billingham, University of Sussex,
Plastics in the environment - Boon or bane?
In association with The North East Polymer Association.
- December 2 Dr M Jaspers, Department of Chemistry, University of Aberdeen,
Bioactive compounds isolated from marine invertebrates and
cyanobacteria.

1999

- January 19 Dr J Mann, University of Reading,
The elusive magic bullet and attempts to find it?
- January 27 Professor K Wade, Department of Chemistry, University of Durham,
Foresight or hindsight? Some borane lessons and loose ends.
- February 9 Professor D J Cole-Hamilton, St. Andrews University,
Chemistry and the future of life on earth.

Appendix B – Colloquia, Lectures and Conferences attended.

- March 9 Dr Michael Warhurst, Chemical Policy issues, Friends of the Earth,
Is the chemical industry sustainable?
- March 10 Dr A Harrison, Department of Chemistry, The University of Edinburgh,
Designing model magnetic materials.

POSTGRADUATE AND POSTDOCTORAL SEMINARS (University of Bath 1999-
2000).

- October 18 Dr T. Hibbert, Silicon-29 NMR as a tool for probing polysilanes.
Dr H. Broadbent, Detecting explosives.
- October 25 Dr R. Price, Alkali metal complexes of phosphonium ylides.
Dr K. Jenkins, Catalytic electronic modification of organic substrates.
- November 1 Dr A. Swain, Polydialkylsilanes ; a random walk into the blue.
Dr C. Bubert, Asymmetric ruthenium-catalysed transfer hydrogenation
reactions.

2000

- January 11 N. Patmore, Boron clusters.
A. Kana, Synthesis of precursors for the CVD of mixed metal sulphides.
R. Jazsar, High pressure/temperature infra-red spectroscopy.
- January 18 J. Hartley, Cowboys and Indium.
M. Lunn, Novel group IV polymerisation catalysts.
D. Cooke, Simulating iron oxide surfaces.
- February 29 M. Wiseman, Gold rings and silver crowns.
D. Snell, The use of ultrasound in emulsion polymerisations.

Conferences and Symposia Attended

RSC National Congress and Young Researchers Meeting, University of Durham (U.K.), 6-9 April 1998.*

The 48th Annual Gathering of Nobel Prize Winners, Lindau (Germany), 25-29 June 1998.

Universities of Scotland Inorganic Club (U.S.I.C.) 1998 meeting, University of Strathclyde (U.K.), 15-16 September 1998.*

BCA Intensive X-ray Crystallography School, University of Durham (U.K.), March 1999.

IMEBORON X, University of Durham (U.K.), 2-6 July 1999.

Dalton Half-Day Symposium, RSC London (U.K.), 8th Nov 1999.

I.C.I. Department of Chemistry Poster Competition, University of Durham (U.K.), 20th December 1999.*

Dalton Full-Day Symposium, University of Bristol (U.K.), 11th Jan 2000.

South-West Area Dalton Meeting, University of Cardiff (U.K.), 13th April 2000.*

* Poster presented.

Work in Other Laboratories

Two weeks in the laboratories of Professor Fernando Lopez-Ortiz, Universidad de Almeria (Spain), 11th-25th March 2000.